













# THE CRYSTALLINE STATE

VOL. I

A GENERAL SURVEY



# THE CRYSTALLINE STATE—VOL. I

Editor: SIR LAWRENCE BRAGG

---

## THE CRYSTALLINE STATE A GENERAL SURVEY

By

SIR LAWRENCE BRAGG,

D.Sc., F.R.S.

CAVENDISH PROFESSOR OF EXPERIMENTAL PHYSICS  
IN THE UNIVERSITY OF CAMBRIDGE

LONDON

G. BELL AND SONS LTD

1949

*First Published 1933.*  
*Reprinted 1939.*  
*Reprinted with corrections 1949.*

PRINTED IN GREAT BRITAIN BY  
BRADFORD AND DICKENS, LONDON, W.C. 1

## INTRODUCTION TO THE FIRST EDITION

THE study of the microstructure of matter by means of X-rays has developed very rapidly during the last decade, and a new branch of Science, the physics and chemistry of the solid state, is largely dependent on it for its experimental basis. When the first edition of *X-rays and Crystal Structure* was written in 1914 it was possible to describe in a short volume the main discoveries in the new field which Laue's classical experiment on the diffraction of X-rays had opened up two years previously. In planning the extended edition which was published in 1924 it was already impossible to cover the whole ground. A choice had to be made between the original simple scheme of the book as an introduction to the subject, and a much more complete survey which would be useful as a book of reference. The first alternative was adopted and the new edition followed the former editions in its main outlines, although several sections on more recent work were included.

Since then the subject has grown so fast, and has had so many ramifications, that it is now necessary to recast entirely the plan of the book. The results of X-ray analysis are of interest to workers in many branches of Science, and hence we feel that this book, if it is to be of service to them, must give a broad general survey of the subject which shows its possibilities in different directions. At the same time we wish it to have the character of a book of reference. Many good books on the subject have appeared in recent years written by Ewald, Niggli, Mark, Wyckoff, Schiebold, Mauguin, Ott, and others. There is place, however, for a book in the English language which includes work much of which as yet is only to be found in original papers scattered amongst many journals. A large body of the work has been carried out in this country, and a characteristic technique and viewpoint have been developed.

We have therefore adopted the following scheme. The



first volume is intended to give a survey of the whole subject and to form an introduction to the remainder of the book. All branches of X-ray analysis are briefly described. It has been our aim to make the treatment one which can be followed by anyone who is interested in the main principles of the new subject, and who wishes to understand its achievements and possible future applications. This first volume is therefore complete in itself, and is a text-book on the crystalline state which it is hoped may be useful to many students who do not require a full treatment. The various branches are developed in greater detail in the succeeding Vols. II and III. We are writing these volumes with the assistance of a number of collaborators, each of whom has been responsible for that part of the subject of which he has expert knowledge. We wish to emphasize that it is not necessary to read the specialised sections consecutively. The General Survey serves for all sections, and the reader can pass directly from it to a further study of any part of the subject which interests him especially. For instance, the reader who wishes to know the results of analysis rather than to study the way in which these results have been obtained, can omit the section on 'X-ray Optics,' which goes somewhat deeply into the theory of diffraction, the section on 'Crystal Symmetry,' and the technical discussion of 'Methods of Analysis.'

The sections included in Vols. II and III represent a natural division of the subject-matter into the theory and technique of X-ray analysis on the one hand, and, on the other, the discussion of the results of analysis with their significance for crystal physics and crystal chemistry. Vol. II includes sections on X-ray optics, crystallography and space-group theory, and the technique of analysis. Vol. III includes sections on inorganic and organic compounds and metals, on crystal physics and chemistry, on growth and deformation-structures, on semi-crystalline bodies, liquids, and gases, and on the technical applications of X-ray analysis.

It was our original intention to include in a fourth volume an atlas of space-groups and a set of tables used in analysis, but this is no longer necessary since the material is given in the International Tables.

The adoption of this arrangement for the book makes a certain amount of repetition inevitable, because subjects dealt with briefly in the General Survey are treated with greater thoroughness

in the remainder of the book. We feel, however, that it is well worth while to run the risk of a certain amount of reduplication if we succeed in making the book useful in a dual capacity—a review of the subject and a work of reference.

W. H. BRAGG

W. L. BRAGG

### PREFACE TO VOL. I.

IN writing this General Survey I have used again much of the material and many of the diagrams of *X-rays and Crystal Structure*, which my father and I first published in 1915, and of *An Introduction to Crystal Analysis*, which my father published in 1928 after giving a course of lectures at University College, Aberystwyth. I have been assisted in countless ways by the collaborators whom we have invited to contribute sections to Vols. II and III, and in planning the present volume I have always had in mind the necessity of making it a suitable introduction to their expert sections. Many other colleagues have lent me photographs and diagrams, or have given me permission to reproduce these from their works. Acknowledgment is made in the text, but I take this opportunity of thanking them. References to original papers have not been given in this volume, since a full list will be given in the later sections, but some of the more important papers or books are quoted in the historical chapter. I wish to express my indebtedness to Dr E. C. S. Dickson for his kindness in reading the proofs, and to my wife for preparing the Index.

W. L. BRAGG

MANCHESTER UNIVERSITY

August 1933

## NOTE ON THIRD IMPRESSION

When this Volume I of "The Crystalline State" was written in 1933, it was intended that it should form an introduction to subsequent Volumes II and III dealing at greater length with the technique and results of X-ray analysis. Owing to my leaving Manchester for new responsibilities at the National Physical Laboratory, to the interruption of all scientific work by the war, and to my father's death, this plan had to be abandoned. It is only now that a Volume II on X-ray Optics has been written by Professor R. W. James and will, it is hoped, soon be published. Great advances have been made since the present volume first appeared; if the subsequent volumes had followed it as originally intended they would now be sadly out of date. The treatment in Volume I, however, is of so general a nature that it still serves as an introduction to X-ray analysis; it is therefore being reprinted in its original form. The only changes I have made consist in the correction of a certain number of errors in the original volume; I am indebted to many kind colleagues who have drawn my attention to them. I have also brought the "Bibliography" up to date by including recent publications. In making these changes I have been assisted by Dr Helen D. Megaw, and wish to express my warmest thanks for the help which she has given me.

W. L. B.

Cavendish Laboratory,  
Cambridge.  
*September 1948.*

# CONTENTS

## CHAPTER I

### THE CRYSTALLINE STATE

	PAGE
The Crystal Pattern . . . . .	I
Lattice-planes and Crystal Faces . . . . .	5
The Law of Rational Indices . . . . .	6
Crystal Zones . . . . .	9
Crystal Symmetry . . . . .	9
External Form and Internal Structure . . . . .	11

## CHAPTER II

### DIFFRACTION BY THE CRYSTAL LATTICE

Reflection by the Planes of the Crystal Lattice . . . . .	13
Diffraction by the Three-dimensional Grating . . . . .	17
Influence of the Unit of Pattern . . . . .	20
Summary . . . . .	20

## CHAPTER III

### EXPERIMENTAL METHODS OF CRYSTAL ANALYSIS

The Laue Photograph . . . . .	23
The Ionisation Spectrometer . . . . .	27
The Rotation Photograph . . . . .	30
The Powder Photograph . . . . .	33
Other Methods of Analysis . . . . .	37
Summary . . . . .	37

## CHAPTER IV

### EXAMPLES OF CRYSTAL ANALYSIS

Potassium Chloride and Sodium Chloride . . . . .	39
Laue, Powder, and Rotation Photographs of KCl and NaCl . . . . .	46
The Analysis of Zincblende, Diamond, and Fluor . . . . .	51
Crystal Structures with Parameters . . . . .	56
Iron Pyrites . . . . .	57
Summary . . . . .	61

## CHAPTER V

## CRYSTAL SYMMETRY

	PAGE
The Space-lattice . . . . .	63
The Point-group and the Classes of Crystal Symmetry . . .	67
The Space-group . . . . .	75
The 230 Space-groups . . . . .	81
Space-group Notation . . . . .	84

## CHAPTER VI

## THE PRINCIPLES OF STRUCTURE ANALYSIS

The Determination of Space-lattice and Space-group by X-ray Methods . . . . .	90
Friedel's Law . . . . .	93
The Numbers of Equivalent Positions in the Unit Cell . . .	95
The Structure Amplitude . . . . .	96
The Atomic Scattering Factor . . . . .	100
The Comparison of Calculated and Observed Intensities of Reflection . . . . .	101
The Analysis of Inorganic Crystals . . . . .	102
An Example of Analysis: Beryl . . . . .	104
The Analysis of Organic Crystals . . . . .	108
Summary . . . . .	111

## CHAPTER VII

## CHEMICAL AND PHYSICAL CRYSTALLOGRAPHY

Interatomic Forces . . . . .	112
Inorganic Compounds . . . . .	124
Metals and Alloys . . . . .	142
Organic Compounds . . . . .	159
The Energy of the Crystal Lattice . . . . .	171
Twinning . . . . .	176
Refractive Index . . . . .	180

## CHAPTER VIII

## CRYSTAL TEXTURE

The Transition from the Crystalline to the Amorphous State . .	188
Diffraction by Amorphous Solids, Liquids, and Gases . . .	191
Crystal Orientation . . . . .	196
The Structure of Natural Fibres . . . . .	203

# CONTENTS

xi

## CHAPTER IX

### X-RAY OPTICS

	PAGE
The Scattering of X-rays by the Atom . . . . .	208
The Intensity of Diffraction by a Crystal . . . . .	213
Formulae for Diffraction by a Mosaic Crystal . . . . .	216
Thermal Movements. The Temperature Factor . . . . .	217
Tests of the Theory of Diffraction with Simple Crystals . . . . .	219
The Use of 'Absolute Measurements' in Crystal Analysis . . . . .	219
The Representation of the Crystal as a Fourier Series . . . . .	221
Examples of Fourier Series . . . . .	224
The Fourier Representation as an Optical Image . . . . .	229
The Reciprocal Lattice . . . . .	231
Summary . . . . .	236

## CHAPTER X

### APPLICATIONS OF X-RAY METHODS TO PROBLEMS OF PURE AND APPLIED SCIENCE. A SUMMARY

Chemical Composition . . . . .	238
The Structure of Alloys . . . . .	240
Identification . . . . .	241
Coefficients of Thermal Expansion . . . . .	242
Technical Applications . . . . .	243

## CHAPTER XI

### THE DIFFRACTION OF ELECTRONS

The Wave-mechanics of Electrons . . . . .	244
Powder Photographs of Electron Diffraction . . . . .	248
The Experiments of Davisson and Germer . . . . .	250
The Wave-length of the Electron Beam . . . . .	253
The Atomic Scattering Factor for Electron Waves . . . . .	254
Diffraction by Single Crystals . . . . .	259
Distortion of the Small Crystal . . . . .	260
Diffraction by a Small Crystal . . . . .	261
Interaction between the Incident and Diffracted Beams . . . . .	263
The Kikuchi 'P' Pattern . . . . .	264
Electron Diffraction by the Molecules of a Gas . . . . .	264

## CHAPTER XII

## HISTORICAL

	PAGE
The Theory of Crystal Structure before the Discovery of X-ray	
Diffraction . . . . .	268
The Early X-ray Investigations . . . . .	271
The Development of X-ray Technique . . . . .	275
Space-group Criteria . . . . .	276
The Use of Intensity Measurements in Analysis . . . . .	278
X-ray Optics . . . . .	279
Crystal Chemistry . . . . .	280
Crystal Physics . . . . .	285
BIBLIOGRAPHY . . . . .	287

## APPENDIX I

## THE PRODUCTION AND PROPERTIES OF X-RADIATION

The Production of X-rays . . . . .	289
Line Spectra . . . . .	291
Energy Levels and X-ray Spectra . . . . .	295
The Continuous Spectrum . . . . .	298
X-ray Absorption . . . . .	300
The Compton Effect . . . . .	305
Apparatus . . . . .	306
Refraction, Reflection, and Interference of X-rays . . . . .	309

## APPENDIX II

EMISSION SPECTRA AND ABSORPTION EDGES . . . . .	318
---	-----

## APPENDIX III

ABSORPTION COEFFICIENTS . . . . .	325
-----------------------------------	-----

## APPENDIX IV

ATOMIC SCATTERING FACTORS . . . . .	328
-------------------------------------	-----

## APPENDIX V

DEDUCTION OF THE FORMULÆ FOR INTENSITY OF REFLECTION . . . . .	335
--	-----

## APPENDIX VI

NOMENCLATURE OF THE SPACE-GROUPS . . . . .	341
--	-----

INDEX OF SUBJECTS . . . . .	347
-----------------------------	-----

INDEX OF AUTHORS . . . . .	350
----------------------------	-----

## CHAPTER I

### THE CRYSTALLINE STATE

#### THE CRYSTAL PATTERN

THE most familiar external characteristic of a crystal is its geometrical form. Crystals are bounded by plane faces meeting in edges and corners, and these faces are often symmetrically related to each other. Quartz, for example, forms crystals which are six-sided prisms terminated by six-sided pyramids; alum crystallises in octahedra, sodium chloride and iron pyrites in cubes. The geometrical form may not be perfectly regular, for some of the corresponding faces on a crystal may have developed more than others owing to accidental conditions of growth. It is found, however, that the angles between the faces in different specimens of the same crystalline substance are characteristic. However much a crystal of quartz departs from a regular six-sided form, the angle between the prism and pyramid faces is always  $38^{\circ} 13'$ . The external form of the crystal is only one of many properties which are related in a precise way to certain definite directions in the crystalline specimen. Cleavage, hardness, electrical conductivity, thermal conductivity, and refractive index are all directional properties of the crystal.

Long before direct evidence was available, these crystal characteristics were correctly interpreted as arising from a regular arrangement in space of certain units, of which the crystal structure is built. When shot lying on a tray are concentrated towards one end by a tilt of the tray, the shot will 'crystallise.' In order to take up the least area, they will pack together and form a regular pattern such that all are placed at the corners of a network of equilateral triangles. In the same way, when a solid crystallises out from the dissolved or molten state, the molecules are arranged regularly, because this arrangement has a lower potential energy than that of an irregular assemblage.



Haüy at the end of the eighteenth century supposed the crystal to be composed of small blocks, each having the shape of the cleavage figure, and accounted for the various faces of a crystal as alternative ways of terminating the stacking together of the blocks. Fig. 1 shows Haüy's explanation of the shape of

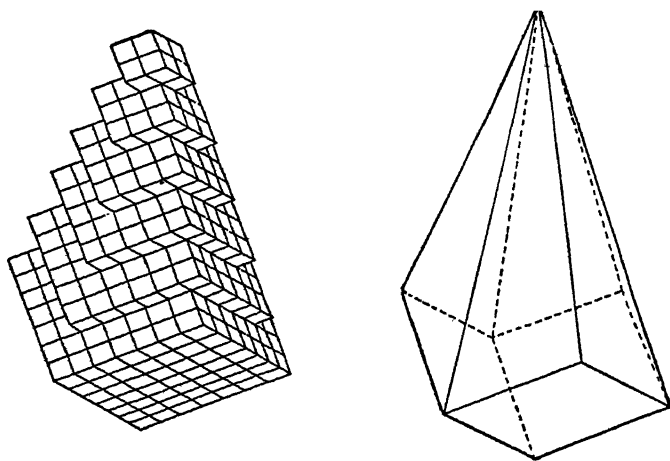


FIG. 1.—Haüy's explanation of the origin of crystal faces  
(From *Mineralogy*, H. A. Miers; Macmillan, 1929)

a calcite crystal, composed of the cleavage rhombs of calcite as units. We would now substitute for Haüy's cleavage rhomb the unit of pattern of the structure, but the principle of their stacking together remains the same.

In a two-dimensional design, such as that of a wall-paper, a unit of pattern is repeated at regular intervals. Let us choose some representative point in the unit of pattern, and mark the position of similar points in all the other units. If these points be considered alone, the pattern being for the moment disregarded, it will be seen that they form a regular network. By drawing lines through them, the area can be divided into a series of cells each of which contains a unit of the pattern. It is immaterial which point of the design is chosen as representative, for a similar network of points will always be obtained.

This is a fundamental characteristic of any pattern. As an instance, fig. 2 (which is taken from Walter Crane's *Line and Form*) shows the construction of wall-paper designs, in which the artist has drawn a framework of dotted lines and filled each cell with a unit of pattern. The cell which encloses the complete

pattern consists of two squares in the upper design and one square in the lower. It will be clear that if we take the design itself and wish to outline the framework on which it is constructed, the choice of a characteristic point is quite arbitrary; the framework has no unique position, but merely indicates the intervals at which the pattern is repeated.

A pattern in three dimensions is correspondingly built up on what is termed a 'space-lattice.' In the crystalline arrangement there must be innumerable points such that, if an observer capable of taking up a position within the crystal and making notes of his surroundings could be translated from one of these points to another, he would find no change in the outlook in any given direction in space. This is the fundamental characteristic of the crystal, which distinguishes it from an irregular arrangement. The

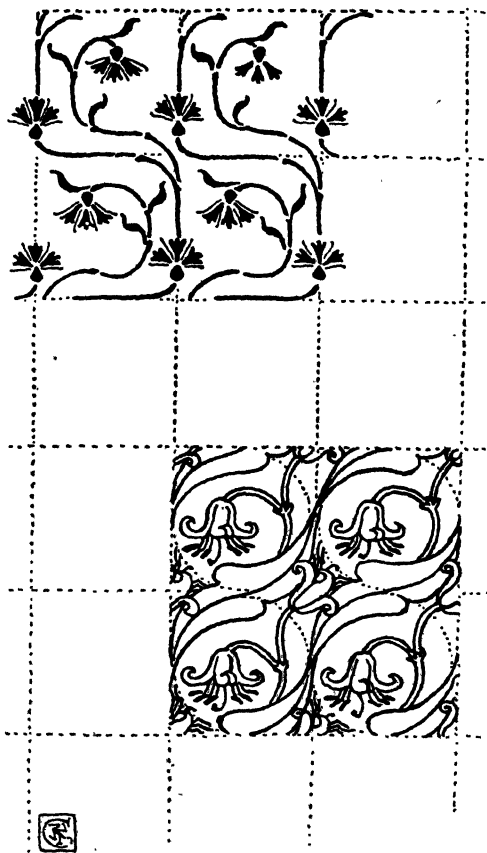


FIG. 2.—The basis of a design upon a network  
(From *Line and Form*, Walter Crane; Bell, 1900)

framework of similar points is shown in fig. 3, in which each point is placed at the intersection of the dotted parallels drawn in three directions in space. The lines of the diagrams are not necessary; rows of points might have been used. The lines serve to make the construction clearer to the eye, and they serve a further purpose in showing that space can be divided into cells. The cells are exactly alike, the eight corners of each being situated at eight of the points.

The arrangement of points is a 'space-lattice,' and the cells are 'unit cells' of the crystal. Each cell contains a complete representation of a unit of pattern, the repetition of which builds up the crystal. As in the case of the wall-paper, it is immaterial which point of the pattern unit is chosen, so long as all points are similarly situated. The space-lattice is a scale showing how the design repeats in three dimensions.

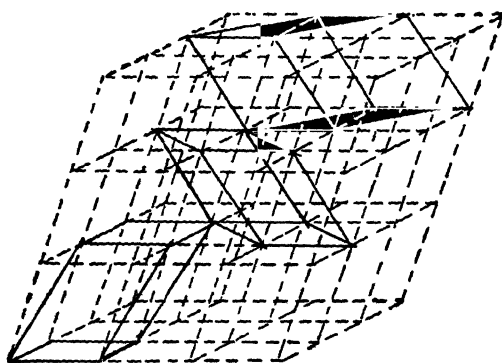


FIG. 3.—The space-lattice, showing alternative ways of outlining the unit cell

The relative positions of the points are always the same for a given pattern, but the way in which the cells are outlined is arbitrary, so that the crystal can be divided into cells in an infinite number of ways. A few alternatives to the dotted lines are shown by the full lines in the diagram.

Such cells, which have a point at each corner, have the same volume whatever their shape, and there are always as many points as cells. Each cell has eight corners, but the point at each corner is common to eight cells, and there is therefore a one-to-one correspondence. This is merely another way of stating that each cell contains a complete unit of pattern.

It is sometimes convenient to refer the crystal to a lattice framework whose cells are not simple cells containing only one unit of pattern. A cell which has, in addition to the points at its corners, a point at its centre or at the centre of one or all of its faces, may be better adapted to display the symmetry of the crystal than a simple cell. Such cases are more fully described in a later chapter. They form no exceptions to the above rules, which apply to all simple cells of the lattice. In general, it is convenient to choose a method of drawing the cells which makes their edges as short as possible, and at the same time is in accord with the symmetry.

The cell is defined by the length of its edges and by the angles between them, as in fig. 4.

$$\begin{array}{ll}
 OA = a & BOC = \alpha \\
 OB = b & AOC = \beta \\
 OC = c & AOB = \gamma
 \end{array}$$

The lengths  $a$ ,  $b$ ,  $c$  are termed the axial lengths, and the vectors  $OA$ ,  $OB$ ,  $OC$  define the axes of the crystal. The axes provide a framework by which the position of any point of the pattern with respect to a given origin can be defined. If the co-ordinates

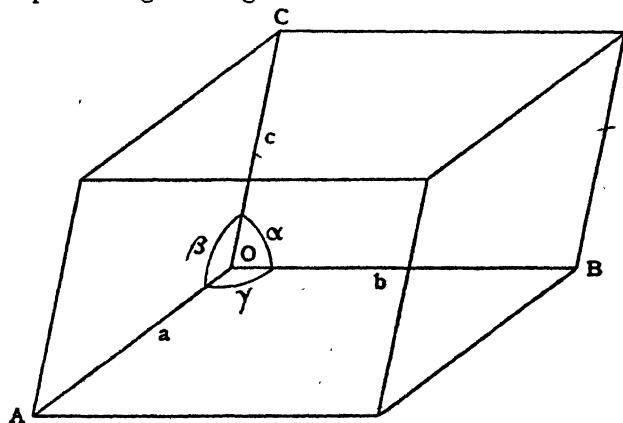


FIG. 4.—The unit cell

of this point are  $x$ ,  $y$ ,  $z$ , measured parallel to the axes, there will be a similar point at  $x+pa$ ,  $y+qb$ ,  $z+rc$ , where  $p$ ,  $q$ ,  $r$  are any integers.

#### LATTICE-PLANES AND CRYSTAL FACES

The points of a space-lattice can be arbitrarily arranged in an infinite number of ways in parallel equidistant sheets. The corresponding geometrical feature of a two-dimensional pattern is very evident when one looks at a hop-garden or orchard where planting has been done in a regular way, and where parallel rows seem to radiate from the observer in a number of directions. The most obvious and densely packed rows are far apart, while more complex rows can be seen which are closer together, though the plants are spaced more widely along any one row. In the three-dimensional pattern the analogues to these rows are series of parallel sheets. Examples are easily traced in fig. 3, for if any face of the various unit cells in that pattern be produced it would pass through a network of points.

The faces of a crystal are parallel to these net-planes, and it is for this reason that the interfacial angles are the same in different specimens. The dependence of the directions of the crystal faces upon the underlying space-lattice leads to a geometrical relationship called by the crystallographer the 'Law of Rational Indices.'

### THE LAW OF RATIONAL INDICES

Let us suppose that we have a series of points constituting a space-lattice, and wish to define one of the ways in which the points can be arranged on parallel equidistant planes. The dotted lines in fig. 5 indicate the positions of these planes, and

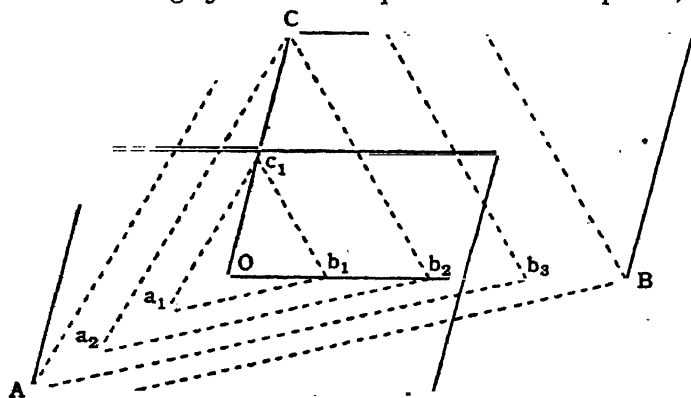


FIG. 5.—The law of rational indices

another plane of the series will pass through the origin  $O$ . It will be clear that if  $O$ ,  $A$ ,  $B$ , and  $C$  lie on one or other of the planes, all points of the lattice will also lie on planes of this set, for any point is arrived at from the origin  $O$  by a suitable repetition of the translations  $OA$ ,  $OB$ ,  $OC$ . The equidistant planes divide the axis  $OA$  into an integral number of equal intercepts,  $Oa_1$ ,  $a_1a_2$ , etc., and the same holds for the other axes. If  $OA$  is divided into  $h$  parts,  $OB$  into  $k$  parts, and  $OC$  into  $l$  parts, the planes are distinguished by the indices  $(hkl)$ . Alternatively, we may define the set of planes by stating that the next plane to that passing through the origin makes intercepts  $a/h$ ,  $b/k$ ,  $c/l$  on the axes. In the figure, for instance, the planes which have been drawn have the indices  $(342)$ . In the special case of a plane parallel to an axis, the corresponding index is zero, since the intercept is infinite.

Guided by the external form of the crystal, descriptive crystallography has arrived at a corresponding method of naming crystal faces. Three non-parallel faces of the crystal are chosen whose intersections give the directions of the crystal axes  $OA$ ,  $OB$ ,  $OC$  (fig. 6). A fourth face is then chosen which cuts all three axes, and is called the standard plane. If  $ABC$  is such a plane, the *relative* lengths of the intercepts  $OA$ ,  $OB$ ,  $OC$  are made to define the crystal axes  $a$ ,  $b$ ,  $c$ . Since it is only the relative lengths which are material in defining external form,  $b$  is usually taken to be unity. The empirical law which is found

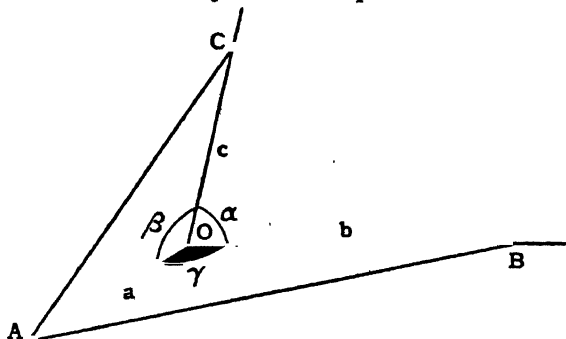


FIG. 6.—The definition of the crystal axes

to govern the directions of all other faces of the crystal is as follows: "Faces of the crystal are parallel to planes making intercepts  $a/h$ ,  $b/k$ ,  $c/l$  on the three axes, where  $h$ ,  $k$ ,  $l$  are small whole numbers."

This law is a consequence of the foundation of the crystal upon a space-lattice, and holds good however the axes and standard plane have been chosen. The true space-lattice cannot be found from the external form alone, and the crystallographer has been guided in his choice of crystal axes by the symmetry of the crystal, and by the criterion that the most suitable axes to take are those which assign the simplest values of  $(hkl)$  to the commonly occurring crystal faces. It will be clear, however, that the law of rational indices must always hold, even if the axes chosen by measuring the external form do not correspond to the edges of a simple cell. They must in any event be parallel to rows of points in the lattice, and the interval between any two points is necessarily divided into equal intercepts by the set of parallel planes to which each crystal face is parallel. The true

space-lattice can be found by X-ray analysis, and in most cases (though by no means always) the axial ratios which have been chosen as the result of observation of the external form are found to be in the proportion of the edges of the cell. It is of course impossible to find the actual length of the edges from external observations.

The indices ( $hkl$ ) which define a crystal face are known as the 'Millerian Indices,' after Miller, who first employed them. A face which is parallel to an axis has a corresponding index zero. It is necessary to distinguish between positive and negative intercepts, the latter being denoted by a bar placed above the index. For instance, the indices ( $hkl$ ), ( $\bar{h}\bar{k}\bar{l}$ ) denote two parallel faces on opposite sides of the crystal.

The naming of faces may be illustrated by the forms of a cubic crystal, shown in fig. 7. In the cubic system the three

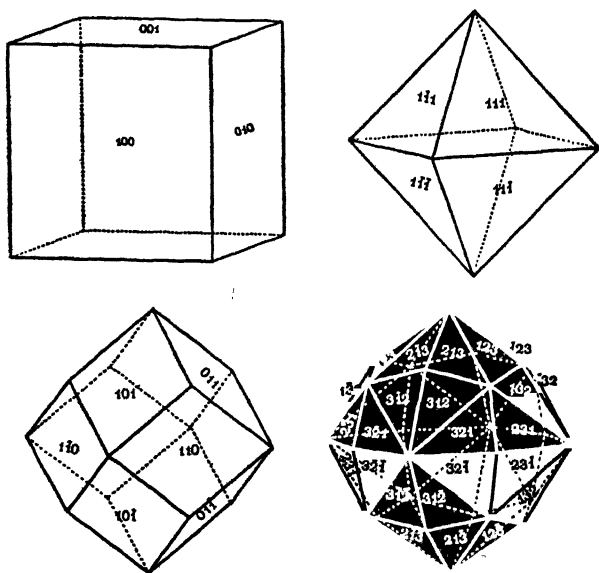


FIG. 7.—The assigning of indices to the faces of a cubic crystal  
(From *Crystallography*, A. E. H. Tutton; Macmillan, 1922)

axes are equal and at right angles to each other, and the method of assigning indices can be readily followed. A complete set of crystal faces which are identical in type is known as a crystal 'form,' and the form is denoted by a set of indices in curly brackets  $\{hkl\}$ , which implies the appropriate permutations.

## CRYSTAL ZONES

The points of a lattice can be arranged in rows. A line joining any two points passes, when produced, through a row of equally spaced points. The direction of such a row is called a 'zone axis' of the crystal. If a point at the origin is joined to another point whose co-ordinates are  $ua, vb, wc$ , the direction will be that of the zone axis  $[uvw]$ , which is denoted by three indices in square brackets to distinguish it from a crystal face.

Just as simple indices can be assigned to the faces of a crystal, so groups of these faces can be selected which are parallel to a common zone axis with simple indices. Such a group of faces is called a 'zone.' A plane can be pictured as passing through a row of points and rotating about this as an axis. Whenever it passes through any other point of the lattice it becomes a net-plane with a sheet of points lying on it. Any densely packed zone axis of the crystal will thus be parallel to a number of important planes which form a zone.

The indices ( $hkl$ ) of a face which is common to the zones  $[uvw]$  and  $[u'v'w']$  are given by the rule

$$h = vw' - v'w, \quad k = wu' - w'u, \quad l = uv' - u'v.$$

## CRYSTAL SYMMETRY

An example has been given above (fig. 7) of several forms of a cubic crystal, and an actual crystal may assume combinations of these or of many other forms. It may appear at first sight strange that all these forms should be classed together as 'cubic.' The name given to the system, though sanctioned by custom, is misleading, and the system is sometimes more appropriately called 'regular.' The reason for grouping these various forms together in a crystal class is that they all show symmetry of the same type.

The symmetry of a body, as, for example, a cube, consists in the geometrical property that it can be brought into self-coincidence by certain symmetry operations, the completed operation making no apparent change. The cube can be reflected, for instance, across a symmetry plane through its centre, which is parallel to a cube face; the original cube and its reflection are identical. Other symmetry planes pass through opposite pairs of edges. An axis through the centre and parallel to an edge is



a fourfold symmetry axis ; after a quarter turn about it in either direction the new position is indistinguishable from the old. Similarly each cube diagonal is a threefold axis of symmetry, and each line joining the centres of opposite edges is a twofold axis of symmetry. The centre of the cube is a symmetry centre or centre of inversion, being midway between pairs of corresponding points of the cube.

These elements of symmetry characteristic of the cube are shown in fig. 8. At the same time, the diagram shows that they

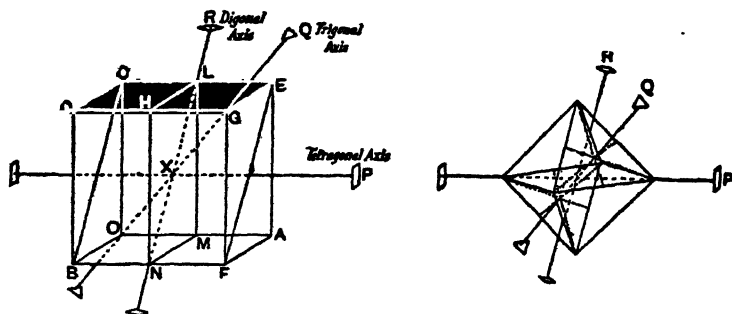


FIG. 8.—Identical symmetry elements of the cube and the octohedron

are also possessed by the octahedron, and indeed by any crystal of this cubic class provided that it is bounded by a regularly developed system of faces. The symmetry is characteristic of the crystalline structure itself, and any manifestation of that structure, including the growth of faces, will reveal it. All crystal properties, such as refractive index, hardness, conductivity, and so forth, are governed by the same symmetry scheme.

The full account of crystal symmetry is postponed to a later chapter, because it will be easier to illustrate its principles when some simple crystal structures have been described which can be used as examples. It will then appear that crystals can be classified according to the nature of their symmetry into seven systems, of which the cubic is one ; the others are the hexagonal, rhombohedral, tetragonal, orthorhombic, monoclinic, and anorthic systems. It is a fundamental point that these seven classes are comprehensive of all possible modes of symmetry. The number of modes is not infinite, but limited, and it will be one of the principal features of the discussion to show how this limitation arises.

## EXTERNAL FORM AND INTERNAL STRUCTURE

In the past, the study of external crystalline form has been of the greatest importance, because it has been the principal means of identification and classification. The goniometer has occupied the foremost place amongst crystallographic apparatus. It has been natural, therefore, to devote great attention to the symmetry of crystals as revealed by their external form.

The fundamental property of the crystal, however, is its atomic pattern, and the external form is only one result of this pattern—a relatively unimportant feature which depends in a complex way on external factors. Further, though a study of symmetry is essential in analysing the atomic arrangement, the symmetry itself has no very close connection with the most important features of that arrangement. Crystals which are closely related in their atomic grouping and bonding may differ widely in the nature of their symmetry.

Owing to the new methods of crystal analysis the centre of interest has changed. The new methods probe deeply into the crystal structure, telling us how the atoms are arranged, and throwing light on the nature of the molecule and the relation between structure and physical properties. If they had been available at the outset, it is probable that the study of external crystal form would have received comparatively little attention. Historically, this study has been of vital importance, as one of the few indications of the underlying structure. The analysis of crystal symmetry was inspired by it, and all the formal apparatus was prepared long before it could be fully applied to actual atomic arrangements. Our views are still coloured by this historical development.

The new view-point should now be adopted. The right basis for commencing the study of crystal structure is the conception of a pattern based upon a space-lattice, and it will only occasionally be necessary to consider the external crystalline form in our treatment.

## CHAPTER II

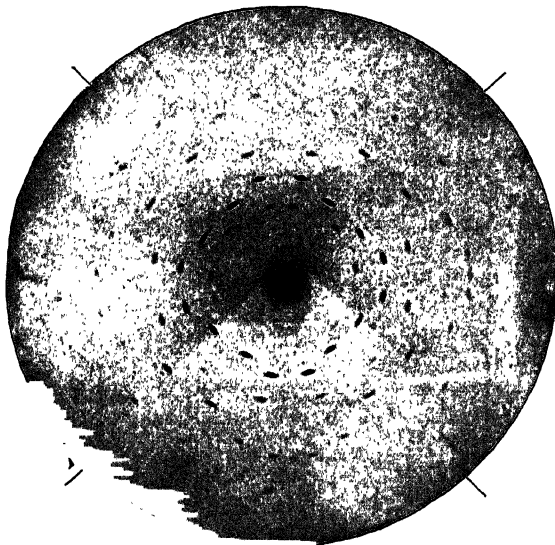
### DIFFRACTION BY THE CRYSTAL LATTICE

THE famous experiment which led to the development of X-ray crystallography was suggested by M. v. Laue in 1912, and carried out by Friedrich and Knipping in the University of Munich. It was designed to test the wave nature of X-rays. Previous attempts to obtain diffraction effects with X-rays having proved inconclusive, Laue had the inspiration to use a crystal as diffraction grating. A narrow beam of X-rays was passed through a crystal and fell upon a photographic plate. The plate when developed showed a pattern of spots around the intense central spot due to the undeviated beam. Using a section of zincblende, a crystal with cubic symmetry, Laue was able to show that the positions of these spots were consistent with diffraction of very short waves by a cubic arrangement of scattering atoms or molecules in the crystal. The wave-lengths of the diffracted X-ray beams which made the spots could be estimated, and proved to be of the expected order many thousand times smaller than wave-lengths in the visible region. It was clear that X-rays could be diffracted like light waves.

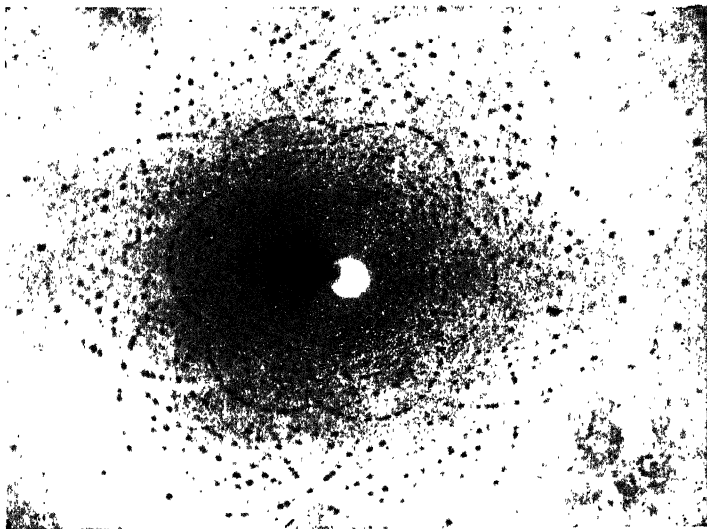
Examples of 'Laue photographs' are given in fig. 9, Pl. I. The symmetry of the pattern corresponds to that of the crystal structure, showing that diffraction is taking place in the body of the crystal.

The Laue photograph has continued to be one of the important methods of crystal analysis, but it is not the most simple in principle, for, as we shall see, it depends upon the presence of a band of 'white' X-radiation containing all wave-lengths within a certain range. It is simpler to consider in the first place the effect of the crystal upon a beam of monochromatic X-rays, such as is used in most methods of investigation. The complete study of this effect is a very complex matter, and has in fact opened up a fascinating new branch of physical optics. Its

PLATE I



A. Zinoblende,  $\text{ZnS}$ . Incident radiation parallel to  $[100]$   
 (*Kristalle und Röntgenstrahlen*, P. P. Ewald; Julius Springer)



B. Beryl,  $\text{Be}_3\text{Al}_2\text{Si}_6\text{O}_{18}$  (Wm. Lehmann). Incident radiation  
 parallel to  $c$  axis

FIG. 9.—Examples of Laue photographs



main principles, however, can be illustrated by the analysis of crystals of simple form.

### REFLECTION BY THE PLANES OF THE CRYSTAL LATTICE

Diffraction effects are produced when a monochromatic beam of X-rays passes through the regular pattern of atoms constituting the crystal. Each atom scatters a minute fraction of the incident wave-train as a train of secondary waves. We wish to find what conditions must be satisfied in order that the scattered waves may reinforce each other so as to build up a strongly diffracted beam.

In the first place, each complex unit of the crystal pattern can be replaced for the present calculation by a representative point at which we suppose the scattering to take place. When light is diffracted by a line grating, the positions of the spectra depend only upon the grating constant, or interval at which the lines repeat. Similarly the conditions for diffraction by the crystal depend only upon the intervals at which the pattern repeats in three dimensions, and the crystal pattern can therefore be considered as a set of scattering points arranged upon a *space-lattice*. The nature of the unit of pattern is highly important, for it determines the relative intensities of the diffracted beams; but for the present we are only concerned with the directions in which diffracted beams are built up.

A train of monochromatic waves sweeps through a set of scattering particles arranged in a space-lattice. In order that the scattered waves may reinforce each other they must be in phase. However this requirement is expressed, it must involve the satisfying of three conditions. For instance, it is necessary and sufficient that the wave scattered at the point O in fig. 4 be in phase with that scattered by the points A, B, and C. The waves scattered by these points will then be in phase with their next neighbours, and so on throughout the crystal.

Two of these conditions can be satisfied by a rule which can be stated very simply. In every case of X-ray diffraction the diffracted waves appear as a *reflection of the incident waves in one or other of the sets of crystal planes*. As the incident waves pass over a set of points in a lattice-plane (fig. 10), the secondary wavelets build up a reflected wave according to the well-known Huygens construction. The transmitted wave passes on, with the

loss of a small portion of its energy, which has been converted into that of the reflected wave. This relation of reflected to incident wave ensures that the waves scattered by all points in

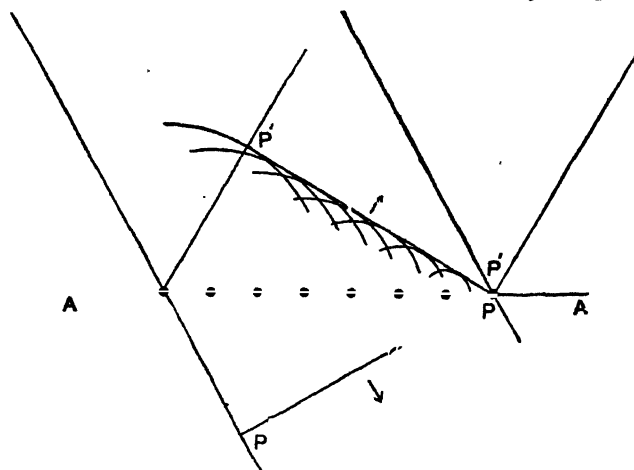


FIG. 10.—The reflection of a wave-front by points lying on a plane

two directions in space, over the lattice-plane, are in phase with each other.

In general, the waves reflected by successive lattice-planes

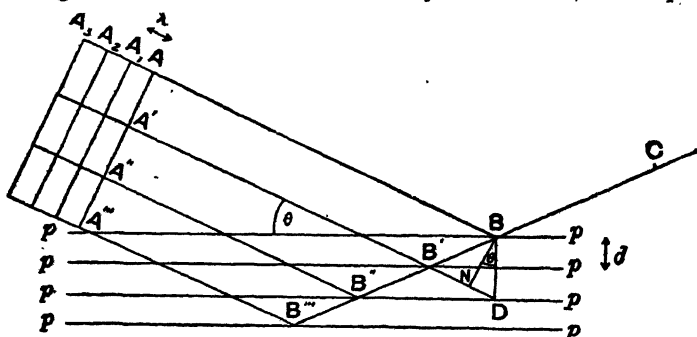


FIG. 11.—The reflection of a wave-train by successive lattice-planes

will not be in phase; but this further condition can be satisfied by adjusting the angle of incidence of the beam upon the crystal planes. Waves falling upon a series of planes are shown in fig. 11, the sheets being represented by the horizontal lines. Those reflected from the upper sheet have a shorter optical path than those reflected from the lower sheet. The difference of

path is that between A'B'C and ABC, which is equivalent to ND, since B'B=B'D. If the planes are spaced a distance  $d$  apart, and the glancing angle is equal to  $\theta$ ,  $ND=2d \sin \theta$ . For reinforcement the path difference must be a whole number of wave-lengths, hence the condition for a diffracted beam is

$$n\lambda = 2d \sin \theta.$$

When this condition is satisfied, the scattered waves from all points throughout the lattice will reinforce each other, and a strong beam will be diffracted. At other angles of incidence destructive interference will make the beam vanishingly small.

This way of regarding the conditions for diffraction is convenient, and the diffracted beams are often termed 'reflections' of the X-rays in the corresponding crystal planes. By putting  $n=1, 2, 3$  we obtain a series of angles at which reflections of the first, second, and higher orders take place. Fig. 12, for instance, shows the effect of 'reflecting' a beam of monochromatic X-rays from the cleavage plane of a crystal of  $\beta$ -corundum. In this crystal the spacing  $d$  of the cleavage planes is large compared with the wave-length  $\lambda$  of the radiation, so that a large number of orders can be observed. The crystal is turned so that the glancing angle varies from one to thirty-six degrees. Values of  $\theta$  are plotted as abscissæ, and the strength of the reflected beam (measured by an ionisation chamber) is plotted as ordinate. It will be seen that the reflections flash out whenever  $\theta$  assumes a value given by the above equation, nineteen orders having been measured in this case.

The difference between optical diffraction by the line grating or cross grating and diffraction by the three-dimensional crystal grating must be noted. In the former case, a series of spectra is formed whatever the direction of the incident light. In the latter case, the 'spectra' flash out one by one as the crystal is turned into the appropriate position for each. Many sets of planes can of course reflect the X-rays in several orders, but the total number of possible reflections of all kinds is limited. The equation  $n\lambda = 2d \sin \theta$  cannot be satisfied by any value of  $\theta$  if  $n\lambda$  is greater than  $2d$ . Hence, for a given wave-length and lattice there is a definite number of possible reflections or 'spectra,' since the more complicated ways of arranging the lattice-points on planes lead to too small a value of  $d$  for even a first-order reflection.



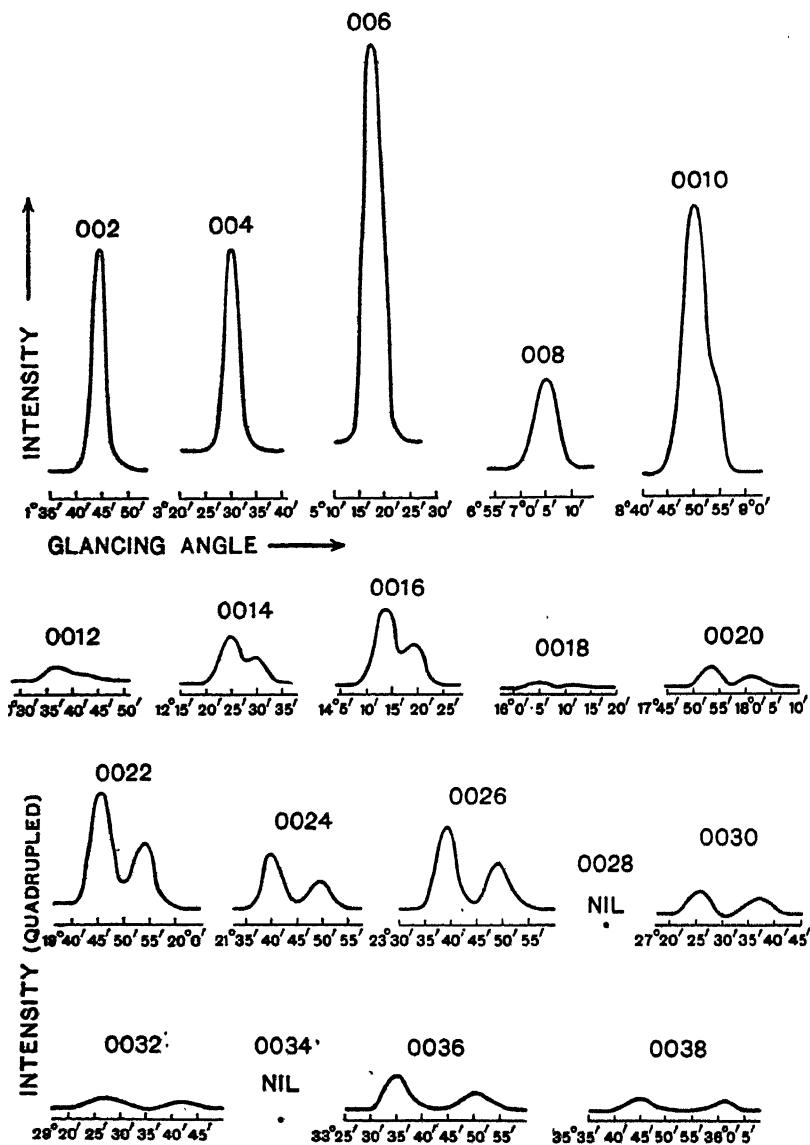


FIG. 12.—Reflections by the basal plane of  $\beta\text{-Al}_2\text{O}_3$ . The  $K\alpha$  line of rhodium used in this case is actually a doublet, and a progressive resolution of the  $\alpha_1$  and  $\alpha_2$  components is evident in the higher orders.

## DIFFRACTION BY THE THREE-DIMENSIONAL GRATING

The above treatment of the diffraction as a reflection in the crystal planes has been given first because it is simple to grasp. The problem was originally solved in a more general way by Laue, and the following description is based on his treatment.

When light falls upon a line grating, the spectra of different orders are built up in the manner shown in fig. 13. Wavelets spread from all lines of the grating, represented in the figure as apertures through which the light can pass. The wavelets

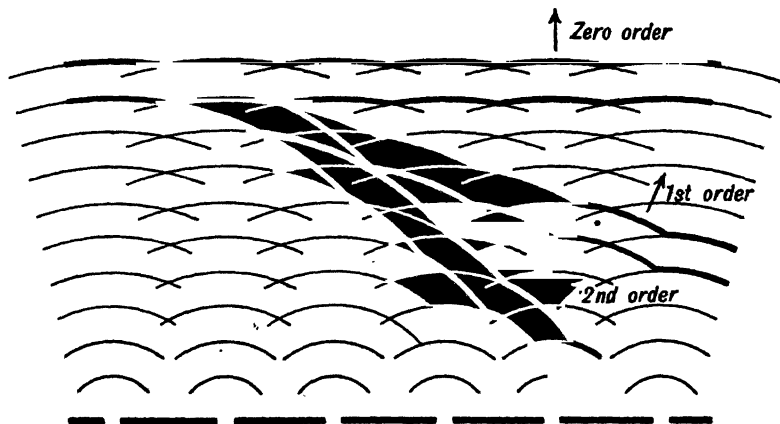


FIG. 13.—Formation of spectra by line grating

combine to build up plane wave-fronts, in directions which give spectra of the zero, first, and higher orders as shown in the figure. The wave-front of the first order is outlined by linking up wavelets such that the path difference, for waves going through successive lines of the grating, is one wave-length; for the second order it is two wave-lengths, and so on for higher orders. In the figure the incident waves fall normally on the grating, but the condition remains the same for any angle of incidence. Let the incident beam make an angle  $\psi_0$  with the grating, whose spacing is  $a$ , and let the diffracted beam make an angle  $\psi$ . The path difference is then  $a(\cos \psi - \cos \psi_0)$  or  $a(a - a_0)$ , where  $a$ ,  $a_0$  are equal to  $\cos \psi$ ,  $\cos \psi_0$  (fig. 14). The positions of the spectra are given by the condition

$$a(a - a_0) = n\lambda,$$

where  $n$  is an integer.

When the diffraction is produced by a three-dimensional

grating three such conditions must be satisfied. Let the three axes have lengths  $a, b, c$ , the cosines of the angles between them and the incident ray-direction be  $\alpha_0, \beta_0, \gamma_0$ , and the corresponding cosines for the diffracted ray  $\alpha, \beta, \gamma$ . The conditions for diffraction are

$$\begin{aligned} a(\alpha - \alpha_0) &= h\lambda, \\ b(\beta - \beta_0) &= k\lambda, \\ c(\gamma - \gamma_0) &= l\lambda. \end{aligned}$$

These are the Laue equations. The triple set of integers  $hkl$

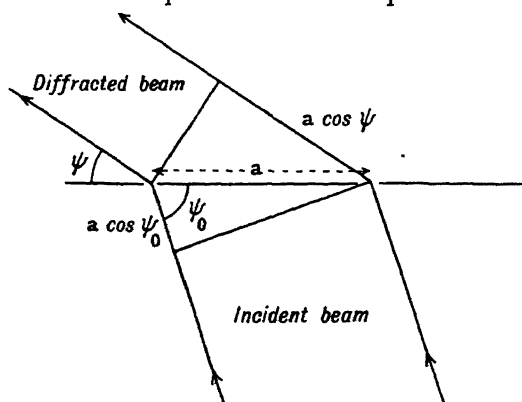


FIG. 14.—Relation between directions of incident and diffracted beams

denotes the order of the spectrum, just as  $n$  denotes its order for the simple grating. Every spectrum formed by the crystal must be labelled by three indices in this way.

It is not difficult to see that this condition is equivalent to the condition for reflection. The three axes of the lattice  $a, b, c$  are shown in fig. 15. By definition the directions of incident and diffracted rays are such that waves scattered by A, B, C are  $h, k, l$  wave-lengths ahead respectively of the wave scattered by O. Let  $OA' = a/h$ ,  $OB' = b/k$ ,  $OC' = c/l$ . Then the waves scattered by A'B'C' are each one wave-length ahead of the wave scattered by O, and consequently are in phase with each other. This is equivalent to saying that the diffracted ray appears to be the *reflection* of the incident ray in the plane A'B'C', since the equality in optical path for points distributed over the plane is the condition for reflection. As we have seen above, the plane A'B'C' is parallel to a set of planes on which points of the lattice lie.

We can see also that the diffracted ray defined by the Laue equations obeys the law  $n\lambda = 2d \sin \theta$ , and at the same time

realise an important distinction between the indices  $hkl$  which define a *reflection*, and the indices which define a *crystal face* or a set of *planes of the lattice*, which to avoid confusion will be called  $h'k'l'$ . A reference to fig. 5 will make it clear that the latter indices never have a common factor. Suppose, for instance, that they were all even so that they could be written  $2h''$ ,  $2k''$ ,  $2l''$ . The successive planes of the lattice would then divide OA, OB, and OC into  $2h''$ ,  $2k''$ , and  $2l''$  parts respectively. We could

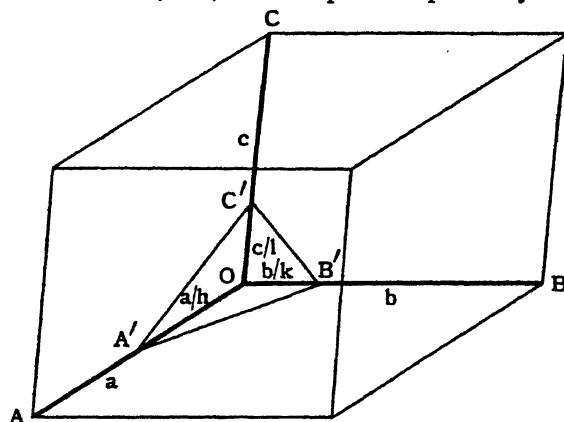


FIG. 15.—Equivalence of 'Laue' and 'reflection' conditions

now omit every alternate plane and still have O, A, B, and C, and so every point of the lattice, lying on planes. The possible planes of the lattice are described, therefore, by combinations of  $h'k'l'$ , which have no common factor. The same is true for indices of a crystal face, since they only describe its orientation. However, the indices  $hkl$  which define the number of wave-lengths in the path difference for waves scattered at O on the one hand, and at A, B, C on the other hand, may have a common factor.

Suppose we are considering the  $n$ th order of reflection by the lattice-planes ( $h'k'l'$ ). The path difference for waves reflected at successive planes is  $n$  wave-lengths. There are  $h'$  planes between O and A, hence the waves scattered by A will be  $nh'$  wave-lengths ahead of waves scattered by O. The same holds for B and C. The Laue indices  $hkl$  are related to the indices of the reflecting planes by the equations

$$\begin{aligned} h &= nh', \\ k &= nk', \\ l &= nl'. \end{aligned}$$

To put this in another way, the set of indices  $hkl$  completely describes a beam by defining both the reflecting plane and the order of reflection. In conformity with this method of description, the first order from (111) planes of the lattice is termed 111, the second order 222, the third order 333, and so forth. This convention is now generally adopted.

It has become customary to use the same letters  $h$ ,  $k$ ,  $l$  for defining both crystal faces and reflections. To avoid confusion, the indices of a face will be put in brackets ( $hkl$ ) as in descriptive crystallography, and the indices of a reflection will be given as  $hkl$  without brackets.

#### INFLUENCE OF THE UNIT OF PATTERN

So far the diffraction has been discussed as if it were caused by a set of particles placed at the lattice-points. Actually a more or less complex pattern of atoms is grouped around each lattice-point. What will its influence be?

The pattern unit has no effect on the *positions* of the diffracted beams. These depend entirely on the space-lattice, just as the positions of optical spectra depend only on the grating constant. The configuration of the unit has, however, an important effect upon the *intensities* of the different spectra. The waves scattered by different parts of one unit may reinforce each other strongly for one set of values  $hkl$ , and interfere destructively for another set. The whole diffracted beam will be strong in the first case and weak in the second. It is, in fact, by studying the relative intensities of the spectra that we deduce the form of the unit of pattern. This will be gone into more fully later, for it is the most important and difficult step in the analysis of crystal structure by X-rays. The effect of a complex unit of pattern may be seen in fig. 12, where the series of reflections from the basal cleavage plane of  $\beta$ -corundum,  $\text{Al}_2\text{O}_3$ , vary greatly in intensity. A similar effect is well known in the case of the optical grating. Each grating gives its own characteristic set of orders, some being weak and some strong according to the way in which the diamond has ruled the lines.

#### SUMMARY

The diffraction of monochromatic X-rays by a crystal is analogous to the diffraction of monochromatic light by an optical grating. The condition which determines the position of the

$n$ th-order spectrum from the line grating is that the path difference for waves coming from successive lines of the grating should be  $n$  wave-lengths. The crystal is a three-dimensional grating, since its pattern is repeated in three directions in space. Hence, what we term the  $n$ th-order spectrum in the case of a grating becomes the order  $hkl$  in the case of the crystal. The path differences for waves scattered by successive units of pattern (in the three directions which have been chosen as crystal axes) are  $h, k, l$  wave-lengths.

A line grating gives several spectra simultaneously for any direction of the incident beam. A crystal grating, on the other hand, can only give one spectrum at a time, and a condition must be satisfied for this to appear. If the diffracted beam is represented as the reflection of the incident radiation in a set of crystal planes with spacing  $d$ , we may express this condition by stating that the angle of incidence  $\theta$  must satisfy the relation  $n\lambda = 2d \sin \theta$ . The diffracted beams flash out one by one as the orientation of the crystal with respect to the incident beam is altered.

This rule gives the directions in which the scattered waves build up a diffracted beam. The intensity of the beam is determined by the form of the crystal pattern-unit, just as the relative strengths of the orders given by an optical grating depend upon the form of the line.

## CHAPTER III

### EXPERIMENTAL METHODS OF CRYSTAL ANALYSIS

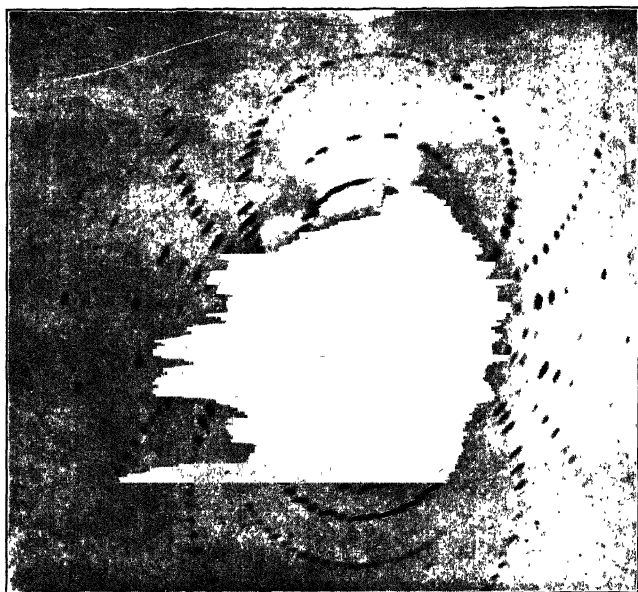
THE radiation from the anticathode of an X-ray tube consists of a continuous range of wave-lengths termed the 'white' radiation, and of components of definite wave-length characteristic of the element forming the anticathode. The white radiation is used in the Laue method; with this exception, methods of analysis depend upon the use of one of the characteristic 'monochromatic' lines in the X-ray spectrum. An account of the production and properties of X-rays is given in an appendix to this volume. The wave-length used in analysis is almost invariably the  $K\alpha$  line, which is the strongest member of the K group or radiation of highest frequency characteristic of each element. The  $K\alpha$  line is actually a close doublet, but for most purposes the two components can be considered as a single line. A suitable wave-length is obtained by choosing the appropriate element for the anticathode, for the wave-length diminishes with increasing atomic number. The most frequently used anticathodes are of molybdenum ( $K\alpha_1 = 0.7120$  A.,  $K\alpha_2 = 0.7076$  A.) and of copper ( $K\alpha_1 = 1.5412$  A.,  $K\alpha_2 = 1.5374$  A.). The choice of wave-length is restricted by the necessity of using a metal which forms a suitable anticathode, for this must have a high melting-point and conduct away the heat generated by the discharge. Chromium, iron, cobalt, nickel, and copper fulfil these conditions in the region of larger wave-length, and molybdenum, rhodium, palladium, and silver at the short-wave end.

It is impossible to excite the  $K\alpha$  lines alone, since the whole group appears when the applied potential is sufficiently high. The  $K\beta$  line, which might otherwise confuse the measurements, can be greatly reduced by using a suitable absorbing screen, which cuts off  $K\beta$  almost entirely, while allowing the  $K\alpha$  radiation to pass with relatively little diminution in intensity.

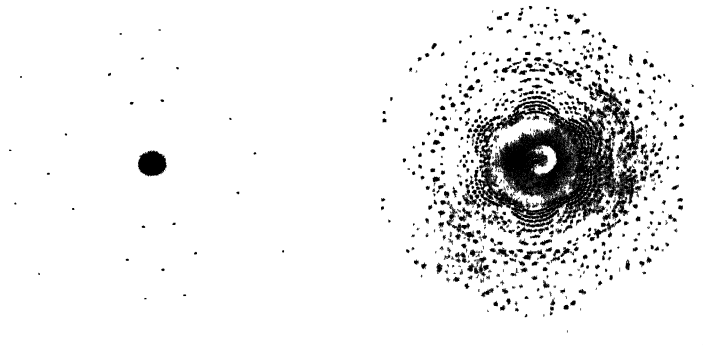




PLATE II



A. Nickel sulphate



B. Iron, incident radiation  
parallel to  $[110]$  (Clark)

C. Kaliophilite, incident radiation  
parallel to  $c$  axis (Bannister)

FIG. 17.—Laue photographs

## THE LAUE PHOTOGRAPH

The Laue method of examining the diffraction of X-rays by a crystal differs from other methods, in that a heterogeneous beam of X-rays is used. The beam falls upon a small crystal, or thin crystal section, and the diffracted beams are recorded on a photographic plate placed at a distance of a few centimetres from the crystal. As an example of the type of apparatus used in this method, an arrangement designed by Müller and made by Adam Hilger is shown in fig. 16, Pl. III, p. 28. The rays are limited to a narrow pencil by the slit system B, the crystal is set at H on a holder which permits adjustment of its orientation, and the photographic plate is placed in the holder D.

A beam with a continuous range of wave-lengths is conveniently obtained by using a bulb with a tungsten anticathode and a tension of about 65,000 volts. This potential is insufficient to excite the characteristic K radiation of tungsten, the presence of which would confuse the record, and the available range of white radiation extends from 0.2 to 1 Å.

It is desirable to screen the directly transmitted beam from the plate, as otherwise a large central area is fogged owing to scattering at the area of impact. The effect of neglecting this precaution is seen in fig. 17A, Pl. II, a photograph of nickel sulphate. A fine photograph of an iron crystal due to Clark is shown in fig. 17B, and one of kaliophilitite in fig. 17C.

In the case of the Laue photograph, the various crystal planes reflect the X-rays as if they constituted a number of mirrors set at different angles. The relation  $n\lambda = 2d \sin \theta$  can be satisfied, although the angle  $\theta$  is fixed for each set of planes, because radiation of the appropriate wave-length can be selected from the continuous range. If the crystal is rotated, the spots change their positions upon the screen, as if they were the reflections of a narrow beam of light by the facets of a cut-glass stopper.

A feature of the Laue photograph, which is very well shown by fig. 17A, is the arrangement of the spots on ellipses which have one end of their major axis at the central spot. The same feature is shown more or less distinctly by all Laue photographs, the spots occurring where the ellipses intersect. All the spots which lie on any one ellipse are due to reflections by planes parallel to a common zone axis, as will be clear from the construction in fig. 18. Incident rays fall upon a crystal at C, which has a zone

axis parallel to  $ZZ'$ , and we consider rays which are reflected by a plane of the corresponding zone. Suppose a reflecting plane to be rotated about  $ZZ'$ ; the reflected beam will trace out a curve  $EE'$  on the plate. If the incident rays make an angle  $\theta$  with the zone axis, the reflected rays will always make the same angle with it, so that they lie on a cone of semivertical angle  $\theta$

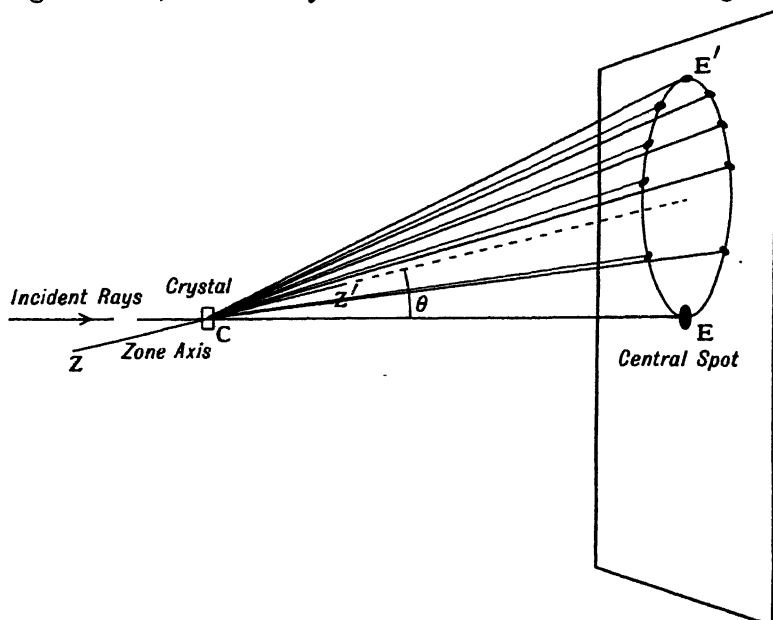


FIG. 18.—The production of a series of spots arranged on an ellipse in a Laue photograph, by reflection at the planes around a crystal zone

around the zone axis. The ellipses in the Laue photograph are the intersections of such cones with the photographic plate. Each spot is at an intersection of ellipses, since a plane parallel to two zone axes is a crystal plane and can reflect the X-ray beam.

A simple model can be made which explains the form of the Laue photograph in a graphic way. If a cylindrical rod of brightly polished metal is placed in an inclined position in a narrow beam of light from a lantern, its surface will reflect radiation so as to trace out the complete curve  $EE'$  in fig. 18, because it represents all orientations of a plane around the axis of the cylinder or zone axis. A group of such rods arranged as in fig. 19 will trace out a pattern like that of rock-salt, the spots



is the point *Z* where the zone axis meets the plate. It is then a simple matter to recognise the zones and to index each point as due to reflection by a plane common to two zones. The requisite formula is given in Chapter I, p. 9. This method is known as the stereographic projection, and some examples are given in the next chapter.

A more convenient projection (the gnomonic projection) is illustrated by the same figure. The point *R* is represented in a

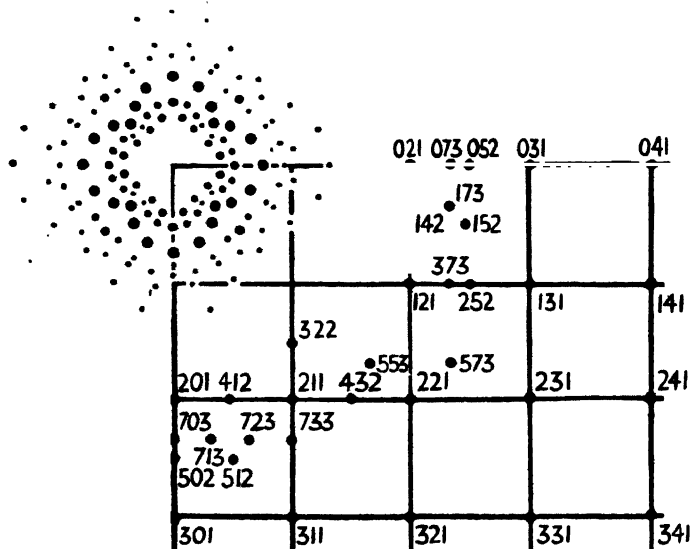


FIG. 21.—The application of the gnomonic projection to a Laue photograph of NaCl (Schiebold)

diagram by the point *G*, where the normal *OG* to the reflecting plane meets the plate. The normals to all planes around a zone lie in a plane at right angles to the zone axis, and this plane cuts the photographic plate in a straight line. Hence the spots of an ellipse transform into points lying on a line, and any such line can be correlated with the corresponding zone axis. The projection can be rapidly made with the aid of a ruler, which is pivoted about *N* and has an *R* scale at the one end and a scale of corresponding *G* positions at the other for a standard distance *ON*.

Fig. 21, due to Schiebold, shows the application of the gnomonic projection to a crystal of NaCl. The pattern of Laue spots is reproduced in the upper left-hand corner, and the corresponding indices are given in the projection.

When a Laue photograph is taken with the rays parallel to an important axis of the crystal, such as the photograph of beryl in fig. 9, it will be noticed that a circular area in the centre is free of spots. We may picture any set of successive planes of the lattice as pivoted about the lattice-points along the axis. As their inclination to the axis is made smaller, both  $d$  and  $\theta$  decrease in the equation  $\lambda = 2d \sin \theta$ , until a point is reached where  $\lambda$  is less than the short-wave limit of the continuous spectrum; reflection is then impossible. A rough estimate of the spacing of the points can thus be directly made, since the short-wave limit is approximately known. The effect is strikingly shown in the photograph of kaliophilite (fig. 17c, Pl. II, p. 23).

The deduction of the crystal structure from the appearance of the Laue photograph is a complicated process, because the intensities of the spots do not depend upon the structure alone. They depend also upon the strength of the components in the continuous range of the original beam to which they are respectively due, and each spot may be composed of several orders superimposed. They are also influenced by the different blackening effect of radiation of different wave-length, and complications arise here owing to the absorption of the X-rays by the silver and bromine in the photographic plate. In spite of these difficulties, the Laue photograph can be made a sound method of analysis, and has, for instance, been used with striking success by Wyckoff. Advantageous features are the ease and certainty with which indices can be assigned to the spots, and the wealth of information represented by a single photograph. Nevertheless, the methods which employ monochromatic radiations are more direct and powerful.

### THE IONISATION SPECTROMETER

The ionisation spectrometer was originally designed to measure singly the reflections of a monochromatic X-ray beam by different sets of planes within the crystal, according to the law  $n\lambda = 2d \sin \theta$ . The spectrometer shown in fig. 22, Pl. III, p. 28, is of historical interest, because the first determination of X-ray wave-length and the original crystal analyses were made with it.

A narrow pencil of X-rays is defined by a slit system, and falls upon a crystal. In the earliest experiments a natural or artificial crystal face was used, which was parallel to a set of

lattice-planes ; but it was also found convenient to reflect the rays by the interior planes of a thin crystal section through which the rays passed, or to bathe a small crystal in the radiation. The crystal is mounted on a rotating table, whose orientation can be read by a scale and vernier as in an optical spectrometer. The reflected radiation passes through a further slit into an ionisation chamber, where it is measured. In order to increase the effect in the ionisation chamber it may be filled with a heavy gas such as methyl bromide ; a chamber 15 cm. in length containing this gas at N.T.P. absorbs 80 per cent. of a beam of molybdenum  $K\alpha$  radiation. The outer wall of the ionisation chamber is insulated and connected to a steady source of high potential of several hundred volts. An inner electrode, which must be out of the path of the beam entering the chamber, serves to collect the ions. It is connected to an electrometer, and the ionisation in a given time is measured. The ionisation chamber revolves about the same axis as the crystal table, so that the direction of the reflected beam can be measured on the circular scale. The slits limiting the incident beam, the crystal, and the chamber correspond to the collimator, grating, and telescope of a spectrometer.

The orders of reflection due to a given crystal plane, set so that it is parallel to the axis of the instrument, are measured individually. One method is to set the crystal at a series of angles differing by a few minutes of arc or less, and to measure the amount of radiation reflected at each setting (fig. 23). Another

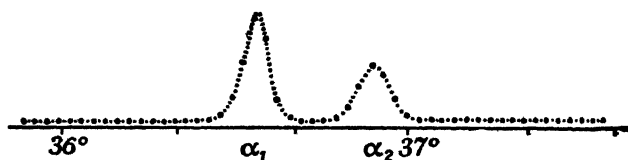


FIG. 23.— $K\alpha_1$  and  $K\alpha_2$  of rhodium in diamond, 444

method consists in setting the chamber with wide slits so as to receive the reflected beam, and turning the crystal through the angle of reflection at a constant angular speed. In the latter case an integrated amount of reflected radiation is measured, as in the ballistic throw of a galvanometer.

The spectrometer method has certain advantages and disadvantages as compared with other methods. Amongst the former must be reckoned the accuracy with which the position

# PLATE III

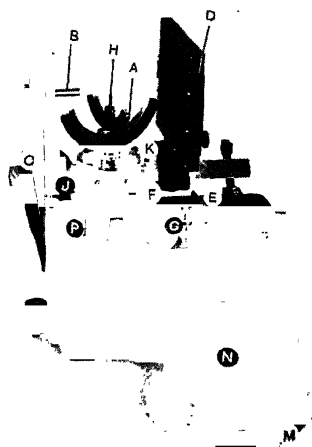


FIG. 16.—Müller X-ray spectrograph, as set up for the Laue and for the rotating crystal methods

B, Slit system. D, Photographic plate. H, Crystal.  
N, Cylindrical camera

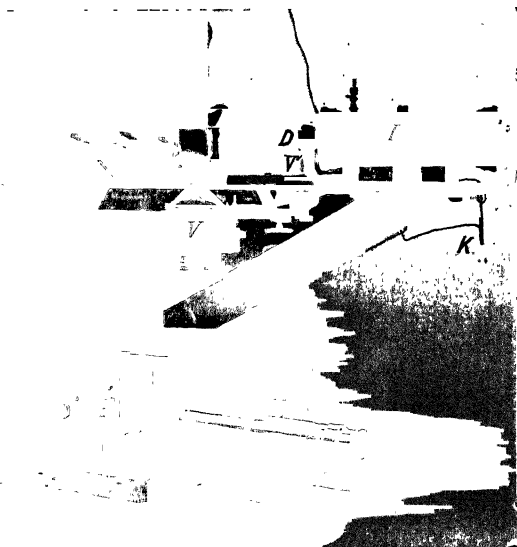


FIG. 22.—The original form of the X-ray spectrometer

LLL, Lead box. V, Vernier of crystal table. A, B, D, Slits. V', Vernier of ionisation chamber. C, Crystal. K, Earthing key. I, Ionisation chamber. E, Electroscope.  
M, Microscope





of the crystal, as well as the direction of the diffracted beam, is known. This makes it a reliable method of assigning the correct indices to reflections. Its greatest advantage, however, is its adaptability to *quantitative measurement*. Photographic methods can be made to give fair estimates of relative intensity when suitable precautions are taken, but the ionisation method is much more accurate.

The instrument has been used to make *absolute measurements*

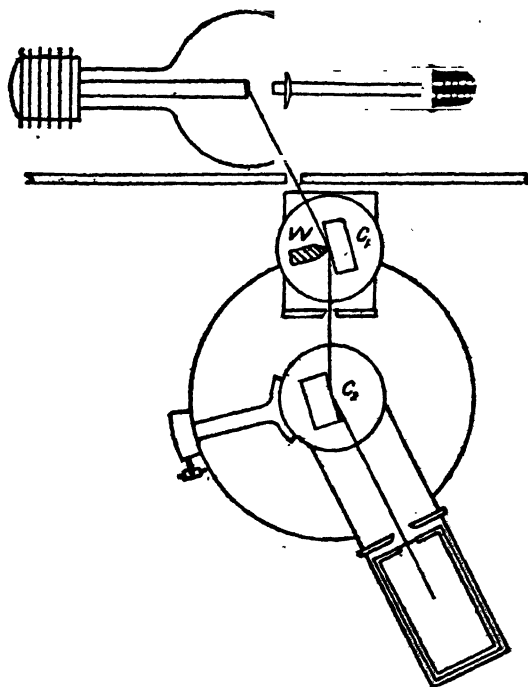


FIG. 24.—The arrangement of the spectrometer for an absolute measurement of intensity of reflection

of efficiency of reflection. An absolute measurement is a comparison of the diffracted beam with the incident radiation, a ratio which has an important theoretical significance. Such measurements are not only useful in the analysis of complex crystals, but also in other important subjects of research, such as the thermal movements of the atoms of the structure, and even the structure of the atom itself. The measurements have no significance unless the primary beam of rays is monochromatic.

Consequently, the X-rays are twice reflected, first by a crystal  $C_1$ , which separates a monochromatic beam from the general radiation, and then by the crystal under investigation. The ionisation chamber can be set so as to measure the intensity of the monochromatic beam incident upon  $C_2$ , and then moved round so as to receive the reflected beam as shown in fig. 24. The first measurements of this type were made by A. H. Compton.

It is a disadvantage of the instrument that spectra must be examined one at a time. A photographic method, on the other hand, gives a simultaneous survey of all the reflections which take place within the limits set by the geometrical conditions. The spectrometer method is laborious, and in crystal analysis is most conveniently reserved for such points of structure as have proved too difficult for the photographic methods. It is a siege battery to be brought into action when the lighter artillery fails.

### THE ROTATION PHOTOGRAPH

In this method, which Schiebold and Polanyi were the first to develop, a fragment of crystal is placed in a narrow beam of monochromatic radiation, and is turned around an axis perpendicular to the beam while the exposure is taking place. It is either rotated completely, or moved backwards and forwards throughout a limited arc. The diffracted beams are recorded photographically upon a plate or upon a film bent into a cylinder around the axis of rotation. The apparatus shown in fig. 16 can be used for both Laue and rotation photographs, the crystal being rotated in the latter case by a clockwork mechanism contained in the metal box. The flat plate which is shown mounted in the figure can be replaced by the cylindrical camera in the foreground. Though this method requires single crystals, which should be as perfect as possible, extremely small crystals suffice. The best results are obtained with crystals whose dimensions in each direction are only a fraction of a millimetre, so that they are completely bathed by the incident radiation. The diffracted rays then give small distinct spots on the plate or film. As the crystal revolves, one plane after another is brought into such a position that it reflects the radiation. The plate when developed shows a number of spots due to various planes which have passed through the requisite positions. Specimen photographs are shown in fig. 25, Pl. IV.

PLATE IV

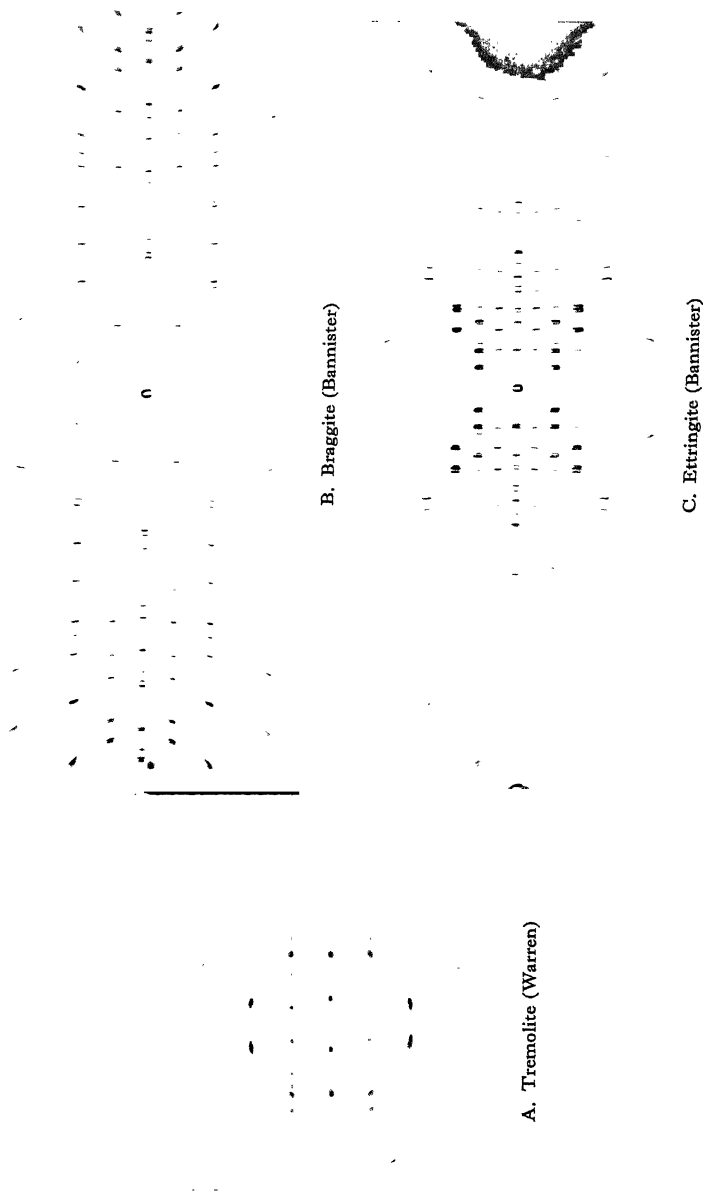


FIG. 25.—Rotation photographs



The geometrical interpretation of rotation photographs is more complex than that of Laue photographs or of the powder photographs, which will be described below. The orientation of the crystal, which is different for each spot, is unknown. At best, we only know that it lies within a certain range when the crystal has been turned through a limited arc. One feature of the photographs is, however, very striking, and has a simple explanation. This is the arrangement of the spots in layers when an important zone axis of the crystal is parallel to the axis of rotation. In fig. 26, PO represents the distance between successive lattice-points along the zone axis, about which the crystal is rotated.

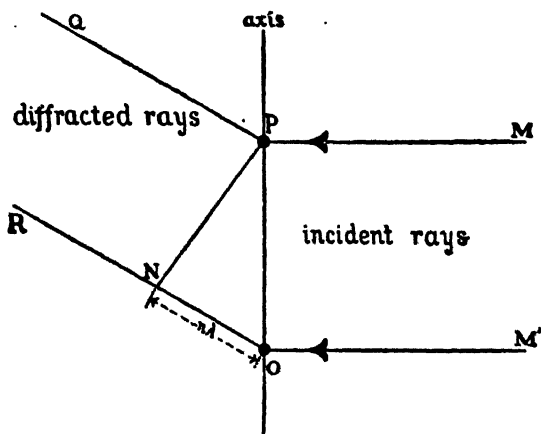


FIG. 26.—The production of 'layer lines' in the rotation photograph

The incident rays are at right angles to this axis. For diffraction to take place, it is a necessary condition that the path difference for rays scattered by P and O should differ by a whole number of wave-lengths, so that ON in the figure is equal to  $n\lambda$ . This condition determines the angle which the diffracted rays make with the zone axis. As the crystal is rotated it will pass through a number of positions suitable for diffraction, which have in common a path difference of  $n\lambda$  between O and P. All the corresponding spots lie on a 'layer line,' which will be the  $n$ th above or below the equatorial line in the photograph.

For instance, let us suppose that the crystal is rotated about a vertical  $c$  axis. Planes parallel to the  $c$  axis reflect rays horizontally, and the spots corresponding to reflections  $hko$  form a horizontal row on the plate level with the central spot. This

is the zero layer line. Reflections with indices  $hkl$  are thrown upwards, making an angle  $\phi_1$  with the horizontal given by

$$c \sin \phi_1 = \lambda.$$

Such reflections constitute the first-layer line. In general, reflections with indices  $hkl$  lie on layer line  $l$ . The beams which produce the spots of a given layer line lie on a cone, which cuts the photographic plane in a hyperbola, or gives rise to a level row when a cylindrical film is used (fig. 27). Since the vertical

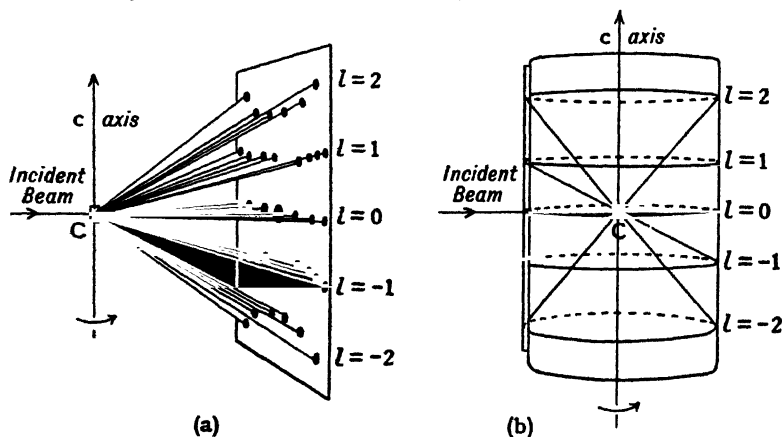


FIG. 27.—Layer lines of a rotation photograph (a) on a plate, (b) on a cylindrical film

spacing of the layer lines depends only upon the distance between lattice-points on the axis about which the crystal is rotated, this distance can be immediately deduced from the photograph. The method thus affords a direct and certain way of measuring the 'identity period' in any chosen direction in the crystal, and so of deducing its space-lattice.

The indexing of the spots involves somewhat intricate geometry, and various graphical methods have been devised for the purpose; they have to be carried out with care in order to avoid errors, and many cases have occurred where incorrect structures have been deduced owing to mistakes in indexing. As an indication of the nature of the transformation, we may note another characteristic of the rotation photographs, the 'row' lines. Let us suppose that a crystal is being rotated about its  $c$  axis as above, and that its  $a$  axis is at right angles to the  $c$  axis. The crystal is rocked backwards and forwards through a small

arc of several degrees on either side of a position such that the  $a$  axis always makes a small angle with the incident beam. The result is a photograph whose appearance suggests that of the spectra given by an optical 'cross-grating,' because the spots are arranged in vertical row lines as well as in horizontal layer lines. The majority of spots are due to reflections by planes parallel to the  $a$  axis, and their indexing is very simple. The spots on the zero layer lines have indices  $010$ ,  $020$ ,  $030$ ,  $040$ ; those on the first layer line  $011$ ,  $021$ ,  $031$ ,  $041$ , etc. The pattern is, in fact, a distorted network of cross-spectra, and a geometrical transformation which converts it into a rectilinear network enables indices to be assigned with ease. A complete rotation causes several of these series of cross-spectra to be superimposed; in fig. 25c the row lines and layer lines are clearly shown.

The method of the rotation photograph is the most useful of all the various methods. A single crystal is a requisite, but extremely small crystals suffice. The usual dimensions are of the order of  $0.1$  mm.<sup>3</sup>, and much smaller crystals weighing  $10^{-6}$  gram can be used. It is almost always possible to obtain a single crystal of these dimensions in the case of any crystallised substance. The space-lattice and space-group are readily deduced. Each photograph gives a wide range of reflections, and a very fair idea of their relative intensities can be obtained. The majority of analyses are carried out by this means.

### THE POWDER PHOTOGRAPH

The methods described above employ a single crystal. The powder method, developed independently by Debye and Scherrer, and by Hull, uses material in which the individual crystals are very small and oriented at random. A narrow beam of monochromatic radiation falls upon the microcrystalline aggregate. Amongst the vast number of small crystals there will always be some which are so oriented that a given reflection  $hkl$  is possible. The crystalline fragments which give these reflections must be so set that the angle of incidence of the rays is correct, but they may have any orientation around the incident rays as axis. Hence the diffracted beams  $hkl$  will all lie on a circular cone. If recorded upon a plate perpendicular to the incident beam, each type of diffraction  $hkl$  appears as a ring or halo surrounding the central spot, as in fig. 28. It is more convenient to employ a



cylindrical photographic film whose axis is perpendicular to the incident radiation as in fig. 29 (a). Beams are then recorded which are bent through all angles up to nearly  $180^\circ$ , and when the film

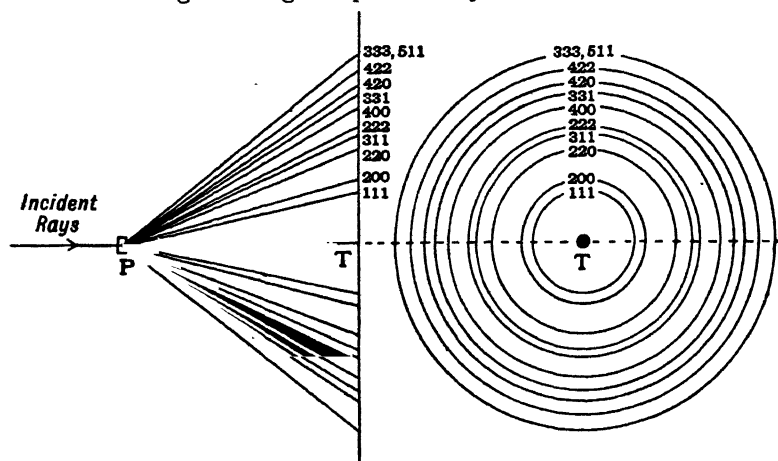


FIG. 28.—The rings of a powder photograph on a flat plate. The positions of the rings are those typical of a face-centred cubic lattice

is unrolled it has the appearance shown in fig. 29 (b). Rays diffracted through a small angle make arcs around the central spot on the film, like an inner halo on the plate. When they are diffracted through  $90^\circ$  the cone becomes a flat sheet, and the

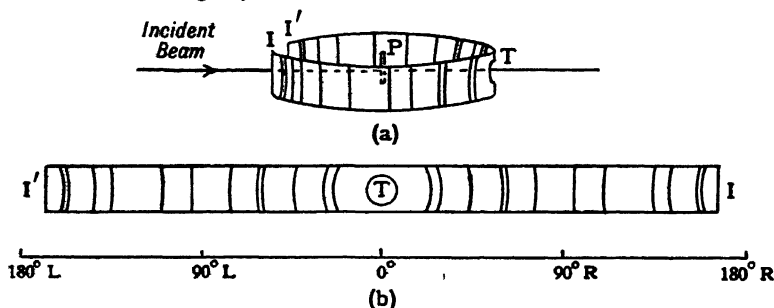


FIG. 29.—Powder photograph on a cylindrical film

corresponding trace on the film is a straight line. When diffracted through a larger angle the curvature is reversed, and when the angle approaches  $180^\circ$  the traces consist of nearly circular arcs around the point where the *incident* rays entered the camera. Thus the curvature of the lines changes from the centre to the outside of the film. The series of powder

photographs in Chapters VII and X illustrates their typical appearance.

If the material to be investigated is a microcrystalline conglomerate such as a metal, a thin rod or plate can be used. Otherwise it is ground into a fine powder, which is placed in a very thin tube, or moulded into a rod with an adhesive, or fastened to a hair, placed along the axis of the camera. A very small amount of powder adhering to a hair gives excellent results. A powder which is too coarse gives a series of spots in place of lines, because all orientations of the crystalline particles do not occur. In such a case, the photograph can be greatly improved by rotating the specimen during the exposure. Fig. 30, Pl. V, p. 48, shows two photographs of the same material, the upper one being taken with the powder fixed, and the lower with the powder rotating. We are indebted to Dr Burgers for supplying this illustration.

Types of camera used for powder photographs are described in a later volume; although their principle is simple, the obtaining of clear sharp photographs depends upon a number of technical details of construction. It is desirable to avoid fogging of the film by scattered radiation, and with this object a hole is cut in the film through which the primary beam escapes, and the slit system is carefully designed.

The  $K\alpha$  radiation from a metal of low atomic number, such as copper or iron, is generally used in the powder method, since the longer wave-length (as compared with  $K\alpha$  molybdenum) increases the separation from each other of the many lines upon the film, and also there is less general scattering. A filter is used which absorbs the  $K\beta$  radiation. An extended use of the powder method, in fact, necessitates a battery of tubes, or a tube with an interchangeable anticathode, so that chromium, iron, cobalt, nickel, copper, or molybdenum radiation can be used as best suits the investigation. The examples of powder photographs in Chapter X illustrate these points.

The lines of a powder photograph are identified by deducing the spacings of the corresponding planes from the positions of the lines, and finding by trial a crystal cell which will give the same spacings. The ease with which this can be done depends upon the number of variables to be dealt with. In a cubic crystal there is only one variable, the length of the unit cube edge. Hexagonal, rhombohedral, and tetragonal crystals have two

variables, a length and an axial ratio. It is feasible to identify the lines in their photographs; Hull's graphs are widely used for this purpose. In these graphs the values of the axial ratio are measured on the vertical axis. For each axial ratio the values of  $\sin \theta$  for the various reflections are plotted on a horizontal line to a logarithmic scale, so that a change in the scale of the structure simply corresponds to a bodily displacement of all the points to right or left. Curves are drawn connecting the points for a given  $hkl$  at different levels. We now plot the observed values of  $\sin \theta$  logarithmically on a strip of paper, and move it about over the graphs, keeping it horizontal, until a match is obtained. The axial ratio and scale can then be read.

In crystals of lower symmetry there are more than two variables, and the number of lines becomes very great. It is almost impossible to unravel them unless something is known about the form of the unit cell from other sources.

An interesting feature which is shown best by the powder photograph is, that the 'resolving power' becomes very high when the reflected ray is thrown back through an angle  $2\theta$ , which is nearly  $180^\circ$ . If the spacing  $d$  is varied in the equation  $2d \sin \theta = n\lambda$ , we have

$$\Delta d \cdot \sin \theta + d \cos \theta \cdot \Delta \theta = 0,$$

$$\Delta \theta / \Delta d = -\tan \theta / d.$$

As the angle of incidence  $\theta$  approaches  $90^\circ$ ,  $\Delta \theta / \Delta d$  becomes very great. Such rays make the curves on the film in the neighbourhood of I, I' in fig. 29 (b). Small variations in  $d$ , such as occur in an alloy when the proportions of the metals are varied, cause large alterations in the positions of the lines in this part of the film, and therefore can be accurately measured. The ordinary type of camera with a diameter of about 8 cm. will yield results accurate to 1/30,000 if full use of the region of high resolving power is made.

The powder photograph is a very widely used method of investigation. It can be applied to any type of matter with crystalline arrangement, since it does not require single crystals. Each crystal gives its characteristic arrangement of lines upon the film, so that the constituents in mixtures of different crystals can be recognised and their quantities roughly estimated. It has been most useful in the investigation of metals and alloys, where single crystals are often impossible to obtain. It is fortunate

that these structures are generally of a highly symmetrical type, for, as explained above, the powder photographs are very hard to analyse when the symmetry is lower than cubic, tetragonal, or hexagonal. The use of the powder method as a method of analysis has therefore been limited almost entirely to the simpler forms of crystal, although as a method of identification it has a much wider and very valuable application.

### OTHER METHODS OF ANALYSIS

Other methods of analysis, differing more or less widely in principle from those described above, can be used. In the Weissenberg goniometer, monochromatic radiation falls upon a small single crystal, which is rotated around a zone axis as in the rotation photograph. Screens are so disposed as to cut out all but a single layer line, and the cylindrical film is displaced bodily parallel to its axis during the exposure, by a movement linked mechanically to the turning of the crystal. This makes it possible to record the setting of the crystal for each diffracted spot, since the crystal orientation can be deduced from the displacement of the spot in a direction parallel to the rotation axis. One layer line only can be examined at a time, but the indices of each spot can be found immediately from its position. The ionisation spectrometer can be adapted to the powder method by measuring with the chamber the ionisation due to beams diffracted by the powder. The spectrometer can also be used in a way analogous to that of the rotation photograph. By mounting the crystal on a vertical graduated circle, placed on the central table of the spectrometer, it is possible to turn it into such positions that all the diffracted beams recorded as spots in the rotation photograph can be measured individually. These methods and others are described in the section on technique in Vol. II.

### SUMMARY

The methods employed in analysing crystal structure are adapted to the form in which the crystalline material is available. If single crystals can be obtained, the rotation photograph is the most appropriate method. It generally gives all the information required for a complete analysis, though it has the drawback that the estimates of intensity are only approximate. The Laue

method is useful as an indicator of the symmetry or pseudo-symmetry of the crystal. Though it has been successfully used for the analysis of crystals with a small number of parameters, it is not so powerful as the methods employing monochromatic radiation. The spectrometer, yielding precise measurements of intensity, gives the most information and may be used where other methods fail, but it is tedious and requires well-developed crystals. When the material is in the form of a finely divided powder, or is microcrystalline in texture, the powder method must be used. Its limitations as a method of analysis arise from the difficulty of indexing the lines, in the case of orthorhombic, monoclinic, and anorthic crystals. Its main field has been the investigation of very simple compounds, and of alloy structures, which almost universally have one of the highest forms of symmetry.

# CHAPTER IV

## EXAMPLES OF CRYSTAL ANALYSIS\*

### POTASSIUM CHLORIDE AND SODIUM CHLORIDE

EXAMPLES of the analysis of certain simple crystals will be given in this chapter, in order to illustrate the application of the methods described in Chapter III.

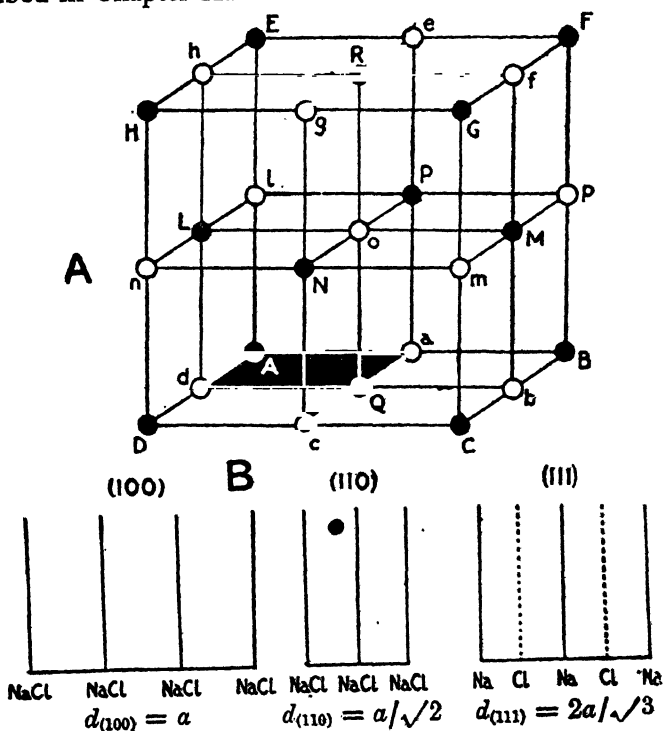


FIG. 31.—Structure and arrangement of planes in sodium chloride

One of the simplest types of structure, which was the first to be analysed by X-ray methods, is that representative of both

\* Throughout this chapter, which discusses some of the first investigations of crystal structure, the earlier convention has been followed of listing under a heading such as '(100) reflections' all reflections of type  $h00$  permitted by the space group.

potassium and sodium chlorides. The structure is shown in fig. 31, A. The crystals have cubic symmetry, and their structure is based on a lattice-work of cubes whose corners are occupied alternatively by metal and chlorine atoms, as shown by the dark and white spheres in the diagram. Either black or white may represent the metal, since they are equivalent positions. In the

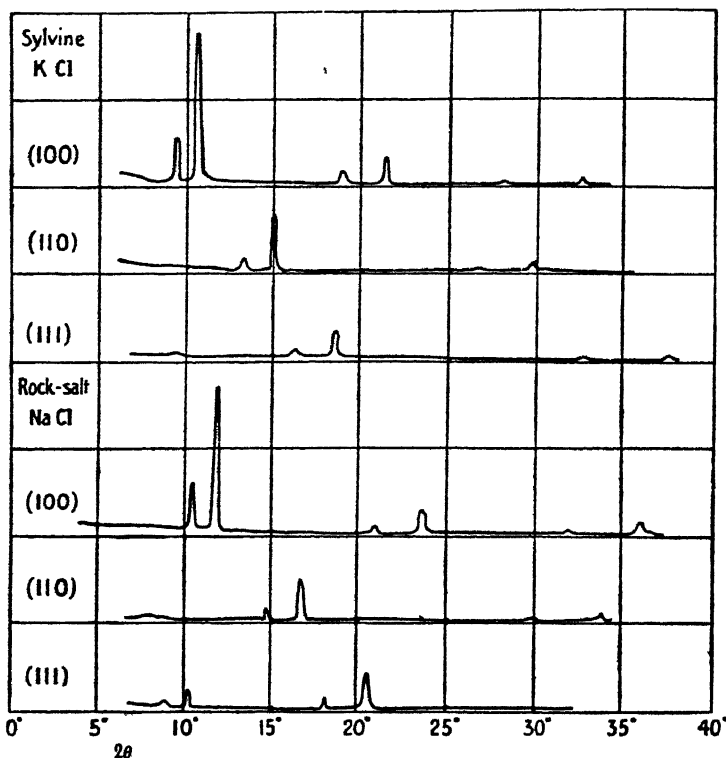


FIG. 32.—Measurement of reflections by KCl and NaCl made with the ionisation spectrometer

diagram, black appears at corners and face centres of the large cube, and white at the centre of the edges and the cube centre, but if the alternative had been adopted of placing the cube corner at a white circle, obviously the positions would be reversed without causing any real difference.

This solution of the structure was arrived at by means of Laue photographs and by measurements made with the ionisation spectrometer. The spectrometer measurements are shown graphically in fig. 32, and were made on natural or artificial faces

with indices (100), (110), (111). The crystal face was set at a series of glancing angles  $\theta$  over a range between  $4^\circ$  and  $20^\circ$ . The ionisation chamber was set in each case at the angle  $2\theta$ , so that it received the reflected beam, and the strength of the beam was measured by observing the ionisation when the X-ray bulb was operated for an interval of about four seconds. The anticathode in the experiment was made of palladium, and the two peaks which appear in different orders in the curves for all faces are the  $K\alpha$  and  $K\beta$  lines in the palladium spectrum, the  $K\alpha$  peak being the stronger of the two.

At the time these first experiments were made nothing was known either about the arrangement of the atoms in the crystals or the wave-length of the palladium K radiation. The information represented by the diagram solved both problems. Consider first the curves for potassium chloride, which have the simpler form. Each face gives a series of peaks superimposed upon a continuous curve which represents the white radiation, the peaks diminishing regularly as the glancing angle increases. The  $K\alpha$  peak reflected from the (100) face occurs at glancing angles whose sines are in the ratio  $1 : 2 : 3$ , these being reflections of the first, second, and higher orders according to the equation

$$n\lambda = 2d \sin \theta.$$

The same relation holds for the other faces.

If next the angles be compared at which the first reflection from the faces (100), (110), (111) takes place, the relative spacings of the corresponding planes can be measured, since  $d$  is inversely proportional to  $\sin \theta$ . Let the spacings parallel to these faces be  $d_{(100)}$ ,  $d_{(110)}$ ,  $d_{(111)}$ ; the first spacing must be the greatest, since it occurs at the smallest angle. A comparison of the sines shows that within the errors of measurement

$$1/d_{(100)} : 1/d_{(110)} : 1/d_{(111)} = 1 : \sqrt{2} : \sqrt{3}.$$

This ratio is to be expected from a series of scattering points in simple cubical array, which has a unit cell as in fig. 33 (*a*). The planes parallel to the face (100) have the spacing  $OA$ , which will be called  $a$ . The face (110) is parallel to one axis of the cube and makes equal intercepts on the other two. BEFC is a plane parallel to this face, and clearly the spacing  $d_{(110)}$  is given by

$$d_{(110)} = OP = a/\sqrt{2}.$$



Similarly ABC is parallel to (111), and the spacing OQ is given by

$$d_{(111)} = OQ = a/\sqrt{3}.$$

We therefore infer from these measurements made with KCl that the crystal contains a simple array of similar diffracting units arranged at the corners of a cubic lattice.

When the results for KCl and NaCl are compared, it will be seen that corresponding spectra occur at a slightly smaller angle for KCl than for NaCl. For instance, the first-order spectrum from the (100) face was found at  $5^{\circ} 23'$  for KCl and  $6^{\circ} 0'$  for NaCl. The planes must be more widely spaced in the first case, with the ratio

$$\sin 6^{\circ} 0' : \sin 5^{\circ} 23' = 1.115 : 1.$$

If the crystals have the same structure, this difference in scale should correspond to the difference in molecular volumes (the molecular weights divided by the densities) of the crystals, which are 37.2 and 26.7 respectively. The cube root of the molecular volume should be proportional to  $d_{(100)}$ . Actually

$$\sqrt[3]{\frac{37.2}{26.7}} = 1.117,$$

agreeing with the ratio calculated from the angles of reflection, and affording a check on the assumption that the two crystals are similar in structure.

In the next place, the spectra from the (111) face of NaCl show a weak peak near  $5^{\circ}$ , as well as the stronger peak near  $10^{\circ}$ , which corresponds to the first order from the (111) of KCl. This is the real first-order reflection, and corresponds to a spacing  $2a/\sqrt{3}$ , not  $a/\sqrt{3}$  as in potassium chloride. The diagrams in fig. 31 explain the difference.

In KCl, the potassium and chlorine atoms have nearly the same scattering power for X-rays, owing to the closeness of their atomic numbers, which are 19 and 17 respectively. Hence the lattice appears to have equal diffracting centres at all corners of the small cubes, whether black or white, as we had already concluded from a study of the reflections. In rock-salt, however, the true relative spacing of the planes shows up, being no longer disguised by a similarity in scattering power between metal and chlorine such as exists in KCl. The planes parallel to (100), (110), (111) have the structure shown in fig. 31, B. The first

two sets contain both sodium and chlorine atoms in equal numbers, and consequently successive sheets are identical. The last set, parallel to (111), consists of alternate sheets of sodium and chlorine atoms. If Na and Cl had been identical, and the lattice therefore simple cubic, the spacings would be in the ratio  $1 : 1/\sqrt{2} : 1/\sqrt{3}$ . Actually they are in the ratio  $1 : 1/\sqrt{2} : 2/\sqrt{3}$

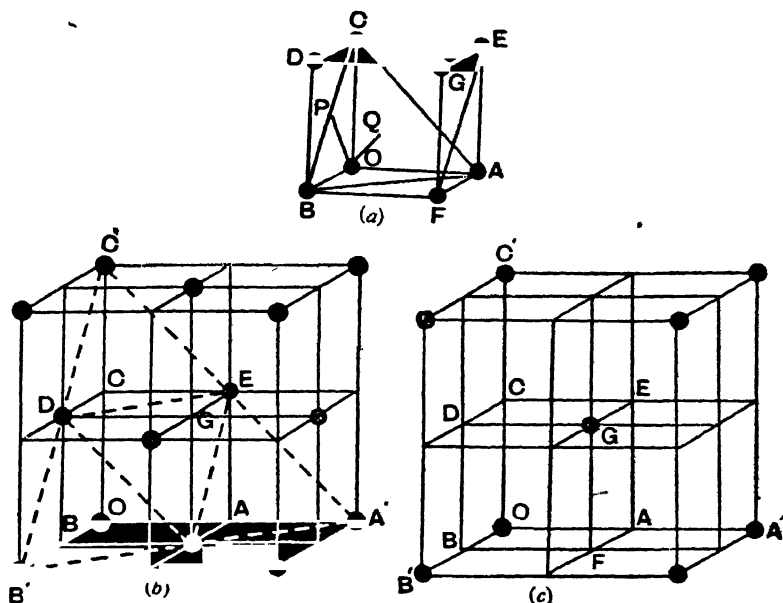


FIG. 33.—The three types of lattice with cubic symmetry  
(a) simple, (b) face-centred, (c) body-centred

as shown, since we must measure spacings between identical planes.

The first-order spectrum from planes parallel to (111) is weak, because waves reflected by the chlorine planes are opposed by waves reflected from the intermediate sodium planes. For the second order there is a path difference of two wave-lengths for waves reflected from successive chlorine planes, and thus the waves reflected by the intermediate sodium planes add their effects to those reflected from the chlorine planes. In general, odd orders will all be weak, even orders strong. Thus all features of the observed reflections are explained by the structure of fig. 31, A.

We may consider the relations between these spacings in

another way. There are three types of space-lattice which possess cubic symmetry. These are the simple cubic lattice, the face-centred cubic lattice, and the body-centred cubic lattice, and each is illustrated in fig. 33. The unit cubes of the two latter structures must be taken to be defined by the axes  $OA'$ ,  $OB'$ ,  $OC'$ ; the edge will in all cases be called  $a_u$ . It will be clear from the figure that reflections for all indices  $hkl$  are not always possible. For instance, the face-centred lattice of fig. 33 (*b*) has *two* planes parallel to (100) between  $O$  and  $A'$ . The only possible reflections are 200, 400, 600, etc., since those with odd indices are destroyed by interference. Similarly, 110 is impossible, and only the reflections 220, 440, 660 occur. On the other hand, the dotted lines show that 111 is a possible reflection, for the presence of the additional points on the face centres does not introduce intervening planes in this case. In general, it can be seen that the indices  $hkl$  of a possible reflection are all odd or all even.

In the body-centred lattice of fig. 33 (*c*) the rule is different. Again, 200, 400, 600 are alone possible. On the other hand, 110 is possible, while the first reflection from the (111) face has the indices 222. For this lattice, the rule holds that  $h+k+l$  must be even.

The reflections of lowest order, and the relative values of  $\sin \theta$  at which they occur, are therefore given by the following table:—

	Indices	$\sin \theta$ is proportional to	
Simple cubic lattice	100	1	$h, k, l$ have all values.
	110	$\sqrt{2}$	
	111	$\sqrt{3}$	
Face-centred cubic lattice.	200	2	$h, k, l$ are all odd or all even.
	220	$2\sqrt{2}$	
	111	$\sqrt{3}$	
Body-centred cubic lattice.	200	2	$h+k+l$ must be even.
	110	$\sqrt{2}$	
	222	$2\sqrt{3}$	

If  $a_w$  is the length of unit cube side, it is easy to show that

$$d_{(hkl)} = \frac{a_w}{\sqrt{h^2 + k^2 + l^2}},$$

$$\sin \theta_{(hkl)} = \frac{\lambda}{2d_{(hkl)}} = \frac{\lambda \sqrt{h^2 + k^2 + l^2}}{2a_w}.$$

The spacings hitherto calculated are simple examples of this rule.

Finally, once the arrangement of any crystal structure is definitely known, both its scale and the wave-length of an X-ray beam can be determined. In the NaCl structure, one atom or half a molecule is associated with each of the eight small cubes of fig. 31. A cubic element has eight corners, but each of these is shared between eight cubes. Thus the mass associated with unit cube must be  $Mm/2$ , where  $M$  is the molecular weight and  $m$  is one-sixteenth the mass of an oxygen atom. This must be equal to  $\rho a^3$ , where  $\rho$  is the density of the crystal. Therefore

$$a^3 = \frac{Mm}{2\rho}.$$

In the case of NaCl, the equation leads to the value

$$a = 2.814 \times 10^{-8} \text{ cm.}$$

Substituting the observed angle of reflection of the rays from the face with this spacing in the formula

$$\lambda = 2a \sin \theta,$$

the value  $0.586 \times 10^{-8} \text{ cm.}$  is obtained for the wave-length of the PdK $\alpha$  radiation.

It has been assumed in this calculation that the diffracting centres are atoms, and not groups of atoms. This assumption was a natural one to make in the case of the original analysis, because it led to so simple an explanation of the difference between potassium and sodium chlorides. It is confirmed in several independent ways, such as by the quantum relationship between the X-ray wave-lengths and potential, and by the diffraction of X-rays by a ruled grating.

Such a calculation now determines the linear scale for all X-ray diffraction processes. Unknown crystal spacings can be measured by using a known wave-length, or conversely the wave-length of a spectral line can be measured by using a crystal

with a known spacing or 'grating constant.' In particular, we can measure the absolute dimensions of the unit cell when investigating a new crystal, and thus by using the density and molecular weight determine how many molecules (it is always a small integer) there are in each cell.

#### LAUE, POWDER, AND ROTATION PHOTOGRAPHS OF KCl AND NaCl

The rules for reflections by these structures, considered above for a few special planes, can now be stated in a general way for reflections with any indices.

(a) Indices  $hkl$  must be all odd or all even. This is so because the structure is founded on a face-centred cubic space-group (examples, 200, 220, 111).

(b) When the indices are odd, the reflection is due to an opposition of the effect of chlorine and sodium or chlorine and potassium. In the former case the reflection is weak, and in the latter case its intensity is vanishingly small (examples, 111, 333).

(c) When the indices are even, the effects of chlorine and metal are combined, and the reflection is strong (examples, 200, 220, 222).

The features of Laue, powder, and rotation photographs of KCl and NaCl may be interpreted by these rules. We take these in order.

Figs. 34 and 35 represent diagrammatically the Laue photographs, which were originally used to establish the structures along with the determination by the spectrometer. The intensities of the spots are indicated by the sizes of the black circles. The incident radiation is parallel to a cube axis in each case. The chief characteristic of the KCl diagram is its simplicity, for all intersections of the circles representing the main zones, throughout a certain region, appear with a regular gradation of intensity. This feature can only be ascribed to a simple arrangement of diffracting points at cube corners.

If we contrast with this the NaCl diagram in fig. 35 it will be seen that the distribution of spots is not so regular. In particular, the innermost zone shows spots with indices  $151$ ,  $351$ , which are absent in the case of KCl. This is so because the first-order reflection from these planes, possible in the case of

the NaCl structure, falls within the range of white radiation, whereas in the case of KCl the first order is destroyed by interference, as has been explained above, and a second-order reflection falls outside the short-wave limit.

The first crystal analysis was actually made with the aid of these diagrams, though the development of the spectrometer

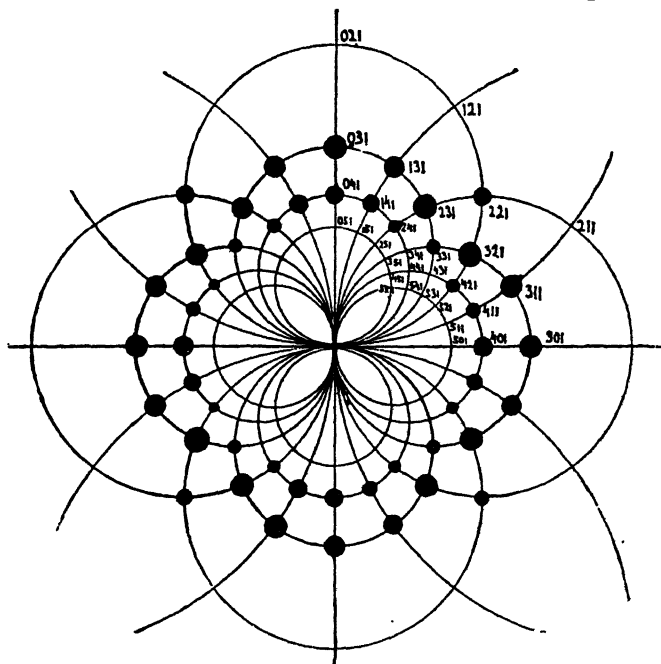


FIG. 34.—Stereographic projection of Laue photograph of KCl

immediately afterwards provided a much more direct and powerful method.

The powder photographs of KCl and NaCl, using copper  $K\alpha$  radiation, are shown in fig. 36, Pl. V, p. 48. The  $K\beta$  line has been cut out by means of a nickel filter. Each line is identified by means of the glancing angle  $\theta$  at which it has been reflected, which can be calculated from a measurement of the film and a knowledge of the radius of the camera. The latter constant is generally measured by calibrating the camera with a powder of known structure. Since  $\sin \theta = \lambda \sqrt{h^2 + k^2 + l^2} / 2a_w$ , we can find by trial integers  $hkl$  which lead to the same value of  $\sin \theta / \sqrt{h^2 + k^2 + l^2}$  for each line.

The indices of the lines are marked in the diagram. Lines which appear in both diagrams are indexed above, the correspondence being shown by the links between the two photographs. The additional lines which appear in NaCl alone are indexed below. In certain cases different sets of planes have the same

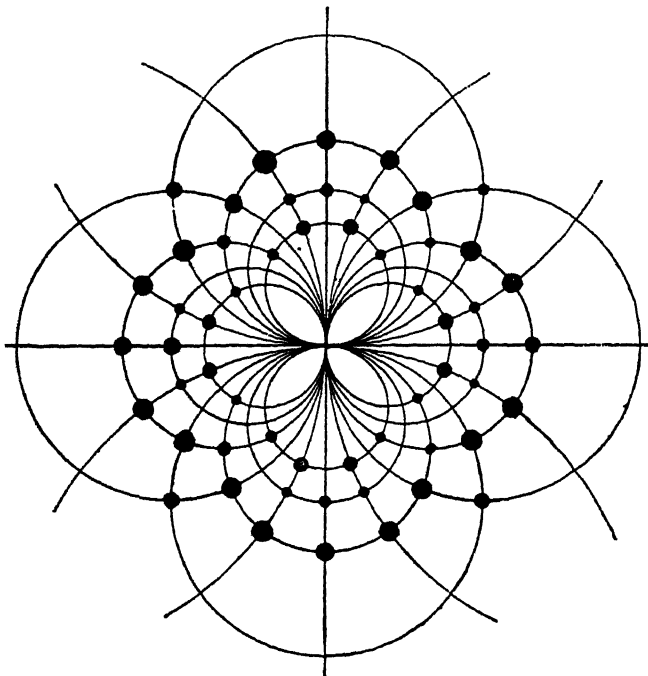


FIG. 35.—Stereographic projection of Laue photograph of NaCl

spacing, and the corresponding line is due to a superposition of both reflections. For instance,

$$5^2 + 1^2 + 1^2 = 27 = 3^2 + 3^2 + 3^2,$$

$$4^2 + 4^2 + 2^2 = 36 = 6^2 + 0^2 + 0^2, \text{ etc.}$$

A comparison of the two photographs reveals the same rules as in the case of other methods of analysis. KCl gives only such reflections as correspond to even indices, whereas NaCl gives in addition a weaker set of lines for which the indices are all odd, and which are due to planes in which Na and Cl sheets alternate. The foundation upon a face-centred lattice is proved by the appearance of all-even and all-odd indices alone. It is also apparent that the NaCl structure is built on a smaller scale than

# PLATE V

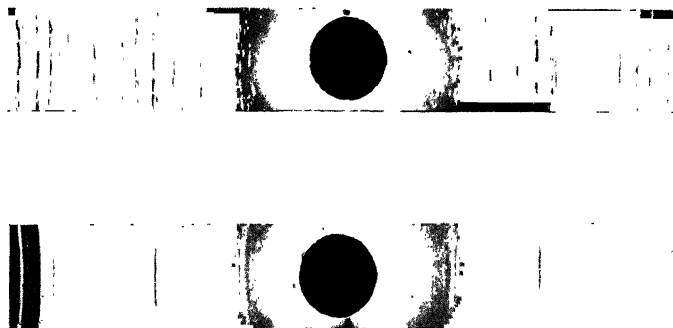


FIG. 30.—Powder photographs taken with the same material (a carbide of tantalum) but with the powder stationary in the upper photograph and rotated during the exposure in the lower photograph (Burgers, Philips Laboratory, Eindhoven)

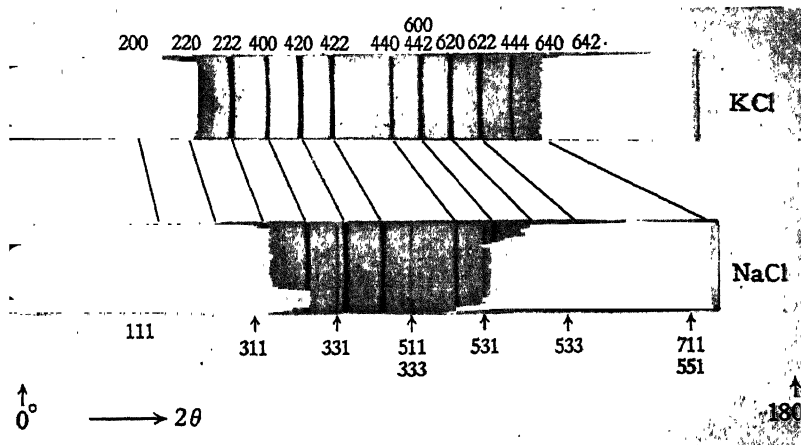


FIG. 36.—Powder photographs of KCl and NaCl





the KCl structure, because corresponding lines occur at greater angles.

Although the KCl structure is simple, there is no regular gradation in the intensity of its lines. The photograph illustrates very well an important factor—the number of contributing planes. Each ring or line in a powder photograph is due to the fortuitous orientation of a number of small crystals in a position for reflection. A crystal particle can contribute to 200, for instance, if any one of its six cube faces (100), (010), (001), ( $\bar{1}$ 00), (0 $\bar{1}$ 0), (00 $\bar{1}$ ) are set correctly. On the other hand, it can contribute to a reflection for which all the indices are unequal, such as 642 or 531, if any one of 48 faces of the crystal is set correctly, since there are 48 permutations of these indices. There is therefore a much higher chance of such a plane being in the right position, or in other words, many more crystalline particles will contribute to 642 than to 200. This effect is well marked in the photograph. The factor is, for instance, 8 for 222, 6 for 400, 24 for 420, and again 8 for 444, 24 for 640, and 48 for 642. Allowance for this factor is essential to the interpretation of the photograph.

Other factors influencing the intensity of the lines depend in a continuous way upon the angle, and can be allowed for (the complete formula is given in Chapter IX). In an accurate investigation the density of the lines is measured by a microphotometer, and compared with a scale of density printed on the same film by a stepped exposure to the direct radiation.

The results of an examination of KCl and NaCl by the method of the rotation photograph are shown by the diagrams of fig. 37. The photographs were obtained by turning the crystals about the cube edge, face diagonal, and cube diagonal as axes respectively. The indices of each spot can be found if we consider it as placed at the intersection of a layer line with one of the haloes which a powder photograph of the same crystal would yield.

Circles have been drawn in each case corresponding to the innermost haloes 111, 200, 220, 311, 222, 400 of a powder photograph. A spot with one of these sets of indices, or its permutations, must lie on the corresponding halo, and at the same time it must lie on the appropriate layer line. The layer lines when the crystal is rotated about the  $c$  cube edge correspond to

$$l = -2, -1, 0, 1, 2, \text{ etc.}$$

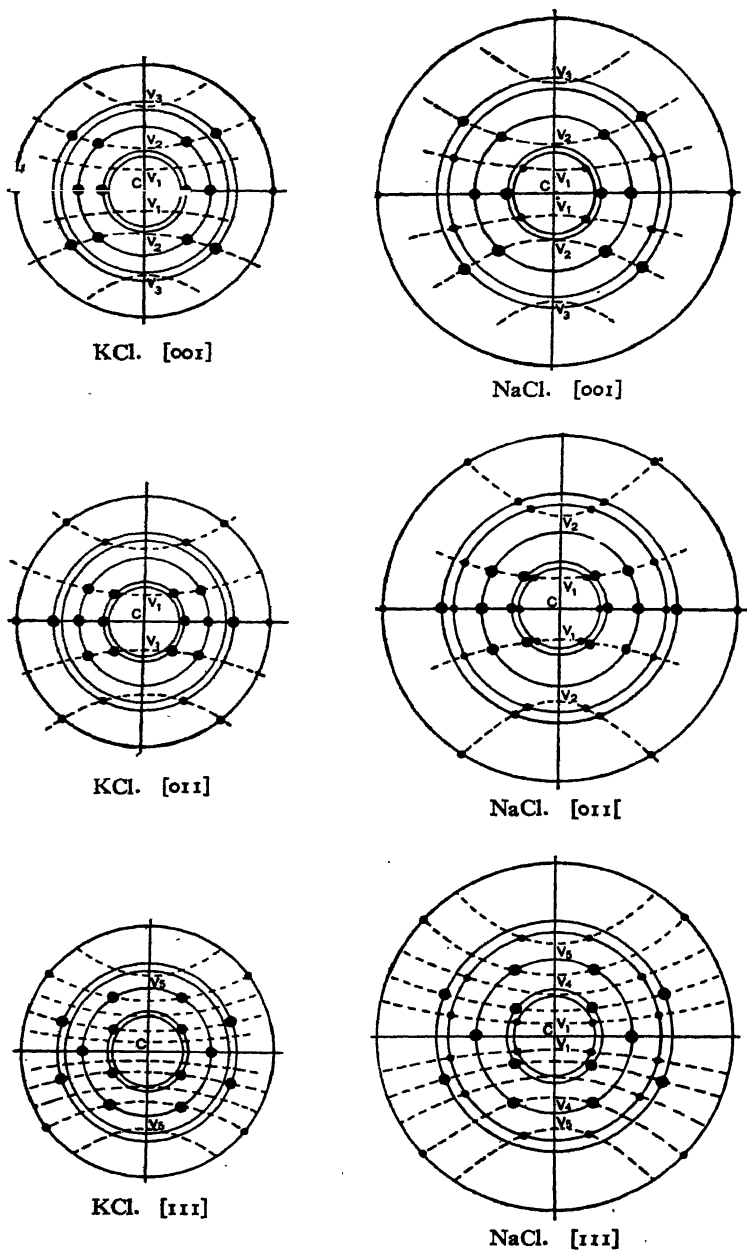


FIG. 37.—Diagrams representing rotation photographs of KCl and NaCl taken with  $\text{CuK}\alpha$  radiation

It can be shown that in the other cases the layer lines have the following characteristics:—

Rotation about  $[011]$ ,  $k+l = -2, -1, 0, 1, 2$ , etc.

Rotation about  $[111]$ ,  $h+k+l = -2, -1, 0, 1, 2$ , etc.

These conditions determine the possible indices in each case.

The evidence of the rotation photograph decides in favour of the same structure of NaCl and KCl as that found by the other methods, and may be briefly summed up. In the first place, the NaCl results show that the layer lines are farthest apart when the crystal is rotated about  $[011]$ , the face diagonal. Hence the lattice-points are closest along this diagonal, and the space-lattice is therefore face-centred cubic. This is a simple example of a very useful property of rotation photographs. They determine with certainty the form and dimensions of the space-lattice, since the layer lines give the spacing of the lattice-points along each important crystal zone. In NaCl, any spot lying on a halo with odd indices  $111, 311$  is weak in comparison with such as lie on haloes with even indices. Similarly the spots on the odd layer lines are weak when rotation is about  $[100]$  or  $[111]$ . In KCl spots lying on haloes  $111, 311$  are too weak to observe. The smaller scale of the NaCl structure as compared with KCl is again evident by the larger scale of its photograph.

#### THE ANALYSIS OF ZINCBLLENDE, DIAMOND, AND FLUOR

Zincblende,  $\text{ZnS}$ , is another binary compound which forms crystals belonging to the cubic system. The spectra of zincblende are shown in fig. 38, the angles  $2\theta$  and intensities being indicated by the positions and heights of the vertical lines.

In the three sets of spectra illustrated here, the first-order spectra have the same relative positions for the three faces as have those of NaCl, and a more complete examination shows that this is true for all reflections given by the crystal. It is clearly based, like NaCl, on a face-centred cubic lattice. The side of the unit cubical cell, determined by the angle of reflection, is  $5.42 \text{ \AA}$ . From the density and molecular weight of  $\text{ZnS}$ , it can be deduced that there are four molecules in the unit cell. Since the lattice itself has four points in each cell, it is a necessary consequence that the atoms of zinc lie on one face-centred cubic lattice, and the atoms of sulphur on a second lattice interpenetrating the first.

The relative positions of zinc and sulphur cannot, however, be the same as in NaCl, as a comparison of the spectra will show. The (110) reflections alone show a normal decrease towards the higher orders, indicating that the sulphur atoms lie on the same sheets as the zinc atoms, for any other arrangement would cause the intensities to fluctuate. The (100) reflections, on the other hand, have a small first order and a large second order, like the (111) reflections of NaCl. The sulphur sheets must alternate with the zinc sheets so as to reduce the odd orders. If the

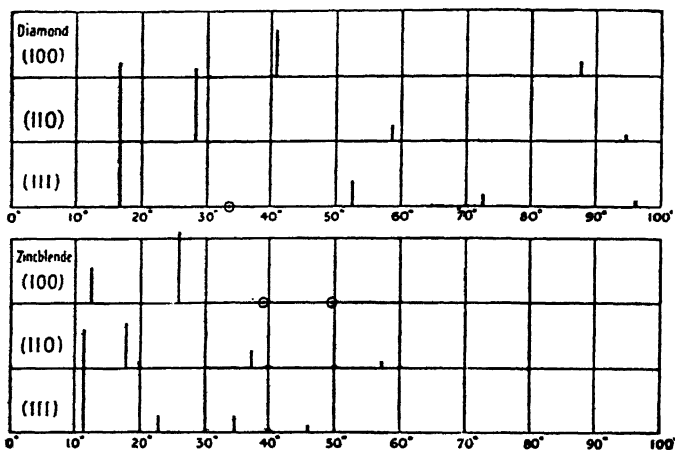


FIG. 38.—Spectrometer measurements on diamond and zincblende

sulphur atoms are to lie in the (110) sheets, and between the (100) sheets, each atom must be placed at the centre of one of the small cubes in fig. 39, A.

Only four sulphur atoms can be shown in the figure, inside the unit cell, but if cubes such as this were stacked side by side so as to continue the pattern, it would be obvious that the sulphur atoms are also on a face-centred lattice like the zinc atoms.

The arrangements of the planes parallel to (100), (110), (111) are shown in the lower part of the figure. The planes parallel to (111) are of a new type, the spacing being such that the distance Zn–Zn is four times the distance Zn–S. It is not hard to see how this will affect the spectra, explaining their appearance in fig. 38. For the second order 222 the waves from the sulphur sheets are in opposite phase to those from the zinc sheets, because the phase difference between Zn and Zn for 222 is  $4\pi$ , and that

between Zn and S is one-quarter of this amount, or  $\pi$ . Hence the second order should be weakened relatively to the first and third as the diagram shows. The arrangement of zinc and sulphur atoms thus explains all the observations satisfactorily.

The next crystal considered is simpler than zincblende, but the latter has been discussed first, because its spectra reveal more clearly the face-centred cubic lattice, which is the basis of both structures.

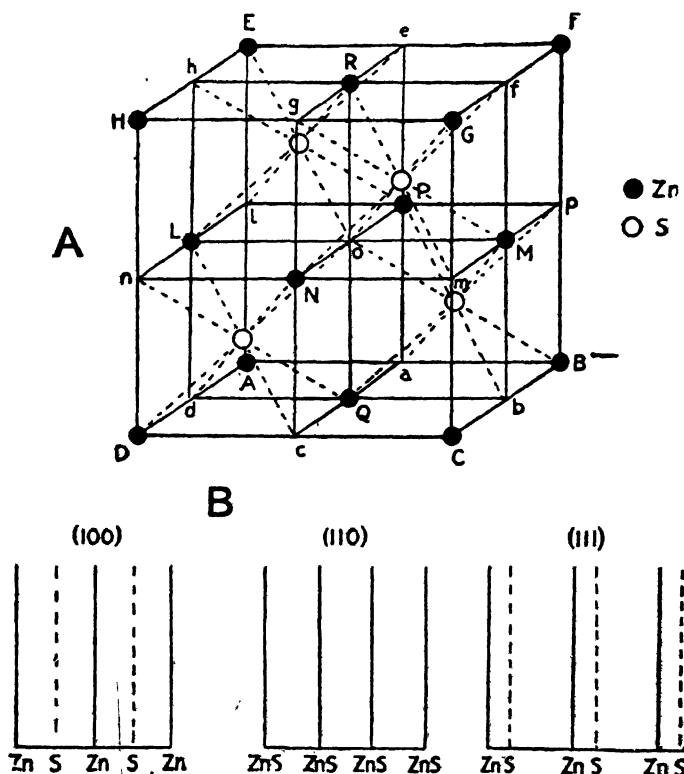


FIG. 39.—Structure of zincblende, and arrangement of its planes

Diamond, one of the modifications of carbon, forms crystals belonging to the cubic system. The reflections are shown in the diagram of fig. 40. The first spectra occur at angles whose sines are in the ratio

$$2 : \sqrt{2} : \sqrt{3}/2.$$

This ratio is not characteristic of any space-lattice. Moreover,

the spectra reflected from the face (111) are peculiar in that the second order is exceedingly faint, although the first, third, fourth, and fifth spectra are quite large.

The nature of the structure which produces these effects can

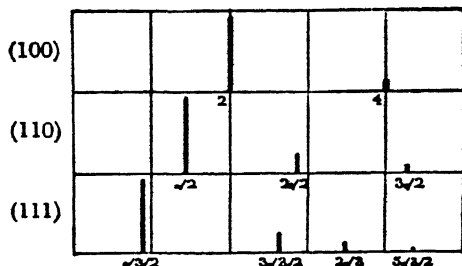


FIG. 40.—Diagram representing the relative positions and intensities of reflections by the diamond structure

be understood by comparing this case with that of zincblende. In the latter crystal, 222 is small because Zn and S oppose their effects, and 200 is small for the same reason. If Zn and S are replaced by identical atoms, 222 and 200 would disappear entirely, and the spectra would resemble those

given by diamond. We are thus led to substitute carbon atoms for both black and white spheres in fig. 39, A, obtaining the structure

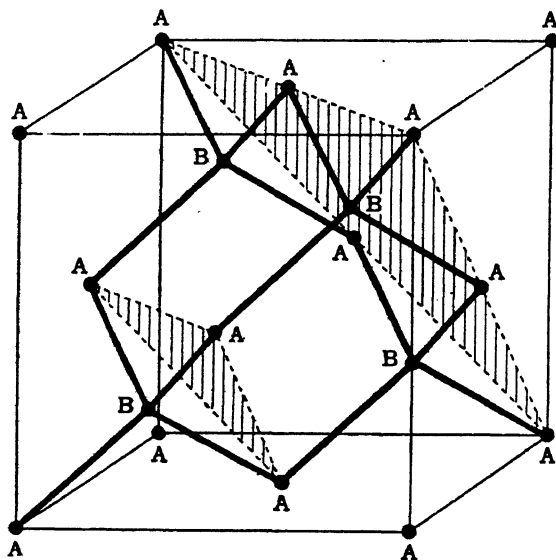
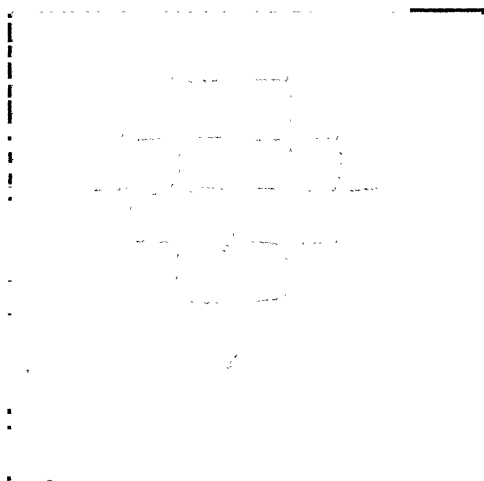


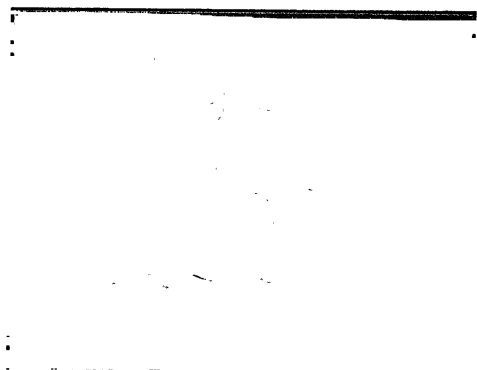
FIG. 41.—Structure of diamond. Successive 111 planes of the unit cube have been shaded

shown in fig. 41. In concordance with this solution, it can be verified from the density that the unit cube contains eight atoms

## PLATE VI



Model of diamond  
Horizontal and vertical planes perpendicular to  
the paper are (110) planes



Model of diamond  
Horizontal planes perpendicular to the paper  
are (111) planes

FIG. 42.—Structure of diamond





of carbon. The resulting structure is an elegant one, which was one of the first achievements of the new methods of crystal analysis. The carbon atoms are arranged in two interpenetrating face-centred lattices. Each atom of lattice B is surrounded by four atoms of lattice A, and *vice versa*. This suggests a simple way of considering the structure; links can be drawn from atom to atom in such a way that each is joined to four neighbours. The scaffolding of the cubic cells can be dispensed with, and a structure is obtained which is shown in fig. 42, Pl. VI, p. 54. The model illustrates well the pairs of planes parallel to each (111) face.

An interesting point of X-ray optics arises in connection with the diamond structure. If the atoms were spherically symmetrical, the 222 spectrum should vanish. Actually it can be observed, though it is very weak. Its existence can be explained by a distortion of the carbon atoms, which reduces their symmetry to that of a tetrahedron, and such a distortion would be produced by the linking of each atom to four neighbours. It can be shown that this distortion would, in fact, produce a very weak 222 spectrum. On the other hand, the 200 spectrum should still vanish even if this distortion is present, and in agreement with this the spectrum is not observed.

One other structure may be briefly described, because it illustrates a point of interest. The reflections given by the cubic crystal fluor,  $\text{CaF}_2$ , resemble those given by diamond. The structure which accounts for these reflections is very simple; it is based, like the others considered so far, on a face-centred cubic lattice, and has four molecules of  $\text{CaF}_2$  in the unit cell. The calcium atoms are arranged on a face-centred cubic lattice, and the fluorine atoms occupy the centres of the small cubes as do the sulphur atoms in zincblende. In this case, however, there are twice as many fluorine atoms as calcium atoms. The fluorine atoms must be placed at the centres of all the small cubes, instead of in one-half of these cubes as in the zincblende structure. The arrangement of the principal planes is then given by fig. 43.

As in diamond, it is found experimentally that the reflections 200 and 222 are weak or absent. However, the vanishing of the spectra is not due to the destructive interference of waves from planes containing identical atoms, but to the interference of waves from planes containing Ca and  $\text{F}_2$  respectively. The calcium planes and fluorine planes must be nearly equivalent as regards reflecting power. It appears that one calcium atom

(atomic number 20) nearly balances two fluorine atoms (atomic number 9).

This example shows that, in order to examine the diffraction of X-rays by crystals more closely, it is necessary to know the efficiencies of various atoms as scatterers of X-rays. In the earlier experiments it was assumed that the scattering power was proportional to the atomic number, or number of electrons contained in the atom. Such cases as that of fluorspar gave support to this assumption as being a first approximation to the truth. Actually, the problem is considerably more complicated. At small angles of scattering, the amplitude of the waves scattered by the atom is approximately proportional to the atomic number, but the amount scattered by a given atom falls off as the angle

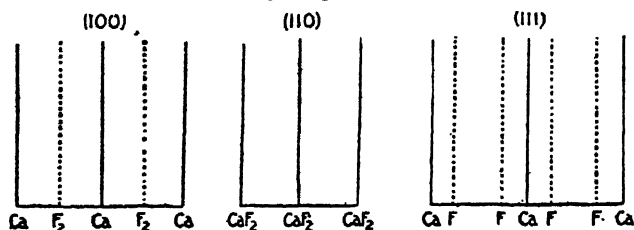


FIG. 43.—Arrangement of planes in fluor

increases. The fall is very rapid for the light atoms, less so for heavy atoms. For instance, the 600 reflection by fluor is appreciable, because at this greater angle Ca scatters more than F<sub>2</sub>. The *f* curves, which enable the amounts scattered by the various atoms at different angles to be estimated, are highly important in analysis, and will be described more fully in a subsequent chapter.

#### CRYSTAL STRUCTURES WITH PARAMETERS

In the crystals considered so far, the atoms are situated at certain definite points of the space-lattice, such as cube corners or centres, and face centres. They cannot be displaced from these precise positions without a degradation of the symmetry of the crystal. One may have to choose between certain alternatives in placing the atoms, but each alternative is precisely defined, and this simplifies the analysis. Such simple cases are very exceptional. In the vast majority of crystals, a typical atom of one of the components may lie at any point along some axis, or on some plane, or be in what is termed a 'general position' with no

geometrical restraints. As long as other atoms occupy corresponding positions, the arrangement is in accord with the crystal symmetry. Instead of choosing between certain definite alternatives, it is necessary to fix for each atom the value of one, two, or three *parameters*, which determine the atomic position, and which may have any values over wide limits. The greater the number of these parameters, the more difficult it is to analyse the structure.

Sodium chloride, zincblende, diamond, and fluor are examples of structures with no parameters. Some structures with one or two parameters will now be considered. It must be realised, however, that such cases are still extremely simple. The more typical crystal may have ten, twenty, or forty parameters, to all of which values must be assigned before the analysis of the structure is complete.

### IRON PYRITES

Iron pyrites,  $\text{FeS}_2$ , is an example of a crystal with one parameter. The cubic unit cell has an edge of 5.405 Å., and contains four molecules of  $\text{FeS}_2$ . The integrated reflections\* from the principal faces are given in Table I, and it will be at once obvious that they are a more complicated set than any as yet considered. In no case is there a regular succession of spectra diminishing in intensity towards the higher orders, and the planes parallel to all three types of faces must have a complex arrangement.

TABLE I

*Integrated Reflections ( $\rho$ ) by Iron Pyrites, measured with the Ionisation Spectrometer (PARKER and WHITEHOUSE)*

$hoo$	$\rho \times 10^4$	$hhh$	$\rho \times 10^4$	$hho$	$\rho \times 10^4$
200	99.7	111	44.0	220	54.4
400	0.32	222	36.4	440	37.6
600	3.12	333	19.7	660	3.58
800	14.2	444	0.14	880	3.60
1000	3.92	555	9.29	..	..
1200	1.11	666	1.51	..	..
..	..	777	1.15	..	..

\* These integrated reflections are expressed in *absolute measure*, in a way described in Chapter IX.

A simple way of arranging the atoms of iron and of sulphur would be that of the fluor structure. The iron atoms would then lie on a face-centred cubic lattice, and the sulphur atoms occupy the centres of all the small cubes. It is clear, however, that this will not explain the observed reflections. Sulphur has an atomic number of 16, iron of 26, and the (100) planes of a fluor-like structure would have alternate sheets of Fe and  $S_2$ . This should give very weak 200, strong 400, weak 600, strong 800, etc., whereas the observed intensities are of a very different type. Similarly, a fluor-like structure would give a very weak 222, whereas it is present as a strong reflection. The sulphur and iron atoms in  $FeS_2$  cannot be in these very symmetrical

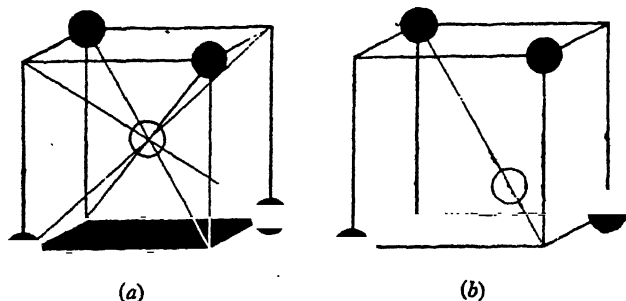


FIG. 44.—Elements of the structures of  $CaF_2$  and  $FeS_2$ , showing the displacement of the sulphur atom in the latter structure

positions, and some of the symmetry elements of fluor must be sacrificed in order to explain the observations.

Fig. 44 (a) represents a small cube of the fluor structure. It has a fluorine atom at the centre and four calcium atoms at the corners. The four diagonals which are drawn intersecting in the centre of the cube are axes of threefold symmetry of the whole structure, and are, of course, continuous through a row of cubes. Four such axes pass through each corner of the cube, as would be apparent if the structure were continued.

If the atom at the centre of the cube is to be displaced from its position, it is impossible to retain the four axes of symmetry passing through it. One at most can be retained, the atom sliding along a diagonal as in fig. 44 (b). The sulphur atom must remain on this one axis, as otherwise all trigonal symmetry would be destroyed, and the crystal must possess trigonal axes since it is cubic. Each iron atom and each sulphur atom now lies on one, and only one, trigonal axis. In fig. 44 (b) the axis going

through one of the iron atoms is shown; the axes which pass through the other three iron atoms are supplied by neighbouring cubes. This arrangement, which is rather hard to visualise, may be made more clear by fig. 45, which shows eight of the cubes stacked together in two sets of four, the sets being separated so as to make the construction more obvious. Each cube contains one trigonal axis, and none of these axes intersects any other. Each trigonal axis is continued in both directions, so as to pass through a string of cubes of the extended structure.

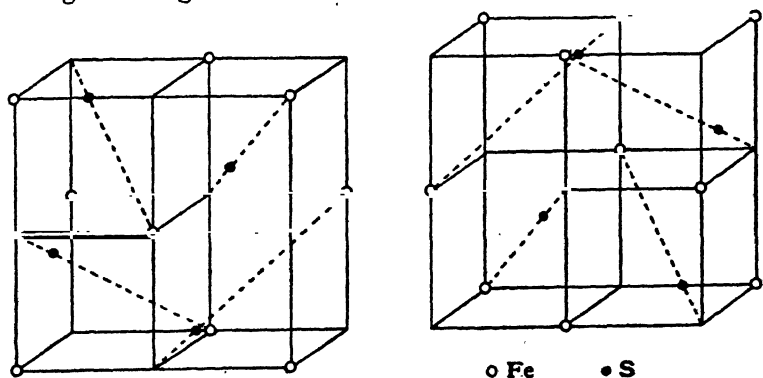


FIG. 45.—The unit cubical cell of the  $\text{FeS}_2$  structure. The front and rear sections are shown separate in order to make the arrangement more clear

It will be clear that there is one parameter to be determined in this structure, this being the distance of the sulphur atom from the cube corner. Symmetry is satisfied if all sulphur atoms are displaced equally, and the amount of displacement must be determined by finding a value which explains the observed reflections. The four iron atoms, on the other hand, are in fixed positions, since they lie at symmetry centres.

A first approximation to the position of the sulphur atoms can be got from the (100) reflections. The reflection 200 is large, 400 and 600 are very weak, 800 and 1000 strong for reflections at so high an angle. The sheets of atoms are shown in fig. 46. If the distance Fe-S were one-quarter of the distance Fe-Fe, sulphur and iron would act in opposition for 400. If it were one-sixth, they would act in opposition for 600. Since both 400 and 600 are weak, the actual distance must be about one-fifth. In order that the sheets may have this spacing, the sulphur atom must be displaced along the diagonal until it divides it in the ratio 1 : 4. As far as these planes go, the displacement

from the centre of the cube may take place either towards or away from the iron atoms along the diagonal, but consideration of the (111) reflections shows that the displacement takes place away from the iron atoms and towards the empty corner, as in fig. 45.

The sheets of atoms parallel to (100), (110), (111) will now be arranged as in fig. 46. These sheets are of a more complicated kind than the simple AB, AB type of arrangement hitherto considered. The intensity of reflection can be calculated, however, in exactly the same way, except that we must now find the

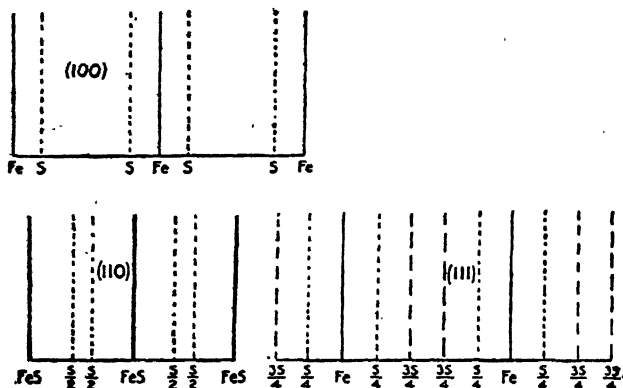


FIG. 46.—Arrangement of planes in  $\text{FeS}_2$  structure

resultant of waves from several sets of planes. As an instance, we may consider the reflections from (100), assuming the distance between Fe and S to be exactly one-fifth of the distance between successive sheets of iron atoms. The phase difference of the reflected waves is  $2\pi/5$  for 200,  $4\pi/5$  for 400, and so forth. If  $f_1, f_2$  represent the amplitudes of waves scattered by these atoms, the amplitudes for the different orders are as follows :—

$$\begin{aligned} 200 \quad f_1 + 2f_2 \cos (2\pi/5) &= f_1 + 0.62f_2, \\ 400 \quad f_1 + 2f_2 \cos (4\pi/5) &= f_1 - 1.58f_2, \\ 600 \quad f_1 + 2f_2 \cos (6\pi/5) &= f_1 - 1.58f_2, \\ 800 \quad f_1 + 2f_2 \cos (8\pi/5) &= f_1 + 0.62f_2, \\ 1000 \quad f_1 + 2f_2 \cos (10\pi/5) &= f_1 + 2f_2. \end{aligned}$$

Remembering that one would expect  $f_2$  for sulphur to be rather greater than one-half of  $f_1$  for iron, and that the intensities of the reflections are dependent upon the *squares* of the amplitudes, we should therefore expect the 200 and 800 orders to be present

in about their normal ratio, but 400 and 600 to be extremely weak, which is in fact observed. Similar calculations show that for the (110) planes 440 is enhanced as compared with 220, and that for the (111) planes the first and fourth orders should be relatively weak and the fifth enhanced. In both cases this agrees with observation.

The above calculations have been given in an approximate form, since the main point has been to illustrate the principles involved in the determination of a parameter. The results of a precise determination are given in Table II. The integrated intensities are converted into estimates of efficiency of diffraction, or F values, by the formula given in Chapter IX. These are compared with F values based on the known scattering efficiencies of iron and sulphur at different angles (the iron and sulphur *f* curves), and the parameter is adjusted until the best agreement is obtained. The measurements were made by Parker and Whitehouse. Their results show that the displacement of the sulphur atom as described above is more than one-fifth of the diagonal in fig. 44, the actual amount being 0.228. The agreement obtained by using the parameter is seen in the table, which affords a good example of more precise methods of measurement.

TABLE II

*Comparison of Observed and Calculated F Values of Iron Pyrites*

The F values are those for the unit  $\text{FeS}_2$ . Parameter  $u=0.114$

<i>hoo</i>	F, obs.	F, calc.	<i>hhh</i>	F, obs.	F, calc.	<i>hho</i>	F, obs.	F, calc.
200	22.9	22.9	111	12.4	-13.1	220	18.2	17.2
400	1.5	-1.4	222	16.1	15.0	440	21.9	23.5
600	6.2	5.8	333	14.6	-14.4	660	8.4	9.4
800	16.7	16.7	444	1.4	-0.5	880	9.5	10.7
1000	10.1	11.7	555	15.5	-14.5	...	...	...
1200	...	2.1	666	6.1	6.1	...	...	...
...	...	...	777	5.2	-5.7	...	...	...

## SUMMARY

The foregoing examples illustrate the principles on which crystal analysis is based. A series of diffracted beams is observed by one of the experimental methods. Measurement of the glancing angles at which these beams are reflected from the



crystal planes makes it possible to determine the spacing of these planes, and so to construct a framework or space-lattice on which the crystal pattern is built. The density of the crystal gives the number of molecules in the unit cell of the lattice. Various arrangements of the atoms are then tried in an attempt to find one which explains the strength of all the diffracted beams, and so can be accepted as correct.

In the examples, a complete and logical deduction of the structure has not been attempted. The original analyses of these simple structures were based on the examination of a few planes. Though further work has confirmed their correctness, the data would now be considered insufficient, and it is clear that the analyses were successful because X-rays were only used to decide between a few definite alternatives. A proper treatment involves the examination of a large number of reflections of all classes.

Before describing the general procedure in analysing more complex crystals, it is necessary to go more deeply into the symmetry of the crystalline arrangement. When the atomic positions depend upon a large number of parameters, the difficulty of testing different arrangements and discovering the true one is greatly increased. As a first step in this search it is possible to deduce the scheme of symmetry according to which the atoms or molecules are disposed, the 'space-group,' which will be dealt with in the next chapter.

## CHAPTER V

### CRYSTAL SYMMETRY

A LOGICAL treatment would place the description of crystal symmetry earlier in this volume, before the sections on methods and results of X-ray analysis. This course has not been followed, because it is easier to discuss symmetry by referring to actual structures such as those described in the last chapter. The complexities of crystal symmetry are more apparent than real, and a few diagrams and models serve to illustrate the main principles. It is essential to grasp the significance of the terms *space-lattice*, *point-group*, and *space-group*, and to see how these geometrical attributes of a crystal can be determined. Once the fundamental ideas are clear, it is easy to treat any particular case with the aid of lists and diagrams of space-groups which have been expressly designed for X-ray analysis.

#### THE SPACE-LATTICE

The space-lattice has already been described. It is formed by taking a series of points in the crystal pattern which are identical in every respect, and it is a measure of the intervals at which the pattern repeats.

The most general type of space-lattice has unequal axes  $a$ ,  $b$ ,  $c$  enclosing angles  $\alpha$ ,  $\beta$ ,  $\gamma$  which are not right angles. Comparatively few crystals, however, are based on a lattice of this type. In most cases the pattern has some elements of symmetry, involving a special relationship between the axes and angles. For instance, when there are three equal axes at right angles, the space-lattice has symmetry of the cubic type.

If we try other special relationships between the axes and angles, we find that this is not the only lattice which has cubic symmetry. Suppose the simple cubic lattice to be extended or compressed along the diagonal  $OO'$  in fig. 47, so that its three equal axes continue to make angles with each other which are

equal but are no longer right angles. When the mutual inclination is  $60^\circ$ , points of the lattice again arrange themselves in a cubic manner as in fig. 47 (b), where some points of neighbouring unit cells have been included. The cube outlined by dotted lines is not a unit cell of the space-lattice, since it has four points associated with it, but it is convenient to think of the lattice in terms of this cube, since it displays the full symmetry. We therefore speak of such a lattice as a 'face-centred cubic lattice,' since the points are at corners and face centres of a set of cubes. Another type of so-called cubic lattice is obtained when the angle between each pair of axes of the true lattice is  $109^\circ 28'$ , and this

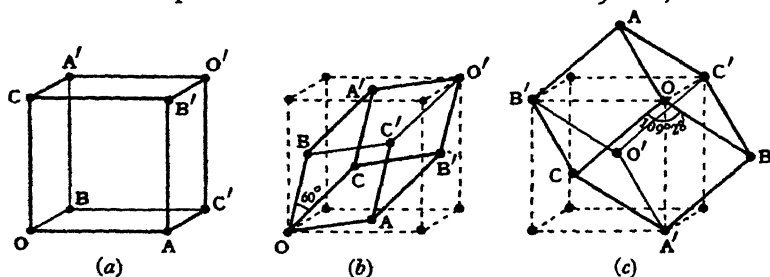


FIG. 47.—The three cubic space-lattices

is known as the 'body-centred cubic lattice' (fig. 47 (c)), the points being at corners and centres of a set of cubes. An alternative way of arriving at the form of these cubic lattices is to start with three equal axes  $OA$ ,  $OB$ ,  $OC$  making equal angles with each other, and to note that cubic symmetry occurs (a) when  $OA$ ,  $OB$ ,  $OC$  are at right angles; (b) when  $AA'$ ,  $BB'$ ,  $CC'$  are at right angles; (c) when  $OA'$ ,  $OB'$ ,  $OC'$  are at right angles. Trial shows that only these three space-lattices have symmetry of the cubic type.

Other lattices have symmetry of a special type, and in all there are fourteen kinds of space-lattice which have symmetry of seven distinct types. These correspond to the seven 'systems' in which all types of symmetry observed in crystals can be grouped.

- |                                       |   |
|---------------------------------------|---|
| Triclinic or anorthic (1).            | Three unequal axes, making unequal angles with each other.            |
| Monoclinic (2, 3).                    | Three unequal axes, one of which is at right angles to the other two. |
| Rhombic or orthorhombic (4, 5, 6, 7). | Three unequal axes at right angles.                                   |

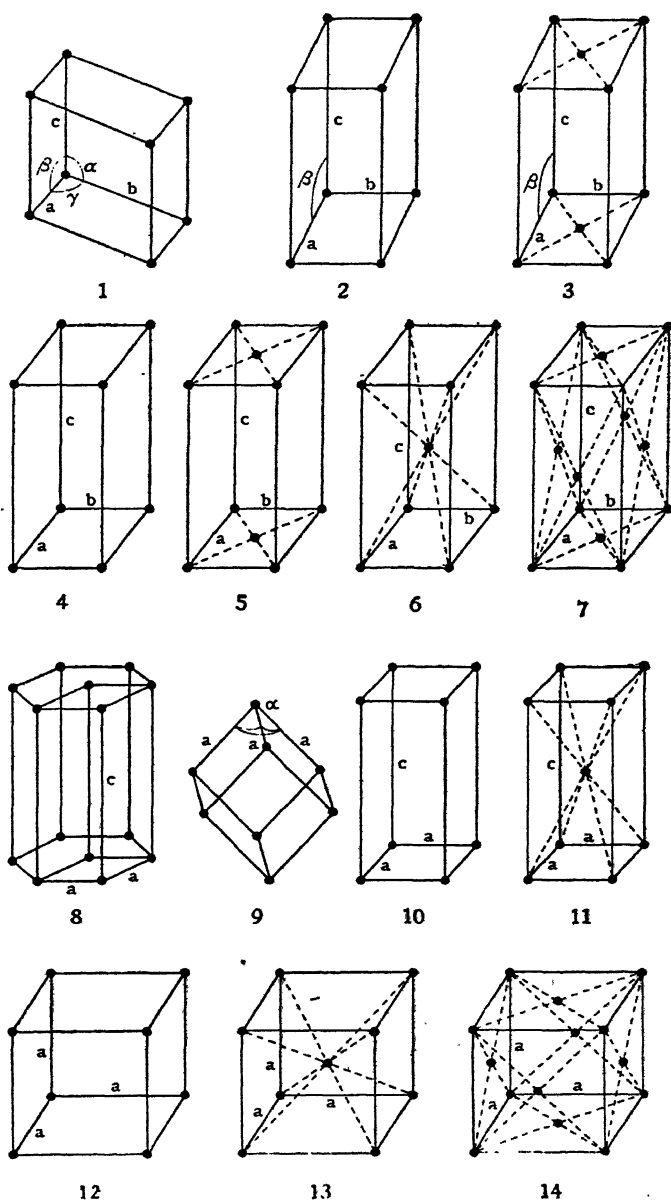


FIG. 48.—The fourteen space-lattices

1.  $P\bar{1}$ , triclinic. 2.  $P2/m$ , monoclinic. 3.  $C2/m$ , monoclinic, one face centred; other arrangements  $A2/m$ ,  $I2/m$ ,  $F2/m$ . 4.  $Pmmm$ , orthorhombic. 5.  $Cmmm$ , orthorhombic, one face centred; other arrangements  $Ammm$ ,  $Bmmm$ . 6.  $Immm$ , orthorhombic body-centred. 7.  $Fmmm$ , orthorhombic, all faces centred. 8.  $C6/mmm$ , hexagonal; other symbol  $H$  in certain space-groups. 9.  $R\bar{3}m$ , rhombohedral. 10.  $P4/mmm$ , tetragonal; other arrangement  $C4/mmm$ . 11.  $I4/mmm$ , tetragonal body-centred; other arrangement  $F4/mmm$ . 12.  $Pm\bar{3}m$ , cubic. 13.  $Im\bar{3}m$ , cubic body-centred. 14.  $Fm\bar{3}m$ , cubic face-centred.

Hexagonal (8).	Two equal axes inclined at $120^\circ$ , and a third unequal axis at right angles to them.
Rhombohedral or trigonal (9).	Three equal axes, making equal angles with each other.
Tetragonal (10, 11).	Three axes at right angles, of which two are equal.
Regular or cubic (12, 13, 14).	Three equal axes at right angles.

These special types of space-lattice are shown in fig. 48. That they are all true space-lattices can be verified by noting that it does not matter which point is taken as the corner of a cell, the arrangement of the surrounding points is always the same. It is not so immediately obvious that these are the only possible

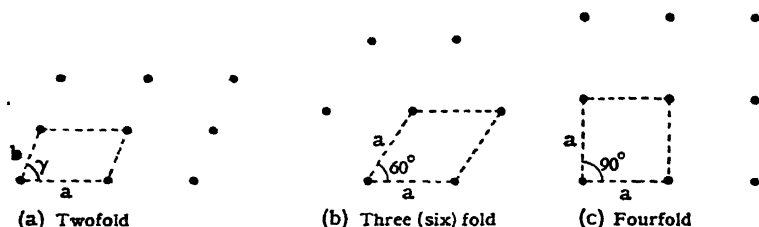


FIG. 49.—Symmetry axes at right angles to a two-dimensional net

space-lattices. We might imagine, for instance, another type of tetragonal lattice with points at the corners and face centres of a tetragonal cell. All points would then be equivalent, and so this is a true lattice. However, by referring this lattice to new  $a$  axes at  $45^\circ$  to the original axes, it becomes identical with the body-centred lattice in fig. 48, 11, so that it is not really a new type. Similarly, the monoclinic lattice with two opposite faces centred can be regarded as body-centred or centred on all faces by alternative ways of outlining the monoclinic cell.

It will be noted that the symmetry of these special space-lattices is limited to twofold, threefold, fourfold, or sixfold types. It is geometrically impossible to construct lattices with other types of symmetry, as can be seen by considering a plane network of points. This has at least a twofold axis of symmetry at right angles to the plane, as in fig. 49 (a). If the two axes are equal and inclined at  $60^\circ$  or  $120^\circ$ , the net takes the form (b), which has a sixfold axis, implying as well a threefold axis. If the two equal axes are at right angles to each other the symmetry is fourfold (c).

Other kinds of symmetry, such as five-, seven-, or eightfold, are incompatible with a continued network. A limitation to the possible symmetry of a plane network must also apply to a three-dimensional lattice.

The hexagonal lattice is unique in that it is conveniently referred to *four* axes rather than to three as in all other cases. It will be seen from the figure that, perpendicular to the  $c$  axis, there are three equal axes inclined at  $120^\circ$  to each other. To choose two arbitrarily, and name the faces accordingly, would disguise the hexagonal symmetry of the lattice. If a face makes intercepts  $a/h$ ,  $a/k$  on two of the equal axes, it can be shown that it makes an intercept  $-a/(h+k)$  on the third. Faces (or reflections) of a hexagonal lattice are therefore named as follows :

$$(h, k, \overline{h+k}, l).$$

Permutations of the first three indices and the usual reversals of signs then give all corresponding faces. For instance, the six sides of a beryl prism have indices  $(10\bar{1}0)$ ,  $(1\bar{1}00)$ ,  $(01\bar{1}0)$ ,  $(\bar{1}010)$ ,  $(\bar{1}100)$ ,  $(0\bar{1}10)$ .

### THE POINT-GROUP AND THE CLASSES OF CRYSTAL SYMMETRY

A crystal, regarded as a whole, has certain elements of symmetry. This symmetry is shown by its external form, for the more ideal the conditions under which the crystal is grown, the closer is its approach to a regular geometrical figure, such as a cube or a hexagonal prism terminated by a hexagonal pyramid. The symmetry is apparent, not only in the growth of the crystal faces, but also in all the properties of the crystal, such as its elasticity, thermal expansion, electrical conductivity, and optical constants. A description of the nature of the symmetry for each class of crystal is provided by a group of symmetry elements, which is termed collectively a *point-group*.

The conception of a point-group may be conveniently understood by considering a perfect crystal on which all faces which are of the same nature have developed to exactly the same extent. Alternatively we may represent the symmetry of any crystal by drawing from a point lines which are normal to each of the crystal faces. The group of lines will then have the symmetry of the ideal crystal, although the actual crystal may be distorted

by unequal development of corresponding faces. In some cases a plane can be drawn through the centre of the crystal such that one-half is the reflection of the other half in the plane; the crystal is then said to have a 'plane of symmetry.' A line may be drawn through the centre such that a rotation of the crystal through half a turn brings it into self-coincidence, the new position being indistinguishable from the old. The crystal is then said to have a 'twofold symmetry axis.' Threefold, fourfold, and sixfold axes are also possible. If every point of a crystal is matched by a corresponding point, such that the line

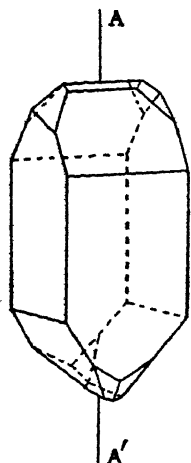


FIG. 50.—Crystal of chalcopyrite, with fourfold axis of rotatory inversion  $AA'$ .

joining the two is bisected at the centre of the crystal, there is a 'centre of inversion' or 'symmetry centre.' For instance, a cube has a centre of inversion, whereas a tetrahedron, while possessing planes and axes of symmetry, has no such centre.

Finally, there is a type of symmetry where the crystal is brought into self-coincidence by a rotation followed by an inversion. In fig. 50, for instance, the crystal has a fourfold axis of rotation-inversion. The crystal comes into self-coincidence if it is turned through  $\pi/2$  about the axis  $AA'$ , and then inverted about its centre.

The operations of reflection, rotation, inversion, and rotation combined with inversion are called 'symmetry operations.' All symmetry operations can be reduced to rotation, inversion, or rotation combined with inversion, because the operation of reflection across a plane is equivalent to a rotation through  $\pi$  about an axis normal to the plane, followed by inversion at a point where plane and axis meet, as fig. 51 shows.

Operations of symmetry are distinguished as being of the 'first' or 'second' kind. Rotations constitute operations of the first kind. If an unsymmetrical object, such as a right-hand glove, is repeated by the operation of a symmetry axis, the whole set will consist entirely of right-hand gloves. On the other hand, an inversion converts it from right hand to left hand. A plane of symmetry does the same, as follows from the equivalence of a plane to a rotation combined with an inversion. Symmetry

operations which turn 'right-handed' into 'left-handed' in this way are termed operations of the second kind.

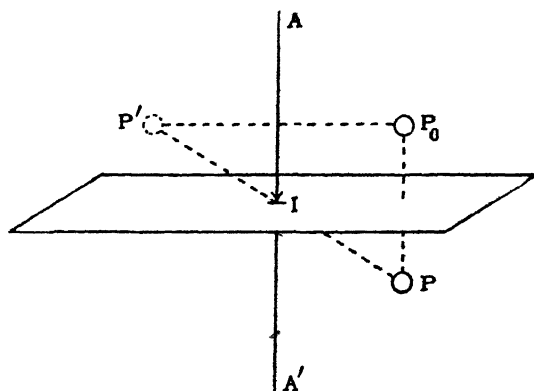


FIG. 51.—Equivalence of a twofold axis of rotatory inversion, and a reflection plane.  $P_0$  becomes  $P'$  by rotation about the axis  $AA'$ , and  $P'$  becomes  $P$  by inversion at the centre  $I$ .

A crystal has in general a number of these symmetry elements, forming an associated group which describe its symmetry, and the combination is termed a 'point-group.' We have used the idea

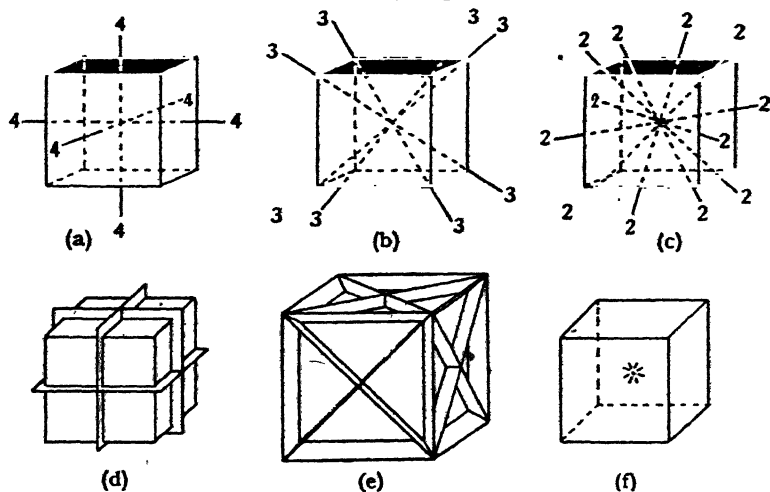


FIG. 52.—Symmetry of elements of a cubic crystal

of a perfect crystal to illustrate the nature of the point-group, but it is clearly a more fundamental property of the crystal and independent of the external form. It expresses the relationship



to each other of all symmetrically disposed properties of the crystal.

It has been seen that the space-lattices can be classified in seven systems, according to the symmetry of the special forms they assume. It follows that crystals, which are based on one or other of these lattices, fall into the same seven divisions or systems. However, the crystals which belong to any one system may have different point-group symmetry.

For instance, consider the point-group which represents the symmetry of a perfect cube. It has (*a*) three fourfold axes at right angles to each other, each passing through the centre of the cube. It has also (*b*) four threefold axes, and (*c*) six twofold axes, as shown in fig. 52. It has (*d*) three reflection planes perpendicular to the fourfold axes, (*e*) six reflection planes perpendicular to the twofold axes, and (*f*) a centre of inversion. These symmetry elements have been arrived at by considering the cube, but they are equally characteristic of any of the forms which a perfect cubic crystal can assume, as will be seen by the series of forms given in fig. 7, Chapter I.

However, all cubic crystals do not possess so high a type of symmetry, though they qualify for inclusion in the cubic system,

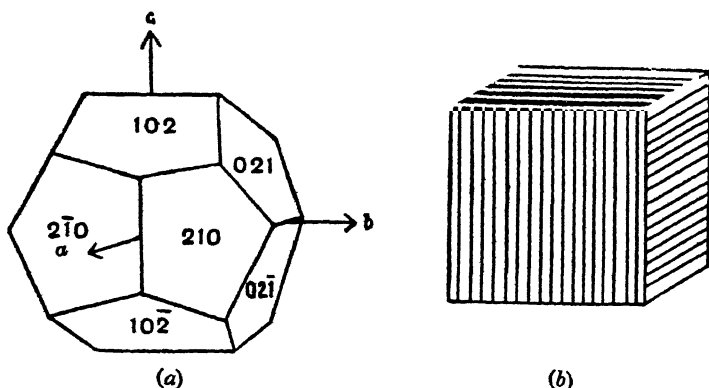


FIG. 53.—Symmetry of iron pyrites

because they can be referred to three identical axes at right angles. A crystal of iron pyrites, for instance, may grow as in fig. 53 (*a*), or show upon its cubic faces striations which are arranged as in fig. 53 (*b*). Comparing this type of crystal with the perfect cube in fig. 52, it will be seen that it possesses the elements (*b*), (*d*), (*f*), but (*c*) and (*e*) are absent, and (*a*) is replaced by three twofold axes at right angles.

Zincblende and tetrahedrite have symmetry of the type represented by a tetrahedron (fig. 54). In this case (b) and (e) are present, while (c), (d), (f) are absent. (a) is replaced by fourfold axes of *rotatory inversion*.

More than one point-group may therefore characterise crystals of a given system. Actually there are five point-groups for cubic crystals, seven for tetragonal crystals, and so forth, the total number of possible point-groups being 32. These are

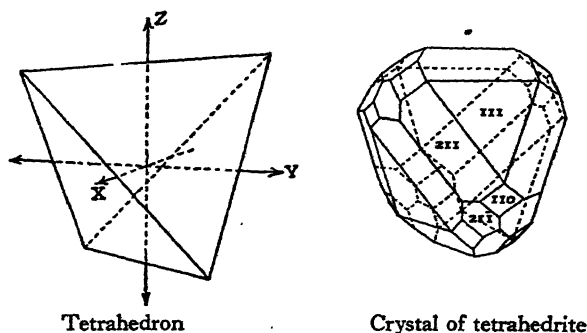


FIG. 54

(From *Mineralogy*, H. A. Miers; Macmillan, 1929)

called the *crystal classes*. Such properties as external form, optical behaviour, elasticity, thermal expansion, and electrical conductivity place a crystal in one or other of these classes.

Fig. 55 (A and B), which is taken from Miers' *Mineralogy*, illustrates the symmetry of these 32 classes.

The existence of several classes in each crystal system, such as the five classes in the cubic system, is due to the different kinds of symmetry which the unit of pattern may possess. The lattices all have the highest possible symmetry of the system to which they belong, and a crystal composed of single atoms grouped at the points of a lattice would also have this symmetry. It is possible, however, for the pattern grouped around each lattice-point to confer a lower symmetry on the structure as a whole than that of the lattice itself.

A two-dimensional example may be used as an illustration. The patterns of fig. 56 are all arranged on a square net. In fig. 56 (a) the units of the pattern are so disposed that the full symmetry of the lattice is retained, and the pattern as a whole has the highest type of 'square' symmetry. In fig. 56 (c) the units are rotated. The fourfold axes of symmetry are retained,

## THE CRYSTALLINE STATE

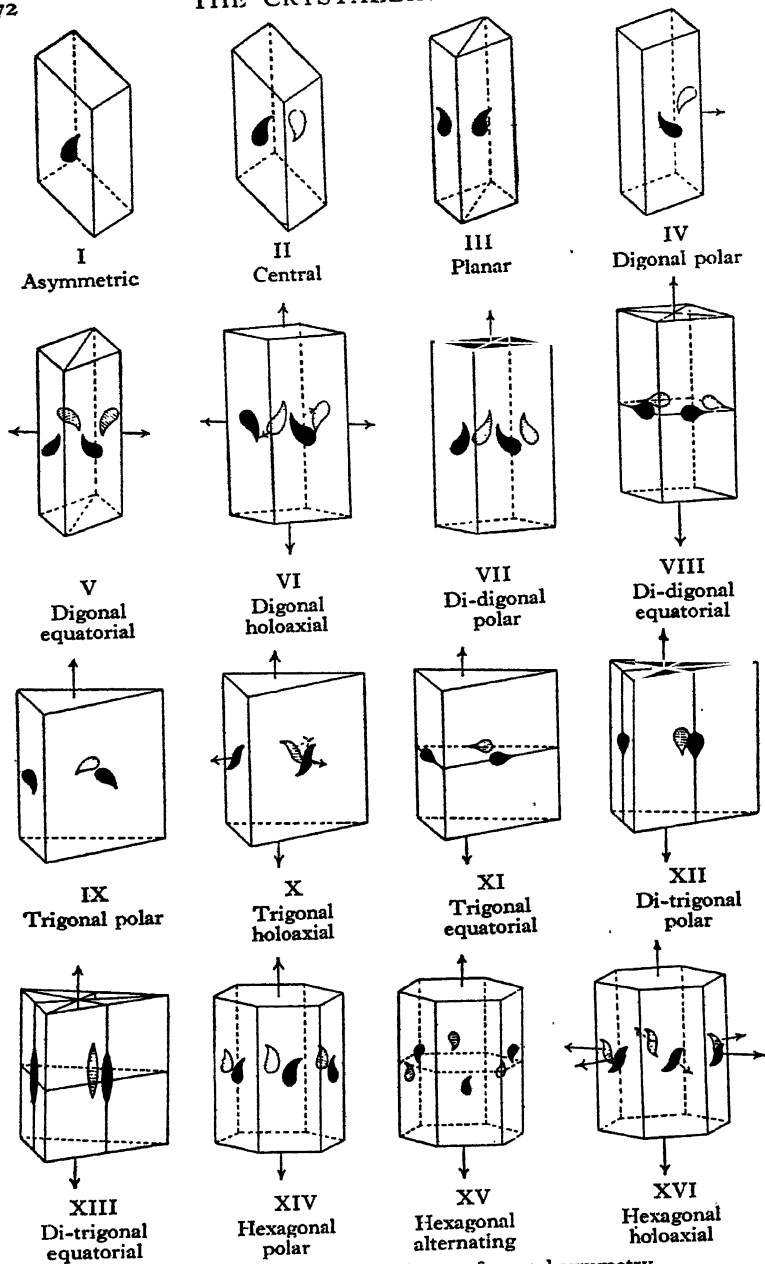
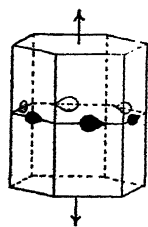
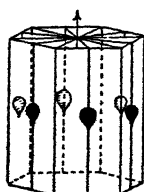


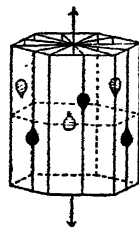
FIG. 55A.—The thirty-two classes of crystal symmetry  
(From *Mineralogy*, H. A. Miers; Macmillan, 1929)



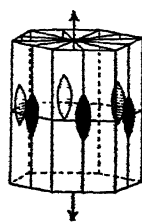
XVII  
Hexagonal  
equatorial



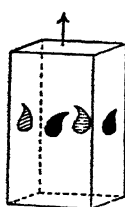
XVIII  
Di-hexagonal  
polar



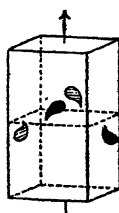
XIX  
Di-hexagonal  
alternating



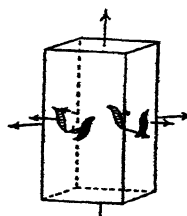
XX  
Di-hexagonal  
equatorial



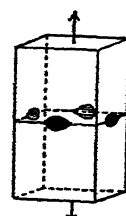
XXI  
Tetragonal  
polar



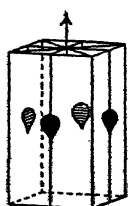
XXII  
Tetragonal  
alternating



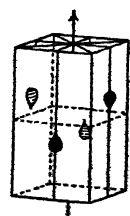
XXIII  
Tetragonal  
holoaxial



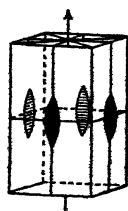
XXIV  
Tetragonal  
equatorial



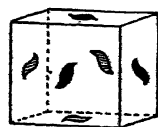
XXV  
Di-tetragonal  
polar



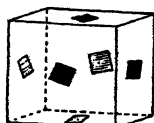
XXVI  
Di-tetragonal  
alternating



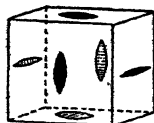
XXVII  
Di-tetragonal  
equatorial



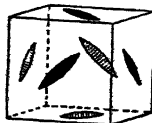
XXVIII  
Tesseral  
polar



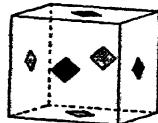
XXIX  
Tesseral  
holoaxial



XXX  
Tesseral  
central



XXXI  
Di-tesseral  
polar



XXXII  
Di-tesseral  
central

FIG. 55B.—The thirty-two classes of crystal symmetry

The symmetry is shown by etched forms  
(From *Mineralogy*, H. A. Miers; Macmillan, 1929)

but the planes of symmetry have disappeared. The pattern still belongs to the 'square' system, but to a less symmetrical 'class.' In fig. 56 (*b*) the units have no fourfold symmetry. Although they have been placed in the figure upon a similar square net (*d*), the pattern can no longer be classified in the square system. In the two former cases the symmetry of the unit led directly to the equality of the two axes at right angles, whereas in this last case the equality of the axes could only be fortuitous, and in general they might have any ratio. The number of classes

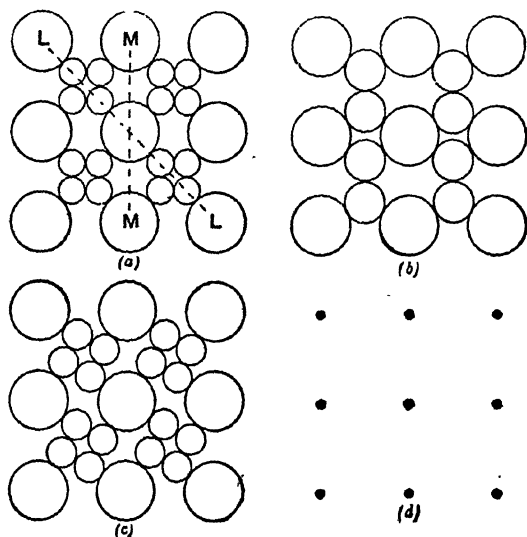


FIG. 56

in the square system is limited to two, in other words, because the unit must have such symmetry as to involve two equal axes at right angles.

In the same way the symmetry of the unit in the cubic system must be such as to involve three equal axes at right angles, and trial shows that the five point-groups are the only possible types. The same holds true for other crystal systems, and leads to the enumeration of the 32 crystal classes.

A crystal which belongs to the class of highest symmetry in a system has the maximum number of similar faces in the general form  $\{hkl\}$ . In a crystal of a lower class, half of the faces are different from the other half (*e.g.* in zincblende the tetrahedron is

formed by four faces of the octahedron {111} developing disproportionately to the other four). A crystal of the first type is called 'holohedral,' and of the second 'hemihedral,' for this reason. A still lower class, such as XXVIII in fig. 55B, is 'tetartohedral.'

### THE SPACE-GROUP

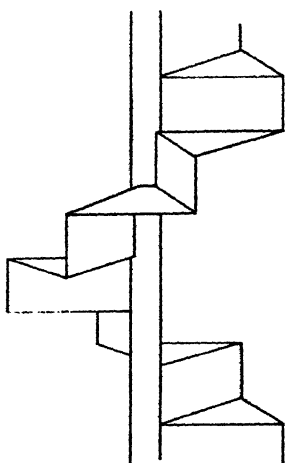
We must now consider a more detailed aspect of the crystal symmetry, the 'space-group,' or symmetry according to which the atoms in the crystal are arranged. Whereas the point-group of a crystal can be deduced from its macroscopic properties, such as external form, optical properties, etc., these properties alone do not determine the space-group, and the assigning of the appropriate space-group to particular crystals was first made possible by X-ray methods. The geometrical theory of space-groups had been developed, however, many years before its practical application became possible, and so a complete framework was ready within which the X-ray results could be incorporated.

Consider the sodium chloride structure, which is shown in fig. 31, extended indefinitely in space. The structure itself (as distinct from the crystal regarded as a single unit) possesses a number of symmetry elements. It has rotation axes, symmetry planes, and symmetry centres. These are not a limited set describing the symmetry of the whole crystal, as in the case of the point-group, but are distributed as an extended pattern in space. We can picture them as existing quite independently of the sodium chloride structure; they form a self-consistent set of operations such that any symmetry operation or lattice translation brings all the remaining symmetry operations into self-coincidence. This system of symmetry operations is collectively termed a *space-group*. In this way we have freed ourselves from the consideration of any particular structure, and it becomes a purely geometrical problem to investigate the different schemes of symmetry according to which three-dimensional patterns in general can be arranged.

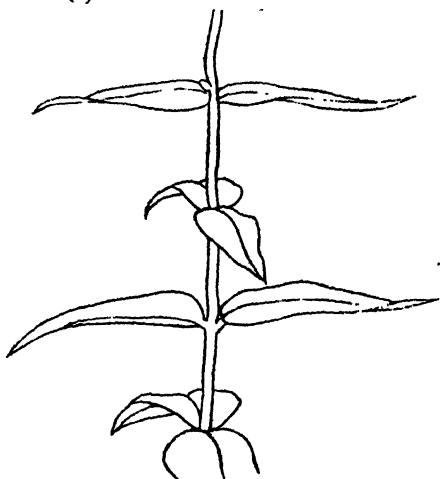
If one sodium and one chlorine atom be put in appropriate places in the space-group, and each be multiplied by all the symmetry elements, the result will be an extended sodium chloride structure. The symmetry elements of the space-group are like the mirrors of a kaleidoscope, which repeatedly reflect

a small asymmetrical collection of glass beads and other objects, and so convert it into a symmetrical pattern.

New symmetry operations are possible in a space-group which have no place in the operations of a point-group. There



$6_1$  Screw Axis (Spiral Staircase)



$4_2$  Screw Axis (Penstemon)

(b)

FIG. 57.—Examples of glide planes and screw axes. (a) Pattern based upon glide plane. (From *Line and Form*, Walter Crane.) (b) Examples of screw axes

may be *glide planes* as well as reflection planes, and *screw axes* as well as rotation axes. A glide plane is such that the structure is brought into coincidence by reflection across the plane, and a simultaneous movement of translation parallel to the plane. Many designs are arranged on this principle, such as the pattern

in fig. 57 (a). The translation must be for a distance which is one-half that of neighbouring points in the lattice, since two successive reflections and translations are equivalent to a translation of the space-lattice. The operation of a screw axis rotates the structure through an angle  $2\pi/n$ , and simultaneously translates it parallel to the axis. A common arrangement of leaves around a stem, or the steps of a spiral staircase, afford examples of this type of symmetry (fig. 57 (b)). The operation, repeated  $n$  times, is equivalent to a translation of the space-lattice. These new operations are possible, because each point of the structure need

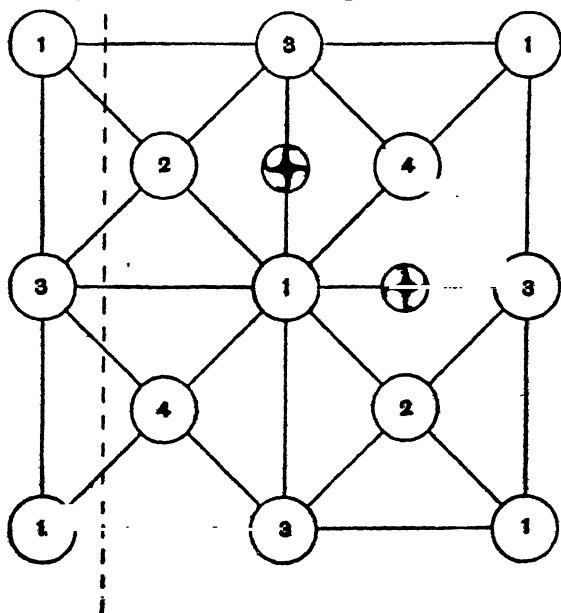


FIG. 58.—Structure of diamond, projected upon a cube face

not be finally brought back to its original position as in the case of a point-group operation, but only to a similar position in another cell of the lattice.

If the space-group contains a parallel set of either reflection planes or glide planes, the corresponding point-group has a single reflection plane parallel to this set. The translation of the glide plane is of atomic dimensions and is not apparent in the symmetry of the crystal as a unit. Similarly, a set of either rotation axes or screw axes in the space-group is represented by a rotation axis in the point-group.



Typical relations between space-group and point-group may be illustrated by examples chosen from the simple structures of the last chapter. In the case of rock-salt, the different axes and planes, and the symmetry centres, are all obvious in the structure of fig. 31. The crystal as a whole will clearly have corresponding fourfold, threefold, and twofold axes, reflection planes and a symmetry centre. Compare with this the structure of diamond, which is shown in plan in fig. 58. The atoms on the upper centred face of a unit cube are marked (1), those in the next layer

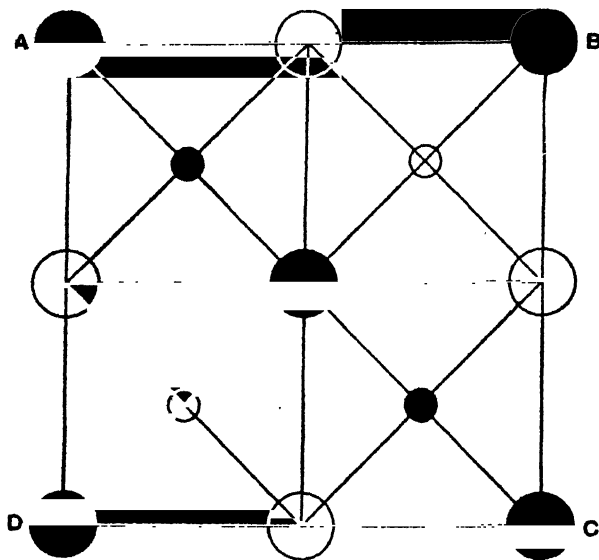


FIG. 59.—Structure of zincblende, projected upon a cube face

(centres of small cubes) are marked (2), and so forth. The diamond crystal as a whole has the highest cubic symmetry, with, for instance, fourfold axes parallel to the cube edges. The structure, however, has no fourfold *rotation* axes, as will be clear from the figure. It has only fourfold *screw* axes in the positions indicated. These axes, half of which are right-handed and the remainder left-handed, turn (1) into (2), (2) into (3), (3) into (4) in a spiral manner. Similarly, the structure has no *reflection* planes parallel to a cube face, but the dotted line in the figure shows the position of a *glide* plane. (1) is reflected across it, and translated along and downwards so as to turn into (2), when (2) turns into (3), (3) into (4), and so forth, by the same movement.

These screw axes and glide planes give the crystal as a whole the symmetry of fourfold rotation axes and reflection planes.

The structure of zincblende,  $\text{ZnS}$ , is very similar to diamond, and is shown in fig. 59. The large black circles are zinc atoms on the upper face of the unit cell; then come smaller black circles representing sulphur, then zinc (large white) sulphur (small white) on successive layers, as in the former figure. Comparing this with the diamond structure, it will be seen that the non-equivalence of zinc and sulphur has destroyed the fourfold screw axes and the glide planes parallel to the cube faces. The whole crystal, therefore, has no corresponding rotation axes or symmetry planes. There are reflection planes parallel to  $(110)$ , and fourfold axes of rotatory inversion parallel to  $[100]$  through each zinc and sulphur atom, and such elements give the crystal the point-group symmetry of a tetrahedron. This difference may be expressed in various ways. In diamond, each atom is at the centre of a tetrahedral group of four others, but the tetrahedra around any nearest pair of atoms face opposite ways, so the symmetry as a whole is the highest cubic type. In zincblende the tetrahedral groups of sulphur atoms around each zinc atom all point the same way, and the crystal as a whole must reflect this tetrahedral arrangement.

The  $[111]$  axes of the  $\text{ZnS}$  crystals are 'polar,' having a difference in nature between opposite ends. This is shown, for example, by an opposite electrification of the two ends when the crystal is warmed or cooled. In proceeding along an axis in one direction the pairs of atoms are encountered in the order sulphur-zinc, whereas in the opposite direction the order is zinc-sulphur. The same is true of the sheets of atoms parallel to  $(111)$  which occur in pairs, described in the case of diamond. The order is  $\text{C} \cdot \text{C} \dots \text{C} \cdot \text{C} \dots \text{C} \cdot \text{C}$  in diamond, whereas in zincblende it is  $\text{Zn} \cdot \text{S} \dots \text{Zn} \cdot \text{S} \dots \text{Zn} \cdot \text{S}$  for the one direction, and  $\text{S} \cdot \text{Zn} \dots \text{S} \cdot \text{Zn} \dots \text{S} \cdot \text{Zn}$  for the other. It follows that the crystal faces  $(111)$  and  $(\bar{1}\bar{1}\bar{1})$  will have a different character in zincblende, though they are identical in diamond.

If a model of iron pyrites is projected on a cube face, it will have the appearance of one of the forms shown in fig. 60; we will assume it to be that on the left. The structure has no fourfold axes, for the sulphur atoms in the projection are in vertical pairs. When the model is turned around so that we view a neighbouring face, the projection changes to that shown on the

right. A property of the crystal which was vertical for the one face has become horizontal for the other. Such a relationship

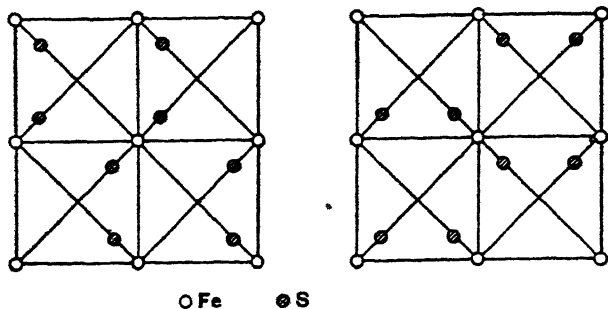


FIG. 60.—Structure of pyrites, projected upon two adjacent cube faces

explains the peculiar symmetry of iron pyrites which is shown in fig. 53. Experiment shows that the striations on each cube face are parallel to the pairs of sulphur atoms in the projection on

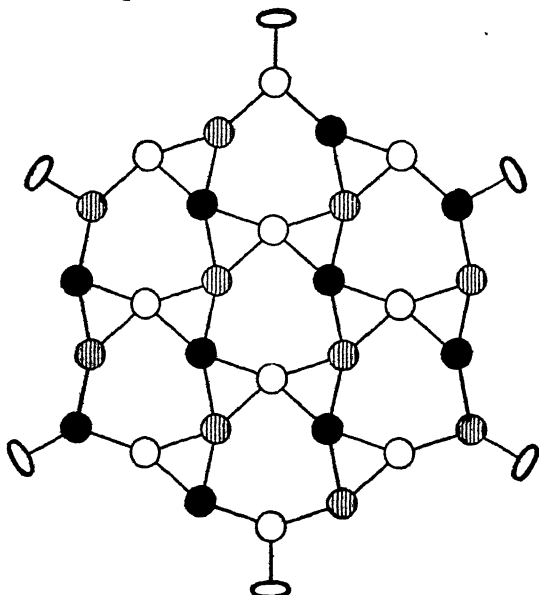


FIG. 61.—Projection of the silicon atoms of a quartz

that face. Without attempting to explain why the striations are in the one direction rather than the alternative direction at right angles, we can see that the underlying structure gives these two directions different properties.

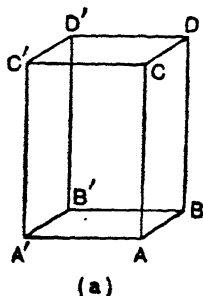
The structure of  $\alpha$ -quartz,  $\text{SiO}_2$ , is illustrated in fig. 61, viewed in a direction along the threefold axis. The positions of the silicon atoms are alone indicated; actually each silicon atom lies between four oxygen atoms, two of which are slightly above it and two below it in the figure, so that the four form a tetrahedral group with the silicon at the centre. The successive layers of silicon atoms are shown as black, shaded, and plain circles. The threefold axes are *screw* axes, which turn black into shaded, shaded into plain, and plain into the next layer of black. The figure shows that (in contrast to the diamond structure already considered) the screw axes are all in the same sense. Now quartz crystals are of two kinds, right- and left-handed; polarised light travelling along the threefold axis may have its plane rotated in the one direction or the other according to the kind of crystal. We again see how the symmetry of the crystal as a whole is related to the symmetry of the atomic pattern. The structure has only threefold screw axes and twofold axes at right angles to them. The point-group of the crystal has therefore threefold and twofold rotation axes, but no centre of symmetry, and the crystals can be right-handed or left-handed.

### THE 230 SPACE-GROUPS

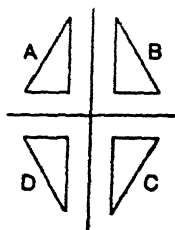
These examples illustrate the nature of the space-group. It is an extended network of reflection planes or glide planes, of rotation axes or screw axes or axes of rotatory inversion, and of centres of inversion, which is based on a space-lattice or system of translations which relate identical points in the structure. We can picture a space-group as existing quite independently of any particular atomic arrangement. Its operations are self-consistent in that any symmetry operation or translation brings all the others into self-coincidence. The space-group is a property of three-dimensional patterns in general, and it is a problem of pure geometry to find how many ways there are of arranging symmetry elements in space. There are many more space-groups than crystal classes, for it has been seen in the case of rock-salt and diamond that two crystals belonging to the same class can be based on a completely different pattern of symmetry elements. The enumeration of the different types of space-group was made independently by Schoenflies, Fedorov, and Barlow, who showed that the number, though large, is limited, and that in all

there are 230 space-groups distributed amongst the 32 crystal classes.

To see how it is that so many possibilities arise, we may take the case of one set of space-groups and illustrate the different possibilities. We will suppose that an orthorhombic pattern is based upon the simple lattice of fig. 62 (a), and that the pattern as a whole has a point-group symmetry represented by two reflection planes at right angles. In how many ways may an asymmetrical unit of pattern be arranged so that this point-group symmetry is achieved?



(a)



(b)

FIG. 62

it could not then have symmetry about two planes at right angles. The orientations marked B, C, D must also occur somewhere in the structure. The upper face of the triangle is supposed to differ from the lower side, since there is no symmetry plane parallel to  $ABA'B'$  in the figure.

The simplest way of arranging the triangles would be to put four at each corner of the lattice, as in the first example of fig. 63. The space-group of this pattern has itself reflection planes corresponding to the reflection planes of the point-group. We can find, however, nine other ways of arranging the triangles, all of which lead to a point-group with two reflection planes. This is done by introducing *glide planes* into the space-group. The translation of the glide plane may be parallel to a horizontal edge or to a vertical edge (these are to be reckoned as different, because the reflection planes of the crystal are vertical), or it may be from the corner to the centre of a vertical face. The permutations of these possibilities lead to the ten arrangements shown in the figure. The unit of the structure is in each case a group of four triangles with the different aspects of fig. 62 (b).

There are other space-groups belonging to the same crystal

class. We have only enumerated those which are based on a simple orthorhombic lattice, and the lattice may be centred on

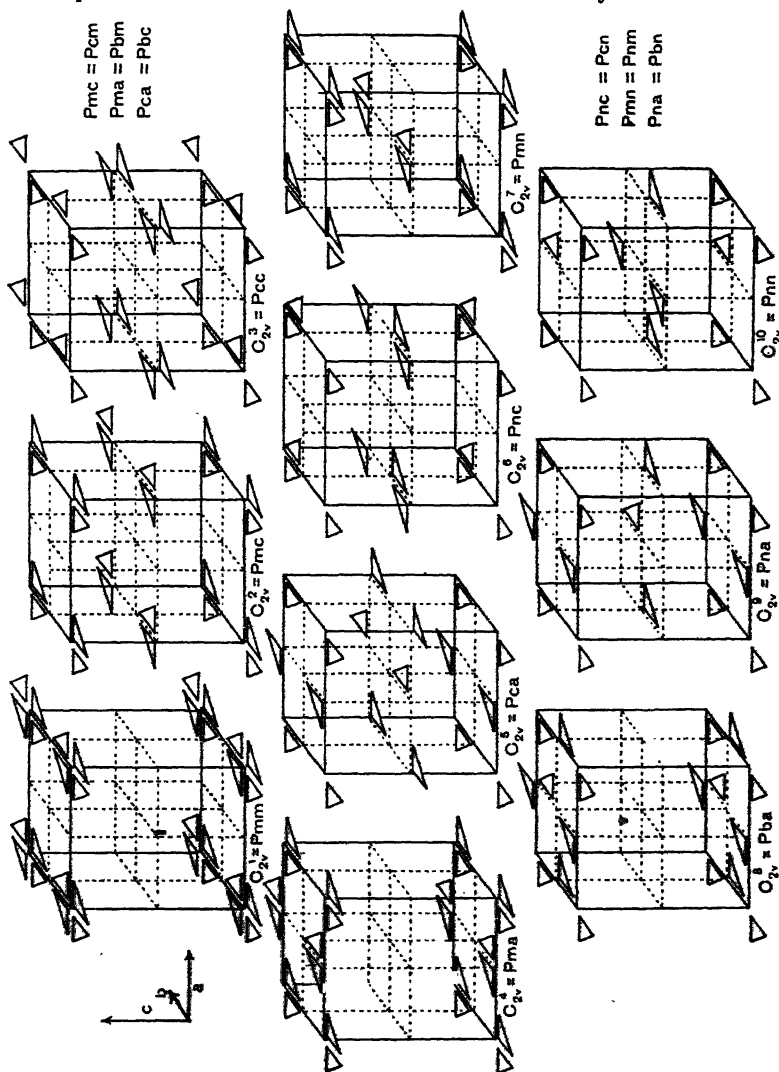


FIG. 63.—The ten space-groups of the orthorhombic polar class, based upon a primitive lattice

one face, or on all faces, or be body-centred as in fig. 64. Examination shows that there are seven further arrangements belonging to the first of these lattices, two to the next, and three to the last. There are in all twenty-two possible arrangements of the un-symmetrical triangles which give the required symmetry.

The same enumeration must be carried out for each of the 32 classes, and it will be clear why the total number is so large.

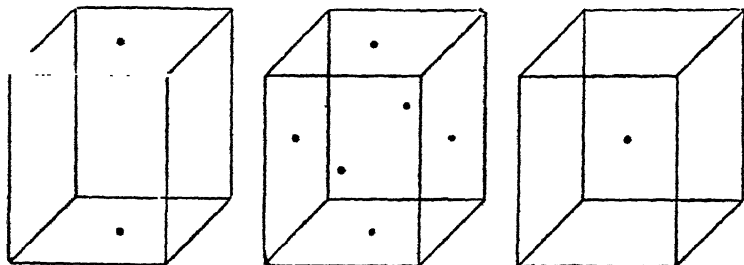


FIG. 64

The number of space-groups in all classes of each system is as follows :

Cubic	.	.	.	.	.	.	.	36
Tetragonal	.	.	.	.	.	.	.	68
Rhombohedral and hexagonal	.	.	.	.	.	.	.	52
Orthorhombic	.	.	.	.	.	.	.	59
Monoclinic	.	.	.	.	.	.	.	13
Triclinic	.	.	.	.	.	.	.	2

### SPACE-GROUP NOTATION

The notation of the space-groups which was originally proposed by Schoenflies has been hitherto generally adopted. In the notation a symbol is used to designate the point-group, such as  $C_{2v}$  for the holohedral monoclinic system. Indices are then added to distinguish the various space-groups which have this point-group symmetry, in this case

$$C_{2v}^1, C_{2v}^2, C_{2v}^3, C_{2v}^4, C_{2v}^5, C_{2v}^6.$$

The order of the groups in each class is that of their derivation by Schoenflies.

Recently a new notation has been adopted by wide consent on the part of those engaged in crystal analysis. This notation has the advantage that it both labels the space-group with a brief and convenient symbol, and indicates its symmetry elements in a kind of shorthand. Anyone familiar with the conventions could draw a diagram of a space-group with its complete set of symmetry elements, when given the symbol for it. A symbolism

of this type was first drawn up by Hermann, and the present form is a simplified version due to Mauguin.

The symbol consists of a series of letters and numbers. The designation of the lattice comes first. P denotes a simple or primitive lattice; A or B or C, lattices which are centred on the  $a$ ,  $b$ ,  $c$  faces respectively; F, a lattice which is centred on all faces; and I, a body-centred lattice. The symbols describing the lattices in fig. 48 illustrate the use of these letters.

A special provision has to be made for the rhombohedral and hexagonal systems, which are interrelated in an intricate way. Crystals belonging to the same class may be based either on a hexagonal or a rhombohedral lattice. In the former case it is sometimes convenient to refer the crystal to the primitive hexagonal cell, and sometimes to a larger cell with its  $a$  axes at right angles to those of the primitive cell. C and H are used for these alternatives, C being chosen because the hexagonal lattice may be regarded as an orthorhombic lattice with its C face-centred.

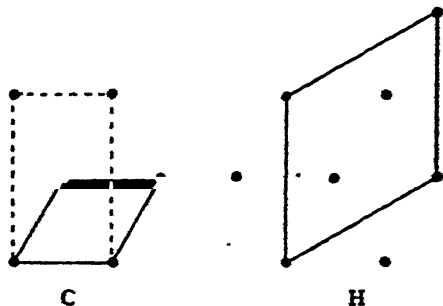


FIG. 65.—Alternative methods of outlining a hexagonal cell. The dotted lines indicate the orthorhombic cell, which it is often convenient to use because its axes are at right angles

Fig. 65 explains the two methods of outlining the unit cell. The rhombohedral lattice, though it might be termed P, as it is primitive, is for convenience given the special symbol R.

The next symbol in general denotes the principal axis of the crystal. Rotation axes are denoted by 1, 2, 3, 4, 6. 1 signifies no symmetry, since any structure must come back into coincidence after a complete rotation. Axes of rotatory inversion are  $\bar{1}$ ,  $\bar{2}$ ,  $\bar{3}$ ,  $\bar{4}$ ,  $\bar{6}$ .  $\bar{1}$  implies a simple centre of inversion, and, as we have already seen,  $\bar{2}$  is equivalent to a reflection plane. Reflection planes are so important a feature of the structure that the symbol for a plane,  $m$ , is written instead of  $\bar{2}$ . If the principal axis of the crystal has a reflection plane at right angles to it, this is written as part of its symbol, i.e.  $2/m$ ,  $3/m$ ,  $4/m$ ,  $6/m$  (see again fig. 48).

'Secondary' axes may also be present in the point-group, in



general at right angles to the principal axis, or secondary reflection planes parallel to the principal axis. In the particular case of the cubic system the secondary axes are the threefold axes inclined to the principal axis. Appropriate symbols for these elements follow those for the primary elements. Tertiary axes (such as those parallel to  $(11\bar{2}0)$  in the hexagonal system or  $(110)$  in the tetragonal system) or the corresponding planes come next in order.

The following scheme gives the point-group symbols for the 32 crystal classes, in both the Schoenflies notation and the new notation. The Roman numerals correspond to the diagrams in fig. 55, but the classes have been rearranged so as to show their analogies more clearly.

I $C_1=1$	II $C_2=\bar{1}$					
IV $C_2=2$	III $C_2=m$ ( $=\bar{2}$ )	V $C_{2h}=2/m$		VII $C_{2v}=2mm$	VI $V=222$	VIII $V_h=mmm$
IX $C_3=3$	XV $C_{3i}=\bar{3}$			XII $C_{3v}=3m$	X $D_2=32$	XIX $D_{3d}=\bar{3}m$
XXI $C_4=4$	XXII $S_4=\bar{4}$	XXIV $C_{4h}=4/m$	XXVI $V_4=\bar{4}2m$	XXV $C_{4v}=4mm$	XXIII $D_4=42$	XXVII $D_{4h}=4/mmm$
XIV $C_6=6$	XI $C_{2h}=\bar{6}$	XVII $C_{6h}=6/m$	XIII $D_{2h}=\bar{6}m$	XVIII $C_{6v}=6mm$	XVI $D_6=62$	XX $D_{6h}=6/mmm$
XXVIII $T=23$		XXX $T_h=m\bar{3}$	XXXI $T_d=\bar{4}3m$		XXIX $O=432$	XXXII $O_h=m\bar{3}m$

In the space-group there may be rotation or screw axes, and reflection or glide planes, and a very neat notation is used to indicate their nature.

Fig. 66 shows the five different types of hexagonal screw axis. The numbers within the circles denote the height of each with respect to the plane of the diagram. 0 and 6 are at top and bottom of the unit cell, and the other numbers are equally spaced between these extremes.  $6_1$  implies an axis that rotates through  $1/6$  of a turn in a clockwise direction, and translates a distance  $c/6$  in the same sense as a right-handed screw. It thus turns 0 into 1, 1 into 2, etc., in fig. 66.  $6_2$  rotates through  $1/6$  of a turn, and translates a distance  $2c/6$ . It turns 0 into 2, 2 into 4, and 4 into 6, which is equivalent to 0. The other relations follow in a similar

way. Note that  $6_5$  is similar to  $6_1$ , but in the opposite sense, and that the same is true for  $6_4$  and  $6_2$ .  $6_3$  may be regarded as either

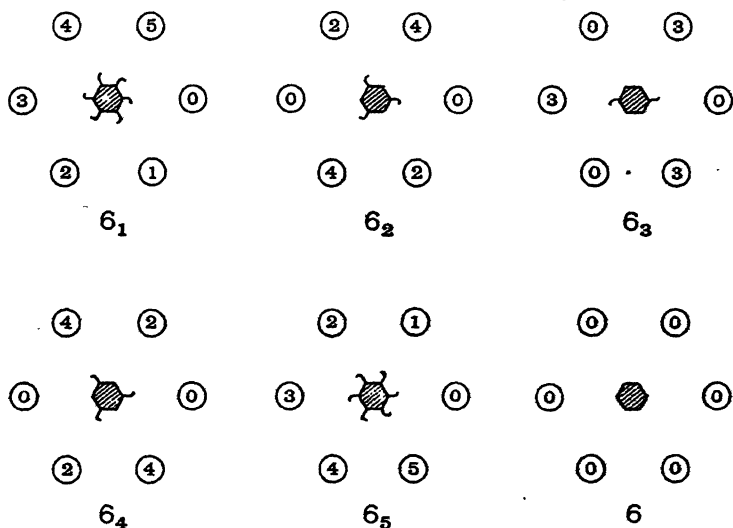


FIG. 66.—The different types of hexagonal screw axis

right- or left-handed. We can thus denote the direction of the screw as well as its nature. The complete set of axes is as follows :

6	$6_1$	$6_2$	$6_3$	$6_4$	$6_5$	also	$\bar{6}$
4	$4_1$	$4_2$	$4_3$			„	$\bar{4}$
3	$3_1$	$3_2$				„	$\bar{3}$
2	$2_1$					„	$\bar{2}$
1						„	$\bar{1}$

Glide planes are distinguished by their movement of translation.  $m$  is a reflection plane, as stated above.  $n$  implies a glide plane with a translation from the corner to the centre of the face which is parallel to the plane.  $a$ ,  $b$ ,  $c$  are glide planes with translations of  $a/2$ ,  $b/2$ ,  $c/2$  respectively. In some cases (*e.g.* diamond described on p. 78) translations of one-quarter of a face-diagonal occur, denoted by  $d$ . The ten orthorhombic space-groups in fig. 63 illustrate the indexing of the glide planes and reflection planes. Trial will show that these ten groups include all possible combinations of the planes  $m$ ,  $n$ ,  $a$ ,  $b$ ,  $c$ , if it is borne in mind that the  $a$  and  $b$  axes are interchangeable, but are different in character to the  $c$  axis to which the planes are parallel.

It is not possible to give a full account of the nomenclature here, and such an account could hardly be clear without a knowledge of the various space-groups. The general principle is that only such symmetry elements are included in the symbol as determine the space-group uniquely, the remainder being omitted since they follow as a necessary consequence. A few instances may be given.

$Pmmm$  is a space-group based on a primitive lattice with three reflection planes at right angles—therefore an orthorhombic space-group. It is not necessary to include the twofold axes, as these follow from the reflection planes.

$Pnma$  is also an orthorhombic space-group,\* since there are three planes at right angles.  $n$  indicates a glide plane perpendicular to the  $a$  axis, with translation  $b/2 + c/2$ .  $m$  is a reflection plane perpendicular to the  $b$  axis.  $a$  is a glide plane perpendicular to the  $c$  axis, with translation  $a/2$ . This illustrates the further point that the symbol shows how the crystal has been 'set up,' i.e. which axes of the space-group have been chosen as  $a$ ,  $b$ ,  $c$  axes. The same space-group, oriented differently, might be

$$Pnam; Pbnm; Pcmn; Pmnb; Pmcn.$$

$Fm\bar{3}m$  is a cubic space-group with reflection planes perpendicular to both  $\{100\}$  and  $\{110\}$ , based on a face-centred lattice. The symbol  $\bar{3}$  indicating a *secondary threefold axis* is sufficient to identify the lattice as cubic, since no other system has such axes. This is the space-group of the rock-salt structure.

It is desirable to memorise the conventions of this nomenclature, not only because they form a convenient basis for the study of space-groups, but also because they embody the rules by which space-groups can be recognised by means of X-rays, as described in the next chapter. Until the advent of X-ray analysis the theory of space-groups had little practical application in crystallography, because it was not possible to assign the appropriate space-group to any given crystal. It is now of fundamental importance in crystal analysis, and it is interesting to see how the new results fit into the framework prepared many years before.

A list of space-groups is given at the end of this volume.

\* This frequently occurring space-group is described in detail in the next chapter. It is Schoenflies'  $V_h^{16}$ .

## CHAPTER VI

### THE PRINCIPLES OF STRUCTURE ANALYSIS

THE general principles of structure analysis may now be reviewed in a more systematic manner.

The first step in the analysis of a new structure is the determination of its space-lattice and space-group. The determination of the space-group is a necessary preliminary when dealing with a structure of any complexity, and we must see how it is possible to carry it out by X-ray analysis. The measurement of the space-lattice, combined with a knowledge of the density of the crystal and its chemical constitution, determines the numbers of atoms of each kind in the unit of pattern. All these processes can be carried out by following definite rules. Though they require care if mistakes are to be avoided, they are essentially mechanical.

The final process of discovering the positions of the atoms is the difficult part of an analysis, and there is no well-defined road to success. The analysis of the structure is made by intelligent guessing. A plausible arrangement of atoms is sought for, and this is tested by comparing the observed intensities of reflection with those which the assumed structure would give. The 'structure amplitude' which is used in this comparison expresses the dependence of the intensity upon the arrangement of the unit of pattern.

The more the investigator is familiar with the probable features of atomic arrangement in the type of crystal he is studying, the more rapid his success will be in divining the true structure without an excessive number of barren trials along wrong lines. The positions of the atoms depend upon a very large number of parameters, and the observations may extend to several hundred diffracted beams. An exhaustive test of all combinations of parameters is of course impossible. The labour is shortened in various ways, of which a brief account is given in the following sections.

THE DETERMINATION OF SPACE-LATTICE AND SPACE-GROUP  
BY X-RAY METHODS

A study of the external forms and other properties generally makes it possible to assign a crystal to one or other of the 32 classes, but gives no clue to the space-group or even the space-lattice. On the other hand, the space-lattice can always be measured by X-ray methods, and the space-group can also be found, provided that the crystal class is known. The determination of the space-group is possible, because the observations

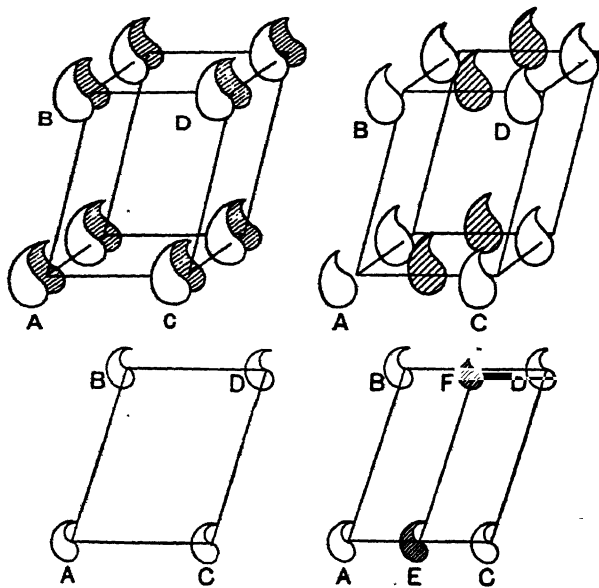


FIG. 67.—Absent spectra owing to glide plane

discriminate between a reflection plane or a glide plane, and between a rotation axis or a screw axis.

Fig. 67 is a representation of the unit cells of two simple monoclinic patterns, in which an asymmetric group of molecules is represented as a comma. Both structures would have the same point-group symmetry, consisting of a reflection plane parallel to ABCD, but in one the symmetry is due to reflection planes in the space-group, whereas in the other it is due to glide planes. A reflection turns the white comma into a black comma, and in the second case the reflection is accompanied by a translation of  $AC/2$ . When experimental measurements are made of

the reflections from many planes of these two patterns, spacings of the planes deduced from these spectra will in general be the same for both, being those characteristic of the unit cell. There will be a difference, however, in the reflections from all sets of planes perpendicular to ABCD, which will discriminate between the two space-groups.

The projections of the unit cells on ABCD are shown in the lower two figures. In the one case, the black and white commas are superimposed, while in the other the black comma is midway between the two white commas. From this point of view the axis of the second unit cell will appear to be AE and not AC, and only such reflections will occur as correspond to a cell AEFB. If AC and AB are taken to be the  $a$  and  $c$  axes, with  $b$  perpendicular to them, the reflections under discussion will have indices  $hol$ . For the one crystal, all values of  $h$  and  $l$  will appear in the indices of the  $hol$  reflections, whereas for the other, reflections corresponding to even values of  $h$  will alone appear. This rule only applies when  $k$  is zero, since from other points of view the black comma will not be similar in outline to the white commas nor half-way between them. The reflections  $hol$  therefore reveal the nature of a reflection or glide plane parallel to (010). If all reflections with an odd value of  $h$  or  $l$  are absent, the translation of the glide plane is  $a/2$  or  $c/2$  respectively. If odd values of  $h+l$  are absent, the translation is  $a/2+c/2$ , because the face appears to be centred in the projection. If all values of  $h$  and  $l$  occur, the plane is a reflection plane of the space-group.

The existence of a screw axis is shown by the absence of certain orders of reflection from the face at right angles to the axis. Fig. 68 shows, for example, a threefold screw axis which turns atom 1 into 2, 2 into 3, and so forth. The  $c$  axis of the crystal, to which the screw axis is taken to be parallel, has a length equal to the distance between 1 and 4. The sheets of atoms perpendicular to the axis are repeated three times in the length  $c$  at equal intervals, as the horizontal dotted lines show. Hence the only orders of reflection possible are the third, sixth, ninth, etc., or, in other words,  $l$  must be a multiple of 3. Planes not perpendicular to the axis have their full spacing, as is shown by the inclined dotted lines.

In this way a screw axis can be distinguished from an axis of simple rotation, which produces no absent spectra, and the

translation of the screw axis can be determined by noting which orders are absent.

It is therefore possible to tell whether a reflection plane of the crystal corresponds to reflection planes or to glide planes in the space-group, and whether a symmetry axis of the crystal corresponds to rotation axes or screw axes of the space-group, the translations being also determined for the latter alternatives. Since each space-group in a crystal class is distinguished from the others by its possession of characteristic sets of reflection or

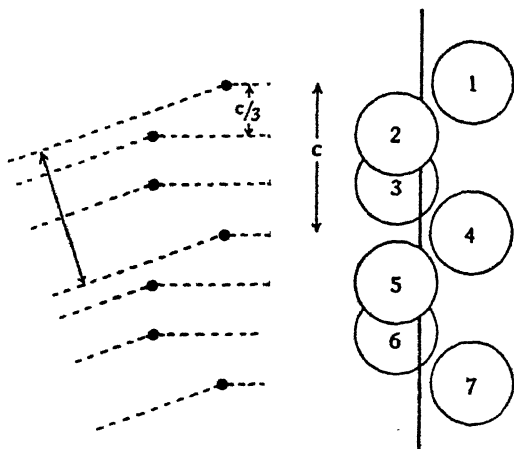


FIG. 68.—Absent spectra owing to screw axis

glide planes, and rotation or screw axes, it is possible to assign to a crystal one of the 230 space-groups. Systematic tables for this purpose have been prepared by Niggli, Wyckoff, and Astbury and Yardley, and such tables are given in a later volume.

The true values of  $hkl$  cannot be assigned to the reflections, and so the absence of sets of reflections demonstrated, until the dimensions of the unit cell are determined. For example, the measured spacing of the planes parallel to  $(0001)$  in quartz is 1.79 Å. This may either be due to a  $c$  axis 1.79 Å. in length, or to a  $c$  axis 5.37 Å. in length combined with threefold screw axes. The latter alternative is recognised to be correct, because all other planes than those parallel to  $(0001)$  indicate a  $c$  axis 5.37 Å. long. It is a universal rule that the smallest unit cell which is consistent with assigning integers  $hkl$  to all reflections is a true cell of the lattice. If a trial set of axes is chosen, and the corresponding values of  $h$  prove to be always even, it means that

the true  $a$  axis is half the assumed length. If some of them are fractional, a longer  $a$  axis must be taken. The layer lines of a rotation photograph about each axis in turn provide the most ready means of finding the lengths of the axes, since so wide a review of reflections of all types is obtained.

Another point must be borne in mind. Axes are so chosen as to be in accord with the symmetry of the crystal, and in many cases this involves a unit cell which is not a simple cell of the lattice. If the cell is body-centred,  $h+k+l$  will be even for *all* reflections. If the  $a$  face of a cell is centred,  $k+l$  will be even for *all* reflections, and similarly for other faces.\* These are characteristics of the lattice itself, which are independent of glide planes or screw axes, and can be recognised because the limitations apply to reflections of every type and not to particular sets.

To sum up, the choice of the correct crystal axes, the discrimination between simple or face-centred or body-centred cells, and the recognition of missing sets of spectra due to glide planes or screw axes, are all interwoven in such a way that analysis must be carried out systematically. The crystal axes must first be measured by a method which establishes their length without ambiguity, such as that of the rotation photograph. Indices  $hkl$  are then assigned to all the observed reflections, and missing sets of spectra are looked for. If some limitation applies to the general reflections  $hkl$ , the cell is body-centred or face-centred. A further limitation applying only to a special set of indices associated with a zone, or to orders of reflection from a plane, must be due to a glide plane or screw axis respectively. The nature of the limitation gives the amount and direction of the translation involved in the glide plane or screw axis. The tables are then used in order to see which space-group has corresponding symmetry operations.

#### FRIEDEL'S LAW

The complete process of space-group determination cannot be carried out by X-ray analysis alone, because the X-ray measurements cannot distinguish between the presence or absence of a centre of inversion. Other tests must be used to determine this point.

In a crystal which has no centre of inversion, the general

\* The discussion of the three types of cubic lattice on p. 44 illustrates this point.



face ( $hkl$ ) has different properties to the face ( $\bar{h}\bar{k}\bar{l}$ ). This difference is due to a reversal in the order in which the atomic sheets are encountered, in proceeding in one direction or the other normal to the faces. Zincblende, discussed in the last chapter, is an example; the order is ZnS . . . ZnS . . . ZnS in one direction perpendicular to (111), and SZn . . . SZn . . . SZn in the reverse direction. The reflected beam is due to the resultant of the waves reflected by zinc and sulphur sheets. When two or more waves of given amplitude, with given phase differences between them, are combined into a resultant wave, the magnitude of the resultant will be the same if the signs of the phase differences are all reversed. Hence the intensities of reflection from ( $hkl$ ) and ( $\bar{h}\bar{k}\bar{l}$ ) will be identical. No method of X-ray measurement can distinguish between these two faces, and a crystal which has no centre of inversion appears to belong to a more symmetrical type which has such a centre. A Laue photograph of zincblende, for instance, taken with the incident rays parallel to [100], has perfect fourfold symmetry (see fig. 9, A, Pl. I, p. 12) although the crystal itself has only a twofold axis in this direction. The addition of a centre of inversion to the symmetry elements already possessed by zincblende would raise it to the highest class of the cubic system, and the photograph has the corresponding symmetry.

This addition of a centre of inversion in X-ray diffraction pictures was first explained by Friedel and is generally known as Friedel's Law. It is necessary to test for a centre of inversion by other characteristics of the crystal, such as its external form, the shape of the etch figures on its faces when it is acted on by a solvent, or the pyro-electric property which endows opposite faces of the crystal with opposite electrical charges when its temperature is altered.

Friedel's Law is only true if the phase difference between the waves reflected from the atomic sheets is the same in magnitude for reflections  $hkl$  and  $\bar{h}\bar{k}\bar{l}$ . In general this condition is obeyed to a sufficient approximation, but it may not hold. If the wavelength of the radiation is in the neighbourhood of the absorption edge of one set of atoms, it is found that an anomalous phase change on scattering by these atoms exists. In contrasting reflections by ( $hkl$ ) and ( $\bar{h}\bar{k}\bar{l}$ ), the sign of this anomalous phase change is not reversed, while all phase differences due to the positions of the atoms are reversed, and hence the resultant waves

have a somewhat different amplitude. Coster and Prins, for instance, have been able to demonstrate the breakdown of Friedel's Law by reflecting from (111) and ( $\bar{1}\bar{1}\bar{1}$ ) of zincblende a group of X-ray spectral lines whose range of wave-lengths includes the zinc absorption edge, and showing that the relative intensities of the lines differ in the two cases.

In iron pyrites, the departure from the highest cubic symmetry is shown by such crystal forms as in fig. 53 (a), p. 70. Instead of the four faces (210), (2 $\bar{1}$ 0), (201), (20 $\bar{1}$ ) around the  $a$  axis, only (210) and (2 $\bar{1}$ 0) appear. Since the crystal has a symmetry centre, the difference between the two sets of planes must be of another type than that in zincblende. Fig. 69 shows a plan of the atomic arrangement parallel to (210) and (201). This different arrangement and the consequent lower symmetry can of course be distinguished by X-ray methods. The 210 planes have twice as great a 'spacing' as the 201 planes, and the first-order spectrum appears at a lower angle. A Laue pattern of iron pyrites, with the incident rays normal to (100), has twofold symmetry and not fourfold symmetry, and the X-rays therefore show that the crystal does not belong to the highest class.

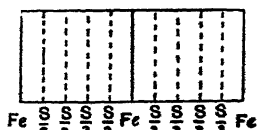
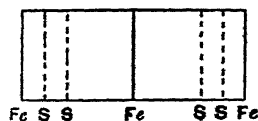


FIG. 69.—Arrangement of 210 and 201 planes in iron pyrites

### THE NUMBERS OF EQUIVALENT POSITIONS IN THE UNIT CELL

If an atom is placed at an arbitrary point, it is multiplied into a set of atoms by the operations of the space-group. The number of atoms in the set depends upon the class of symmetry of the crystal. For instance, the orthorhombic class of the highest type has three reflection planes at right angles, intersecting in three twofold axes. There is a fundamental eightfold nature in the symmetry of such a crystal. Any general face ( $hkl$ ), or any arbitrarily chosen feature of the crystal, appears eight times over because of its reflection across the planes, once in each of the octants into which the planes divide the crystal. An asymmetrical unit of structure in the space-group must correspondingly be one of a group of eight, since all aspects must be present so

as to give the symmetry. It is a general law that a crystal with an  $n$ -fold nature in its symmetry will have  $n$  asymmetrical units associated with each lattice-point, whatever its space-group. Fig. 63, p. 83, illustrates the point. The crystal class is such that  $n$  is four, due to two reflection planes at right angles. Each of the different arrangements illustrated in the figure, which correspond to different space-groups, has four asymmetrical triangles in the unit cell. Naturally, if the unit cell has more than one lattice-point associated with it, as is the case for face-centred and body-centred cells, the number of asymmetrical units in the cell will be correspondingly multiplied.

When an atom is not in the general position, but is situated on a reflection plane or rotation axis, or at a symmetry centre, the number of corresponding atoms is reduced. If the atom is on a plane, it must be reckoned as equivalent to two asymmetric units, and so there will only be  $n/2$  atoms associated with each lattice-point. The number will be  $n/2$  if it is at a symmetry centre, and  $n/2$ ,  $n/3$ ,  $n/4$ , or  $n/6$  if it is on a two-, three-, four-, or sixfold axis. If it is at the intersection of a twofold axis with a reflection plane, the number will be  $n/(2 \times 2)$ , or  $n/4$ , and so forth. It will be clear that the reduction in number only occurs for positions on reflection planes or rotation axes, and not for positions on glide planes or screw axes.

### THE STRUCTURE AMPLITUDE

In the case of the simple crystals of Chapter IV, it was convenient to consider the reflection by sheets of atoms whose arrangement could be readily pictured. When the unit cell contains many atoms, the process would be cumbersome if carried out for all the reflections.

A more general way of considering the problem of diffraction is as follows. A unit of structure, composed of a number of atoms, is grouped around each point of the space-lattice. Each of these atoms scatters radiation, and the contribution of the unit as a whole to the wave forming the diffracted beam with indices  $hkl$  is the resultant of these separate waves. We can form a general expression for the resultant which is termed the 'structure amplitude  $F(hkl)$ .'

A suitable origin in the unit cell being chosen, let the co-ordinates of a typical atom referred to this origin be  $x$ ,  $y$ ,  $z$ ,

measured parallel to the axes whose lengths are  $a, b, c$ . The amplitude of the wave scattered by the atom is represented by the symbol  $f$  (the atomic scattering factor). The different scattered waves may be conveniently combined by finding the phase difference between each and a standard wave supposed scattered at the origin itself. From the definition of the indices  $hkl$  (see p. 19) it follows that the translations  $a, b, c$  involve phase changes of  $2\pi h, 2\pi k, 2\pi l$  respectively when the  $hkl$  reflection is taking place. The partial translation  $x$  in the  $a$  direction therefore involves a phase change of  $2\pi hx/a$ , and the total phase change in going from the origin to the point  $xyz$  will be

$$2\pi hx/a + 2\pi ky/b + 2\pi lz/c.*$$

The 'structure amplitude  $F(hkl)$ ' is thus the resultant of a number of waves each with amplitude  $f$  and phase

$$2\pi(hx/a + ky/b + lz/c).$$

referred to the origin. The resultant can be found by the usual rule for compounding vectors.

The most concise way of expressing the amplitude is by using complex quantities,

$$F(hkl) = \sum f e^{2\pi i(hx/a + ky/b + lz/c)},$$

where the complex resultant expresses both amplitude and phase of  $F$  according to the usual conventions. Alternatively

$$I \propto |F(hkl)|^2 = \{\sum f \cos 2\pi(hx/a + ky/b + lz/c)\}^2 \\ + \{\sum f \sin 2\pi(hx/a + ky/b + lz/c)\}^2,$$

where  $I$  is the intensity of the diffracted beam. The summation extends over every atom in the unit cell.

As a simple instance, let us take a structure composed of atoms on a face-centred lattice, with an origin at one of the atoms. Other atoms in the lattice are at points  $0\frac{1}{2}\frac{1}{2}$ ,  $\frac{1}{2}0\frac{1}{2}$ , and  $\frac{1}{2}\frac{1}{2}0$ .\* The structure amplitude is therefore, since the sine terms are zero,

$$F(hkl) = f\{\cos(0) + \cos 2\pi(k/2 + l/2) + \cos 2\pi(h/2 + l/2) \\ + \cos 2\pi(h/2 + k/2)\}.$$

\* Fractional co-ordinates  $u, v, w$  are often used in place of  $x, y, z$ , where  $u = x/a, v = y/b, w = z/c$ . The expression then becomes

$$2\pi(hu + kv + lw).$$

By combining these cosines by trigonometrical rules, this expression can be transformed to

$$F(hkl) = 4f \cos \pi(h+k+l) \cos \frac{\pi(k+l)}{2} \cos \frac{\pi(h+l)}{2} \cos \frac{\pi(h+k)}{2}.$$

This expression contains the rules for possible reflections from a face-centred lattice. It is zero unless  $k+l$ ,  $h+l$ ,  $h+k$  are all even, which involves the condition that  $h$ ,  $k$ ,  $l$  are all even or all odd integers. In this case it is equal to  $4f$ .

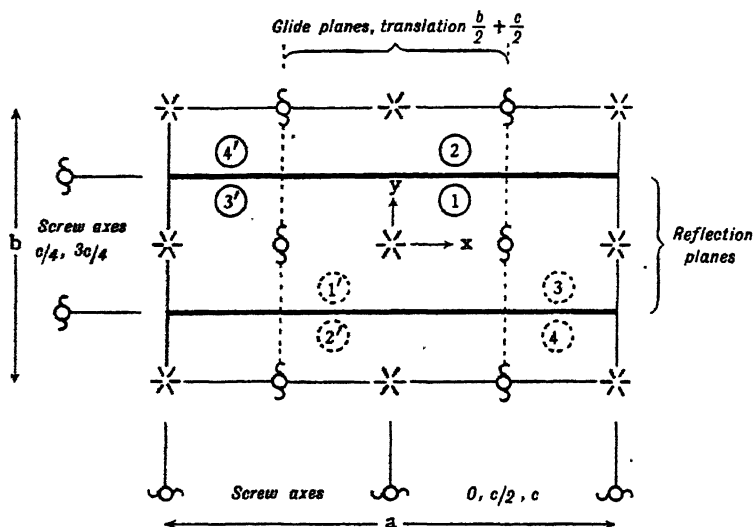


FIG. 70.—The symmetry elements of the space-group  $V_h^{16} = Pnma$ , and the set of equivalent atoms in a general position

The face-centred lattice is a very simple case, and the expression for the structure amplitude is generally much more complicated. We can formulate it, however, for any given space-group. If an atom is in some position  $xyz$  in the cell of the space-group, there will be several other atoms in the cell which are equivalent in that they turn into each other by the symmetry operations. The contribution of the whole group to the structure amplitude can be written, and in most cases it can be simplified by combining the trigonometrical functions as has been done above.

Fig. 70 illustrates the space-group  $V_h^{16}$  or  $Pnma$ , an orthorhombic group which has been found to be the basis of an exceptionally large number of crystals. The directions of the

$a$  and  $b$  axes are indicated in the diagram, the  $c$  axis being normal to both. There are reflection planes  $m$  perpendicular to the  $b$  axis, denoted by heavy lines in the diagram. Glide planes  $n$  perpendicular to the  $a$  axis are denoted by dotted lines, and the translation associated with them is  $\frac{b}{2} + \frac{c}{2}$ . Glide planes  $a$  perpendicular to the  $c$  axis, and so parallel to the plane of the figure, are at levels  $c/4$  and  $3c/4$  from the base of the unit cell, and the translation is  $a/2$ . The positions of the three sets of twofold screw axes are shown in the figure. Centres of inversion are shown as stars, at levels 0,  $c/2$ , and  $c$ , and it will be seen that the unit cell has been outlined so as to have a centre of inversion at its centre. It is always convenient to do this when centres of inversion are present, because the structure amplitude then assumes a simpler form.

The circle 1 represents an atom at a general point  $x, y, z$ , the origin being at the centre of the cell. The operations of symmetry reproduce this atom at the following points, eight in all:

$$\begin{aligned} 1, 1' & \pm (x, y, z) \\ 2, 2' & \pm \left(x, \frac{b}{2} - y, z\right) \\ 3, 3' & \pm \left(\frac{a}{2} - x, -y, -\frac{c}{2} + z\right) \\ 4, 4' & \pm \left(\frac{a}{2} - x, -\frac{b}{2} + y, -\frac{c}{2} + z\right). \end{aligned}$$

The structure amplitude is:

$$\begin{aligned} & 2 \cos 2\pi \left\{ \frac{hx}{a} + \frac{ky}{b} + \frac{Lz}{c} \right\} \\ & + 2 \cos 2\pi \left\{ \frac{hx}{a} + k \left( \frac{1}{2} - \frac{y}{b} \right) + \frac{Lz}{c} \right\} \\ & + 2 \cos 2\pi \left\{ h \left( \frac{1}{2} - \frac{x}{a} \right) - \frac{ky}{b} - l \left( \frac{1}{2} - \frac{z}{c} \right) \right\} \\ & + 2 \cos 2\pi \left\{ h \left( \frac{1}{2} - \frac{x}{a} \right) - k \left( \frac{1}{2} - \frac{y}{b} \right) - l \left( \frac{1}{2} - \frac{z}{c} \right) \right\}. \end{aligned}$$

The sine terms cancel owing to the occurrence of the atoms in pairs on either side of the origin at the centre of inversion. By

combining these terms trigonometrically, the amplitude becomes

$$8 \cos \pi(h+k+l) \cos \pi\left(\frac{h+k+l}{2} + \frac{2hx}{a}\right) \cos \pi\left(\frac{k}{2} + \frac{2ky}{b}\right) \cos \pi\left(\frac{h+l}{2} + \frac{2lz}{c}\right)$$

We have thus obtained a single expression for the combined effect of all eight atoms. It will be seen that this expression contains the rules for recognising the space-group.

(1) If  $h$  is zero, the second factor (and so the whole amplitude) is zero when  $k+l$  is odd. Reflections  $okl$  only appear if  $k+l$  is even. This is due to the glide plane perpendicular to  $a$  with translation  $\frac{b}{2} + \frac{c}{2}$ .

(2) If  $k$  is zero, there is no restriction, because the third factor then becomes unity.

(3) If  $l$  is zero, the fourth factor is zero when  $h$  is odd. Reflections  $hko$  are only possible when  $h$  is even. This is due to the glide plane perpendicular to  $c$  with translation  $a/2$ .

To obtain the total structure amplitude for a given reflection  $hkl$ , this expression is evaluated for each kind of atom in turn, by substituting its co-ordinates  $x, y, z$ , and its atomic scattering factor  $f$  appropriate to the angle of scattering. The contributions are added, due account being paid to their signs, and so a number  $F(hkl)$  is obtained which represents the diffracting power of the unit cell for the reflection considered, and which may be compared with the experimental measurement of intensity of reflection.

### THE ATOMIC SCATTERING FACTOR

The atomic scattering factor  $f$  which appears in the formula for the structure amplitude is a measure of the efficiency of the atom in scattering X-rays. It is defined in such units that the atom scatters  $f$  times as much as would be scattered, according to the classical formula, by a single free electron. Its theoretical significance is dealt with in the chapter on X-ray Optics, but certain features may be conveniently summarised here. It depends both upon the wave-length  $\lambda$  of the X-rays and the glancing angle  $\theta$ , but in such a way that it is a function of  $(\sin \theta)/\lambda$ . Values of  $f$  for different atoms can therefore be plotted as ordinates against  $(\sin \theta)/\lambda$  as abscissa, and such curves are known as  $f$  curves and are indispensable in analysis. At small values of  $(\sin \theta)/\lambda$ ,

the  $f$  ordinates are nearly equal to the atomic numbers of the atoms, or more precisely to the number of electrons they contain, since they may be ionised. The curve falls away with increasing  $(\sin \theta)/\lambda$ , because waves coming from different parts of the atom interfere, the fall being much more rapid for the light elements than for the heavy ones. Typical  $f$  curves are given in Chapter IX.

#### THE COMPARISON OF CALCULATED AND OBSERVED INTENSITIES OF REFLECTION

The final process of analysis consists in postulating an arrangement of the atoms, and testing whether it explains the observed intensities of reflection.

These intensities depend upon several factors. In the first place, there is the factor which we are primarily concerned with here, the square of the structure amplitude. Large structure amplitudes correspond to strong diffracted beams, and small structure amplitudes to weak diffracted beams. In addition there are other factors which will be described in the chapter on X-ray Optics. They can be calculated for certain defined conditions of experiment; there is in general a falling off in the intensity of diffraction with increasing angle, but the laws according to which it takes place are different for different experimental methods. Both sets of factors must be considered when calculated and observed intensities are compared.

If a photographic method of registration is used, the estimates of intensity are in general relative. In most cases such measurements suffice for analysis. In a rotation photograph, for instance, the spots may be labelled as very strong, strong, moderate, weak, very weak, and listed in order of increasing  $(\sin \theta)/\lambda$ . A structure for which the calculated structure amplitudes show a parallel set of large and small values, which check against the observed intensities of the spots, may be accepted as accurate if the correspondence holds good over a wide range.

The most precise and powerful method, however, is the use of absolute measurements such as are given by the spectrometer. An absolute measurement, or comparison of the intensity of the incident and diffracted beam, can be converted into a measurement of  $F(hkl)$  by using the formula appropriate to the experimental method employed. The value of  $F(hkl)$  for each reflection is to be matched by the structure amplitude calculated



from the proposed structure. This is a more stringent test than a mere check of strong or weak reflections against large or small amplitudes, and so leads much more directly to the atomic positions by eliminating impossible configurations. An example of the comparison of  $F$  values is given by the results for iron pyrites quoted at the end of Chapter IV. This method is reserved for cases where a structure is to be examined in detail, or is of a type difficult to analyse, because the experimental measurements demand so much labour. The agreement of theory and experiment in such cases is evidence of the sound basis of the optical theory.

In the vast majority of analyses less precise methods can be used. An approximate allowance for the factors other than the structure amplitude can be made, and the qualitative comparison is sufficient.

### THE ANALYSIS OF INORGANIC CRYSTALS

It is convenient at this point to consider the analysis of inorganic and organic crystals separately, because the further stages of analysis present different features.

We will suppose that we are analysing a complex inorganic crystal, such as a salt or a silicate. The lattice, space-group, and numbers of atoms of each kind in the unit of pattern have been determined. We wish to use every possible device to indicate the form of the structure before embarking upon the final test of comparing observed and calculated intensities.

Certain atoms may be in special positions, lying on symmetry planes and rotation axes or at centres of inversion. This must be so if the number of such atoms in the unit cell is less than the number characteristic of a general position. A limitation of this kind is of assistance because it reduces the number of parameters, and it is particularly useful when some important atom in the structure is pinned down by a position at a symmetry centre. This atom then forms a nucleus around which the rest of the structure can be built up.

The packing together of the atoms or groups of atoms is a very helpful guide. Ions are packed into a structure as if they were spheres of approximately constant size. These ionic sizes are described in Chapter VII; they vary from one atom to another, and it is a general rule that the negative ions are considerably larger than the positive ions. The former are therefore the

more important in the packing of the structure, and the positive ions may be broadly said to occupy the interstices between the negative ions. Acid groups such as  $\text{CO}_3^-$ ,  $\text{SO}_4^-$  may also be assigned definite dimensions, though their figure is not spherical but resembles a cluster of spheres pressed compactly together.

In packing the ions together the domains of neighbours must not overlap, and this has an important bearing upon their position relatively to the symmetry elements. 'Purely geometrical reasoning may in this way take us a long step forward in the search for the right structure. Let us suppose that an oxygen ion, with a radius of 1.33 Å., is to be incorporated into a structure, and that the space-group has reflection planes. Since an oxygen atom must not overlap with its own reflection in the plane, the atomic centre must either lie exactly on the plane or be distant from it by more than the oxygen radius. There is therefore a layer on either side of the reflection plane which is forbidden territory, as it were, to the centre of any oxygen atom. Similarly, the atom must lie on a twofold axis, or at a centre of inversion, or be more than 1.33 Å. distant from either. It must be still further away from axes of higher symmetry, if it is not actually on one of them. If these forbidden areas are outlined, it is often found that the atom is left with quite a limited range. The same holds true for the complex acid groups, which must not overlap symmetry elements.

These considerations are geometrical, and the physical aspect of the structure may now be considered. As the structure is held together by the attraction of positive and negative ions, these ions may be expected to alternate so that a positive is surrounded by negatives, and *vice versa*. Pauling's rule, which is of fundamental importance in the theory of ionic structures, puts this condition in a quantitative form. Briefly expressed, it states that there is as far as possible a localised neutralisation of electrical charge in the crystal; the rule is explained in Chapter VII. When regard is paid to the packing together of the ions, and to the satisfying of Pauling's rule, it is often found that only a few alternative structures need be tested.

The general conditions outlined above are used to simplify as far as possible the final process of testing various atomic arrangements in order to obtain one which explains the X-ray results. We can only give a general idea of the methods employed in the final analysis, because they vary so greatly with the type of crystal.

The spectra with small values of  $hkl$  are used to indicate the approximate positions of the atoms, because small variations in the parameters do not affect the structure amplitude greatly when the indices are low. The higher orders are then used in a process of fine adjustment. If one or more atoms have a high atomic number compared with the others, their contribution to the  $F(hkl)$  is so large that it dominates, and heavy atoms are therefore easy to place. This is particularly the case for the higher orders, since, as we shall see later, the scattering of light atoms falls away more quickly with increasing  $(\sin \theta)/\lambda$ , and so the heavy atoms stand out from the rest.

The most important guide of all is the knowledge obtained from previous determinations of similar crystals, and the laws of crystal structure which these determinations have revealed. All these features enable the investigator to get a first approximation to the atomic arrangement, which is then improved by trying small movements of the atoms and comparing the calculated and observed intensities.

#### AN EXAMPLE OF ANALYSIS: BERYL

The analysis of beryl,  $\text{Be}_3\text{Al}_2\text{Si}_6\text{O}_{18}$ , illustrates many of the features which have been described. This crystal belongs to the holohedral, or highest class of the hexagonal system. It is one of some complexity, containing a large number of atoms in the unit cell whose fixation involves the determination of seven parameters. In spite of this, the structure may be found very simply and directly.

Since all crystals of this class are based on one type of lattice (the hexagonal lattice), it is a simple matter to find the axes from the observed reflections. The ratio  $c : a$  usually adopted as the result of crystallographic measurements is 0.4989 : 1, but the X-ray measurements show that the true ratio is twice as great:

$$c = 9.17 \text{ \AA}, \quad a = 9.21 \text{ \AA}, \quad c : a = 0.9956 : 1.$$

The unit cell contains two molecules of  $\text{Be}_3\text{Al}_2\text{Si}_6\text{O}_{18}$ .

The space-group is found by noting which series of reflections are absent. A survey of the possibilities could be made by consulting space-group tables, but it will be carried out from first principles here, because it forms an example of the very simple way in which the various space-groups arise.

A portion of the hexagonal lattice is shown in fig. 71, the  $c$  axis being normal to the plane of the diagram, or what will be referred to as the 'vertical' direction. In order that the structure may have the highest form of hexagonal symmetry, there must be twenty-four asymmetrical units around each point of the lattice. We need only consider a set of twelve here, because there is in each case a horizontal reflection plane, so that each

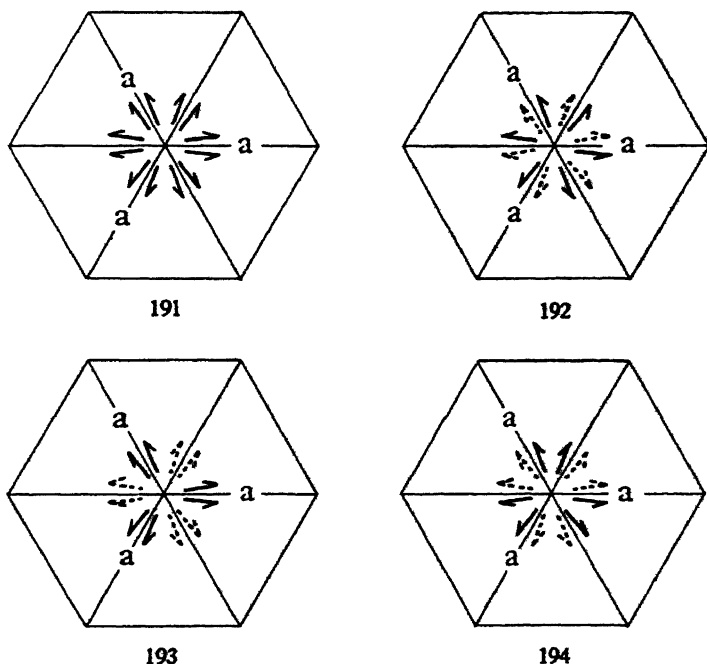


FIG. 71.—The four hexagonal space-groups of highest symmetry

unit in the diagram actually represents a pair. Our problem is that of finding in how many ways the twelve can be arranged so that the full symmetry is represented.

Fig. 71 shows that this can be done in four ways, the units being represented conventionally as half-arrows. We may put all twelve in one plane (191). Alternatively six (drawn in full line) may be put at top and bottom of the cell, and six (in dotted line) half-way up the cell at height  $c/2$ . There are three ways of effecting the latter arrangement. We may either have six arrows rotating in one sense at the top, and six in the opposite sense at height  $c/2$  (192), or two sets of three pairs, a pair being either

reflections across a plane parallel to  $a$  (193), or a plane perpendicular to  $a$  (194). The figure illustrates the possibilities better than a description.

Another way of arriving at the result is to recognise that the point group or crystal class has vertical reflection planes  $\{10\bar{1}0\}$  and  $\{11\bar{2}0\}$  parallel and perpendicular to  $a$  respectively. These must be represented by either reflection or glide planes in the space-group. The possibilities are therefore

$(10\bar{1}0)$	$(11\bar{2}0)$	Group number	Symbols
Reflection	Reflection	191	$D_{6h}^1$ , $C6/mmm$ .
Glide	Glide	192	$D_{6h}^2$ , $C6/mcc$ .
Reflection	Glide	193	$D_{6h}^3$ , $C6/mcm$ .
Glide	Reflection	194	$D_{6h}^4$ , $C6/mmc$ .

Planes perpendicular to  $(10\bar{1}0)$  have indices  $(mm\bar{2}ml)$ , and planes perpendicular to  $(11\bar{2}0)$  have indices  $(mo\bar{m}l)$ . Remembering the rules for the apparent halving of the  $c$  axis due to a glide plane, the criteria are seen to be

191. All reflections present.
192.  $l$  must be even for  $mo\bar{m}l$  and  $mm\bar{2}ml$ .
193.  $l$  must be even for  $mo\bar{m}l$ .
194.  $l$  must be even for  $mm\bar{2}ml$ .

In beryl, whereas such reflections as  $12\bar{3}1$ ,  $12\bar{3}3$  show the true length of the  $c$  axis, it is found that  $10\bar{1}1$ ,  $10\bar{1}3$ ,  $10\bar{1}5$  . . . and  $11\bar{2}1$ ,  $11\bar{2}3$ ,  $11\bar{2}5$  . . . are absent. Therefore the space-group of beryl is  $D_{6h}^3$  or  $C6/mcc$ .

The framework of symmetry elements has now been found, and it remains to fit the numbers of atoms represented by  $2Be_3Al_2Si_6O_{18}$  into the unit cell. The framework is complicated, and for simplicity only a part of the unit cell will be considered. At the top of the unit cell there is a network of horizontal twofold axes represented by lines in the figure; vertical axes are denoted by appropriate symbols. At a distance  $c/4$  below the top of the cell there is a reflection plane parallel to  $(000l)$ , the plane of the diagram. We will consider the portion between the horizontal axes and the reflection plane, this being the top quarter of the cell (fig. 72).

The oxygen atoms are the largest units in the structure, being about 2.7 Å. in diameter, and 36 of them must be put into the unit cell without overlapping. Suppose an oxygen atom be placed in a general position, such as  $O_1$ . It must not intersect a symmetry plane or an axis, for this would involve an overlapping. We may picture the twofold axes in the figure as a set of rods, which are at a distance of  $c/4$  or 2.29 Å. above a plane. A sphere 2.7 Å. in diameter must be placed between the

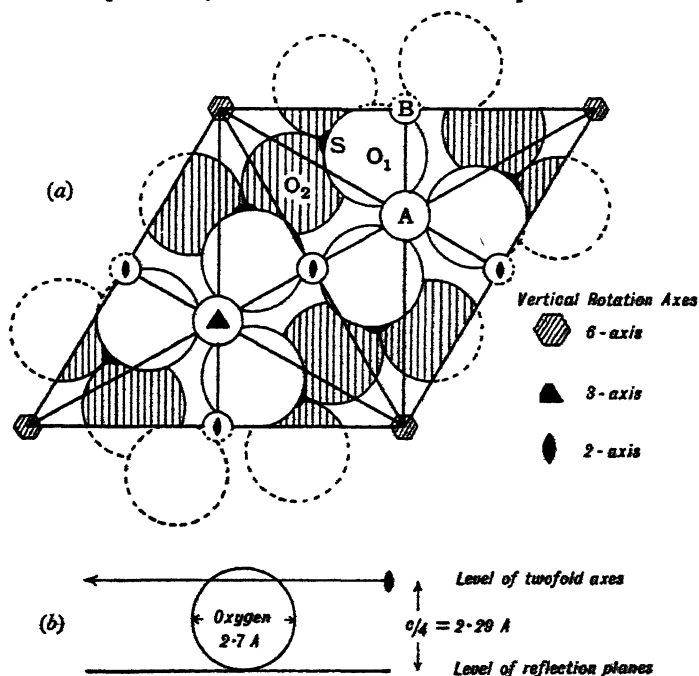


FIG. 72.—Deduction of the structure of beryl,  $\text{Be}_3\text{Al}_2\text{Si}_6\text{O}_{30}$

rods and the plane. Trial shows that only one position is possible, the sphere being wedged between three rods and the plane at  $O_1$ . The sphere bulges somewhat above the level of the rods, as in fig. 72 (b). The symmetry operations turn  $O_1$  into a group of 6 atoms within this section of depth  $c/4$ , and hence into 24 in the whole unit cell. There are 36 oxygen atoms in all, and as an atom in the general position is one of a group of 24, the remaining 12 must lie on some symmetry element. Places on twofold axes are ruled out, because overlapping with the other 24 atoms would result. There remains as a possibility

a position on the horizontal reflection planes, and it is again found that there is just sufficient room for one at  $O_2$ . The atoms of the group are shaded in the figure. Six appear on the reflection plane considered, and another set of six on the reflection plane at a depth  $3c/4$ . The approximate positions of all the oxygen atoms have now been found.

Since there are only 4 aluminium atoms in the unit cell, as compared with 24 atoms in a general position, aluminium must be in a highly symmetrical situation. A few alternatives present themselves, and the X-ray results immediately decide for a position A where the threefold axis intersects three twofold axes. Similarly, the 6 beryllium atoms are found to be at B and its equivalent positions.

The positions of the 12 silicon atoms can be found by trying various situations which are probable from a physical point of view, and seeing which of these explains the X-ray results. Actually, their position at S is obvious. A position on twofold axes is ruled out, for then there would be no forces holding the crystal together across the reflection planes. They must lie on the reflection planes, and suitable places are ready for them between groups of four oxygen atoms.

The X-ray results are now used to test the correctness of the structure and to make final small adjustments to the seven parameters. Such small adjustments present no difficulty when the approximate positions of the atoms are known, since it is easy to find reflections which are especially sensitive to any given parameter. The completed structure is shown in fig. 73. This example has been given in some detail as indicating the way in which a complicated crystal can be treated.

### THE ANALYSIS OF ORGANIC CRYSTALS

The unit of structure in the organic crystal is the molecule. The atoms in the molecule are closely and rigidly bound, whereas they are separated from those of neighbouring molecules by much greater distances. This characteristic feature is responsible for a great difference in the methods of analysis of organic and inorganic crystals.

The initial determination of space-lattice, number of molecules in the unit cell, and space-group is common to both types of investigation, but the subsequent fixation of the atoms by X-ray

methods alone is very difficult in organic crystals. The structures are exceedingly complex, and the atoms of carbon, oxygen, and nitrogen, which form the greater part of any organic molecule, are so alike in their scattering power that they can hardly be distinguished from each other. Hydrogen, the other important constituent of organic compounds, must in general be regarded as a proton embedded in the electronic structure of the molecule, so it has no influence as a unit in scattering X-rays.

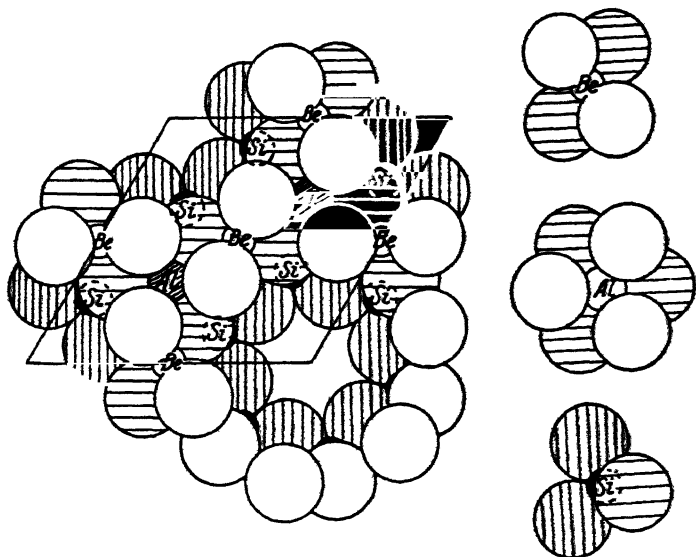


FIG. 73.—The structure of beryl

(From *The Structure of Silicates*, W. L. Bragg; Akad. Verlag, 1930)

On the other hand, the existence of a well-defined molecule in the organic compound opens up a new line of attack. Stereochemistry indicates the way in which the atoms of the molecule are linked to each other. A study of the simpler compounds makes it possible to determine the typical interatomic distances and the angles between the closely knit bonds of the molecule. The much greater distances between neighbouring atoms or atomic groups which do not belong to the same molecule can be found in a similar way. It is possible to build up a model of the molecule, and to consider how such molecules can be made to fit into the framework discovered by X-ray analysis.

A broad generalisation divides the organic units into long molecules such as the carbon chains, flat molecules such as



groups of benzene rings, and complex molecules with three-dimensional extension. It is a curious feature that the long molecules almost always associate in sheets to form platy crystals, whereas flat molecules form needle-shaped crystals with an extension more or less normal to their planes.

The first analyses of organic crystals were concerned with simple aliphatic and aromatic compounds, and did no more than confirm the conclusions of stereochemistry, though they gave a much greater precision to the models. The importance of a more extended application of X-ray methods in this field can hardly be exaggerated, for they can be used to supplement the findings of organic chemistry in the case of highly complex organic molecules whose structure is still uncertain. The researches of Bernal have been largely responsible for advances along these lines.

In the case of a complex compound, chemical methods will generally have suggested the way in which certain portions of the molecule are constructed, even if the complete structural formula is unknown. It is therefore possible to build up alternative models, into which these portions are incorporated. An immediate test is to try which of these models will fit into the cell determined by X-ray analysis. The space-lattice and space-group outline a space of definite dimensions for the molecule, which may or may not include a symmetry element. Such of the proposed models as are too long or too broad to fit into the space provided for them can be discarded as impossible.

Other indications are available. Since the molecules are widely separated the optical properties of the crystal reflect those of the individual molecules rather than the manner of their grouping together. Hence a knowledge of the refractivities associated with certain elements of the structure, such as a double bond or aromatic ring, enables the investigator to correlate the orientation of these features with the directions and magnitudes of the three principal refractive indices. The same holds true for absorption bands due to particular portions of the molecule, and for magnetic properties.

When the molecule is altered by addition or substitution at some part of its structure, it is often found that the crystal structure remains essentially the same except for a change in the dimensions of the unit cell, such as an alteration in the length of one axis. The nature of the change gives information as to the 'lie' of the molecule in the unit cell.

Though the final tests of co-ordinating the structure with the observed intensities of X-ray diffraction cannot be carried out completely, valuable information can often be got from the intensities. This is particularly the case if one or more heavy atoms such as chlorine can be incorporated into the structure without altering the general arrangement. These atoms stand out from the rest owing to their high scattering power, and it is a comparatively simple matter to determine their positions in the unit cell.

The use of such methods brings the study of very complex compounds within the range of possibility, and although only an indication of their nature can be given here, it will perhaps serve to show how such problems are approached.

#### SUMMARY

All methods of X-ray analysis are essentially indirect. It is not possible to substitute the observed intensities in a formula which automatically yields the atomic parameters; a process of trial and error is always necessary. The successful determination of simple structures affords an insight into the mechanics of crystal structure, and this enables more complex structures to be attacked. When one considers a model of a crystal structure with perhaps some hundreds of atoms in the unit cell and a correspondingly great number of parameters, it appears at first sight almost impossible that such a number of variables should have been successfully handled by any process of trial and error. Yet there can be no doubt of such analyses being correct, for the proposed atomic arrangements have a beauty and simplicity of organisation which would carry conviction even if they were not supported by the X-ray results. The rapid advances which have been made hold out promise that the successful application of X-ray methods will in future be extended to all forms of organised structure in matter.

## CHAPTER VII

### CHEMICAL AND PHYSICAL CRYSTALLOGRAPHY

THE main aim of X-ray analysis is the discovery of the atomic arrangement in the solid state. The crystalline structures are the result of an interplay of forces between the atoms, and a structure is a configuration of minimum potential energy like any mechanical system in a stable state. The various forms of structure will be reviewed in the present chapter, and discussed in relation to the types of interatomic force which are responsible for their formation. It is possible to explain why certain associations of atoms are formed and others are not, and this study may be termed Chemical Crystallography. We may then seek to explain the physical properties of the crystal as results of its structure, and here we must distinguish between two main fields of inquiry. Certain properties of the crystal, such as its axial ratios, optical constants, energy of formation, and electrical conductivity, are properties of the ideal atomic arrangement and will be discussed here. On the other hand, many properties are influenced by the size and relative orientation of the crystalline particles, and these features can also be examined by X-ray analysis. The influence upon physical properties of the 'geography' of the crystalline mass, as it may be termed, will be discussed in the next chapter under the head of Crystal Texture.

#### INTERATOMIC FORCES

*The Ionic or Heteropolar Bond.*—Sodium chloride is a typical case of a crystal in which the most important binding forces are due to electrostatic attraction between charged atoms or ions. The properties of the crystal show that it is composed of sodium and chlorine ions. These ions, originally postulated to explain the phenomena of electrolytic conduction in solution, exist also in the solid state. Instead of supposing that the atoms acquire

their charges when the salt is dissolved in water, we must now picture the process as a breaking up of the crystal lattice which already consists of negative and positive ions, as was surmised many years ago by Berzelius. Such a structure explains the regular alternation of the atoms, and the non-existence of a grouping into pairs corresponding to 'molecules of sodium chloride.' Molecule association may exist in the state of vapour, but there is no indication of it in the solid state of such compounds. Each ion is immediately surrounded by six of the opposite sign, to all of which it is equally related; the equality in numbers of the two kinds of ion is not the result of molecular association, but of the condition that positive and negative charges must be equivalent in amount throughout the crystal.

The neutral sodium atom contains two electrons in the K shell, eight electrons in the L shell, and a 'valency electron' which is much less firmly held than the remainder. This electron may be removed with a small expenditure of energy, converting the neutral atom into an ion with charge  $+e$ . The remaining electrons then form a structure like that of the inert gas neon, though on a somewhat smaller scale because the nuclear charge is  $11e$  as against  $10e$  for neon. A neutral chlorine atom would have 2, 8, and 7 electrons in the K, L, and M shells respectively. The M shell is incomplete, and by a method described later in this chapter it can be found that the neutral atom has an affinity for an electron, potential energy being released when an electron from outside is absorbed into the M shell and so gives it a full complement of eight electrons. The result is an expanded argon-like structure with a charge  $-e$ .

The ions are attracted together in the crystal by their electrostatic charges, and are held apart by a force of repulsion which increases very abruptly as the ions get within a certain distance of each other. It was first found empirically, and later explained theoretically, that the distance between the centres of the ions approximately obeys an additive law, each ion being packed into the structure as if it were a sphere of characteristic size. 'Ionic radii' can be assigned, the distance between two ions being the sum of the ionic radius of each. The additive law was founded by Fajans and Grimm, W. L. Bragg and Wasastjerna, and has been justified theoretically by Born, Lennard-Jones, and Pauling. Goldschmidt has drawn up tables of the most appropriate values for the ionic radii, which are listed below and are shown graphically in fig. 74.

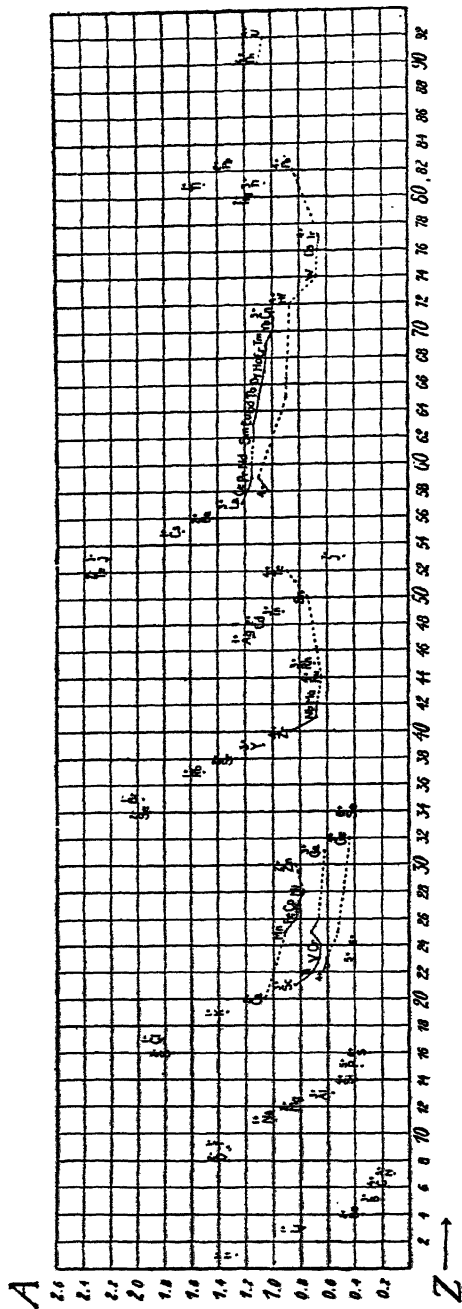


FIG. 74.—The radii of ions in crystals (Goldschmidt)

(*Trans. Far. Soc.*, 258, 1929)

TABLE III

2 -	1 -	0	1	2	3	4
		He	Li 0.78	Be 0.34		
O 1.32	F 1.33	Ne	Na 0.98	Mg 0.78	Al 0.57	Si 0.39
S 1.74	Cl 1.81	A	K 1.33	Ca 1.06	Sc 0.83	Ti 0.64
Se 1.91	Br 1.95	Kr	Rb 1.49	Sr 1.27	Y 1.06	Zr 0.87
Te 2.11	I 2.20	X	Cs 1.65	Ba 1.43	La 1.22	Ce 1.02

TABLE IV

Monovalent ions	NH <sub>4</sub> , 1.43	Tl, 1.49	Ag, 1.13	
Divalent ions	Mn, 0.91	Fe, 0.83	Co, 0.82	Ni, 0.78
	Zn, 0.83	Cd, 1.03	Hg, 1.12	Pb, 1.32
Trivalent ions	Cr, 0.64	Mn, 0.70	Fe, 0.67	
Quadrivalent ions	Mo, 0.68	W, 0.68	V, 1.05	Th, 1.10

Though the additive law is only approximately obeyed, and the above figures are mean values, the importance of the ionic radii both in analysis and in building models of crystal structure can hardly be exaggerated. It is an exceedingly useful conception; when a new structure is being analysed it may be assumed that the distance between the centres of two neighbouring ions will be within 0.1 Å. of that calculated from the above table.

The nearest neighbours in most ionic crystals are ions of opposite sign, as in sodium chloride. The distance between the atomic centres can be measured, but from such crystals alone it is impossible to decide what part of the distance is to be assigned to the ionic radius of the positive ion, and what part to that of the negative ion. We might add a constant amount to all positive radii in our list, and diminish the negative radii by the same amount, and still have a set of numbers which obey the additive law. This ambiguity is removed by a study of crystals whose scale is determined by the packing together of the negative ions. As will be seen from the list, a number of positive ions are small

compared with typical negative ions such as  $O^{--}$ ,  $F^-$ ,  $Cl^-$ . Many oxides in particular show a minimum distance between oxygen centres of about 2.7 Å., and this provides a datum point for the survey of ionic radii. By general consent, a value of 1.32 Å. for oxygen is taken to be the standard; the advantage of this point of departure was first pointed out by Wasastjerna, who in 1923 translated W. L. Bragg's original set of radii into a system almost identical with that now adopted.

It is doubtful whether the assigning of an 'ionic' radius to  $Si^{4+}$  is justifiable, and this is still more doubtful in the case of  $P^{3+}$  or  $S^{6+}$  when these atoms form the centres of acid radicals such as  $PO_4^{3-}$  or  $SO_4^{2-}$ . The packing of such groups into a crystalline structure can best be described by considering them as clusters of appropriate size and shape (see fig. 79 below).

To sum up, the typical ionic bond is a simple electrostatic attraction between ions of opposite sign. These ions may be single atoms, or groups such as  $CO_3$  and  $SO_4$ . The ionic bond is a characteristic feature of inorganic compounds.

Another type of bonding may be referred to here, since it is also electrostatic. Two systems may be electrically neutral, and yet exert an attraction on each other because each consists of a dipole. The field surrounding such a dipole is equivalent to that in the neighbourhood of equal positive and negative charges separated by a short distance so that the system has an electrical moment. The force between two dipoles varies as the inverse fourth power of the distance between them, whereas electrostatic forces between charges vary as the inverse square of the distance; dipole forces have therefore a more restricted range of action.

*The Homopolar Bond.*—In ionic crystals the electronic systems of the positive and negative ions are separated by spaces where the electronic density is extremely small, so that each ion is to a first approximation a distinct entity with a definite number of electrons. On the other hand, when two electronegative atoms are linked together by a homopolar or valency bond, the electronic systems interpenetrate. The simplest case of the hydrogen molecule has been studied in detail by the application of quantum mechanics in the well-known treatment of Heitler and London. The two electrons form an electron-pair bond uniting the hydrogen nuclei. The extension of this treatment to the union of more complex atoms presents considerable mathematical difficulty. Lewis in 1916 postulated the existence of the electron-

pair bond in homopolar combination, and his conception has been partially justified on theoretical grounds by Slater and by Pauling. In general terms, two electrons which are held in common by the two atoms form a bond with a localised distribution of electron density, whose strength is only slightly affected by other bonds which the atom may form. Without entering here into the theory of such bonds, some of the consequences may be stated.

The bonds involve a much closer approach of the atoms than is the case for ionic bonds. Atomic radii lose their significance, and must be replaced by a list of interatomic distances. The bonds are limited in number by the number of unpaired electrons available for their formation, and they are exerted in definite directions around the atom. These properties are in sharp contrast to those of the ionic compounds, where the electrostatic attraction of an ion extends to all ions of opposite sign in the neighbourhood, and is independent of direction. The fusing together of the atomic structures, or 'electron sharing,' is the physical basis of the directed links assumed by van't Hoff in founding stereochemistry. A list of interatomic distances where the links are homopolar is given below, the distances between carbon atoms being of especial interest. The 1.54 Å. found in diamond, where each carbon atom has four neighbours, corresponds to the distance between carbon atoms in typical aliphatic compounds such as the long-chain hydrocarbons, whereas the 1.42 Å. of graphite where the carbon atom has three coplanar neighbours corresponds to the 1.39 Å. in the flat benzene ring.

TABLE V

		A.			A.
C - C	Diamond	1.54	S - S	Pyrites	2.14
C - C	Aliphatic structure	1.51	Cl - Cl	Cl <sub>2</sub> , gas	2.1
C - C	Graphite	1.42		Band spectra	1.98
C - C	Aromatic structure	1.39	Br - Br	Br <sub>2</sub> , gas	2.28
C = C	Stilbene	1.35		Band spectra	2.26
	Band spectra	1.31	I - I	I <sub>2</sub> , solid	2.7
C ≡ C	CaC <sub>2</sub>	1.1?		Band spectra	2.66
	approx.		B - Cl	BCl <sub>3</sub> , gas	1.75
C - N	(NH <sub>2</sub> ) <sub>2</sub> CO	1.33	Si - Cl	SiCl <sub>4</sub> , gas	2.02
C = O	"	?	P - Cl	PCl <sub>3</sub> , gas	2.04
	CO <sub>2</sub>	1.13	B...O	Borates	1.3
C - Si	Carborundum	1.90		Band spectra	1.21
C - S	(NH <sub>2</sub> ) <sub>2</sub> CS	1.64	N...O	N <sub>2</sub> O	1.19
C - Cl	CCl <sub>4</sub> , gas	1.83		Band spectra	1.14
C - Br	CBr <sub>4</sub> , gas	2.2	O - O	Band spectra	1.21
C - I	CI <sub>4</sub> , gas	2.5	S = O	SO <sub>2</sub>	1.37
F - F	Band spectra	1.28	N ≡ N	Band spectra	1.25





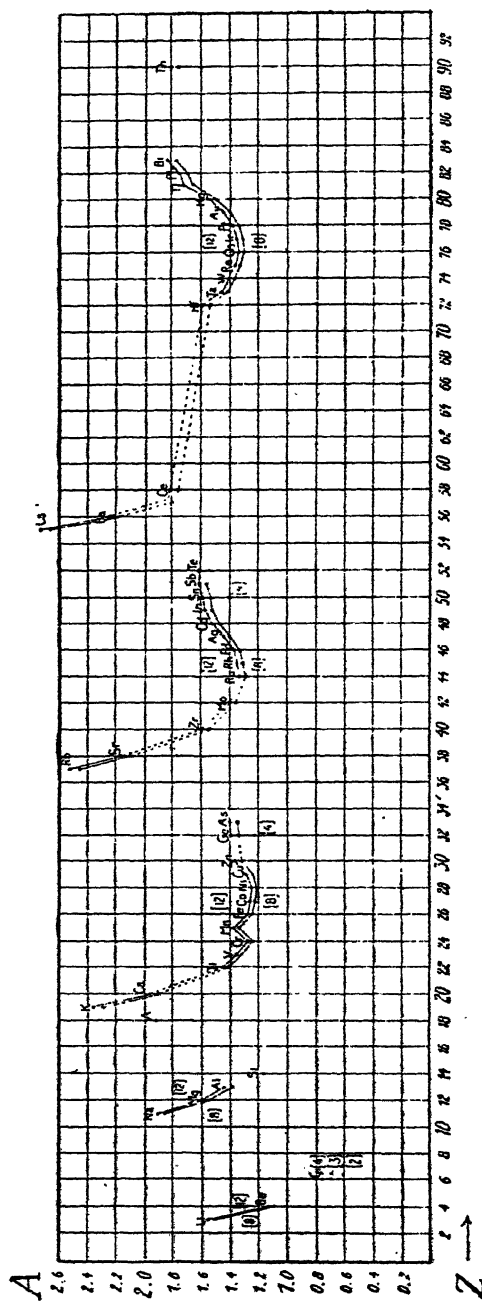


FIG. 75.—The radii of atoms in metals (Goldschmidt)  
(*Trans. Far. Soc.* 258, 1929)

bonds described above, but it may become important when two atoms are pressed closely together in the crystalline structure.

London has obtained an expression for the potential energy which is released owing to the van der Waals attraction when two atoms approach. The expression is proportional to the product of the polarisabilities of the two atoms, and varies as the inverse sixth power of the distance between them. Since the power of the distance is so high, the van der Waals force is only appreciable between neighbouring atoms in the crystal.

The interatomic repulsion sets in very rapidly when the atoms approach to within a certain distance of each other. An estimate of its rate of change in the neighbourhood of the equilibrium distance in crystals can be obtained from a study of their compressibility in a manner which is described below. In an early theory of ionic structures, Born expressed the contribution to the potential energy of the crystal due to the repulsion by an empirical expression,

$$\frac{B}{r^n},$$

and it was found that  $n$  must be given a value of the order 9 in the alkali halides. In a more recent theory this expression has been replaced by an exponential form,

$$b'e^{-r/\rho},$$

or more conveniently

$$be^{(r_1+r_2-r)/\rho},$$

where  $r_1$  and  $r_2$  are the ionic radii, and  $r$  is the interatomic distance. In the latter expression it is found that  $b$  and  $\rho$  are nearly constant for ions of the alkaline halides,  $\rho$  being 0.34 Å. The main point to note is the rapidity with which the repulsion decreases when  $r$  becomes greater than  $r_1 + r_2$ , and *vice versa*, owing to the small value of  $\rho$ . This is the basis of the additive law for ionic radii.

*Interatomic Distances in relation to Atomic Structure.*—The diagrams of fig. 76 have been drawn in order to illustrate the effect of the different types of binding. The curves represent the radial distribution of electron density in atoms, the ordinates being a quantity  $U(r)$  such that there are  $U(r)dr$  electrons between radii  $r$  and  $r + dr$ . These radial distributions are plotted with their origins at a distance apart equal to the actual distance between atoms in typical crystals as measured by X-rays. In crystalline argon

(atomic number 18) the atomic centres are separated by 3.82 Å. The attractive force is of the van der Waals type, and the atomic structures overlap to a very small extent. In KCl (atomic numbers 19 and 17) the overlap is greater owing to the attraction of the opposite charges. In the group  $S_2$  (atomic number 16)

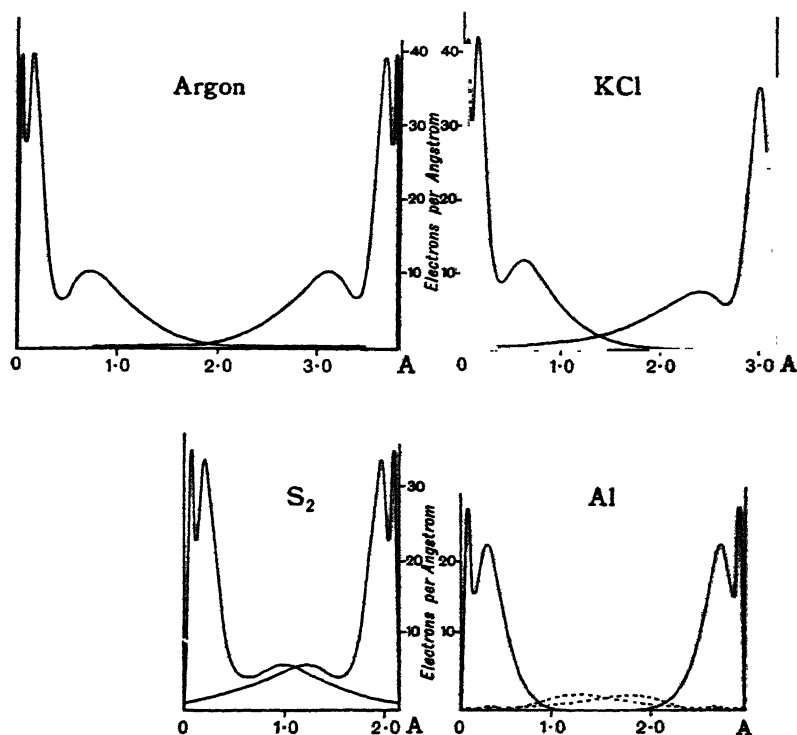


FIG. 76.—The radial electron distribution in various atoms, in relation to the interatomic distance in crystals

the homopolar bond draws the two atoms so close that their outer M shells coincide. It must be stressed that these diagrams are necessarily approximate, since the electron distributions are drawn for free atoms or ions and must be considerably distorted and no longer spherical in the crystal.

The fourth diagram represents metallic aluminium. The full lines represent  $Al^{3+}$  ions, which are seen to be widely separated. The dotted lines show where the valency electrons would be if the ions were free; in the metal they form part of a common structure.

*The Binding of Hydrogen.*—The function of hydrogen is unique, owing to its extremely simple structure. The neutral hydrogen atom consists of a proton as nucleus, with an electron which is lightly bound. When hydrogen is incorporated into the structure of a compound, it cannot be regarded as a separate atom with an electronic structure of its own. It is preferable to regard the proton as a dimensionless centre of force which modifies the electronic structure of the neighbouring atoms. For instance, the group  $\text{OH}^-$  resembles  $\text{F}^-$ , being a negative ion with apparent spherical symmetry and a radius of 1.33 Å. The distance between O and H centres, deduced from band spectra, is 0.98 Å., so that the hydrogen nucleus is embedded in the electronic structure of the oxygen atom. The ammonium radical  $\text{NH}_4$  is a spherically symmetrical positive ion with a radius of 1.43 Å., approximating to that of rubidium. Similarly in hydrocarbons the hydrogen nuclei are embedded in the carbon structure, and carbon atoms of neighbouring molecules which have hydrogen linked to them have a closest distance of approach of about 3.5 Å., as contrasted with the 1.5 Å. for carbon atoms linked by a homopolar bond.

Hydrogen can appear in another rôle—as a symmetrical link between neighbouring atoms, as was first pointed out by Huggins. These links have been found in many inorganic compounds. In  $\text{KH}_2\text{PO}_4$ , for instance, each oxygen of a  $\text{PO}_4$  group is linked to an oxygen of a neighbouring group by a hydrogen atom symmetrically placed between the two. An example of their occurrence in organic compounds has been demonstrated by Foz and Palacios in the case of crystalline quinhydrone, where oxygen atoms of neighbouring molecules are linked by a common hydrogen atom.

The various forms of binding have been illustrated above by typical cases where each is predominant. In actual crystalline forms there is a continuous transition between them. Lists of crystals can be drawn up which show all gradations between ionic and homopolar, ionic and metallic, or metallic and homopolar types. Nevertheless, a classification in terms of these forces is of great assistance in understanding and describing crystal structures. The division of chemistry into inorganic chemistry, organic chemistry, and metallurgy is fundamentally due to the distinctive properties of compounds in which ionic, homopolar, and metallic bonds are respectively of predominant importance.

A periodic table of the elements, to which frequent reference will be made, is given in Table VI.

TABLE VI.—ATOMIC NUMBERS AND ATOMIC WEIGHTS

	I.	II.	III.	IV.	V.	VI.	VII.	O	VIII.
PERIOD I. (2 Elements.)									
	3 Li	4 Be	5 B	6 C	7 N	8 O	9 F	10 Ne	
"	6-940	9-02	10-82	12-00	14-008	16	19-00	20-183	
	11 Na	12 Mg	13 Al	14 Si	15 P	16 S	17 Cl	18 Ar	
"	22-997	24-32	26-97	28-06	31-02	32-06	35-457	39-944	
	19 K	20 Ca	21 Sc	22 Ti	23 V	24 Cr	25 Mn	26 Fe	27 Co
IV. (18 Elements.)	39-10	40-07	45-10	47-90	50-95	52-01	54-93	56-84	58-94
	28 Ni	30 Zn	31 Ga	32 Ge	33 As	34 Se	35 Br	36 Kr	59-69
	63-57	65-38	69-72	72-60	74-93	79-2	79-916	83-7	
	37 Rb	38 Sr	39 Y	40 Zr	41 Nb	42 Mo	43 Ma	44 Ru	45 Rh
V. (18 Elements.)	86-44	87-03	89-22	91-22	93-3	96-0	—	101-7	102-91
	47 Ag	48 Cd	49 In	50 Sn	51 Sb	52 Te	53 I	54 Xe	
	107-880	112-41	114-8	118-70	121-76	127-5	128-932	131-3	
	55 Cs	56 Ba	57-71 RARE EARTHS	72 Hf	73 Ta	74 W	75 Re	76 Os	77 Ir
VI. (32 Elements.)	132-81	137-36	141-4	145-9	151-8	157-0	162-5	168-0	173-1
	79 Au	80 Hg	81 Tl	82 Pb	83 Bi	84 Po	85 At	86 Nt	87 Pt
	197-2	200-61	204-39	207-22	209-00	—	—	222	195-23
	87 Fr	88 Ra	89 Ac	90 Th	91 Pa	92 U	—	—	—
VII. (1 Elements.)	—	225-07	—	232-12	—	238-14	—	—	—

## INORGANIC COMPOUNDS

It is only possible within the scope of this book to describe the main types of inorganic compounds, illustrating these types by examples chosen from the vast range of substances whose structures have been determined. The simple substances of composition  $AX$ ,  $AX_2$ ,  $AX_3$ ,  $A_2X_3$  have been exhaustively studied by Goldschmidt and his school, and their systematic work has greatly increased our understanding of crystal architecture. Next in order come the salts containing complex acid radicals, such as carbonates and sulphates. Co-ordination compounds, such as  $K_2PtCl_6$ , form another class. The silicates are examples of a class often termed the 'complex oxides,' which are intermediate in character between metallic oxides and salts. Their complexity is due to their containing indefinitely extended frameworks built of silicon and oxygen. Another type contains immense globular acid radicals, such as the ion  $(PW_{12}O_{40})^{3-}$  which occurs in the phosphotungstates. Finally, a brief description is necessary of the various rôles played by 'water of crystallisation.'

*Structure Types of Compounds  $AX$  and  $AX_2$ .*—A striking feature of these compounds is the small number of types represented by their crystals. Goldschmidt has proved that the majority of them have one or other of the structures shown in figs. 77 and 78. These structures are extremely simple, and most of them were amongst the first to be analysed by X-rays. They are arranged by Goldschmidt according to their type of co-ordination, or number of neighbours around atoms of each kind. In the  $AX$  compounds, boron nitride has a structure like that of graphite. Each B atom is surrounded by three N atoms, and each N atom by three B atoms. In the  $ZnS$  and  $ZnO$  types each atom is surrounded tetrahedrally by four of the other kind. In  $NiAs$  and  $NaCl$  the co-ordination is sixfold, and in  $CsCl$  it is eightfold (that this is true for both constituents will be apparent on extending the structure).

In the  $AX_2$  compounds,  $CO_2$  is a molecular structure in which carbon is linked to two oxygen atoms, and oxygen to one carbon atom. In the  $SiO_2$  structure the numbers of neighbours are 4 and 2, in  $TiO_2$  6 and 3, in  $CaF_2$  8 and 4. The type of co-ordination is a more fundamental feature of the crystal than its symmetry.

We may consider first the structures which are of the ionic

type. These are the types of structure represented by CsCl and NaCl amongst the AX compounds, and by CaF<sub>2</sub> and TiO<sub>2</sub>,

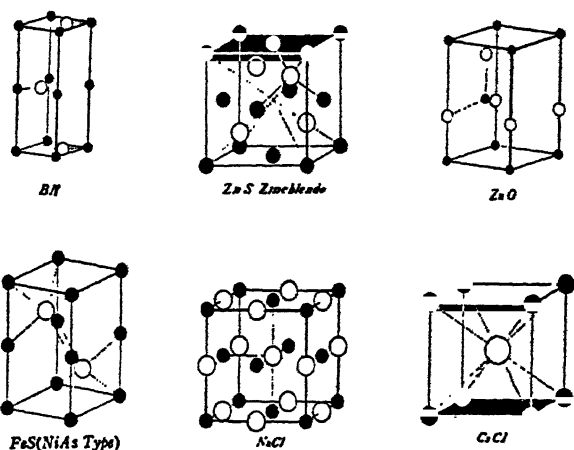


FIG. 77.—Structure types of compounds AX (Goldschmidt)  
(*Trans. Far. Soc.*, 254, 1929)

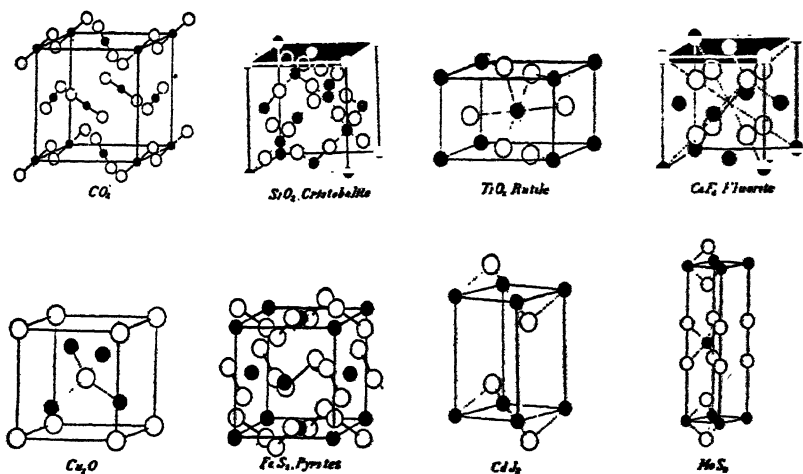


FIG. 78.—Structure types of compounds AX<sub>2</sub> (Goldschmidt)  
(*Trans. Far. Soc.*, 255, 1929)

amongst the AX<sub>2</sub> compounds. Table VII gives a list of the compounds crystallising with NaCl and CsCl structures, the figures being the lengths  $a_u$  of the cubic axes. There is no space in this survey for similar tables for other series of compounds,



but this table is given as an example of the more important and complete series.

TABLE VII  
NaCl Type  
(Type Br in Ewald's *Strukturbericht*)

	F	Cl	Br	I		O	S	Se	Te
Li	4.020	5.143	5.490	6.000	Mg	4.205	5.19	5.45	..
Na	4.619	5.628	5.962	6.462	Ca	4.80	5.68	5.91	6.34
K	5.33	6.277	6.586	7.052	Sr	5.15	6.01	6.23	6.65
Rb	5.63	6.54	6.854	7.325	Ba	5.53	6.37	6.59	6.99
Cs	6.008	..	..	..	Mn	4.42	5.21	5.45	..
NH <sub>4</sub>	..	6.53 *	6.90 †	7.24 †	Pb	..	5.93	6.14	6.44
Ag	4.92	5.54	5.76	..					

Also NiO, 4.17; CoO, 4.25; FeO, 4.28; CdO, 4.70.

\*  $T > 184^{\circ}\text{C.}$

†  $T > 138^{\circ}\text{C.}$

‡  $T > -18^{\circ}\text{C.}$

CsCl Type  
(Type B<sub>2</sub> in Ewald's *Strukturbericht*)

	Cl	Br	I
Cs	4.11	4.287	4.56
NH <sub>4</sub>	3.86 *	4.05 †	4.37 †
Tl	3.84	3.97	4.18

\*  $T < 184^{\circ}\text{C.}$

†  $T < 138^{\circ}\text{C.}$

‡  $T < -18^{\circ}\text{C.}$

The operation of the additive law, and the extent to which it is approximate, can be conveniently studied by comparing the scale of these structures with the list of ionic radii in Tables III and IV.

A large number of difluorides and dioxides crystallise in one or other of the two types, rutile, TiO<sub>2</sub>, and fluor, CaF<sub>2</sub>. Goldschmidt has shown that the factor which decides the type appears to be the ratio between the radii of cation and anion  $R_A/R_X$ . He gives the following list, the numbers denoting the ratio:

#### Rutile Structure

MgF<sub>2</sub> NiF<sub>2</sub> CoF<sub>2</sub> FeF<sub>2</sub> ZnF<sub>2</sub> MnF<sub>2</sub>  
0.59 0.59 0.62 0.62 0.62 0.68

MnO<sub>2</sub> VO<sub>2</sub> TiO<sub>2</sub> RuO<sub>2</sub> IrO<sub>2</sub> OsO<sub>2</sub> MoO<sub>2</sub> WO<sub>2</sub> NbO<sub>2</sub> SnO<sub>2</sub> PbO<sub>2</sub> TeO<sub>2</sub>  
0.39 0.46 0.48 0.49 0.50 0.51 0.52 0.52 0.52 0.56 0.64 0.67

*Fluor Structure*

CdF <sub>2</sub> 0.77	CaF <sub>2</sub> 0.80	HgF <sub>2</sub> 0.84	SrF <sub>2</sub> 0.95	PbF <sub>2</sub> 0.99	BaF <sub>2</sub> 1.08
ZrO <sub>2</sub> 0.66	PrO <sub>2</sub> 0.76	CeO <sub>2</sub> 0.77	UO <sub>2</sub> 0.80	ThO <sub>2</sub> 0.84	

It will be seen that the fluor structure is assumed when the ratio rises above a value of 0.7. Now in the tetragonal rutile structure each cation (black) is surrounded by six anions, and each anion (white) by three cations, whereas in fluor these numbers are eight and four respectively. A group of eight spheres in contact at cube corners, with radii  $R_X$ , has a space at its centre which can accommodate a sphere of radius  $(\sqrt{3} - 1)R_X$  or  $0.73 R_X$ . Hence in the fluor structure as long as  $R_A/R_X > 0.73$ , positives and negatives are in contact, but if  $R_A/R_X < 0.73$ , the positive ion becomes so small that the negative ions come into contact, the positive ion being in a hole between them which is unnecessarily large. The inference is drawn that the rutile structure is therefore taken up, since in this structure positives and negatives are in contact as long as  $R_A/R_X > \sqrt{2} - 1 = 0.41$ . Several such series have been discovered, another example being the change from calcite to aragonite structures amongst the carbonates and nitrates, where the small cations are found in calcite-type structures and large cations in aragonite-type structures.

*Layer Lattices.*—It will be seen that the lattices of CdI<sub>2</sub> and MoS<sub>2</sub> are of a peculiar type. Instead of an alternation of positive and negative ions in every direction, the structure consists of layers. Two sheets of anions (white) are interleaved by a sheet of cations (black), and these composite sheets are laid one above the other. Hund first called such structures *Schichtengitter*, or layer lattices, and it has been shown that they are formed by combinations of positive ions with highly polarisable negative ions. The crystals have been appropriately described as ionic in two dimensions in the layers, and molecular at right angles to the layers. The crystals part and glide very easily along planes parallel to the layers, having a graphite-like structure. Goldschmidt in reviewing the disulphides, diselenides, and ditellurides concludes that the larger ions Zr, Sn, Ti, W, Mo, Pt, Pd form layer lattices, whereas the smaller ions form structures of the pyrites type, e.g. Mn, Os, Ru, Fe, Co, Ni.

*Zincblende and Wurtzite Types.*—Zinc sulphide,  $\text{ZnS}$ , crystallises in two forms, as cubic zincblende and as hexagonal wurtzite with the structure shown for  $\text{ZnO}$  in fig. 77. The structures are essentially the same in principle, each atom being surrounded symmetrically by four of the other kind. These structures resemble that of diamond, and are called 'adamantine.' They show an interesting transition between the ionic and homopolar types.

The condition for the occurrence of these compounds can be described by referring to the periodic table (p. 123). Carbon, silicon, germanium, and tin are tetravalent elements in the same column of the periodic table, and form structures of the diamond type. An adamantine compound is formed between an element which is a certain number of places to the left of the C, Si, Ge, Sn column, and an element which is the same number of places to the right. We have, for instance, the series:

$\text{SnSn}$	2.79	$\text{GeGe}$	2.43	$\text{SiSi}$	2.347
$\text{InSb}$	2.793	$\text{GaAs}$	2.435	$\text{AlP}$	2.360
$\text{CdTe}$	2.799	$\text{ZnSe}$	2.452		
$\text{AgI}$	2.811	$\text{CuBr}$	2.460		

where the two elements are in the same row. Series are also formed by elements in different rows of the periodic table:

$\text{CuI}$	2.618	$\text{MgTe}$	2.76	$\text{CuCl}$	2.341
$\text{ZnTe}$	2.637	$\text{AlSb}$	2.638	$\text{ZnS}$	2.346
$\text{GeSb}$	2.638	$\frac{1}{2}(\text{SiSn})$	2.57	$\text{GaP}$	2.354
$\frac{1}{2}(\text{GeSn})$	2.62	$\text{PIn}$	?	$\frac{1}{2}(\text{GeSi})$	2.39
$\text{AsIn}$	?	$\text{SCd}$	2.521	$\text{AsAl}$	2.437
$\text{SeCd}$	2.62				

The figures represent the distances between atomic centres in these compounds, and it will be noticed that they are practically constant in each group, as was first pointed out by Grimm and Sommerfeld. Now the diamond structure is typically homopolar, and the constancy of interatomic distance in each column of the above series indicates that the distance is determined rather by a bonded electronic structure than by a packing of ions.

*The Nickel-arsenide Type.*—The curious nickel-arsenide structure is found in many compounds of Cr, Mn, Fe, Co, Ni, Cu with S, Se, Te and As, Sb, Bi. The structure is hexagonal.

The metal atoms (black in fig. 77) lie upon a simple hexagonal lattice, and the other atoms (white) upon two interpenetrating lattices, which together build up a structure of hexagonal close-packing. The compounds are more nearly akin to alloys than to ionic compounds. They are conductors and show metallic reflection. The metal atoms not only have six neighbours of the metalloid, but also are nearly 'in contact' in the direction of the  $c$  axis, their interatomic distance parallel to  $c$  being about twice the metallic radius. Finally, the amount of metal can exceed the 50 per cent. (atomic) demanded by the AX formula, a feature which is often found in alloys but which is impossible in a true ionic crystal. It is very striking to find a compound such as FeS, which is of this type, possessing properties characteristic of an alloy.

**Complex Acid Radicals.**—In a large group of inorganic salts the negative ion is composite, as in the nitrites, nitrates, carbonates,

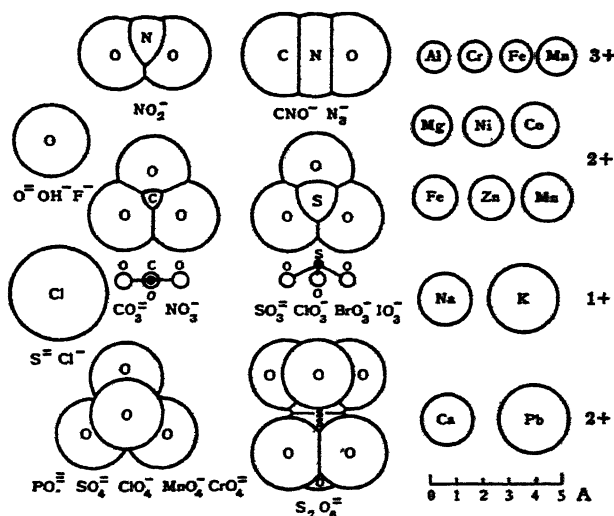


FIG. 79.—The structures and dimensions of some acid radicals

sulphates, and perchlorates. The ion consists of several oxygen atoms arranged around a central atom. Two important features of these acid radicals may be mentioned.

In the first place, an acid radical has the same form in different compounds, within the error of X-ray measurement. The forces binding oxygen to sulphur in an SO<sub>4</sub> group, for instance, appear

to be so strong in comparison with the forces between the group and other ions, that the group preserves a characteristic tetrahedral shape and constant size.

In the second place, the law of constant ionic size holds good here as in the case of simple ions. To represent the packing of the ion into the surrounding structure we must picture spheres of radius 1.32 Å. (the oxygen radius) centred at each oxygen atom, although this makes oxygen atoms which belong to the same group overlap to a considerable extent. Other ions are in contact with these spheres.

Fig. 79 shows the structure and dimensions of a number of common negative ions. For the sake of comparison, several positive ions have been drawn to the same scale. Several structures which illustrate the packing together of positive and negative ions are shown in fig. 80, Pl. VII.

**Co-ordination Compounds.**—Potassium hexachloroplatinate,  $K_2PtCl_6$ , is an example of a group of compounds which represent the co-ordination compounds of Werner's theory. The term co-ordination has been extended by common use in X-ray analysis to many ionic compounds such as have been described above. This extension is natural and legitimate, since the regular arrangement of a set of atoms around a central atom which Werner postulated for co-ordination compounds resembles the typical grouping of one kind of ion round the other in ionic crystals. The chemical formulæ of co-ordination compounds gave a first hint of the much more widespread feature discovered by X-ray analysis. The more restricted term co-ordination compound is appropriately used in such cases as the following :—

Ferrocyanides . . .	$K_4Fe^{++}(CN)_6$
Ferricyanides . . .	$K_3Fe^{+++}(CN)_6$
Cobaltinitrites . . .	$K_3Co^{+++}(NO_2)_6$
Cobaltammines . . .	$Cl_3Co^{+++}(NH_3)_6$ , etc.

The structure of  $K_2PtCl_6$  is shown in fig. 81 (b). Other compounds with the same structure are  $(NH_4)_2SnCl_6$ ,  $(NH_4)_2SiF_6$ ,  $Cl_2Ni(NH_3)_6$ , to name a few examples. The arrangement of these  $R_2MX_6$  compounds is like that of fluor,  $CaF_2$ , R replacing F and the octahedral group  $MX_6$  replacing Ca. A diagram of potassium chloroplatinite,  $K_2PtCl_6$ , is given in the same figure in order to show its interesting  $PtCl_4$  group, which is planar and not tetrahedral.

# PLATE VII



FIG. 80.—Crystal models which illustrate the packing together of ions

a, Sodium chloride  
c, Calcite,  $\text{CaCO}_3$   
e, Iron pyrites,  $\text{FeS}_2$

b, Cesium chloride  
d, Aragonite,  $\text{CaCO}_3$   
f, Anhydrite,  $\text{CaSO}_4$



A number of structures containing *water of crystallisation* are closely allied to the co-ordination compounds. In  $\text{BeSO}_4 \cdot 4\text{H}_2\text{O}$ , for example, there is a tetrahedral group of water molecules around each beryllium atom, and the whole acts as a composite positive ion. In  $\text{NiSO}_4 \cdot 6\text{H}_2\text{O}$  there is a similar sixfold group around nickel. A large number of hydrates, ammoniates, and

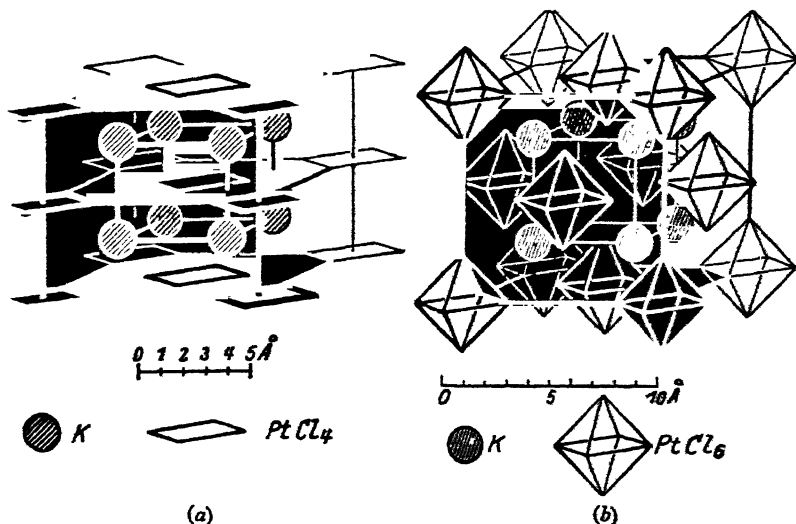


FIG. 81.—The structures of (a)  $\text{K}_2\text{PtCl}_4$ , and (b)  $\text{K}_2\text{PtCl}_6$ .  
(*Strukturbericht*, P. P. Ewald and C. Hermann, Akad. Verlag, 1931)

co-ordination compounds have been studied, especially by Wyckoff and by Hassel. In such compounds as  $\text{NiSnCl}_6 \cdot 6\text{H}_2\text{O}$  there exists both a negative co-ordination group  $\text{SnCl}_6$  and a positive complex  $\text{Ni} \cdot 6\text{H}_2\text{O}$ . The general feature of a symmetrical group surrounding a central atom substantiates Werner's original hypothesis.

*The Silicates.*—The elucidation by X-ray methods of the structures of silicates is a striking example of the application of these methods to a problem of chemical constitution. It is difficult to investigate silicates by purely chemical methods. The majority can only exist in the solid state, and the character of the constituent groups is entirely lost in chemical processes. The composition of any particular species is often so variable that it is difficult to assign a standard formula. Formulae of typical silicates are given below, but it must be stressed that wide variations from these ideal formulae occur in natural compounds



owing to the substitution of one element for another. The groups into which the substances are divided represent a classification according to structure as determined by X-ray analysis.

- |  |  |
|--|--|
| I. Forsterite, $\text{Mg}_2\text{SiO}_4$<br>Phenacite, $\text{Be}_2\text{SiO}_4$<br><br>Zircon, $\text{ZrSiO}_4$<br>Garnet, $\text{Ca}_3\text{Al}_2(\text{SiO}_4)_3$   | Topaz, $(\text{AlF})_2\text{SiO}_4$<br>Cyanite, sillimanite, andalusite,<br>$\text{Al}_2\text{OSiO}_4$<br>Chondrodite, $\text{Mg}(\text{OH})_2 \cdot 2\text{Mg}_2\text{SiO}_4$   |
| II. Melilite, $\text{Ca}_2\text{MgSi}_2\text{O}_7$<br>Hemimorphite,<br>$\text{Zn}_4(\text{OH})_2\text{Si}_2\text{O}_7 \cdot \text{H}_2\text{O}$  | Benitoite, $\text{BaTiSi}_3\text{O}_9$<br>Beryl, $\text{Be}_3\text{Al}_2\text{Si}_6\text{O}_{18}$  |
| III. Diopside, $\text{CaMg}(\text{SiO}_3)_2$<br>Acmite, $\text{NaFe}(\text{SiO}_3)_2$  | Tremolite, $\text{Ca}_2\text{Mg}_5(\text{OH})_2\text{Si}_8\text{O}_{22}$<br>Amphibole, $(\text{Ca}, \text{Na})_2\text{Na}_{9-1}\text{Mg}_1$<br>$(\text{Mg}, \text{Al})_4(\text{Al}, \text{Si})_2\text{Si}_6\text{O}_{22}(\text{O}, \text{OH}, \text{F})_2^*$ |
| IV. Pyrophyllite, $\text{Al}_2(\text{OH})_2\text{Si}_4\text{O}_{10}$<br>Talc, $\text{Mg}_3(\text{OH})_2\text{Si}_4\text{O}_{10}$<br>Kaolin,<br>$\{\text{Al}(\text{OH})_2\}_2 \cdot \text{Al}_2(\text{OH})_2\text{Si}_4\text{O}_{10}$ | Muscovite, $\text{KAl}_2(\text{OH})_2(\text{Si}_3\text{Al})\text{O}_{10}$<br>Phlogopite, $\text{KMg}_3(\text{OH})_2(\text{Si}_3\text{Al})\text{O}_{10}$<br>Margarite, $\text{CaAl}_2(\text{OH})_2(\text{Si}_2\text{Al}_2)\text{O}_{10}$                      |
| V. (a) Orthoclase, $\text{KAlSi}_3\text{O}_8$<br>Albite, $\text{NaAlSi}_3\text{O}_8$<br>Anorthite, $\text{CaAl}_2\text{Si}_2\text{O}_8$  | (b) Analcite, $\text{Na}(\text{AlSi}_3\text{O}_8)\text{H}_2\text{O}$<br>Natrolite, $\text{Na}_2(\text{Al}_2\text{Si}_5\text{O}_{10}) \cdot 2\text{H}_2\text{O}$  |
| VI. Quartz, cristobalite, tridymite, $\text{SiO}_2$  |  |

The clue to the classification of these formulæ is found by considering the silicon-oxygen arrangement apart from the remainder of the structures. If the silicates resembled ordinary salts, this would be equivalent to a classification according to their acid groups, and indeed in the past many hypothetical acids of silicon have been formulated. The structure of the silicates is, however, of a different kind. In some cases the silicon-oxygen structure forms closed groups like ordinary acid radicals, but in general the structure is endless, extending right through each individual crystal. Silicon is in an intermediate position between aluminium and magnesium on the one hand, which form continuous ionic structures with oxygen, and phosphorus, sulphur, and chlorine on the other hand, which form with oxygen discrete acid radicals.

Silicon is always found between four oxygen atoms. The

\* Ferrous iron replaces magnesium, and ferric iron aluminium, in this formula, which is due to Warren and to Berman and Larsen.

crystals of the first group above (orthosilicates) contain independent tetrahedral  $\text{SiO}_4$  groups, like quadrivalent acid radicals. Each oxygen of such a group is linked to one silicon atom, and acts as a centre of negative charge  $-e$  attracting the positive ions of the crystal. It is possible, however, for an oxygen atom to be common to two tetrahedral groups which are thus linked by their corners; such an oxygen is neutral, its valency being satisfied by its two bonds to silicon on either side. One or more corners of each tetrahedral group may be linked each to a neighbour in this way. Different skeletal arrangements of these tetrahedral groups linked by corners form the basis of the vast number of different silicate structures.

Examples of the most prevalent types of grouping are shown in fig. 82. There exist

- I. Independent  $\text{SiO}_4$  groups.
- II. Closed systems, such as two tetrahedra linked to form  $\text{Si}_2\text{O}_7$ , three in a ring to form  $\text{Si}_3\text{O}_9$ , or six in a ring to form  $\text{Si}_6\text{O}_{18}$ .
- III. Endless chains and bands. The simplest type of chain is a string of tetrahedra linked corner to corner, the composition of such a chain being  $(\text{SiO}_3)_n$ . A band is formed by linking two such chains side by side, as shown in the figure, and this band has the composition  $(\text{Si}_2\text{O}_6)_n$ . Chains and bands are found in the pyroxenes and amphiboles respectively, two large families of minerals with a fibrous character (asbestos is an example). The chains are like endless linear acid radicals, and are bound together laterally by the metallic ions.
- IV. Sheets of linked tetrahedra, each tetrahedron sharing three corners. The composition of a sheet is  $(\text{Si}_2\text{O}_5)_n$ . Such hexagonal sheets are found in laminar minerals, such as talc and mica, which cleave with extreme ease parallel to the plates and have a pronounced pseudo-hexagonal symmetry. The sheets are cemented together by metallic ions.
- V. Three-dimensional networks, in which each tetrahedron shares every corner. If such a structure were built entirely of silicon and oxygen, the composition would

## THE CRYSTALLINE STATE

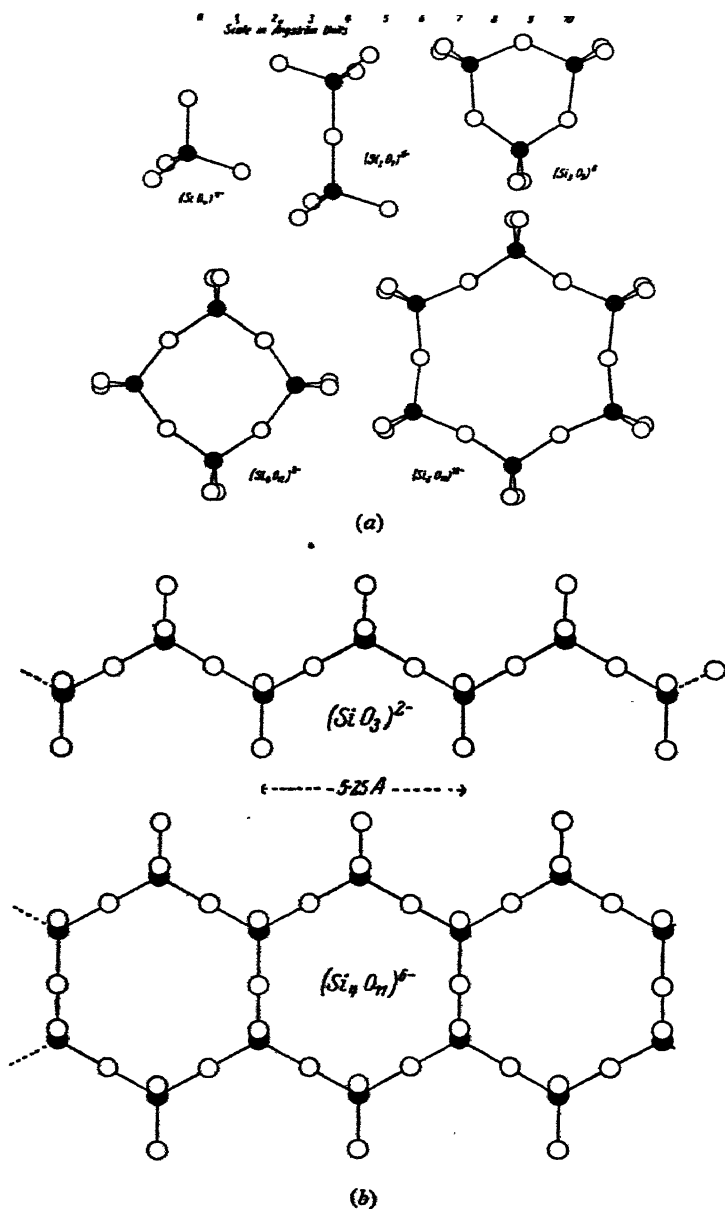


FIG. 82.—Types of silicon-oxygen grouping in the silicates  
 (a) Closed groups. (b) Chains and bands

(*Zeit. f. Krist.*, 74, 269 and 270, 1930)

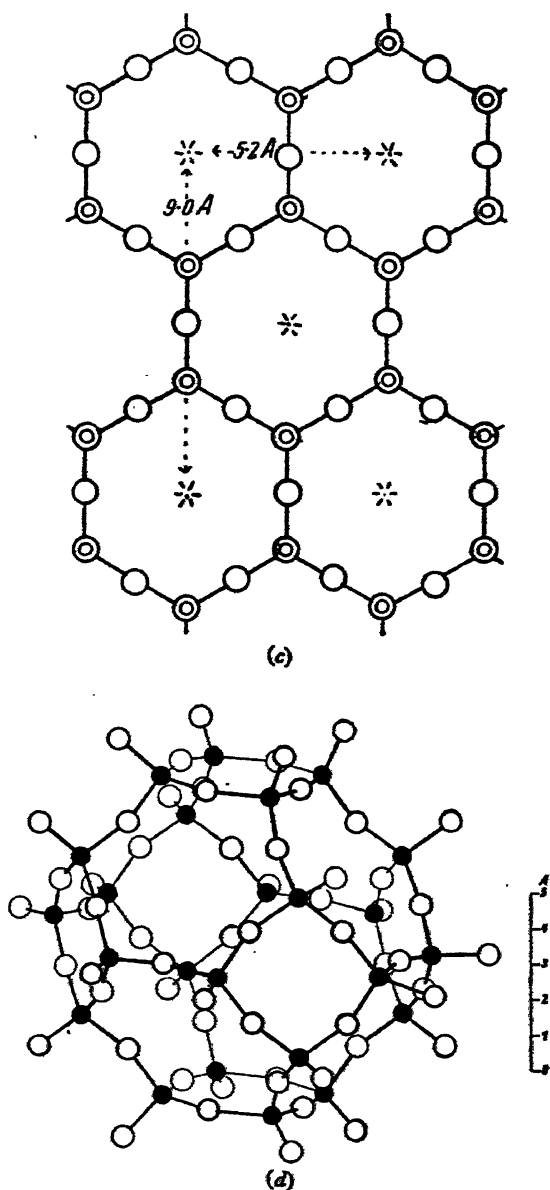


FIG. 82.—Types of silicon-oxygen grouping in the silicates  
 (c) Sheet (mica). (d) Three-dimensional net (ultramarine).  
 (Zeit. f. Krist., 74, 271 and 265, 1930)

be  $(\text{SiO}_2)_n^3$ , and the various forms of silica are of this type. Corresponding silicates exist in which the silicon is partly replaced by aluminium, preserving the ratio  $(\text{Si}, \text{Al})\text{O}_2$ . The tetrahedral framework then has a resultant negative charge, and metallic ions are incorporated in its interstices. The acid radical must be considered as extending throughout the entire crystal. The felspar group of minerals have this structure. The zeolites are similar but the framework is more open, and contains loosely held water molecules.

The different types are characterised by an increasing ratio of silicon to oxygen, viz. :

	Ratio Si : O	
I. $\text{SiO}_4$	1 : 4	Tetrahedron
II. $\text{Si}_2\text{O}_7$	2 : 7	Double tetrahedron
$\text{Si}_3\text{O}_9$ , $\text{Si}_6\text{O}_{18}$	1 : 3	Ring
III. $(\text{SiO}_2)_n$	1 : 3	Chain
$(\text{Si}_4\text{O}_{11})_n$	4 : 11	Band
IV. $(\text{Si}_2\text{O}_5)_n^2$	2 : 5	Sheet
$\{(\text{Si}, \text{Al})_2\text{O}_5\}_n^2$		
V. $\{(\text{Si}, \text{Al})\text{O}_2\}_n^3$	1 : 2	Three-dimensional net
VI. $(\text{SiO}_2)_n^3$		

The replacement of silicon by aluminium within the silicon-oxygen complex may take place in all the extended structures. The consequent increase in negative charge is compensated by the incorporation of additional cations, or by a parallel substitution of one cation by another of higher valency.

The complete structures of silicates are too complex and numerous to be shown here and will be described in the later volume. Their peculiar chemistry is explained by their extended acid radicals ; in particular it will be clear why the radicals cannot be isolated by chemical means but break down when this is attempted. Though the silicates are the most important compounds of this class, the extended radical structure is not confined to them ; Zachariasen has shown, for instance, that similar complexes of linked triangles occur in the borates (see fig. 83).

*The Heteropolyacids.*—It has been seen that the groups consisting of boron between three oxygen atoms, and silicon between four oxygen atoms, are of such a nature that extended linking can take place. An oxygen atom held in common between neighbouring groups links them together, and the process may be indefinitely repeated leading to chains and sheets which are negatively charged and act as extended acid radicals. This

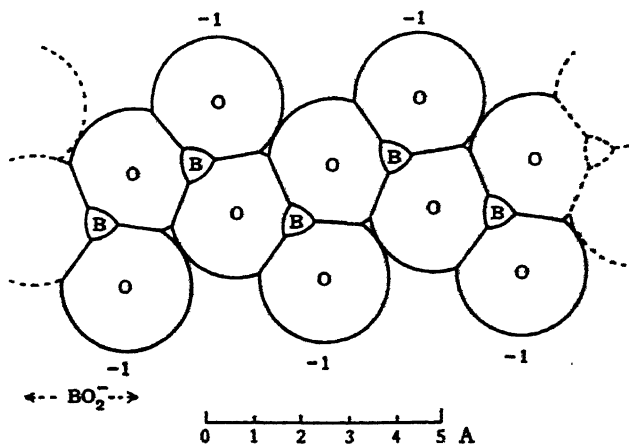
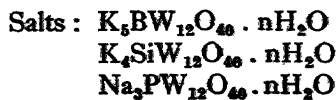
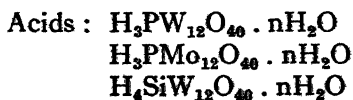


FIG. 83.—The negative ion in  $\text{CaB}_4\text{O}_6$

possibility of extended linking is ascribed to the fact that boron is trivalent and between three atoms, and silicon tetravalent and between four atoms, so that the valency of the oxygen atom is half satisfied by the link to B or Si, and completely satisfied when it is shared by two groups.

Further on in the periodic table atoms exist which we might expect to satisfy the conditions for a similar linkage of groups by sharing an oxygen atom. Tungsten and molybdenum have a valency of six, and in crystals these atoms occur between six oxygen atoms, each of which has its valency half satisfied. It is found, however, that structures built of such groups do not form long chains or sheets, but on the other hand groups unite in clusters to form very large acid radicals of more or less globular form. They are the radicals of the heteropolyacids.

Typical compounds of this kind are :



The acids have peculiar properties. They are easily prepared, very stable, and crystallise readily. The crystals contain a large amount of water of crystallisation; the acid  $\text{H}_3\text{PW}_{12}\text{O}_{40}$  crystallises, for instance, with  $29\text{H}_2\text{O}$  from solution in water. On exposure to a dry atmosphere this water content is reduced to  $5\text{H}_2\text{O}$ . The acids are very soluble both in water and in organic liquids containing oxygen, such as ether and alcohol.

Pauling in 1929 suggested certain structures of linked octahedra for these interesting compounds, basing his predictions on the rules which he had formulated for ionic structures in general. More recently (1933) they have been examined by the X-ray powder method by Keggin, who has analysed the structures of the phosphotungstic and silicotungstic acids. They prove, in fact, to be a cluster of linked octahedral groups, though the actual structure is of a different type from that which Pauling predicted.

The structure found by Keggin for  $\text{H}_3\text{PW}_{12}\text{O}_{40} \cdot 5\text{H}_2\text{O}$  is illustrated in fig. 84. At the centre of the acid radical, which has tetrahedral symmetry, is a phosphorus atom surrounded by four oxygen atoms. Each tungsten atom is at the centre of an octahedral group of six oxygen atoms. We may start to assemble the unit by taking the central tetrahedron and three of the octahedra, as in fig. 84 (a). The three octahedra are linked by making the corner to which two small arrows are attached common to all three, and those to which one arrow is attached common to two. In other words, they form a threefold group in which each octahedron is linked to its neighbour on either side by a shared edge. The common corner is also a corner of the central tetrahedral group. Fig. 84 (b) illustrates the assembling at this stage. A group of three octahedra is linked in a similar way to each corner of the central tetrahedron, and a further linking of octahedra takes place by a sharing of corners between neighbouring groups. Fig. 84 (c) shows two threefold groups linked in this way. The whole unit is shown in a simplified form in fig. 84 (d). The crystalline structure consists of a body-centred cubic packing of the clusters shown in fig. 84 (e), with water of crystallisation between the clusters.

On counting the number of atoms in each cluster, there are found to be a phosphorus atom at the centre, surrounded by four oxygen atoms, which are also linked each to three tungsten atoms. There are twelve tungsten atoms within the octahedra, twelve oxygen atoms which form the extremities of the shared edges, twelve

oxygen atoms forming the shared corners, and twelve outermost oxygen atoms which are linked only to one tungsten. The composition of the whole is  $(PW_{12}O_{40})^{3-}$ . The formula thus arrived at by X-ray analysis is one of several alternatives proposed on chemical grounds.

The structure of these large acid radicals suggests the cause

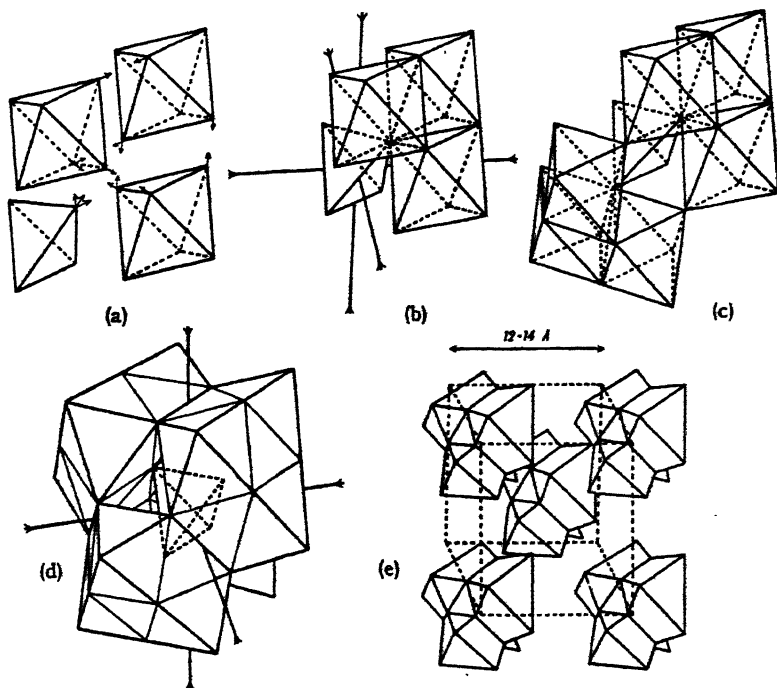


FIG. 84.—The structure of the acid radical in  $H_3PW_{12}O_{40}$

of their peculiar chemical properties. The groups may be expected to be extremely stable, since the internal links are so strong. The resultant negative charge depends upon the central atom, being three for phosphorus, four for silicon, five for boron, and so forth. This charge is distributed over so large an external cluster of oxygen atoms (36 in all) that the surface density is very small as compared with that of other complex anions. The solubility in solvents of such diverse kinds, and the property of forming compounds with complex organic groups, and 'lakes' with basic dyes, must be associated with this peculiar feature. The heteropolyacids are of numerous types, and form a class of



their own with characteristic chemical properties; their explanation is to be sought for by the aid of X-ray analysis of structure as in the case of the silicates.

*Pauling's Principles of Ionic Structure.*—Pauling in 1928 drew up a set of principles which govern the structure of ionic crystals. The basis of these principles is the recognition of the ionic structure as a set of oppositely charged bodies so arranged that the potential energy has a minimal value.

The ions composing the crystal have definite charges and characteristic sizes. If they are thought of as originally dispersed in space, and as then coming together under the influence of their mutual attractions, potential energy is released owing to the disappearance of electrostatic energy in the space surrounding each ion. We have already seen in a qualitative way how the final arrangement is determined. The ions come together until they are packed in contact (the meaning of this has been indicated above), and ions of one sign are surrounded by ions of the opposite sign. The merit of Pauling's principles is their more precise definition of the conditions for least energy. The regular co-ordination of negative ions around positive ions is present in complex compounds as well as in the simple series studied by Goldschmidt, and as a general rule the larger the central ion the larger the number of negative ions around it. For instance, in the silicates the following regular groups of oxygen ions around metal ions are found :—

Threefold group . . .	B <sup>+++</sup>
Fourfold group . . .	Be <sup>++</sup> B <sup>+++</sup> Mg <sup>++</sup> Al <sup>+++</sup> Mn <sup>++</sup> Fe <sup>++</sup> Fe <sup>+++</sup> Zn <sup>++</sup>
Sixfold group . . .	Al <sup>+++</sup> Ca <sup>++</sup> Mg <sup>++</sup> Fe <sup>++</sup> Ba <sup>++</sup>

In simple structures of AX and AX<sub>2</sub> types the regularity of these groups is fixed by symmetry. The important point established by X-ray analysis is that the groups remain approximately symmetrical even when the structure is complex and of low symmetry. Pauling accepted this regular grouping as a general principle, and added a further principle which is of fundamental importance.

The electric charge of each cation is divided between the surrounding anions, and the resulting share of an anion is defined as the strength of the electrostatic valence bond which that cation contributes to it. Pauling's principle states that the electric charge of each anion is numerically equal to the total strength of the electrostatic valence bonds from all the cations around it.

The principle may be illustrated by the beryl structure, shown in fig. 85. Each quadrivalent silicon is surrounded by four oxygen atoms, and the Si - O bond therefore has the value unity. Be<sup>++</sup> lies between four oxygen atoms, therefore the Be - O bond has a value  $1/2$ . Similarly Al<sup>+++</sup> between six oxygen atoms contributes an Al - O bond of  $1/2$ . Turning now to the anions O<sup>-</sup>, they are of two kinds. The one is linked to two Si atoms ( $1 + 1 = 2$ ), and the other to Si, Al, and Be ( $1 + \frac{1}{2} + \frac{1}{2} = 2$ ), so that the charge on oxygen is compensated in both cases.

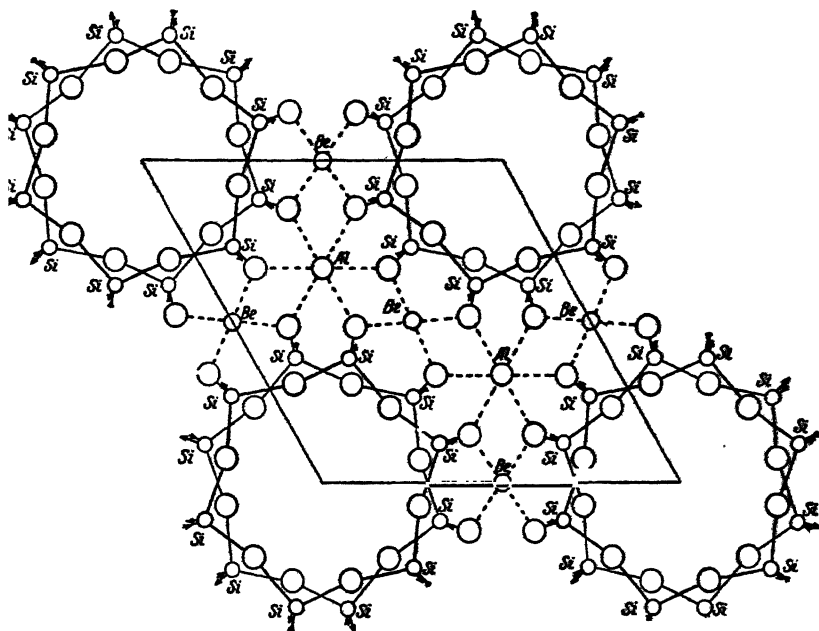


FIG. 85.—The structure of beryl,  $\text{Be}_3\text{Al}_2\text{Si}_6\text{O}_{18}$

(*Zeit. f. Krist.*, 74, 262, 1930)

We can see what this implies if we consider the potential energy as residing in the electrostatic field around the ions, and represent this field by a system of 'lines of force.' All lines of force starting from positive ions end on negative ions, since the total charges balance. The electrostatic energy will be a minimum if the lines of force are as short as possible. This is the case when all lines starting from each positive ion can end on the nearest negative ions instead of being forced to find their negative termination on distant ions. Pauling's rule is the quantitative expression of this condition ; it implies that positive and negative

charges balance locally as far as possible, as well as being equivalent in their total amount. The rule both helps in envisaging possible solutions when analysing a new structure, and in identifying its atoms and understanding its chemical nature. O' and OH' can be distinguished by counting the lines of force ending on them, for instance, although to X-rays they are identical. The rule has been amply justified by the analysis of many structures.

## METALS AND ALLOYS

In no other field has X-ray analysis afforded results which are of such theoretical and technical interest, and of such service in elucidating a maze of hitherto unrelated data, as in the investigation of metals and alloys. The exploration of this field is as yet only partial, but already one can see promise of an ordered scheme.

*Elements.*—Fig. 86 shows the periodic table as arranged by Bohr. In considering the structure of the elements we may make certain well-known generalisations. In the two short groups the character of the elements changes from metallic at the beginning of the group to non-metallic towards its end. In the long periods the metallic property is extended over nearly the whole of each period, and becomes more pronounced as atomic numbers increase. It is convenient to divide the elements which show metallic or semi-metallic properties into three classes :

### I. Alkali and alkaline earth elements.

3 Li 2	11 Na 2	19 K 2	37 Rb 2	55 Cs 2
4 Be 3	12 Mg 3	20 Ca 1	38 Sr 1	56 Ba 2

### II. Transition elements.

IV Period.	21 Sc ?	22 Ti 3	23 V 2	24 Cr 2	25 Mn ..	26 Fe 2, 1	27 Co 1, 3	28 Ni 1	29 Cu 1
V Period.	39 Y ?	40 Zr 3	41 Nb 1	42 Mo 2	43 Ma ?	44 Ru 3	45 Rh 1	46 Pd 1	47 Ag 1
Rare earths									
VI Period.	57 La ?	.. 72 Hf Λ	73 Ta 3	74 W 2	75 Re 2	76 Os 3	77 Ir 1	78 Pt 1	79 Au 1

## III. Elements of B sub-periods.

IV Period.	30 Zn	31 Ga	32 Ge	33 As	34 Se	35 Br
V Period.	48 Cd	49 In	50 Sn	51 Sb	52 Te	53 I
VI Period.	80 Hg	81 Tl	82 Pb	83 Bi	84 Po	85 -

The first class includes the elements which, according to the Bohr scheme, have one or two valency electrons marking the

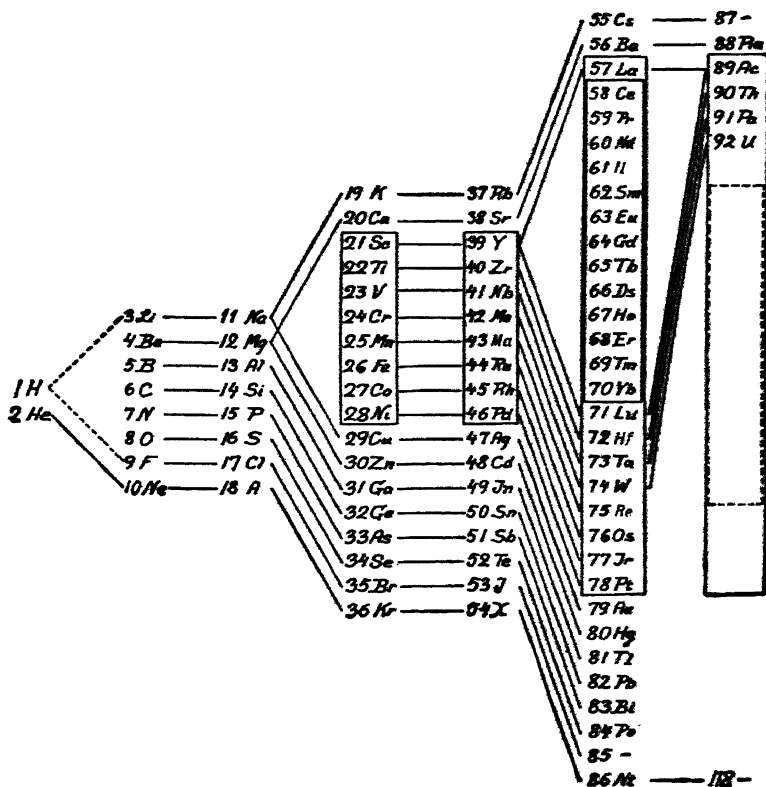


FIG. 86.—Bohr's arrangement of the periodic table

commencement of a new outer electronic shell in the periodic system. In the transition elements, the process of forming a new shell remains in abeyance while the added electrons go into an inner shell. When the inner shell is complete, the process of forming the outer shell recommences in the elements of the B sub-periods. This essential difference in the structure of the atoms is strongly reflected in the crystalline arrangements of

elements, which may be described as due to a compromise between the demands of two opposing tendencies. The first tendency is responsible for the metallic character. The binding forces are non-directional, and the crystal under their influence tends to assume one of the simple arrangements of packed spheres. Nearly all the metals in the first two classes have such a structure, and the few exceptions have an arrangement derived from one of the simple types by a small distortion. The second tendency shows itself as a closer linking of each atom to certain of its neighbours than to the remainder. All atoms in the B sub-periods have more complex structures owing to these specific bonds, and the effect increases towards the end of the period, becoming finally a typical homopolar link in diatomic molecules such as  $F_2$ ,  $Cl_2$ ,  $Br_2$ ,  $I_2$ . Some of the non-metallic elements, for example sulphur and phosphorus, have exceedingly complex structures which have not as yet been analysed:

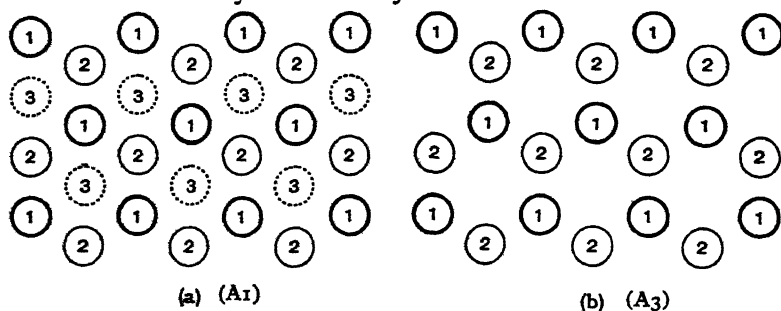
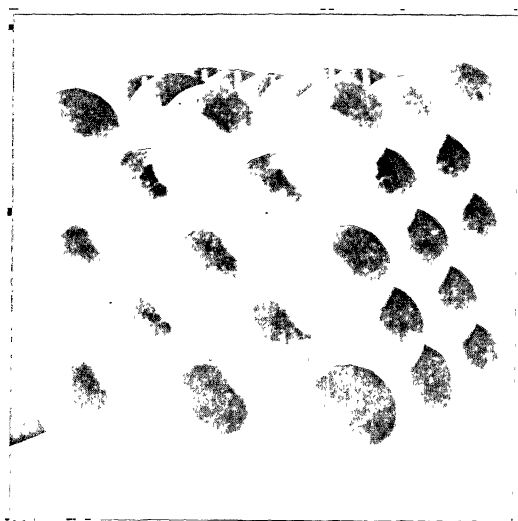


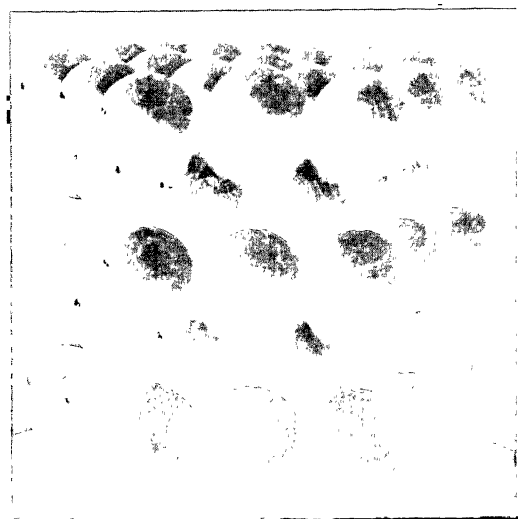
FIG. 88.—The superposition of layers in the two forms of closest packing

The simple structures assumed by many metals are of three types, which are named  $A_1$ ,  $A_2$ ,  $A_3$  in Ewald's *Strukturbericht*, and are shown in figs. 87, 88 and 89. The types  $A_1$  and  $A_3$  are structures of closest packing, or ways of packing equal spheres so that the resulting volume per sphere is the minimum possible. In a close-packed layer of spheres the centres lie at the corners of an equilateral network, marked (1) in fig. 88. The next layer of spheres whose centres are marked (2) fits over (1) if each point is over the centre of the triangle below. In adding the next layer there are two alternatives. It may either be put directly over (1) as in fig. 88 (b), or in the alternative position shown in fig. 88 (a). Fig. 88 (a) is the cubic face-centred lattice viewed along a threefold axis. Fig. 88 (b) is the arrangement of hexagonal closest packing consisting of two hexagonal

PLATE VIII



A<sub>1</sub>, Cubic



A<sub>3</sub>, Hexagonal

FIG. 87.—Cubic and hexagonal closest packing of equal spheres

(From Pope's *Modern Aspects of the Molecular Theory*)



lattices (1) and (2). It is clear that the two ways are equally efficient in packing the spheres as closely as possible. The hexagonal arrangement of closest packing has an axial ratio  $c : a = 1.632 : 1$ . The probability that these two methods of closest packing formed the basis of structures of elements was pointed out by Pope and Barlow many years before crystal analysis became possible.

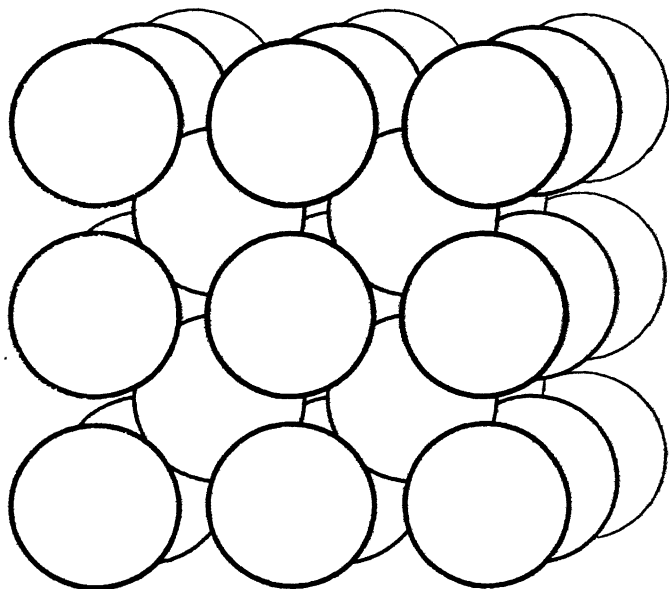


FIG. 89.—Body-centred cubic packing of equal spheres (A<sub>2</sub>)

The third simple structure (fig. 89) has atoms at cube corners and centres and is not so closely packed. In packing together incompressible spheres of radius  $a$ , each of which has a volume of  $4\pi a^3/3$  or  $4.18 a^3$ , the volume of the structure per sphere is  $5.66 a^3$  in A<sub>1</sub> and A<sub>3</sub>, and  $6.16 a^3$  in A<sub>2</sub>. Each atom is surrounded by twelve neighbours in the first two structures and eight in the second. Actually metal atoms do not pack as if incompressible spheres, and it is found that when a metal has alternative structures A<sub>2</sub> and A<sub>1</sub> (or A<sub>3</sub>), as is sometimes the case, the volume per atom is almost the same in both structures because the atoms are slightly closer together in the A<sub>2</sub> structure.

The structures of elements in the first two classes are indicated by 1, 2, 3 in Table VIII, when they belong to the A<sub>1</sub>, A<sub>2</sub>, A<sub>3</sub> types



respectively. The only elements of these classes as yet analysed which have more complex structures are Mn and Hg.

TABLE VIII

The following list of cell dimensions for the simple metallic structures is taken from the *Strukturbericht*:—

Type A1. Face-centred cubic.

	Cu	Ag	Au	Ca	Al	Ce- $\alpha$	Th	Pb	Nb	Fe- $\gamma$
$a_u$	3.61	4.079	4.070	5.56	4.041	5.12	5.08	4.93	4.191	3.63
	Co- $\alpha$	Ni	Rh	Pd	Ir	Pt	A			
$a_u$	3.554	3.520	3.80	3.873	3.823	3.91	5.42			

Type A2. Body-centred cubic.

	Li	Na	K	V	Ta	Cr- $\alpha$	Mo	W	Fe- $\alpha$	Fe- $\beta$	Fe- $\delta$
$a_u$	3.50	4.30	5.20	3.04	3.32	2.872	3.412	3.155	2.800	2.90	2.93

Type A3. Hexagonal closest packing.

	Be	Mg	Zn	Cd	Ce- $\beta$	Tl	Ti	Zr	Hf	Cr- $\beta$	Co- $\beta$	Ru	Os
$a$	2.283	3.20	2.649	2.97	3.65	3.40	2.95	3.23	3.32	2.714	2.514	2.69	2.714
$c$	3.615	5.20	4.930	5.61	5.96	5.51	4.69	5.14	5.46	4.410	4.105	4.28	4.315

The elements of the B sub-periods show very interesting relationships in structure. The tendency towards homopolar binding asserts itself as against the tendency towards close-packing. The bonds obey a rule which was first pointed out by Bradley and which has been extended by Hume-Rothery; each atom is bound closely to  $8 - n$  neighbours when  $n$  is the number of its group in the periodic table. For instance, carbon, silicon, germanium, and grey tin in the fourth period have the diamond structure with each atom surrounded by four others. Arsenic, antimony, and bismuth have a structure in which each atom has three close neighbours and three at a greater distance. In selenium and tellurium the atoms are in chains, each being connected to a neighbour on either side. Atoms in solid iodine are bound in pairs, corresponding to the diatomic molecules of bromine and chlorine. We may even trace the  $8 - n$  rule in zinc and cadmium, where each atom has six near neighbours and six at a slightly greater distance. The structures of the third group do not appear, however, to obey it. We may sum up the  $8 - n$  rule by stating that the bonds correspond to the negative valencies of the atoms; they become more pronounced towards the end of each period.

Fig. 90 shows the structures of Pd, Ag, Cd, In, Sn, Sb, Te, I, Xe, Cs drawn to the same scale, and contains examples of the majority of types. The convention is adopted of drawing the atoms as spheres in contact. When the atoms are closer to one set of

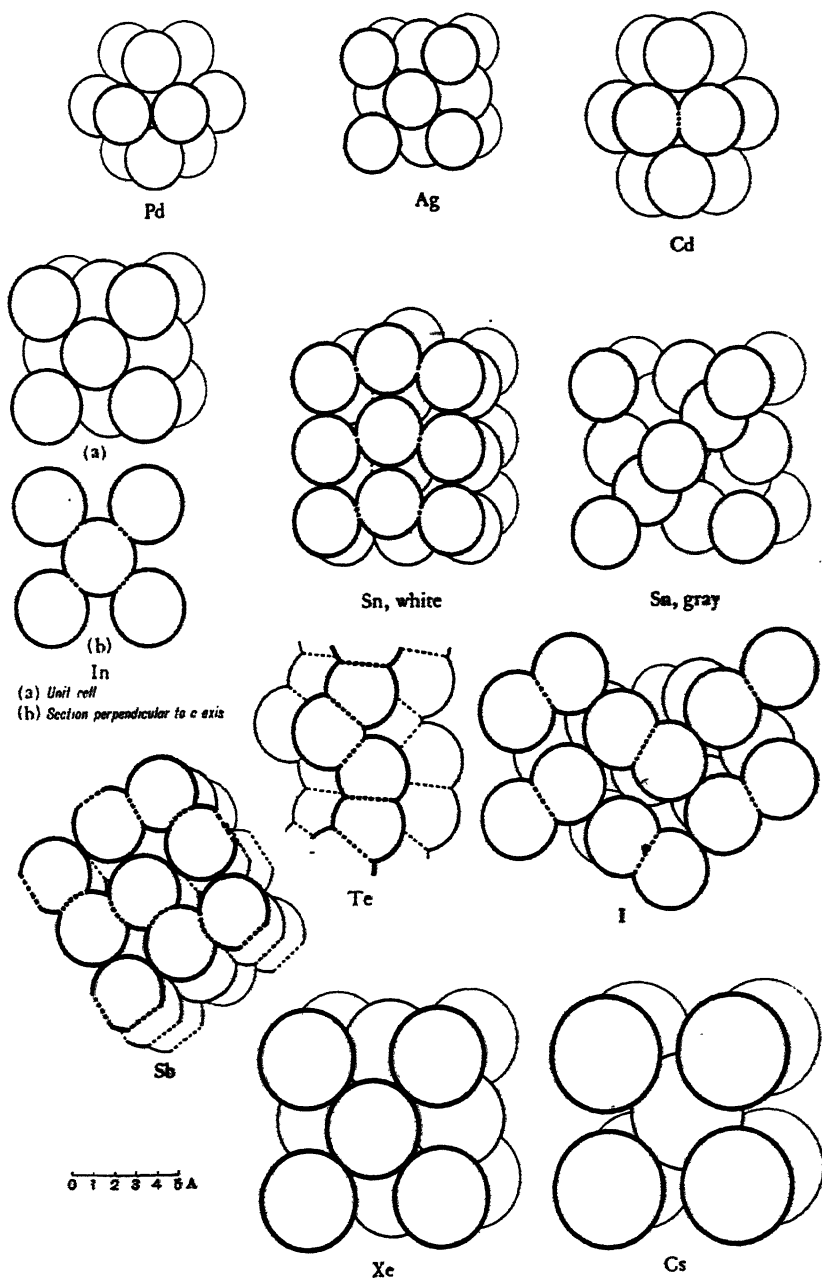


FIG. 90.—Structure of elements from palladium to caesium

neighbours than to another set, the spheres have been made to intersect in the first case and touch in the second, and an intersection is indicated by a dotted line. It will be seen that in indium and white tin the extent of intersection is only slight, and that it becomes increasingly marked in antimony, tellurium, and iodine. The large scale of the caesium structure is very apparent. Such a figure shows very well the regularities which characterise the structures of the elements.

Space forbids a full description of the more complex structures. Manganese crystallises in two forms,  $\alpha$ -Mn and  $\beta$ -Mn, which are cubic with 58 and 20 atoms in the unit cube respectively. The structures resemble those of certain complex alloys, and suggest that the manganese atoms in each structure are of two types. The structures of tetragonal white tin and cubic grey tin are shown in fig. 90. Gallium has a complex orthorhombic structure. The indium structure resembles a face-centred cubic lattice slightly extended in the  $c$  direction. Arsenic and selenium have other modifications, as yet not analysed, in addition to the forms described above.

*The Structure of Alloys.*—In the study of alloy structures we are dealing with a class of solid body whose characteristics are different from those of inorganic and organic compounds. In organic compounds the molecule is a definite entity, composed of a group of atoms whose relative numbers are unalterable. A typical inorganic crystal is composed of positive and negative constituents; the molecule has in general no existence in the structure. It may be possible to substitute one kind of positive ion for another, or of negative ion for another, without altering the nature of the structure as, for instance, in the silicates. These ions occupy definite places in the structure, however, and their substitution is governed by the rule that positive and negative charges should balance. It is therefore possible to assign definite chemical *formulae* to both organic and inorganic compounds, since the atoms are combined in constant proportion. In an alloy of two metals A and B, we are dealing not only with the relation of the two kinds of metal atom to each other, but also with the relation of both to their common system of free electrons, and the laws governing the formation of the structure are correspondingly different; in particular there is a characteristic elasticity in composition. The terms 'solid solution' and 'intermetallic compound' which have been so frequently used in describing

alloys must be based on a recognition of the physical reality to which they correspond, and must not be given a significance only applicable to inorganic and organic compounds. A typical example of an alloy system illustrates the nature of the problem.

Fig. 91 shows the equilibrium diagram of the system silver-cadmium. This example and the X-ray powder photographs in

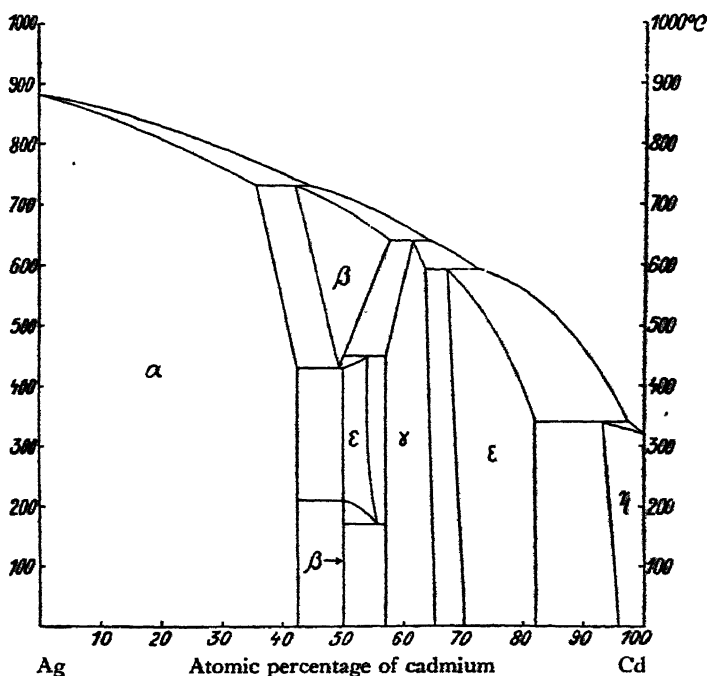


FIG. 91.—Equilibrium diagram of the silver-cadmium alloys  
(*Angewandte Chemie*, 45, 33, 1932)

fig. 92B are due to Westgren, whose work on alloys has been of outstanding importance. The composition varies from silver on the left to cadmium on the right, proportions being expressed in atomic percentage. The regions marked  $\alpha$ ,  $\beta$ ,  $\gamma$ ,  $\epsilon$ ,  $\eta$  cover ranges of composition in which the structure of the alloy is homogeneous. The intermediate regions represent a mixture of the two phases on either side of the region, in proportions which vary from the pure phase of one kind to that of the other.

Fig. 92A, and B (Pl. IX), show the results of an X-ray examination of the alloys. Pure silver has a face-centred cubic structure,

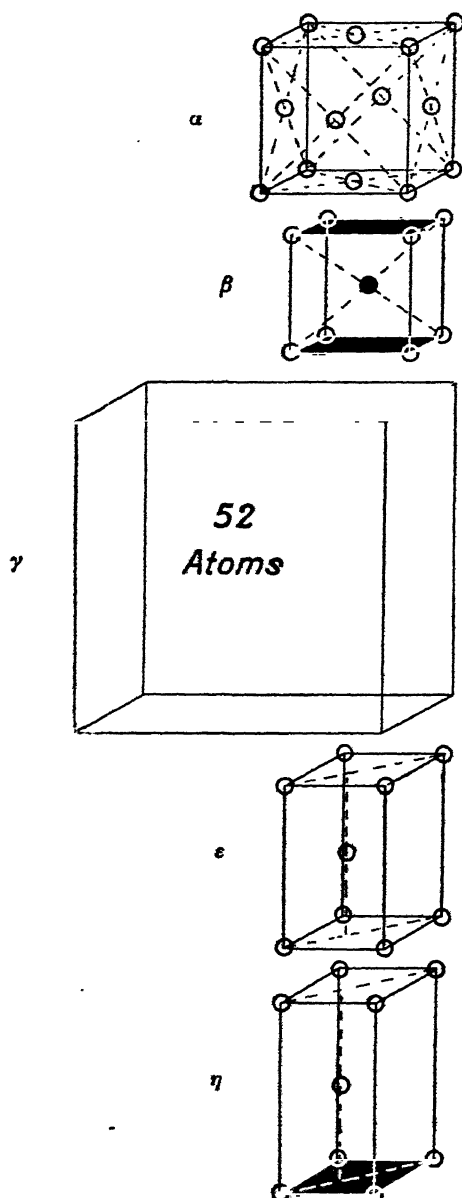


FIG. 92A.—Structure of the silver-cadmium alloy phases  
 (From a paper by A. Westgren and G. Piragmén, "Gesetzmässigkeiten im Aufbau der Legierungen," *Metallwirtschaft*, vii, 1928, pp. 700-703)

# PLATE IX

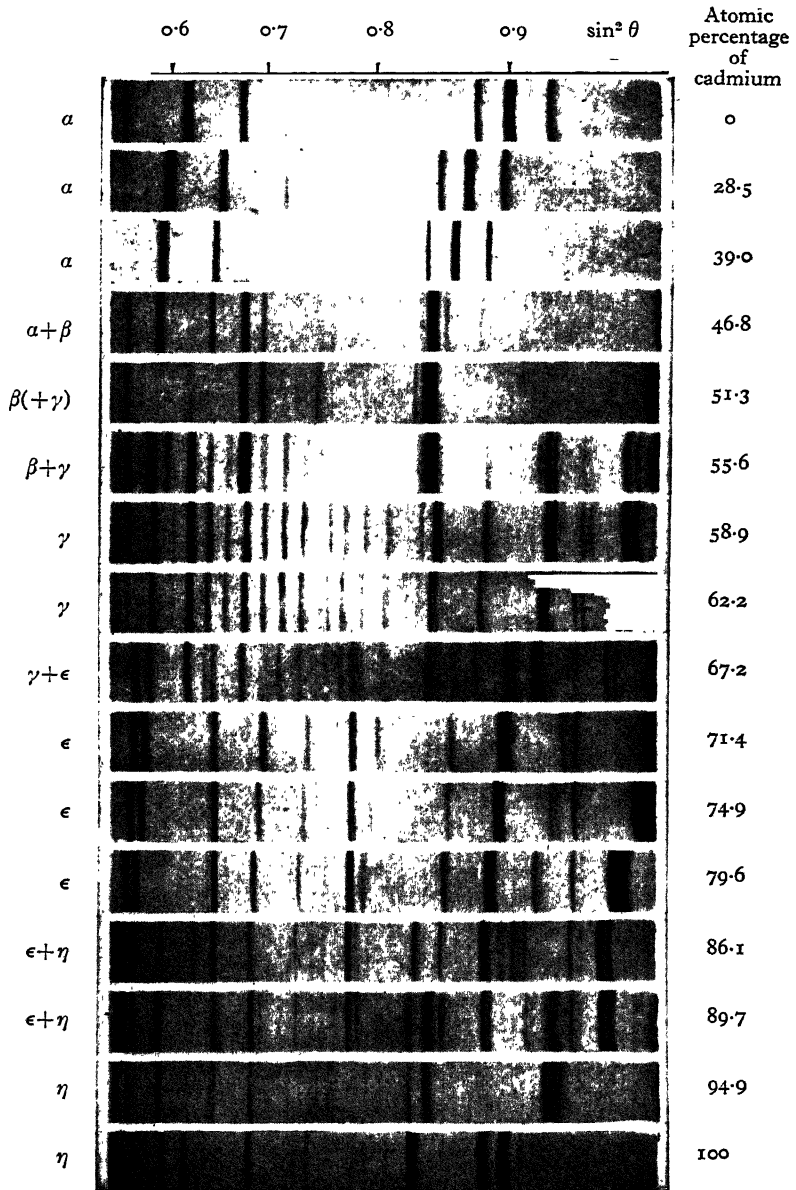


FIG. 92B.—An X-ray examination by the powder method of the silver-cadmium alloys (Westgren). FeK radiation

(From a paper by A. Westgren and G. Phragmén, "Gesetzmässigkeiten im Aufbau der Legierungen," *Metallwirtschaft*, vii, 1928, pp. 700-703)



and throughout the  $\alpha$ -phase this structure is retained. The cadmium atoms appear to replace the silver atoms at random, so that the X-ray powder photograph of the alloy only shows the lines characteristic of the face-centred lattice. This is seen in the three upper photographs of fig. 92B, where the system of lines remains the same. The addition of cadmium merely increases the scale of the structure, as shown by the displacement of all the lines towards smaller values of  $\sin \theta$ . Beyond 40 per cent. Cd a new  $\beta$ -phase appears; the  $\alpha$  lines become fainter and new lines are observed which are characteristic of a CsCl structure. Silver atoms occupy the corners of cubes and cadmium atoms the centres. Since the  $\alpha$ -phase in this two-phase region has taken up the maximum amount of cadmium, its lines show no further shift towards the left. A very narrow region of  $\beta$ -phase follows. The  $\gamma$ -phase, which next appears, is a complicated cubic structure which contains 52 atoms in the unit cell. This structure, which is found in many alloys, and is described below, has a characteristic brittleness and hardness. The  $\epsilon$ -phase is one of hexagonal close-packing, and the  $\eta$ -phase has the same relation to the hexagonal cadmium structure as the  $\alpha$ -phase has to the cubic structure of silver.

The ideas of 'solid solution' and 'intermetallic compound' are based upon such phase diagrams. The process by which the silver lattice accommodates atoms of cadmium or the cadmium lattice atoms of silver is termed solid solution, and there is a simple replacement of one atom by another. On the other hand, the phases which appear in the central portion of the diagram are sometimes termed intermetallic compounds. This is justified in the case of the  $\beta$ -phase, for instance, both by its appearance in the region of 50 per cent. Cd so that it may be assigned a formula  $\text{AgCd}$ , and by its crystalline structure, which suggests equal numbers of Ag and Cd atoms at cube corners and centres respectively. Similarly, the  $\gamma$ -structure is found in a region covering the composition  $\text{Ag}_3\text{Cd}_8$ , and it is natural to suppose that the ideal unit cell with 52 atoms contains 20 Ag and 32 Cd. The  $\epsilon$ -phase corresponds to a composition  $\text{AgCd}_3$ , but in this case there appears to be a random distribution of the atoms between the points of the hexagonal close-packed lattice, and the ratio is not supported by the crystal structure. The existence of a range of composition within each phase is described as due to a solid solution of one constituent or the other in the



phase in question. In the case of many alloy systems some of the single-phase regions are very narrow, and correspond precisely to simple stoichiometrical proportions, so that there is even greater justification for describing them as intermetallic compounds.

Further consideration shows, however, how misleading it is to give too definite a significance to these terms. In the first place, we may give an example to show that a solid solution passes by continuous steps into an intermetallic compound with no abrupt transition between the two. In the second place, a simple ratio between the numbers of the atoms in an intermetallic compound does not necessarily correspond to their ordered distribution in a crystalline structure, as in other classes of compound, though this may be one of the factors determining the proportions of the phase. The relation between the atoms and free electrons also influences this ratio, and may be of such predominating importance that the proportions are quite inconsistent with any geometrical distribution of the atoms amongst the points of the structure.

*Superlattices.*—The transition from random replacement to the regular arrangement of a superlattice, and the consequent change in the physical properties of an alloy, was first studied in detail by Johanssen and Linde in the gold-copper series. We may give here another example of a somewhat more complex type. When aluminium is added to iron in any amount up to 50 per cent. in atomic proportions, it is found that the aluminium atoms replace iron atoms in the body-centred cubic structure characteristic of iron itself. The manner of replacement has been studied in detail by Bradley and Jay, and their results are shown in figs. 93 and 95.

The results are conveniently described in terms of a lattice unit composed of eight body-centred cubes stacked together as in fig. 93. The points of this lattice are divided into four sets, *a*, *b*, *c*, *d*, as indicated in the figure, each set being on a face-centred lattice corresponding in dimensions to the large cube. If the alloys are annealed carefully, two structures appear which might reasonably be called intermetallic compounds. The first has the composition  $\text{Fe}_3\text{Al}$ , and in the structure the positions *a*, *c*, *d* are occupied by iron atoms and *b* by aluminium atoms. In other words, all corners and half the centres of the small cubes are occupied by iron atoms, and the remaining centres by aluminium atoms, in a regular way. The second structure,  $\text{FeAl}$ ,



# PLATE X

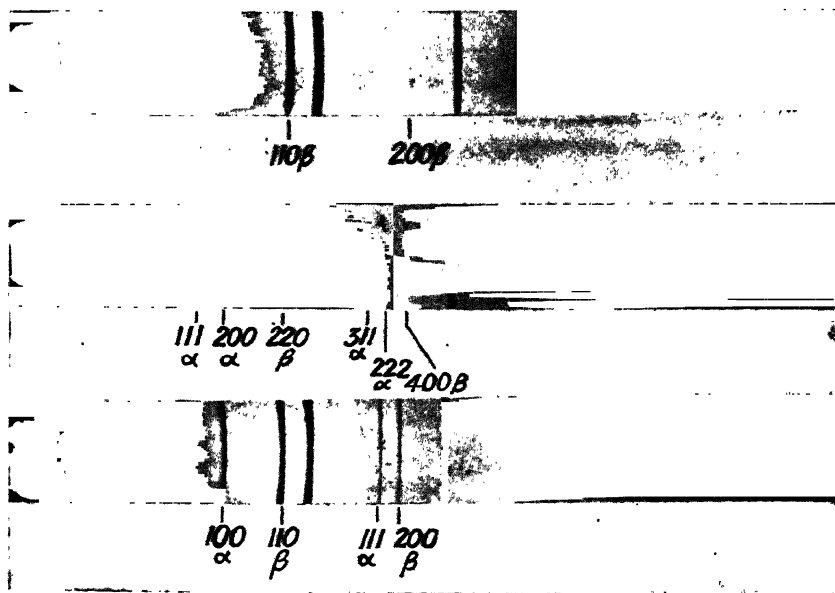


FIG. 94.—X-ray powder photographs of pure iron,  $\text{Fe}_3\text{Al}$ , and  $\text{FeAl}$ .  $\text{FeK}\alpha$  and  $\text{K}\beta$  radiation (Bradley and Jay). The lines of the body-centred lattice (upper photograph) are common to all three photographs. The faint additional lines are caused by the segregation of added Al atoms into regular positions

(*Proc. Roy. Soc., A*, **136**, 224, 1932)

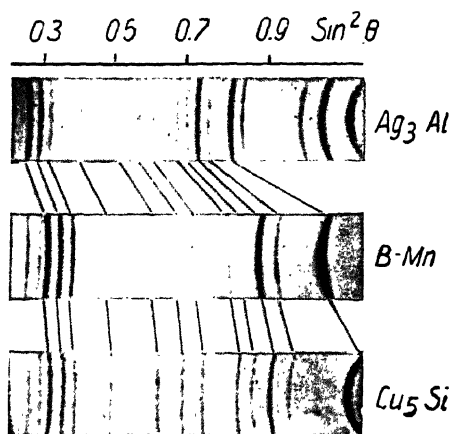


FIG. 97.—X-ray powder photographs of  $\text{Ag}_3\text{Al}$ ,  $\beta\text{-Mn}$ , and  $\text{Cu}_5\text{Si}$ . Corresponding lines are linked (Westgren)

(*Zur Chemie der Legierungen*, *Angew. Chemie*, **45**, 33, 1932)

is of the CsCl type, the corners *a* and *c* being occupied by iron and the centres *b* and *d* by aluminium. Such structures, in which certain regularly chosen positions are occupied by atoms of one kind, are termed *superlattices* ('Überstrukturen'). The interesting features appear when the alloys of intermediate composition are studied, the results being shown in fig. 94, Pl. X, p. 153. Powder photographs of all the alloys show the strong lines of the common body-centred arrangement, but when a superlattice is present, faint additional lines appear due to its structure, and the extent to which the aluminium atoms take up regular positions can be estimated from the strength of these lines (fig. 94). Considering annealed alloys in the first place, it will be seen from fig. 95 that there is a gradual transition from random to ordered replacement. Composition is plotted horizontally in the diagram,

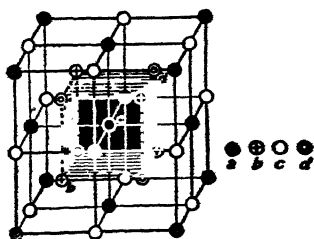


FIG. 93.—The relation of the structure of  $\alpha$ -iron to those of  $\text{Fe}_3\text{Al}$  and  $\text{FeAl}$  (Bradley and Jay)

(Proc. Roy. Soc., A, 136, 221, 1932)

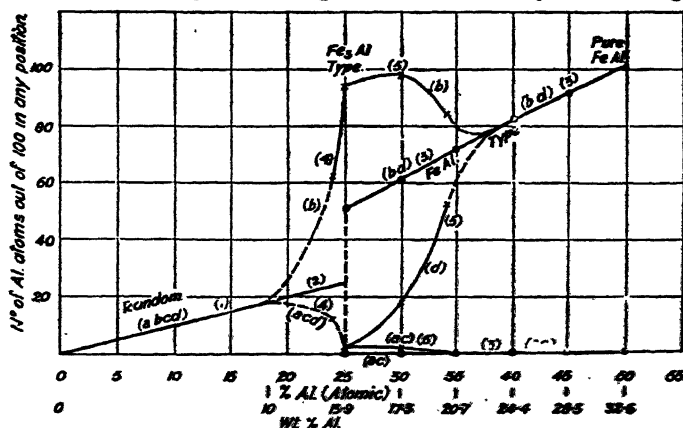


FIG. 95.—Distribution of atoms between the four positions *a*, *b*, *c*, *d* of fig. 93,  $\text{FeAl}$  alloys (Bradley and Jay)

(Proc. Roy. Soc., A, 136, 230, 1932)

and the vertical scale denotes the extent to which any given position *a*, *b*, *c*, or *d* is filled with aluminium atoms up to a maximum of 100 per cent. At first the aluminium atoms replace iron atoms at random, but beyond a certain percentage they segregate into

the  $b$  position and desert  $a$ ,  $c$ , and  $d$ . The process is complete at a composition corresponding to  $\text{Fe}_3\text{Al}$ , where  $b$  is full. Beyond this point additional atoms go into the  $d$  position, deserting  $b$  to a certain extent in order to fill up  $d$ , and finally filling both  $b$  and  $d$  completely. The quenched alloys are also interesting. There is first a random replacement in all positions, and then at a well-marked point a desertion of all  $a$  and  $c$  positions, and concentration in a random way into  $b$  and  $d$ .

It must be emphasised that the alloy consists throughout of a single phase, and that the effect studied is confined to the distribution of atoms amongst the positions characteristic of this phase. The nebulous nature of the boundary between solid solution and intermetallic compound will be obvious. The ordered arrangement must have a slightly lower potential energy than the random replacement, though the quenched structures show how easily this order is destroyed by heat motion.

*Hume-Rothery's Law.*—The above example shows how slight the influence of ordered arrangement may be in determining the relative proportions of the constituents in a phase. Hume-Rothery first pointed out another factor which determines these proportions, the factor being the relative numbers of atoms and free electrons.

The complex structure with 52 atoms in the unit cubic cell, which appears in the  $\text{AgCd}$  system illustrated in fig. 92, was first analysed by Bradley and Thewlis in the form of  $\gamma$ -brass,  $\text{Cu}_5\text{Zn}_8$ . Fig. 96 explains its nature. A body-centred cubic cell contains two atoms, and if 27 such cells are stacked together so as to build a cube of three times as great an edge, the large cube contains 54 atoms as in fig. 96 (a). The  $\gamma$ -structure is derived by removing two atoms per large cube, denoted by circles with crosses, and then allowing the remainder to shift slightly in order to close up the gaps so formed. Fig. 96 (b) shows the nature and extent of the distortion, and the number of atoms in the unit cube is thus reduced from 54 to 52.

This structure occurs in many alloy systems, and appears when the atomic proportions of the constituents are such that there are 21 free or valency electrons to every 13 atoms. For instance, it is found in the copper-zinc system when the composition approximates to  $\text{Cu}_5\text{Zn}_8$ , in copper-aluminium to  $\text{Cu}_4\text{Al}_3$ , in copper-tin to  $\text{Cu}_{31}\text{Sn}_8$ .

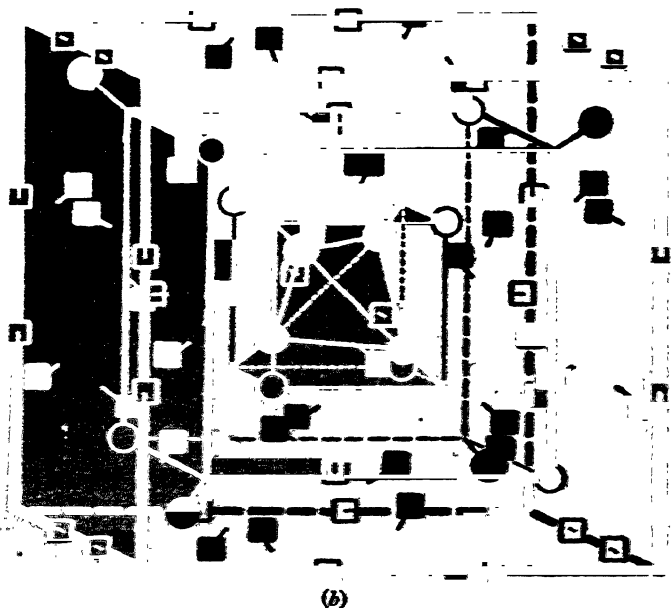
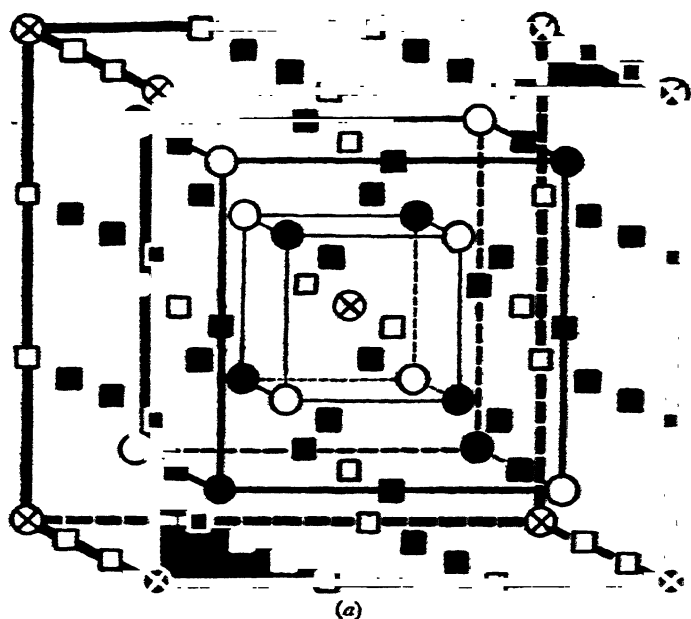


FIG. 96.—(a) The derivation of the structure of  $\gamma$ -brass from a simple cube-centred arrangement of atoms. (b) Structure of  $\gamma$ -brass (Bradley and Thewlis)

(*Proc. Roy. Soc., A*, 112, 681 and 682, 1926)

$\text{Cu}_5\text{Zn}_8$	.	.	$5 + 8 = 13$	$5 + (8 \times 2) = 21$
$\text{Cu}_9\text{Al}_4$	.	.	$9 + 4 = 13$	$9 + (4 \times 3) = 21$
$\text{Cu}_{31}\text{Sn}_8$	.	.	$31 + 8 = 39$	$31 + (8 \times 4) = 63$

Silver and gold may be substituted for copper, and cadmium and mercury for zinc, in the above formulæ. Further, ternary alloys of these metals have the  $\gamma$  structure when the 21 : 13 ratio is obeyed by the constituents. Ekman has also shown that similar  $\gamma$ -structures are formed by Fe, Co, Ni, and by the palladium and platinum triads, such as  $\text{Fe}_5\text{Zn}_{21}$ ,  $\text{Co}_5\text{Zn}_{21}$ ,  $\text{Ni}_5\text{Zn}_{21}$ ,  $\text{Pd}_5\text{Zn}_{21}$ ,  $\text{Pt}_5\text{Zn}_{21}$ . Such alloys fall into line with the 21 : 13 ratio if the first metal is assigned a valency zero.

Some of these proportions are inconsistent with any regular distribution of the two kinds of metal atoms between the points of the  $\gamma$ -structure. The relation between numbers of atoms and electrons in the structural unit overrides the influence of regular arrangement.

Similar rules hold for other characteristic structures. The body-centred  $\beta$  structure, which is illustrated in fig. 92A, as the structure of  $\text{AgCd}$ , appears when the electron-atom ratio is 3 : 2. It is found, for instance, in  $\text{CuZn}$ ,  $\text{Cu}_3\text{Al}$ , and  $\text{Cu}_5\text{Sn}$ , and also in  $\text{FeAl}$ , where again iron must be assigned zero valency. The hexagonal structure  $\epsilon$  is found when the ratio is 7 : 4.

The 3 : 2 ratio in other cases produces a complex structure in which the cubic cell contains 20 atoms, and which is similar to the structure of  $\beta$ -Mn. Examples are  $\text{Ag}_3\text{Al}$ ,  $\text{Au}_3\text{Al}$ ,  $\text{Cu}_5\text{Si}$ , and also  $\text{CoZn}_2$ . Powder photographs are shown in fig. 97, Pl. X, p. 153, and Westgren points out that the complete correspondence of the upper and lower photographs with that of  $\beta$ -Mn indicate a random distribution of the atoms in the alloys amongst the points of the structure. The proportions of atoms are also inconsistent with regular arrangement in a cell containing 20 atoms, so that there is the strongest evidence that the structure is determined by the electron-atom ratio rather than by the requirements of an atomic pattern. The phase ' $\text{Ag}_3\text{Al}$ ' has a very narrow range of composition. If definite composition with a simple ratio entitles a substance to be termed a 'compound,'  $\text{Ag}_3\text{Al}$  must be considered as such, but it is a compound of quite a different type to those which we recognise in inorganic and organic chemistry.

In general, the transition metals alloy with one another with ease, forming phases which have a wide range of composition.

On the other hand, alloys containing metals of the B sub-groups form phases which approach more closely to the ideal of an inter-metallic compound, in which the range of composition is narrow and the different atoms have their appointed places in a regular crystalline structure. They pass by continuous stages into regular compounds such as sulphides and arsenides.

*Metallic Nitrides, Carbides, Borides, and Hydrides. Interstitial Alloys.*—The difference between the transition elements on the one hand, and the elements of the B sub-groups, alkali metals, and alkaline earths on the other hand, is again shown by their compounds with nitrogen, carbon, boron, and hydrogen. Compounds of the transition metals with N, C, B, H are metallic in character, whereas compounds of other metals or metalloids with the same four elements are non-metallic.  $\text{LiH}$ ,  $\text{CaC}_2$ ,  $\text{AsH}_3$ ,  $\text{AlN}$  are examples of the latter class. The metallic nitrides, carbides, borides, and hydrides form a characteristic group with different properties from other alloys. They have been extensively studied by Gunnar Hägg, who has been the first to arrange the facts in an ordered scheme.

As a working hypothesis, Gunnar Hägg associates the peculiar features of this class of compound with the small sizes of the atoms involved. Hydrogen is unique in this respect. In the next row of the periodic table the non-metallic elements B, C, N, O, F come under review. The last two atoms are ionised when combined with metals owing to their strong affinity for electrons, and the compounds are therefore not metallic. The following radii are assigned to the remaining elements N, C, and B, rather as an aid to classification than as having a definite physical significance:—

N, 0.71 Å.      C, 0.77 Å.      B, 0.97 Å.

The compounds with transition elements are of two types. If the metallic radius of the metal (not its ionic radius) is termed  $R_M$ , and that of the other constituent  $R_X$ , the type is determined by the ratio  $R_X/R_M$ .

When  $R_X/R_M < 0.59$ , the compounds have a very simple structure. The metal atoms in practically every case are arranged in one of the forms of closest packing, cubic or hexagonal, or on a lattice which is derived from one of these forms by a small distortion of the axes which does not in any case exceed 4 per cent. The atoms of H, N, C, or B are placed in the interstices



of the metallic structures. They are so light in comparison to the metal atoms that it is difficult to find their positions by X-ray analysis, but these can be inferred from the nature of the structures. The volume per metal atom in the compound is greater than that in the pure metal, as if the metal atoms were forced apart by the foreign atoms. Such structures are called *Einklagerungsstrukturen* by Hägg, and will be referred to here as 'interstitial structures.' On the other hand, when  $R_X/R_M > 0.59$  more complex structures are found, few of which have yet been analysed. The interstitial compounds have in general a wide range of composition within each phase, whereas the complex structures have a narrow range.

All hydrides and nitrides, and some carbides, fall within the first category of interstitial compounds. The most common types have a range of composition grouped around those expressed by the formulæ  $M_2X$  and  $MX$ . The  $M_2X$  compounds are for the most part based on hexagonal closest packing of the metal atoms, examples being  $Zr_2H$ ,  $Ta_2H$ ,  $Ti_2H$ ,  $Ta_2C$ ,  $Mn_2N$ ,  $W_2C$ ,  $Cr_2N$ ,  $Mo_2C$ ,  $Fe_2N$ , though  $Pd_2H$ ,  $W_2N$ , and  $Mo_2N$  are cubic. A cubic closest packing of the metal atoms appears to be the general rule in the  $MX$  compounds, examples being  $ZrH$ ,  $TiH$ ,  $ZrN$ ,  $ScN$ ,  $ZrC$ ,  $TiN$ ,  $VN$ ,  $TiC$ ,  $TaC$ ,  $CrN$ ,  $VC$ . In one case,  $TaH$ , the metal atoms are on a body-centred cubic lattice. In addition, some examples have been found whose composition is expressed by  $MC_2$ , and in which the carbon atoms appear to be bound in pairs which are incorporated as units between the metal atoms.

Examples of the complex structures of the second category are provided by the borides of Fe and Ni, and the carbides of Cr, Mn, Fe, Co, Ni. Regularities also appear in this class. Westgren shows, for instance, that the composition of the carbide phase is richer in carbon the greater the metallic radius, and quotes the series  $TiC$ ,  $V_3C$ , and  $VC$ ,  $Cr_7C_3$  and  $Cr_3C_2$ ,  $Mn_4C$  and  $Mn_7C_3$ , and  $(Fe, Co, Ni)_3C$ , of which the Ti and V compounds are interstitial structures and the remainder complex. It is to be noted, however, that Fe can take up small amounts of carbon not exceeding 8 atomic per cent., with the formation of an interstitial structure, a process which is of fundamental importance in the metallurgy of iron.

*Summary.*—A review shows how widespread is the metallic character. It is possessed by the majority of elements and their

alloys, by the compounds described in the last paragraph, and also by structures of the nickel-arsenide type. It is present, in fact, whenever a supply of free electrons is available, and is absent when the compound contains atoms with a strong affinity for electrons. Typical inorganic non-metallic compounds are thus the halides, and those containing oxygen such as salts and complex oxides. The chemistry of the metallic compounds is of quite a different type to that of organic and inorganic compounds, and the employment of X-ray methods has contributed greatly to its elucidation.

When two metals are alloyed together in a complete range of relative proportions, a series of phases is obtained and each of those phases has its own crystalline arrangement. In contrast to other types of compound, however, it is necessary to distinguish between two characteristics of each phase. The first feature is the manner of arranging the metal atoms irrespective of their nature, or what we may term the arrangement of atomic sites in the phase. Similar arrangements of sites appear in different series of alloys, giving rise to phases with similar properties. Since each phase structure of a given type appears when the ratio of valency electrons to atoms has a characteristic value, it would appear that the arrangement of sites is determined by the interaction between the valency electrons on the one hand and the metal atoms on the other hand. The second characteristic of a phase is the manner of distribution of the two kinds of atom amongst the sites. This appears to be of secondary importance, since it is found in many cases to be influenced by heat-treatment, and sometimes to be random. Further, similar phases in different alloy systems have different ratios between the numbers of atoms, and in some cases these ratios are inconsistent with any regular distribution of the two kinds of atom. The conception of a phase as a characteristic arrangement of atomic sites is thereby confirmed.

### ORGANIC COMPOUNDS

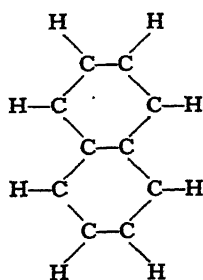
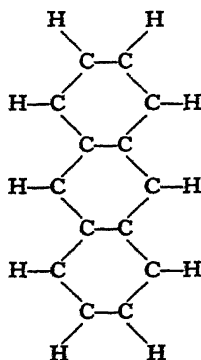
The X-ray analysis of organic compounds was begun considerably later than the analysis of inorganic compounds and metals, and the first results rather confirmed accepted ideas than produced new conceptions. The late beginning was due to the complexity of the structures, for even the compounds of

lowest molecular weight form crystals with a large number of parameters. Further, considerable progress had to be made before the new analysis could attain the point already reached by the organic chemist. The majority of inorganic substances only exist in the solid state and very little was known about their stereochemistry, so that it was possible from the very start to throw light on the problems of their structure; a new crystal chemistry has been created in this field. Similarly, the chemistry of intermetallic compounds and alloys had previously only been inferred from the phase diagrams of metallurgy, and X-ray methods were found to be peculiarly well fitted to supplement the wealth of material which the metallurgists had accumulated. On the other hand, organic chemistry is essentially based on spatial relationships between the atoms in the molecule. The organic molecule has strong internal bonds and a weak external field. It not only remains a unit during melting, evaporation, or solution, but also processes of addition or subtraction may be performed at one point in the molecular structure without altering the constitution of the remainder. Stereochemistry is founded upon this rigidity of form.

The main points of departure in building up stereochemical formulæ of aliphatic and aromatic organic compounds are the conceptions of four valency bonds around the carbon atom arranged tetrahedrally, and of six linked carbon atoms in the benzene ring. In order to lay a foundation for X-ray analysis these conceptions had to be made precise. The distances between atoms united by bonds, the angles between the bonds, and the shapes of such rings as the benzene ring had to be measured. Such elements of structure are almost unchanged in form when they are part of larger molecules, and they can be linked together when models are made.

Although the initial difficulties have been considerable the range of possible applications is immense. By combining the results of chemical analysis, X-ray analysis, and a study of physical and optical properties, stereochemistry takes on a new aspect.

*Aromatic Compounds.*—The first attempt to analyse organic compounds was made in 1921 by W. H. Bragg, who measured the unit cells of naphthalene and anthracene. The molecules are assigned a structure consisting of benzene rings joined side by side.


 Naphthalene,  $C_{10}H_8$ 

 Anthracene,  $C_{14}H_{10}$ 

The crystals are monoclinic. The forms of the unit cells are shown in fig. 98, and it will be seen that there is a close relationship

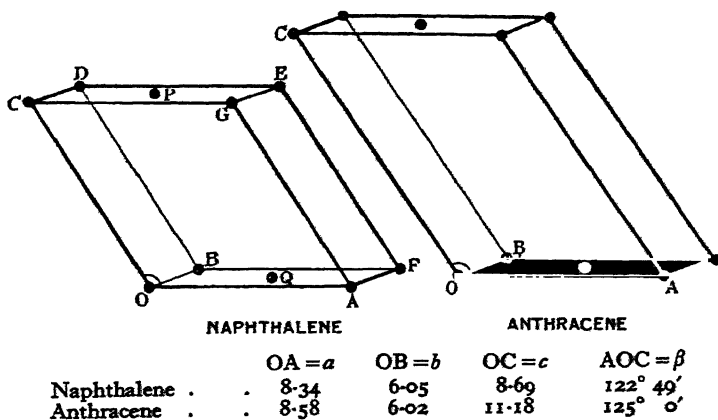


FIG. 98

between them. The  $a$  and  $b$  axes and the angles  $\beta$  are almost the same in each. They differ as regards the  $c$  axis, which is 2.49 Å. longer in naphthalene than in anthracene. Each cell contains two molecules.

W. H. Bragg inferred from this relationship that the long axis of the molecule in each case is parallel, or nearly parallel, to the  $c$  axis of the unit cell. The similarity in the molecular structures accounts for the agreement in values of  $a$ ,  $b$ , and  $\beta$ , while the greater length of the anthracene molecule explains the greater  $c$  axis. This was confirmed by comparing the difference in the  $c$  axis with the probable width of the additional benzene

ring. Hexagonal rings of carbon atoms are very evident both in the diamond and graphite structures, which are shown in fig. 99.

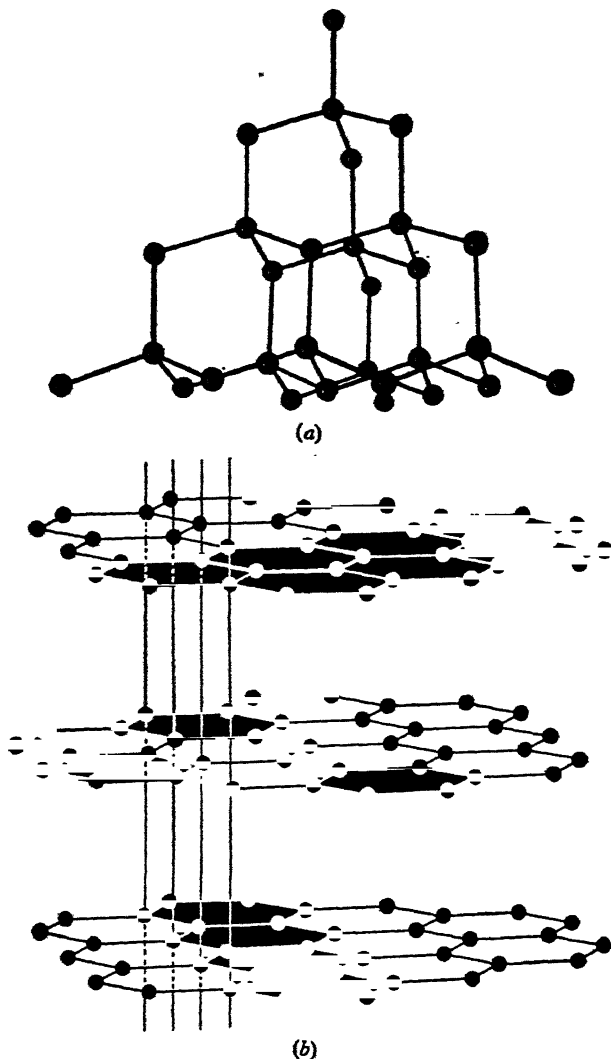


FIG. 99.—The structures of diamond and graphite  
(a) Diamond. (b) Graphite

In diamond the rings are puckered. The carbon atoms are 1.54 Å. apart, and the width of a ring or distance between lines joining opposite pairs of atoms is 2.51 Å. The rings are flat in

graphite ; although the carbon atoms are closer together (1.42 Å.), the width of the ring is 2.46 Å., or nearly as great as in diamond, owing to the atoms being coplanar. In either case, the width of the ring is very nearly equal to the difference 2.49 Å. in the  $c$  axes of the two cells. One is forced to the conclusion that the molecules are nearly parallel to  $c$ , and that the axes  $a$  and  $b$  and the angle  $\beta$  are determined by the packing of the molecules side by side.

The early measurements could not decide more precisely the positions of the molecules in the unit cell, or distinguish whether the rings are flat or puckered. Subsequent analysis has shown

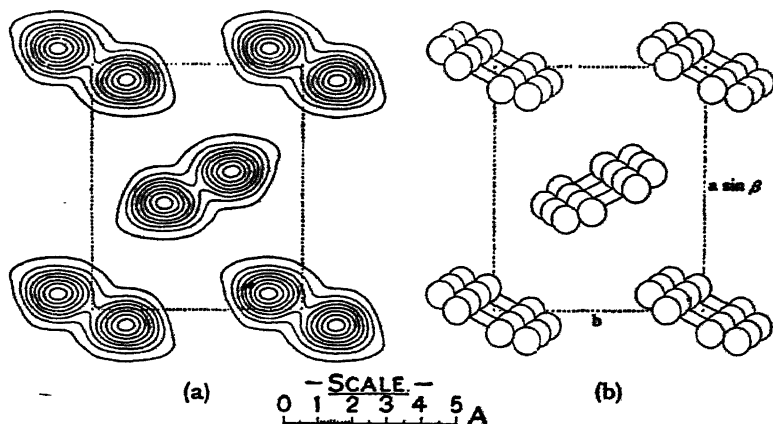


FIG. 100.—The structure of anthracene projected on a plane perpendicular to the  $c$  axis (Robertson)

that they are flat. This was first proved by Mrs Lonsdale for the structure of the benzene ring itself in the compound hexamethylbenzene,  $C_6(CH_3)_6$ , and has been confirmed by a full analysis of anthracene by J. M. Robertson. Results of the latter investigation are shown in figs. 100 and 101. Quantitative measurements of intensity for a large number of reflections by anthracene are used to build up a Fourier series, by a method described in Chapter IX. The Fourier series gives the electronic density of the crystal projected upon a given crystal plane, such as the plane  $ac$  of the unit cell. Contour lines of equal density outline the concentrations which correspond to the atoms. Fig. 100 (a) shows the Fourier projection of the molecules, whose atomic centres are in the positions of fig. 100 (b), upon a plane perpendicular to the  $c$  axis. The plane of the

molecule is slightly inclined to the direction of projection. Fig. 101 shows the group of molecules in the unit cell projected in this case upon the  $ac$  plane. It will be seen that their long axes are, in fact, very nearly parallel to the  $c$  axis. Projections on other faces enable the molecule to be viewed from other aspects, and it can be shown that all the carbon atoms lie in a

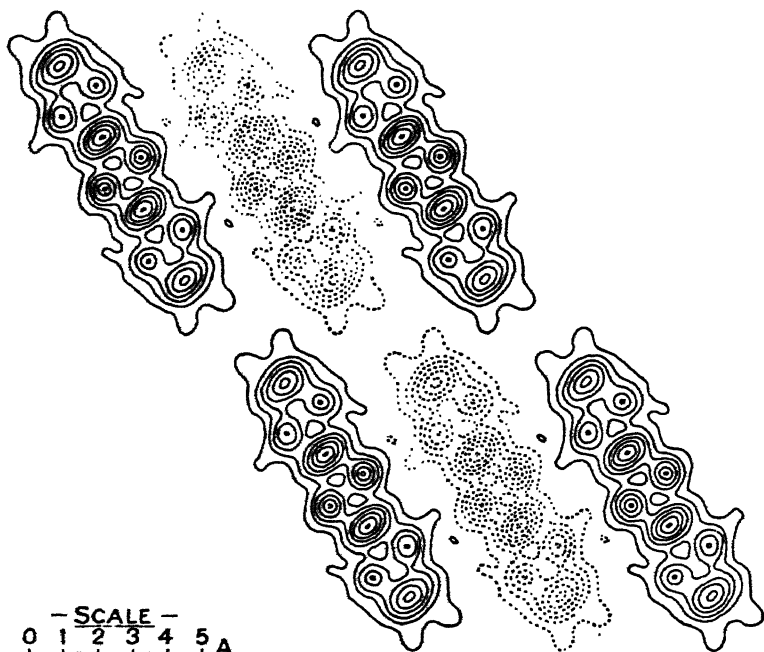


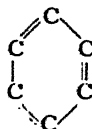
FIG. 101.—The structure of anthracene projected upon the  $ac$  plane. The longer axis is the  $c$  axis, the shorter the  $a$  axis (see fig. 135)

plane. The positions of the atoms can be deduced with considerable accuracy from the Fourier diagrams, and it is found that within the error of measurement the rings are regular hexagons whose sides are 1.41 Å., as compared with 1.42 Å. in graphite.

These results confirm the form of the ring found in crystalline hexamethylbenzene, for which Mrs Lonsdale had proved the carbon ring to be a flat regular hexagon. The carbon-carbon distance in the ring was shown to be  $1.42 \pm 0.03$  Å., and the distance between a carbon of the ring and that of a methyl group to be  $1.54 \pm 0.12$  Å. Though the latter distance is not so

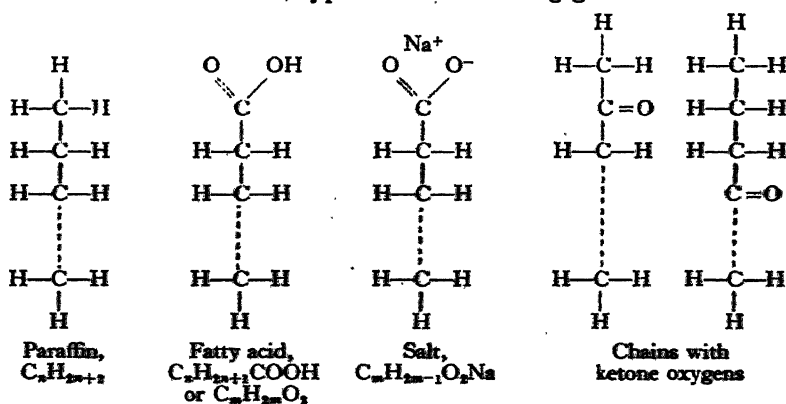
accurately fixed, it indicates a correspondence with the carbon-carbon distance in diamond.

To sum up, these pioneer researches established several points of fundamental importance. The carbon ring in these compounds is flat. It has a regular hexagonal form, there being no indication of two types of bond as in the formula:



The three bonds from the carbon atom lie in a plane, being inclined at  $120^\circ$  to each other. The carbon-carbon distance in an aromatic ring is 1.42 Å. The ring corresponds to the rings found in the graphite structure. Though benzene itself has not as yet been completely analysed, it may justifiably be inferred that the benzene ring has the same features.

*Long-chain Compounds.*—Much investigation has been carried out into the structure of long-chain aliphatic compounds, such as the paraffins and fatty acids. Powder-photograph effects with paraffin wax were obtained as early as 1913 by Friedrich, though their nature was not understood at the time. De Broglie and Friedel, Müller, Piper, Shearer, and Trillat are amongst those who have studied these compounds. They contain a long chain of linked carbon atoms, typical formulæ being given below.



The earlier investigations were carried out by modifications of the powder method, and much information was gained in this way. These results are more easily followed, however, if





1.54 Å. apart, whereas they are separated from carbon atoms of other chains by distances of 3.7–4 Å. The CH<sub>2</sub> elements, regarded as units in contact, have 'radii' of about 1.8 Å. This is indicated in fig. 103, where the packing becomes apparent. The columns representing the AA molecules are almost ellipsoidal in section, and are packed together in an approximately equilateral way, as if in closest packing. Further, the ends of AA and BB columns are related in a close-packed way, each BB end (dotted) coming between three AA ends (line), and *vice versa*. Terminal atoms of AA and BB are separated by a gap of about 4 Å.

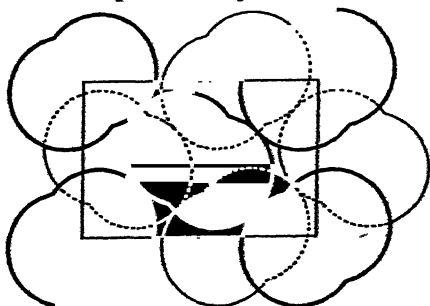


FIG. 103.—Packing of long-chain molecules

A structure of this kind, with its chains of carbon atoms arranged parallel to the long *c* axis, produces interference effects of a correspondingly striking nature. When reflecting from the plane (001), for instance, Müller found that after the first few orders the spectra were all too weak to observe until 0.0.60 and 0.0.62 were reached, which were very strong. This is so because the carbon atoms in the double tier of chains fall almost exactly upon steps obtained by dividing the *c* axis of 77.2 Å. into 60 equal parts. The molecule itself is in fact acting like a diffraction grating with 29 lines, and the spectra 0.0.60 and 0.0.62 of the unit cell fall within its first-order spectrum. Müller was able in this way to measure with the highest accuracy the ratio *S/c* (see fig. 102), which he found to be :

$$S/c = 0.03286 \pm 0.00002.$$

This gives a value of 2.54 Å. for *S*.

If we suppose the distance between carbon atoms to be 1.54 Å., and the angle of the zigzag to be the angle 109° 28' between tetrahedral bonds, the distance *S* should be :

$$2 \times 1.54 \sin \left( \frac{109^\circ 28'}{2} \right) \text{Å.} = 2.52 \text{ Å.},$$

which agrees very closely with the spacing parallel to the chain.

Müller also tried to estimate the distance *W* in fig. 102 (a), so

as to determine  $D$  and  $\psi$  as well as  $S$ . It is much more difficult to attain accuracy here. For  $D = 1.54$  A.,  $\psi = 109^\circ 28'$ ,  $W$  should be 0.89 A., whereas Müller found values between 1.6 and 1.2 A. Müller explains the discrepancy as a real effect due to the influence of the hydrogen nuclei in the  $\text{CH}_2$  group. Hengstenberg, on the other hand, who has carried out a somewhat similar investigation with  $\text{C}_{35}\text{H}_{72}$ , obtained for the same distance an estimate 0.75–0.90 A., which is in closer agreement with the calculated value, though no high degree of accuracy is to be expected.

The above structure has been described in some detail because it helps us to understand the nature of all long-chain crystals, and illustrates well the contrast between the homopolar binding within the chain, and the weak van der Waals forces between neighbouring chains. Typical powder photographs of long-chain compounds are shown in figs. 104 and 105, Pl. XI. These photographs were obtained by smearing the substance or allowing a molten drop to solidify upon a plate. The plate is mounted in a camera and oscillated a few degrees on either side of a small glancing angle about the camera axis during the exposure. The photographs of paraffins in fig. 104 show several orders of a large spacing, increasing with the number of carbon atoms as follows:—

35 carbon atoms	47.7 A.
31    "      "	42.9 A.
27    "      "	37.1 A.
23    "      "	32.2 A.
19    "      "	26.9 A.

This regularity is to be expected if the structures are similar to  $\text{C}_{25}\text{H}_{52}$ . The photographs of fatty acids in fig. 105 indicate similar regularities in spacing. They also show well what are termed the 'side spacings' or spacings of 4–5 A. associated with the lateral packing of the long molecules. These spacings, indicated by the rather diffuse lines at higher angles in the photographs, are almost independent of the length of the chain.

It will be noted in these last photographs that odd orders of the long spacing are strong and even orders weak. This is due to a linking of the fatty acid molecules such that their  $-\text{COOH}$  ends come together as in fig. 106. The consequence is a distribution of scattering matter in the reflecting planes as shown in the lower part of the figure. It is

PLATE XI

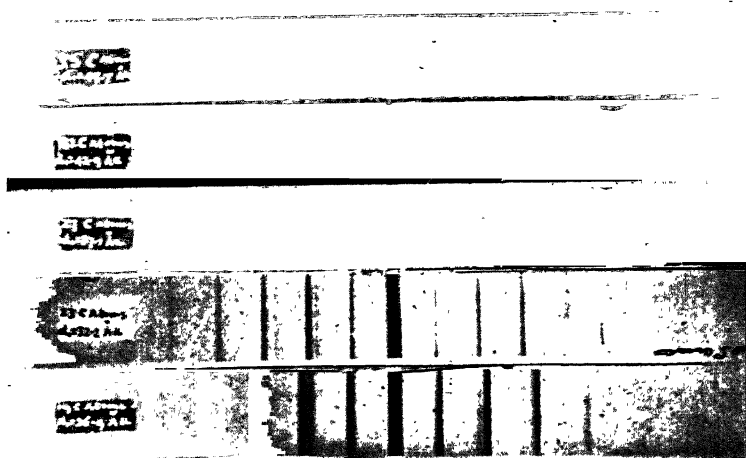


FIG. 104.—Spectra due to various hydrocarbons (Müller and Saville)

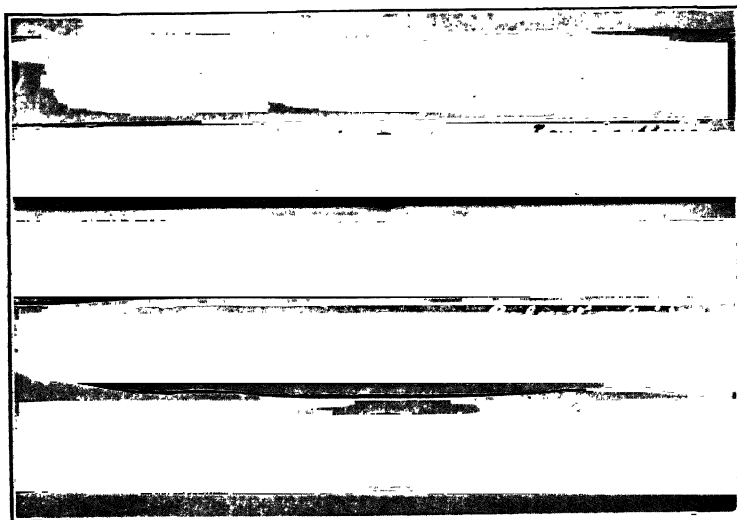


FIG. 105.—Spectra due to various fatty acids (Müller)



constant along the chain, since for these low-order spectra the carbon atoms are smoothed into a continuous distribution. The density is lower where the  $\text{CH}_3$  groups are in contact, and higher where the  $\text{COOH}$  groups come together. A uniform distribution throughout would of course give no low orders of spectra, for they are due to the break in continuity where one chain ends and the next commences; the  $\text{C}-\text{C}$  spacing only produces the very high orders. An excess at the centre and deficiency at each end of the spacing gives the reverse of the effect seen in the  $\text{NaCl}$  (III) spectra due to alternating  $\text{Na}$  and  $\text{Cl}$  planes.

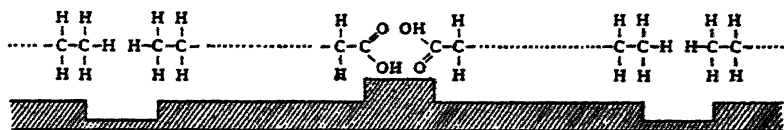


FIG. 106.—Distribution of density in fatty acids, parallel to the long spacing

Odd orders are now enhanced and even orders diminished, because a negative weight must be ascribed to the deficiency.

These examples illustrate the general nature of long-chain compounds. The long molecules pack side by side\* so as to form sheets, which are superimposed in the crystal. The long spacing which we measure is due to the repetition of these sheets. The paraffin chains which have been described are perpendicular to the sheets, and hence each added carbon atom produces a maximum effect in increasing the spacing. In other long-chain compounds the molecules, while remaining parallel, are not at right angles to the sheets, and hence the increase in spacing per carbon atom is less. Allotropic modifications of the same substance contain chains with different tilts. Müller has measured the tilt in crystals of several fatty acids, and found that the spacings are all consistent with a zigzag chain of the form outlined above although the degree of tilt varies widely. Chains with active ends, like the fatty acids, form double layers in which the active ends are in juxtaposition. The dimensions of the chains are in good agreement with the work of Langmuir and Adam on surface films. The small but characteristic difference in physical properties of compounds with odd and even numbers of carbon

\* It does not necessarily follow that these long molecules are rigid, retaining their straight form in all states. In fact, the evidence of electron diffraction by vapours, according to Märk and Wierl, points to their curling up by twisting about the  $\text{C}-\text{C}$  bonds.

atoms is explained by their crystalline arrangement; this and many other interesting points must be left to a more complete account.

*General Features of Organic Compounds.*—The investigations of  $C_{22}H_{22}$  and of anthracene, which have been described, are similar to many investigations of inorganic compounds, in that an attempt is made to determine the positions of all the atoms by X-ray analysis. While it is essential to attain this precision in the case of the fundamental types, it would be impossible to apply rigorous methods to all compounds. Their number and complexity, and the labour of the measurements, prohibit the attempt. It has been seen in such cases as the silicates that the careful investigation of a few types leads to a generalisation of the laws governing their structure, and that highly complex types can then be analysed with the aid of only a few X-ray observations which serve as a check. This holds with even greater force in analysing organic crystals. The rigidity of the molecule, the existence of homologous series, and the possibility of studying the effect of adding, subtracting, or substituting groups in the molecule, all make it possible to get a great deal of information about its structure merely by determining the lattice cell and symmetry by X-rays, without attempting to use the observations to fix all atomic positions. Pioneer work in this field has been carried out by Bernal, and a description of methods has been included in the chapter on the Principles of Structure Analysis.

As a broad generalisation, the form of the organic crystal may be ascribed to the influences of the shape of the molecule and of the binding forces. Apart from the very simple substances of low molecular weight, the molecules may be long and narrow as in the long-chain compounds, flat as in aromatic compounds, or a globular cluster with complicated inter-connections. The binding forces may be of the van der Waals type as in the hydrocarbons. These forces are weak and undirected, and hence the form of the crystal is almost entirely determined by the packing together of molecules of characteristic shape. Anthracene and the paraffins are examples. In the next place, the molecule may have local dipoles such as the OH group, and in such cases they pack together so that dipoles of opposite polarity are in juxtaposition. Sugars and alcohols are examples. Finally, organic acids and bases have

localised electrical charges which attract each other as in inorganic ionic crystals, though even here the shape of the molecule is of fundamental importance as a structure-determining factor. Experience enables the investigator to estimate the influence of these various factors, and so to arrive at possible models of the structure which can be tested.

The main point to be stressed is that complexity of the molecule is no insuperable obstacle to successful analysis. While it would be desperately difficult to find all the atomic positions by X-ray methods alone, these methods may supply just the information which is required to effect a solution when combined with other data. In fact, if X-ray methods are to be of real assistance in organic chemistry, they must be applied to the highly complex substances where purely chemical methods give uncertain results, for the structures of the simpler substances are already known. There can be no doubt that an enormous field for investigation exists, and that results of the highest importance are to be expected.

### THE ENERGY OF THE CRYSTAL LATTICE

In the majority of crystalline types, either we are as yet uncertain of the nature of the binding forces, or the complexity of this problem is too great for it to be possible to calculate the loss of potential energy when the crystal lattice is formed from its constituent units. The simple ionic crystals, however, are bound together by forces which are mainly electrostatic. It is therefore possible to correlate in a quantitative way calculations of lattice energy with observed constants such as heats of formation, of solution, and so forth.

The first calculations of this type were made by Born and Landé in 1918. Although Born has subsequently put forward a more thorough analysis of the forces, the original method is well adapted to illustrate the principles of such calculations.

Let us suppose an assembly of  $\text{Na}^+$  and  $\text{Cl}^-$  ions, arranged as in the  $\text{NaCl}$  pattern, but initially with a very large interatomic distance so that they are widely dispersed in space. They are allowed to come together, always retaining the arrangement of alternate ions. Potential energy will be liberated in the process, because the electrostatic energy in the space around each ion largely disappears owing to the lessened interspace between the



ions. A calculation of the amount of energy which thus disappears was first made by Madelung for the NaCl structure. He showed that it is equal to  $N \cdot 1.747 \cdot e^2/r_0$  ergs,  $N$  being the number of *pairs* of ions which approach, and  $e$  the electronic charge of the univalent ion. The final distance between a positive and negative ion is  $r_0$ , which is in this case one-half the edge of the unit cubical cell.

When the ions are far apart, the forces between them are entirely electrostatic. As they approach closely other forces will come into play, and finally these forces will exercise a repulsion which prevents a closer approach of the ions. In the original treatment, Born and Landé allowed for the repulsive forces by expressing the energy of formation of the lattice per ion-pair as

$$u = \frac{a}{r} - \frac{b}{r^n};$$

or, if  $N$  is the number of molecules in one gram-molecule and  $U$  is the energy per gram-molecule,

$$U = N \left( \frac{a}{r} - \frac{b}{r^n} \right),$$

where  $a$  is the Madelung constant, 1.747, multiplied by  $e^2$ , and  $b/r^n$  represents the work done against the forces of repulsion.

They next showed that both  $b$  and  $n$  could be calculated. In the first place, if  $r_0$  is the equilibrium distance between the atoms measured by X-ray analysis, it follows that

$$\left( \frac{\partial u}{\partial r} \right)_{r=r_0} = 0,$$

whence

$$b = ar_0^{n-1}/n.$$

In the second place, the coefficient  $n$  can be calculated from the observed compressibility of the crystal. A high index  $n$  implies a very rapid increase of the repulsive force as  $r$  is lessened, and so a small degree of compressibility, and *vice versa*. If the crystal under a pressure  $P$  suffers a small alteration in volume,

$$P\delta V = \delta U \quad \text{or} \quad P = \delta U / \delta V,$$

where  $V$  is the volume of one gram-molecule. The compressibility of the crystal  $k$  is defined by

$$k = -\frac{1}{V} \frac{\partial V}{\partial P},$$

$$\frac{1}{k} = -V \frac{\partial P}{\partial V} = -V \frac{\partial^2 U}{\partial V^2}.$$

Since  $U = Na \left( \frac{1}{r} - \frac{r_0^{n-1}}{nr^n} \right)$ , and  $V = 2Nr^3$ , it can be deduced that

$$k = \frac{18r_0^4}{a(n-1)}.$$

Applying this calculation to a number of alkaline halides, Born and Landé found values of  $n$  in the neighbourhood of 9. The energy when  $r = r_0$  is seen to be

$$U = \frac{Na}{2} \left( 1 - \frac{1}{n} \right),$$

and since  $n$  is equal to 9, we can see that the inclusion of the forces of repulsion has diminished the potential energy due to electrostatic forces alone by about 13 per cent. The figures in the table below represent the estimates on this basis of the amounts of heat in large calories liberated when a gram-molecule of salt is formed from dispersed ions.

	F	Cl	Br	I
Na	210.4	170.0	159.7	146.7
K	192.2	159.0	150.6	139.1
Rb	..	154.6	146.5	135.8

These figures cannot be compared directly with the heats of formation of the corresponding compounds. Starting with sodium metal and chlorine gas, the amount of energy liberated in the formation of one gram-molecule of NaCl is the difference between  $U$  calculated above, and the energies required to vaporise the sodium, remove an electron from each atom, dissociate the chlorine molecules into atoms, and add an electron to each chlorine atom. We know the latent heat of vaporisation of sodium, the energy required to remove an electron from a neutral sodium atom (ionisation energy), and the energy required to

dissociate the chlorine molecules. The energy of formation of the salt from the elements is also known. The remaining unknown quantity is the energy required to attach an electron to a chlorine atom. A check on the calculation can therefore be obtained by estimating this amount of energy for each chloride, and noting whether the results are in agreement, which proves to be the case. The energy turns out to be negative—energy is liberated when an electron is absorbed into the system of a neutral chlorine atom. The following estimates of such energies are obtained by the improved method of calculation of Born and Mayer, described below:—

Electron affinities : F, 95.3 k. cal. per gram-atom.

Cl, 86.5    "        "        "

Br, 81.5    "        "        "

I, 74.2    "        "        "

Another check can be obtained from heats of solution. If one gram-molecule of KCl and of RbBr are dissolved in a large quantity of water so that the salts are fully ionised, the end result is the same as if the original salts had been KBr and RbCl. The difference between heats of solution of KCl + RbBr and KBr + RbCl should therefore be equal to the difference in lattice energy of KCl + RbBr and of KBr + RbCl. These differences are small, but satisfactory agreement is found.

The calculation of the Madelung constant is carried out by a triple summation of the mutual potential energies of all the charges in the crystal structure, which involves complex mathematics. An estimate of the constant may be very rapidly obtained, however, by a simple calculation, which may be given here because it affords an easily grasped physical picture although it is only approximate. Let us suppose an ion with charge  $e$  to exist in free space, and then destroy a part of the electrostatic potential energy in its neighbourhood by surrounding it with an earthed spherical conducting shell of radius  $r$  and volume  $V$ . An amount of energy will disappear equal to  $\frac{1}{2}e^2/r$ , or since  $V = 4\pi r^3/3$ ,

$$\begin{aligned}\frac{1}{2}e^2/r &= \frac{e^2}{V^{1/3}} \cdot \frac{3}{2} \sqrt{\frac{\pi}{6}} \\ &= 0.806 \cdot e^2/V^{1/3}.\end{aligned}$$

In the case of NaCl, we may regard the electrostatic energy in the field around each ion as confined to a cube of volume  $r_0^3$ , since beyond that volume the energy is to be associated with the neighbouring ion. The electrostatic energy which disappears as the ions come together to form the crystal is equivalent to that outside the shell considered above. Thus  $V = r_0^3$ , and the energy lost per ion is equal to  $0.806 \cdot e^2/r_0$ . The energy per pair of ions by this simple calculation is  $1.61 \cdot e^2/r$ , as compared with the Madelung value  $1.747558 \cdot e^2/r$ .

In the case of the CsCl structure, the unit cell of volume  $a_w^3$  contains two ions. Therefore

$$V = a_w^3/2.$$

The energy per pair of ions is therefore

$$\begin{aligned} & 2 \cdot 0.806 \cdot e^2/V^{1/3} \\ &= 2 \cdot 0.806 \cdot \sqrt[3]{2} \cdot e^2/a_w \\ &= 2.035 \cdot e^2/a_w. \end{aligned}$$

The corresponding Madelung constant calculated by Landé is

$$a = 2.035356.$$

It will be realised that such a method of calculation can only give very approximate results. The lines of force around each ion are distorted by the neighbouring ions, and the cell inside which we picture the remaining electrostatic energy of the ion to be confined is a polyhedron, which we have taken to be a sphere of equal volume. However, it is interesting to see how closely it yields a value of the constant.

Born and Mayer have more recently established the calculation of the lattice energy upon a firmer basis. Their expression for the energy lost per gram-molecule is

$$-U(r) = \left( -\frac{ae^2}{r} - \frac{C}{r^6} + B(r) + \epsilon \right) N.$$

In this expression,  $a$  is the Madelung constant as above.  $C$  is a constant such that  $C/r^6$  represents the effect of the van der Waals forces of attraction. These forces, for both like and unlike ions, can be calculated from the known polarisabilities of the ions and their optical terms. The term  $B(r)$  is a complex exponential expression which replaces the  $b/r^n$  of the earlier

formula. It is based on the assumption of a potential due to the repulsive force between two ions of the form

$$\phi(r) = be^{(r_1 + r_2 - r)/\rho},$$

which has been referred to earlier in this chapter. The final term  $\epsilon$  is the zero-point energy of the lattice, and is equal to  $\frac{3}{4}h\nu_{\max}$ , where  $\nu_{\max}$  is the highest frequency of oscillation associated with the lattice.

Mayer and Helmholtz have recalculated the lattice energies of the alkaline halides on this basis, with results which may be compared with the table given above (p. 173).

	F	Cl	Br	I
Na	213.4	183.1	174.6	163.9
K	189.7	165.4	159.3	150.8
Rb	181.6	160.7	153.5	145.3

A new point which is brought out by the calculations is the importance of the van der Waals forces. These are usually assumed to be very weak, and, indeed, they make little difference to the lattice energy in most cases owing to their rapid decrease with increase of  $r$ . However, Born and Mayer show that in cases where the ions are large and therefore highly polarisable, they may be so important as to decide the type of crystal structure. The lattice energies of the NaCl and CsCl types are very nearly the same, and on the older theory it was impossible to explain why CsCl, CsBr, and CsI crystallise body-centred, and not with the NaCl structure. In the new theory this is explained by the greater influence of the van der Waals force in their case.

The theory even of these simple ionic structures cannot yet be regarded as complete. Many assumptions have to be made, and there is an artificial element in the division of the forces between the ions into the various types. Nevertheless, the theory has been given at some length here because it represents a first attempt to explain the dynamics of the crystal which has met with at least a partial success.

## TWINNING

A twinned crystal consists of two individuals which are symmetrically united. The one may either be derived from the other

by reflection across a plane, or by rotation around an axis. These operations of reflection or rotation must naturally not be symmetry operations of either individual, since in that case there could be no distinction between them, but the planes or axes are always net-planes or zone axes of each crystal.

In cases where the structures of twinning crystals are known, it appears to be a general rule that the transition takes place

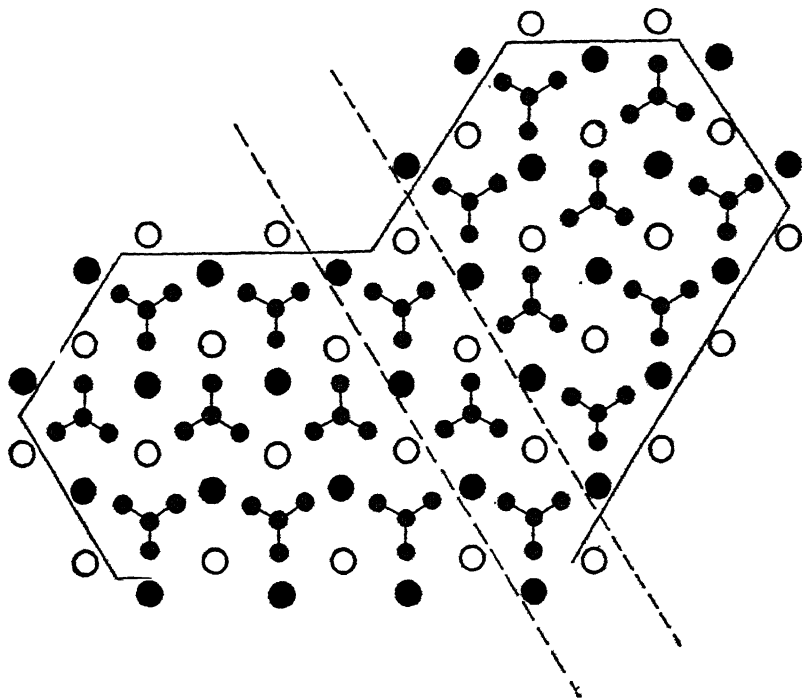
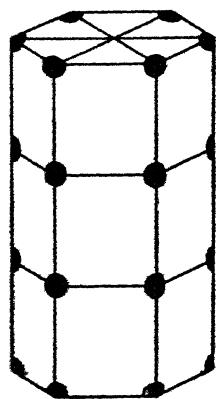


FIG. 107.—Section perpendicular to  $c$  axis of aragonite twinned on  $(110)$   
(*Proc. Roy. Soc., A*, 106, 37, 1924)

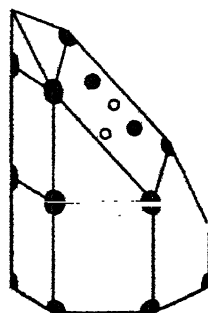
across a finite layer of structure which conforms closely to the pattern of each. The twinning of aragonite affords a simple example. Aragonite is orthorhombic, and twins across the plane  $(110)$ . The projection of the structure upon the plane  $(001)$  is shown in fig. 107, which also represents the union of two individuals of a twin. The left-hand crystal has its  $a$  axis horizontal and its  $b$  axis vertical, and the direction of a twin plane  $(110)$  is shown by the dotted lines. The faces  $(010)$  and  $(110)$  are outlined, and it will be seen that they are nearly parallel to

the sides of a regular hexagon. The structure is in fact pseudo-hexagonal, the calcium atoms (large circles) being arranged in approximately hexagonal closest packing and a  $\text{CO}_3$  group being placed between each group of six calcium atoms. A glance at the figure will show, however, that the symmetry is actually orthorhombic. In the direction  $[100]$  the  $\text{CO}_3$  groups lie in a row with every member parallel, whereas in the directions  $[110]$  and  $[1\bar{1}0]$  the alternate groups point opposite ways. The point to note is that the slab of crystal enclosed within the dotted lines

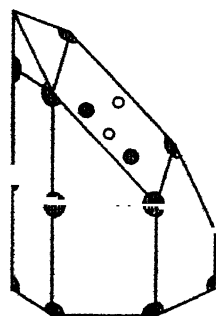


● O  
○ O

FIG. 108



(a)



(b)

FIG. 109

A section of the quartz structure by the plane  $(11\bar{2}2)$ . The individuals in fig. 109 (a) and (b) are right- and left-handed

may be considered as conforming either to the structure on the left or the structure on the right whose  $a$  axis is tilted through nearly  $60^\circ$ . In other words, when building a further section of crystal after crossing one of the dotted lines, the influence which decides the atoms or groups to continue the pattern on the left does not originate in nearest neighbours, for they might equally well belong to the structure on the right, but in more distant neighbours on the other side of the slab. The influence is therefore weak, and an accident of growth may easily initiate a crystal twin. Actually these twins are of such frequent occurrence in the aragonite structure that most specimens simulate by repeated twinning a single hexagonal crystal.

Quartz twins in several ways. The most common is the union of two individuals of the same hand, of which the one is

related to the other by a rotation of  $180^\circ$  about the threefold axis. In a Brazilian twin, right-handed and left-handed crystals are united, being related to each other by reflection across a plane parallel to the threefold axis and perpendicular to the faces of the usual six-sided prism and pyramids. A further type of twinning consists in reflection across a plane perpendicular to

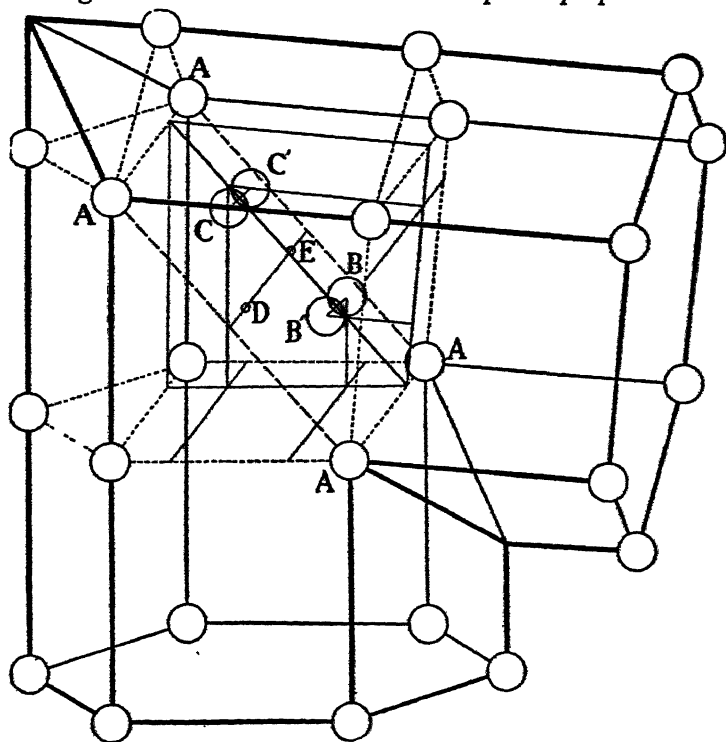


FIG. 110.—One form of twinning of quartz. The silicon atoms B, B' and C, C' are slightly distorted from their normal positions so as to be coincident in the twinned structure

the threefold axis. In all three cases the twins have a common hexagonal space-lattice. A rare form of twinning is illustrated in figs. 108 and 109. The two quartz prisms are nearly at right angles to each other, as shown in fig. 110, and are related by reflection across the plane  $(11\bar{2}2)$ . A number of silicon and oxygen atoms of the structure lie nearly upon the plane, as shown in fig. 109, and by uniting the right- and left-hand quartz structures shown in this figure these atoms will be common to both patterns.



A slab of crystal which can form part of either of the individuals of a twin is naturally frequently found in pseudo-symmetrical crystals, or crystals which are derived from more symmetrical structures by a small distortion. Hence twinning is very frequent in such crystals, and if of the interpenetrating or repeated type, it causes them to appear to belong to a higher class of symmetry.

### REFRACTIVE INDEX

When electromagnetic waves traverse matter, the atoms become polarised under the influence of the electric fields, dipole moments being created by the distortion of their structure. The velocity of the waves in the matter differs in consequence from the velocity *in vacuo*. If the matter is isotropic, like glass or water, the velocity of the waves is independent of their direction. The matter has a characteristic refractive index, equal to the ratio of the velocity *in vacuo* to the velocity in the medium. The greater the polarisation of the medium for a given electrical field due to the waves, the higher is the refractive index.

When the waves traverse a crystal, the extent of the polarisation for a given field in general depends upon the direction of the field. This is so because the polarisation of each atom is caused not only by the electric field of the wave, but also by the dipole moments produced in other atoms in its neighbourhood. Since these neighbours lie in certain definite directions, determined by the crystal structure, it follows that the extent of polarisation, and therefore the velocity of the wave, depends upon the orientation of the electrical stress relatively to the crystal axes. Double refraction arises in this way. A beam of light entering the crystal splits up into two polarised \* components which travel at different rates. The electric intensity of the faster beam is in a direction for which the polarisation of the crystal is a minimum, and that of the slower beam in a direction at right angles to the first for which the polarisation is a maximum, both directions lying in the wave front. Double refraction occurs in all crystals except those belonging to the cubic system.

The complete discussion of the effect of the waves upon the atoms is complicated, and it will only be treated here in a very

\* It is necessary to use 'polarized' to describe both the nature of the electrical field in the light beam and the creation of dipoles in the atoms, but the context will show in what sense the word is used in each case.

general way. We may conveniently divide the influence upon any given atom into three parts. In the first place, as the waves sweep over it, it is polarised by the average electric intensity of the waves. In the next place, the average polarisation of the whole medium around it further increases its own polarisation. Finally, its immediate neighbours produce upon it an effect which may be in any direction, and so may increase or decrease the polarisation due to the first two causes. It is this last effect which leads to double refraction.

The most simple case is that of a number of widely dispersed atoms, such as those of a monatomic gas. When the atom is placed in a field  $E$ , it will be supposed that it becomes a dipole of strength  $Ee^2\lambda$ , where  $e$  is the electronic charge and  $\lambda$  a constant characteristic of the atom. The expression is put in this form for dimensional reasons; it is supposed that an electron with charge  $e$  is displaced by a distance  $\lambda Ee$  when a force  $Ee$  acts upon it, so that the moment of the distorted system is  $\lambda Ee^2$ . If there are  $N$  such atoms per unit volume, the dielectric constant of the medium is

$$K = 1 + 4\pi N e^2 \lambda.$$

If instead of the dielectric constant for a steady field the refractive index for waves of a given frequency is required, this must be written

$$n^2 = 1 + 4\pi N e^2 \lambda,$$

where  $\lambda$  is now a constant for the given frequency, but varies with the frequency.

When the atoms are closer together, so that the polarisation of the medium appreciably influences the polarisation of each atom, the Lorentz formula must be used:

$$\frac{n^2 - 1}{n^2 + 2} = \frac{4\pi}{3} N e^2 \lambda.$$

This reduces to the more simple formula when  $n$  is nearly equal to unity. Considering now one gram-atom of the substance, we

can multiply each side by  $\frac{M}{\rho}$ , where  $M$  is the atomic weight and  $\rho$  its density:

$$\frac{M}{\rho} \cdot \frac{n^2 - 1}{n^2 + 2} = \frac{4\pi}{3} \cdot \frac{M}{\rho} \cdot N e^2 \lambda = \frac{4\pi}{3} N_0 e^2 \lambda,$$

where  $N_0$  is the Loschmidt number, or number of atoms in a gram-atom. The expression on the right-hand side is a constant,

characteristic of the atom for a given light frequency and independent of the degree of dispersion of the atoms.  $\frac{M}{\rho} \cdot \frac{n^2 - 1}{n^2 + 2}$  is therefore defined as the *atomic refractivity*. If the substance is complex, and  $M$  is the molecular weight of a group of atoms,

$$\frac{M}{\rho} \cdot \frac{n^2 - 1}{n^2 + 2} = \sum \frac{4\pi}{3} \cdot N_0 e^2 \lambda,$$

where the sum is taken over all the atoms in the group. It will be clear that it is convenient to use the *molecular refractivity* of a body, and not its refractive index, when seeking to relate the optical properties of the body to its structure.

The third factor, the influence upon an atom of its immediate neighbours, has so far been neglected. It can be shown, however, that in simple crystals of the NaCl or CsCl types the influence of the nearest neighbours exactly cancels out. In such crystals it is therefore to be expected that the molecular refractivity should be equal to the sum of the characteristic refractivities of the positive and negative ions. This is approximately true, as the following table will show. The observed molecular refractivities are compared with the sums of ionic refractivities (in *italics*), the latter being empirical constants obtained by Wasastjerna from the study of a number of salts and their solutions. It is clear from the table, however, that there is a systematic departure from the additive law owing to a distortion of the ions by each other when packed together in the crystal.

TABLE IX

	F, 2.20	Cl, 8.45	Br, 11.84	I, 18.47
Li, 0.15	2.337 <i>2.35</i>	7.587 <i>8.60</i>	10.560 <i>11.99</i>	15.978 <i>18.62</i>
Na, 0.74	3.016 <i>2.94</i>	8.517 <i>9.19</i>	11.560 <i>12.28</i>	17.073 <i>19.21</i>
K, 2.85	5.162 <i>5.05</i>	10.846 <i>11.30</i>	13.983 <i>14.69</i>	19.754 <i>21.33</i>
Rb, 3.41	6.740 <i>6.41</i>	12.549 <i>12.86</i>	15.778 <i>16.25</i>	21.708 <i>22.88</i>
Cs, 7.36	9.507 <i>9.56</i>	15.572 <i>15.81</i>	18.949 <i>19.20</i>	25.143 <i>25.95</i>

It will be seen how much the ionic refractivity varies from one ion to another. A small ion such as Li has a refractivity of 0.15, whereas a large ion such as  $I^-$  has a refractivity of 18.5 or more than one hundred times as great.

The above crystals are optically isotropic owing to their cubic symmetry. The influence of a less symmetrical arrangement of the atoms is illustrated by the carbonates and nitrates of the calcite and aragonite type. In calcite and  $NaNO_3$ , the  $CO_3$  and  $NO_3$  groups are perpendicular to the threefold axis of the rhombohedral crystals. Both crystals have a strong negative birefringence. A ray of unpolarised light entering a calcite crystal is split up into two beams, the ordinary and extraordinary rays. The electrical vibration of the ordinary ray is always perpendicular to the threefold or optic axis of the crystal, and so is parallel to the plane of the  $CO_3$  group. It is the 'slow' ray in the crystal, and behaves as if the crystal had a constant refractive index for a given frequency; this is termed the ordinary refractive index  $\omega$ , and its value for the sodium D line is 1.658. The extraordinary ray does not obey the simple laws of refraction, since its velocity in the crystal depends upon its direction. When the rays are travelling parallel to the optic axis, there is no splitting up into two polarised beams. When travelling normal to the optic axis, the extraordinary ray has its maximum velocity defined by assigning to the crystal an extraordinary refractive index  $\epsilon$  which is less than  $\omega$ .  $NaNO_3$  has an even greater birefringence than calcite, as the following table shows:

Calcite	$\epsilon = 1.486$	$NaNO_3$	$\epsilon = 1.336$
	$\omega = 1.658$		$\omega = 1.587$

The birefringence is more marked when the optical characters are expressed in terms of molecular refractivity:

Calcite	$R_\epsilon = 10.37$	$NaNO_3$	$R_\epsilon = 7.75$
	$R_\omega = 13.31$		$R_\omega = 12.58$

The ionic refractivity of  $Ca^{++}$  is 1.99, and that of  $Na^+$  is 0.74, so that the metal ions make a relatively small contribution to the molecular refractivity. It is clear that the cause of the double refraction is to be sought for in the  $CO_3$  and  $NO_3$  groups. We may sum up the optical characteristics by saying that the polarisation of the  $CO_3$  groups is much greater when the electrical

field is in the plane of the group than when it is perpendicular to the group. The carbonates and nitrates of the aragonite type also contain  $\text{CO}_3$  and  $\text{NO}_3$  groups which are also approximately parallel. Since the crystals are orthorhombic there are three characteristic refractive indices; but again the two nearly equal large indices correspond to vibrations parallel to the groups and the small index to vibrations perpendicular to the groups. In all carbonates of these two types the refractivities of the  $\text{CO}_3$  groups are about 11 and 8 for  $\omega$  and  $\epsilon$  respectively, and in nitrates the corresponding figures are 11.5 and 7.

The reason for this property of the  $\text{CO}_3$  and  $\text{NO}_3$  groups is illustrated by fig. 111. The three oxygen atoms lie at the corners

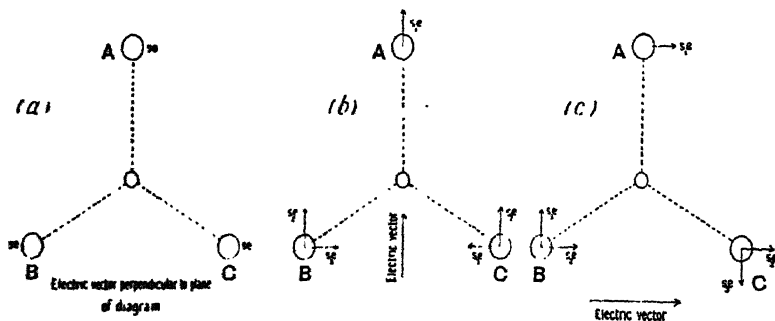


FIG. 111.—Polarisation of the oxygen atoms in the  $\text{CO}_3$  group by an electric field

(*Proc. Roy. Soc., A*, 105, 378, 1924)

of an equilateral triangle. When the field is perpendicular to the plane of the triangle, as in fig. 111 (a), the atoms become dipoles as shown in the figure. The field of each dipole tends to depolarise its two neighbours by acting in a contrary sense to the external field. On the other hand, when the field is parallel to the plane of the group (fig. 111 (b)) atoms B and C reinforce A, and A reinforces B and C. It is true that B and C mutually depolarise each other, but calculation shows that the average gain more than compensates the loss. The same holds for case (c).

The author in 1924 made some calculations on this basis. Assuming the oxygen atoms in the  $\text{CO}_3$  group to be 2.25 Å. apart, as determined by X-ray analysis, and also the whole refractivity of the group to be due to oxygen, the effect of the oxygen atoms upon each other can be calculated. For case (b) the total polarisation of the three oxygen atoms is 1.17 times as great as if they

were separated in space, and for case (a) the factor is 0.815. The molecular refractivity of calcite is made up of two parts,

$$R_e = 10.37 = 1.99 + 8.38$$

$$R_\omega = 13.31 = 1.99 + 11.32$$

where the figure 1.99 is the ionic refractivity of Ca. It will be seen that the ratio 11.32 : 8.38 is almost exactly that of the two refractivities we have calculated for the  $\text{CO}_3$  group, *i.e.* 1.17 and 0.815 times the normal refractivity of the three oxygen atoms.

Actually the calculation cannot be made in quite so simple a way, because the oxygen atoms are affected by the atoms of neighbouring groups as well as by the atoms of their own  $\text{CO}_3$  groups. The following table shows the result of calculating the refractive indices of calcite and aragonite, on the basis of the structure determined by X-rays and refractivities of 1.99 for Ca and 3.30 for oxygen :

		Calculated	Observed
Calcite	$\epsilon$	1.488	1.486
	$\omega$	1.631	1.658
Aragonite	$\alpha$	1.538	1.530 (c)
	$\beta$	1.694	1.681 (a)
	$\gamma$	1.680	1.686 (b)

The letter in brackets denotes the axis of the crystal to which the electrical vibration is parallel. It is to be emphasised again that the velocity of the wave depends upon the direction of the electrical field, not upon the direction in which the wave is travelling.

An instance of an organic compound may be briefly referred to as an example. When examining the magnetic anisotropy of naphthalene crystals, Bhagavantam in 1929 measured their refractive indices. The principal indices of refraction are 1.775 when the electric vector is parallel to the *b* axis, 1.932 when its direction is almost coincident with the *c* axis, and 1.432 when it is perpendicular to both the above. The corresponding molecular refractivities are 57.75, 64.40, and 39.05. The naphthalene molecule, as has been seen earlier in this chapter, consists of

two linked benzene rings, all the carbon atoms lying in one plane. The long axis of this plane assemblage is nearly parallel to the  $c$  axis of the crystal, and, as is to be anticipated, the greatest refractivity of 64.40 corresponds to an electric vector in this direction. We would also expect the least refractivity of the molecule to be perpendicular to its plane, and the intermediate refractivity to be in the plane but at right angles to its long axis. In the naphthalene crystal, the planes of the two molecules in the unit cell are inclined at about  $30^\circ$  on either side of (100). The intermediate refractive index of the crystal 1.775 corresponds to the direction which is most nearly parallel to the two molecules, and the least index 1.442 to the direction most nearly perpendicular to them, again as would be anticipated.

These examples illustrate the close connection between the optical properties of a crystal and its structure. A unit composed of several atoms closely associated in a plane has a larger refractivity parallel to the plane than perpendicular to it. If the crystal contains a number of these groups approximately parallel to each other it will be optically *negative*. Two refractive indices for vibration in the plane will be large and the third small. On the other hand, if the units are parallel rows of atoms, it will be optically *positive*. Two refractive indices corresponding to vibrations perpendicular to the rows will be small, and the third, for a vibration parallel to the rows, will be large. A regular unit like the tetrahedral  $\text{SO}_4$  group is optically isotropic; most sulphates have correspondingly a small birefringence. The laws for organic compounds are simpler in one respect than those for inorganic compounds, because in the former the molecules are widely separated and hence the refractivity of the crystal corresponds closely to that of the molecules themselves, whereas in the latter the structure is more continuous, and we cannot neglect the effect of neighbouring groups upon each other.

The optical properties of organic crystals will probably become the most valuable indications of their molecular arrangement, as Bernal has surmised, because they show the orientation of the molecules in the structure. Under the heading of optical properties are to be included not only the refractivity, but also the absorption of light, Raman frequencies, and so forth. All these properties are linked with certain directions of vibration in the crystal.

PLATE XII

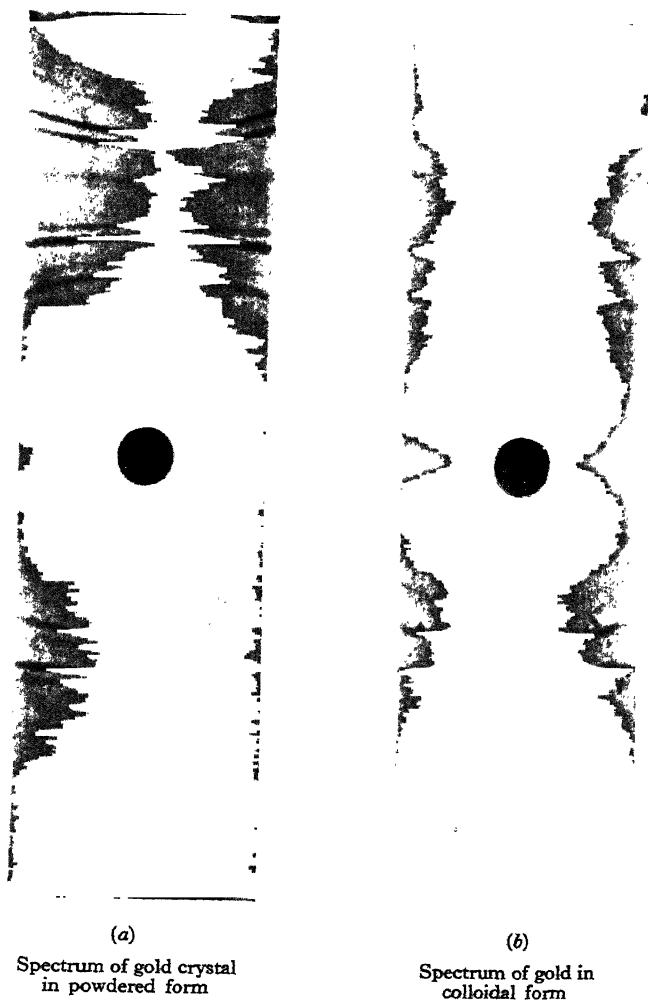


FIG. 112  
(Debye and Scherrer)





## CHAPTER VIII

### CRYSTAL TEXTURE

WE have hitherto only considered the crystal as a definite atomic arrangement which is repeated in a regular pattern. The properties of a crystalline mass, however, do not depend on its atomic pattern alone. Even when it is chemically a single substance, its properties are influenced by the size of the individual crystal blocks, by their orientation, and by the way they are cemented together. Degrees of orderly orientation of the individual crystals are possible, which range from the limiting case of a single highly perfect crystal or the nearly parallel blocks of a mosaic crystal,\* through such partial orientations as exist in worked metals, to the complete disorder of a microcrystalline mass in which the crystal particles are oriented in every direction at random. There may be any degree of extension of the individual particles in a crystalline mass, ranging from coarse grains to particles so small that the amorphous state is approached. The individual crystals may be in a state of strain, causing a distortion and variation in lattice spacing which is revealed by X-rays; the physical properties of the body are correspondingly altered.

Many natural substances, such as cellulose and wool and stretched rubber, are in an anisotropic state which is neither truly crystalline nor amorphous. Though not composed of small units of perfect crystal, there is sufficient order in the linking of one molecule to the next to give rise to diffraction effects with X-rays which resemble those due to crystals. Such an organisation in the structures built up by living matter appears to be widespread, and its study is naturally of immense importance since it will help to explain their properties.

These aspects of structure may be conveniently classed under the heading of Crystal Texture.

\* This term is used to describe crystals in which the continuity of structure is interrupted on a microscopic scale, by faults like those in geological strata, an almost universal feature in actual crystals.

## THE TRANSITION FROM THE CRYSTALLINE TO THE AMORPHOUS STATE

When a powder photograph of a moderately fine crystal powder is taken, the definition of the halo lines on the film or plate depends upon such attributes of the apparatus as the slit system, size of powder specimen, and radius of the camera. Very sharp lines can be obtained when the slits are narrow, and the specimen is small or a focusing device is used. If the particles of crystal are very fine indeed, however, it is found that the haloes become diffuse quite independently of any enlargement due to the geometry of the apparatus. This effect becomes marked when the individual crystal particles are of the order  $10^{-6}$  cm., or 100 Å., in their dimensions in each direction, and the finer the particles the more diffuse are the lines. The broadening of the lines was noticed by Debye and Scherrer in their first experiments with the powder method, and explained by them as imperfect resolution by a crystal grating with a limited number of elements. Fig. 112, Pl. XII, p. 186, shows the photographs of gold in powder form, and of fine particles of colloidal gold. The particles in the former case are sufficiently large to give sharp lines, whereas in the latter case they give diffuse lines owing to their smallness.

The upper photograph in fig. 113, Pl. XIII, is yielded by graphite, the next by lamp-black from the combustion of acetylene, and the remainder by various forms of carbon ranging down to hard gas-carbon. All show analogies with the graphite structure.

The effect is familiar in the case of the optical grating. The width of a spectral line depends upon the number of rulings on the grating. In order to get a high resolving power, or, in other words, to distinguish between two components in the light with wave-lengths which are close together, it is necessary that the number of rulings should be great. For instance, the D lines 5889 and 5896 in the sodium spectrum cannot be separated in the first order by a grating unless it has more than one thousand lines. The images of the  $D_1$  and  $D_2$  lines are otherwise so broad that they merge together, irrespective of the other optical properties of the spectrometer, such as its grating constant or the magnification of the image. An approximate rule for resolution states that, in order to separate two lines in the first-order spectrum

## PLATE XIII

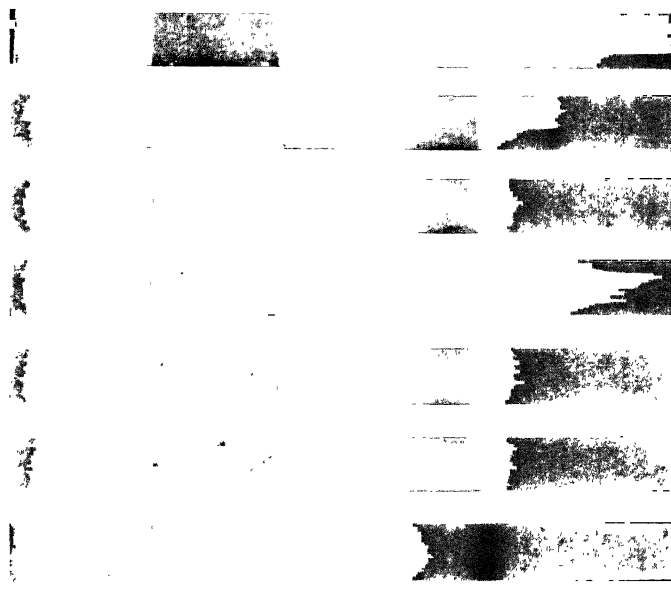


FIG 113.—Powder photographs of graphite and of various forms of carbon

(Reproduced by permission of the Research Laboratories of the General Electric Company, Wembley)



whose difference  $\Delta\lambda$  in wave-length is  $1/N$ th of the mean wave-length  $\lambda$ , a grating of at least  $N$  lines must be used. The resolving power of a grating is defined as  $\lambda/\Delta\lambda$ , and is equal to  $N$  in the first order, or more generally  $mN$  in the  $m$ th order.

The breadth of the spectral line as seen in the telescope depends upon interference between the waves coming from the lines of the grating. The centre of the line corresponds to a direction such that all the waves are exactly in phase. Over a small range of angle on either side of this direction, the scattered waves are nearly in phase and build up an appreciable diffracted beam, and it is not until the deviation from the mean direction is so great that the wave from the first ruling is one wave-length out of step with that from the last, that the diffracted beam is entirely cut out by interference. The smaller the number of lines in the grating and so of component wavelets, the greater will be the extent of the diffraction maximum on either side of the mean angle given by the grating equation

$$\lambda = a \sin \theta.$$

In the same way, when X-rays are reflected by a crystalline particle consisting of  $N$  successive planes, the beam is most strongly reflected at an angle  $\theta$  given by

$$n\lambda = 2d \sin \theta.$$

At the angle  $\theta + \epsilon$ , its intensity has fallen from  $I_{\max}$  to  $I$ , given by a well-known equation of optics:

$$I/I_{\max} = \sin^2 \phi / \phi^2, \quad \text{where} \quad \phi = (2\pi Nd \cdot \epsilon \cos \theta) / \lambda.$$

It is convenient to define the 'breadth' of the line or diffraction maximum, as being the angular range between the two points where the intensity falls to half value. If  $\sin^2 \phi / \phi^2 = \frac{1}{2}$ ,  $\phi = 1.40$  radians ( $80^\circ$ ). Hence the range of glancing angles  $2\epsilon_0$  is given by

$$\begin{aligned} (2\pi Nd \cdot \epsilon_0 \cos \theta) / \lambda &= 1.40 \text{ radians,} \\ 2\epsilon_0 &= 0.445 \lambda / t \cos \theta \text{ radians,} \end{aligned}$$

where  $t (= Nd)$  is the thickness of the crystal. The total angular width  $B$  of the reflected beam is twice this:

$$\begin{aligned} B &= 0.89 \lambda / t \cos \theta \text{ radians} \\ &= 51 \lambda / t \cos \theta \text{ degrees.} \end{aligned}$$

Scherrer gave originally the formula

$$B = 2 \sqrt{\frac{\log_e 2}{\pi}} \frac{\lambda}{t \cos \theta} + b$$

$$= \frac{0.94 \lambda}{t \cos \theta} + b,$$

where  $b$  is the width which the line would have owing to the slit width and other features of the experimental arrangement even if the optical resolution were perfect. The simplified calculation given here leads to nearly the same value of the constant. In a more precise evaluation account must be taken of the lateral extension of the crystal as well as of its depth. In addition, the crystalline particles may not be all of the same size and shape, but may vary over a range on either side of a mean value. Laue has examined the influence of shape and distribution in size of the particles and has obtained more general formulæ. The simple treatment will give, however, an idea of the order of the effect.

It is thus possible to estimate the size of the crystal particles in a microcrystalline mass by measuring with a microphotometer the intensity distribution of each line in a powder photograph.

The resolution or otherwise of the  $K\alpha$  doublet is a convenient index of particle size. As in the case of the optical grating, the two lines will be resolved if

$$nN > \lambda/\delta\lambda,$$

where  $N$  is the number of crystal planes,  $n$  the order of the spectrum,  $\lambda$  and  $\lambda + \delta\lambda$  the wave-lengths of the doublet. The doublet is most conveniently observed in the region where  $2\theta$  is nearly equal to  $180^\circ$ , since dispersion is very high in this region and the components have a wide angular separation. Since  $\sin \theta$  is nearly unity in this case,  $n\lambda$  is approximately equal to  $2d$ , hence resolution is effected if

$$nN = \frac{2Nd}{\lambda} = \frac{2t}{\lambda} > \frac{\lambda}{\delta\lambda}.$$

As a numerical example to illustrate the order of the effect, we may find how large the crystals must be in order to resolve the  $\text{Cu}K\alpha$  doublet. In this case  $\frac{\lambda}{\delta\lambda} = 400$ , and  $t$  must therefore be greater than 200 wave-lengths, or about 300 Å.





# PLATE XIV

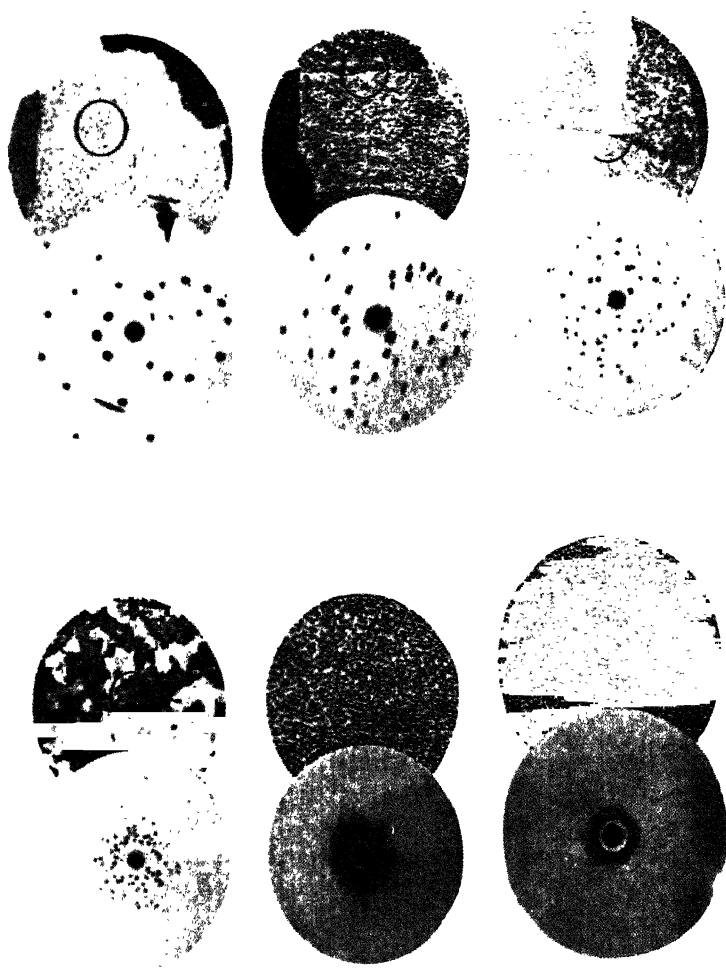


FIG. 114.—Laue patterns obtained with aluminium sheet of various degrees of crystalline grain-size

(By courtesy of George L. Clark)

Diffuse lines may not always be due to the smallness of the crystals. In cold-worked metals, diffuseness is caused by internal strains, which compress or shear individual crystals so that their lattice constants vary from the mean value. It is not always easy to distinguish between the possible causes of diffuseness in any given case, and we can only draw attention here to the alternative explanations.

Unless the crystalline particles have dimensions less than  $10^{-5}$  cm., the broadening due to imperfect resolution is very small. In the range of particle size between  $10^{-5}$  and  $10^{-3}$  cm. the rings are sharp and uniform. For particles of larger size the rings break up into separate spots because all orientations are not present in the aggregate (see fig. 30, Pl. V, p. 48).

The Laue method can be employed to give an estimate of the coarseness of grain in this latter region. A beam of white radiation which has passed through a pin-hole falls upon the specimen. In the extreme case where the grain is so coarse that only a single crystal is encountered by the beam, a simple Laue pattern is the result. The pattern becomes more and more complex as the number of crystalline particles in the beam increases. Fig. 114, Pl. XIV, due to Clark, gives the patterns for the simultaneous diffraction of X-rays by 1, 2, 5, 120, 2000, and 1,000,000 crystal grains of aluminium. The etched specimen is shown in each case for comparison.

#### DIFFRACTION BY AMORPHOUS SOLIDS, LIQUIDS, AND GASES

If the particles in a microcrystalline mass become finer and finer, in the limit all crystalline structure is lost and the solid becomes amorphous. Even in the amorphous state the distribution of the atoms cannot be entirely random. The impossibility of interpenetration of the atoms, and the existence of interatomic binding, implies that certain arrangements of any given atom with respect to its neighbours are more probable than others. This is an extremely interesting problem, and X-ray diffraction by amorphous solids and liquids, when treated by methods similar to those applied to crystal diffraction, can give information about the arrangement.

When X-rays are diffracted by non-crystalline matter, a small number of broad diffuse haloes are observed. Fig. 118, Pl. XV,

p. 195, shows typical haloes of this kind. For convenience, two factors which determine the form of the haloes may be distinguished, which Debye calls 'inner' and 'outer' interference. The first represents the effect of interference between waves scattered

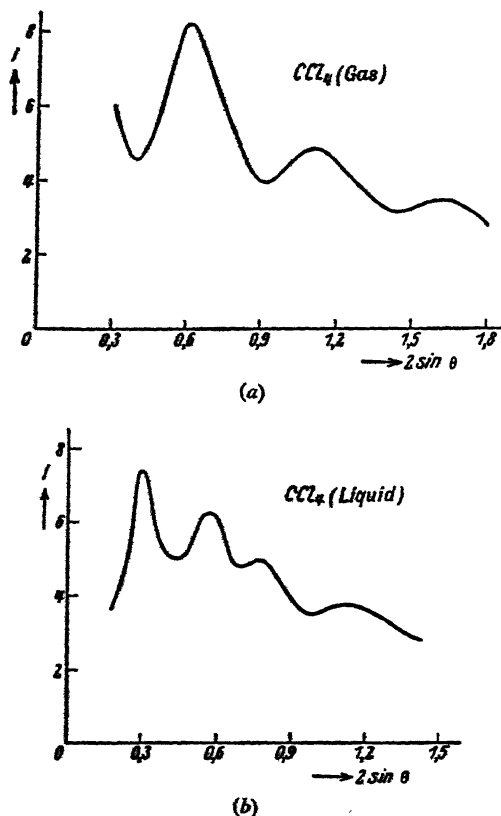


FIG. 115.—Curves illustrating diffraction by (a) gaseous and (b) liquid  $\text{CCl}_4$  (Debye)

(*Ergebnisse der technischen Röntgenkunde*, II, Akad. Verlag, 1931)

by atoms belonging to the same molecule, and the second that of interference between waves from neighbouring molecules. It is convenient to consider cases where these two factors can be separated. Fig. 115, due to Debye, shows the variations of scattered radiation with angle of deviation for liquid and gaseous  $\text{CCl}_4$ . It will be seen that the curves are quite different. In

the case of the gas, we may take it that we are measuring the effect of the first of the above factors alone, because interference between waves scattered by different molecules has no resultant effect owing to their wide separation and random distribution in space. The intensity scattered by the gas will be an average effect, due to molecules which have all orientations relative to the incident and scattered beam. The intensity is given by a formula due to Debye:

$$I = \text{constant} \cdot \sum_1^n i \sum_1^n j f_i f_j \frac{\sin x_{ij}}{x_{ij}},$$

where, for an angle of scattering  $2\theta$ ,

$$x_{ij} = 4\pi l_{ij}(\sin \theta)/\lambda.$$

$f_i$  and  $f_j$  are the atomic scattering factors of atoms  $i$  and  $j$ , and  $l_{ij}$  is the distance between them. The summation is taken over all values of  $i$  and  $j$  up to  $n$ , the number of atoms in the molecule. There are  $n$  terms for which  $i=j$ , giving the effects  $\sum f^2$  of individual atoms. In addition, there are the terms for the pairs of atoms, representing interference of waves scattered by different atoms in the molecule.

It is therefore possible to test molecular models by comparing observation on scattering by a gas with calculation. Debye has carried out such experiments with X-rays, in spite of the technical difficulties due to the very weak intensity of the scattered beam. The method has also received a beautiful application in the hands of Mark and Wierl, who, in their experiments with gas molecules, have used electron diffraction in preference to diffraction of X-rays. Their results are described on p. 264.

The aggregation in amorphous solids or liquids is most simply interpreted when the units are single atoms, so that there is no effect of molecular grouping. Liquid mercury fulfils this condition, since it is monatomic. Experimental measurements and theoretical treatments by Prins and Zernicke, and by Debye and Menke, have led to very interesting results. The curve in fig. 116, due to Debye, represents the distribution of intensity in haloes given by liquid mercury.

The first curve gives a quantity  $E$  as ordinate, plotted against  $s (=2 \sin \theta)$ .  $E$  may be defined as the ratio of the amount of observed diffracted radiation, to that which would be present if the distribution were quite random; in the latter case the effect

of  $N$  atoms is simply  $N$  times the effect of a single atom. At large angles  $E$  approaches to unity, the effects of interference becoming negligible. The oscillations in  $E$  at small angles, which correspond to the haloes observed when X-rays pass through mercury, imply a departure from random distribution. The abscissa  $s$  is on a scale appropriate to experiments with copper  $K\alpha$  radiation, and the curve for these rays ends at  $s = 2 \sin \theta = 2$ , but by incorporating results with shorter molybdenum  $K\alpha$  radiation it is possible to continue the curve, since the scattering is a function of  $(\sin \theta)/\lambda$ .

An interpretation can now be made which is analogous to the application of Fourier series to the measurements of diffraction

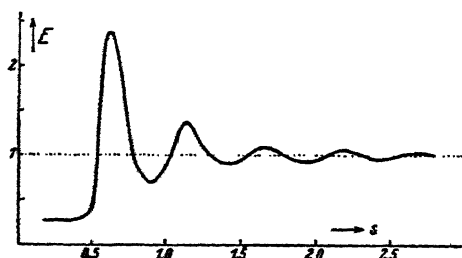


FIG. 116.—Diffraction by liquid mercury (Debye and Menke)  
(*Ergebnisse der technischen Röntgenkunde*, II, Akad. Verlag, 1931)

by a crystal described in Chapter IX. Consider two atoms  $m$  and  $n$  which are in a volume  $V$  of mercury. Let the probability that one atom is within the element of volume  $\delta V_m$ , and the other within the element of volume  $\delta V_n$ , be

$$W \frac{\delta V_n}{V} \frac{\delta V_m}{V}.$$

For an absolutely random distribution,  $W$  would be everywhere unity. Actually,  $W$  is a function of the distance  $r$  between the atoms, and in particular  $W$  must be zero for small values of  $r$ , because the atoms cannot interpenetrate. It is shown that the distribution function  $W$ , and the scattering function  $E$ , are related as follows:—

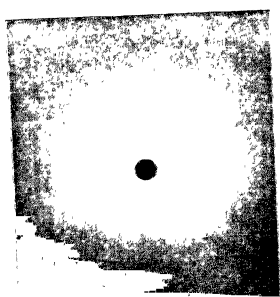
$$s(1 - E) = \frac{2N\lambda^3}{V} \int_0^\infty \frac{r}{\lambda} (1 - W) \sin \frac{2\pi sr}{\lambda} d\left(\frac{r}{\lambda}\right),$$

from which it follows that

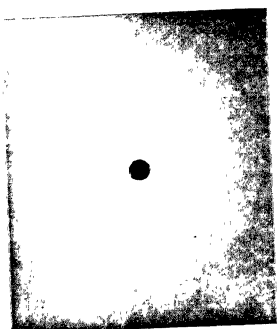
$$\frac{r}{\lambda} (1 - W) = \frac{2V}{N\lambda^3} \int_0^\infty s(1 - E) \sin \frac{2\pi rs}{\lambda} ds,$$



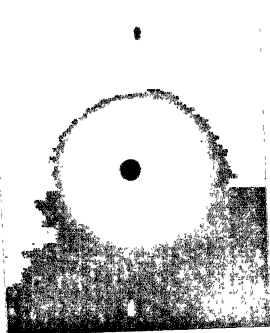
# PLATE XV



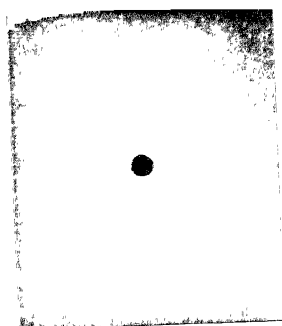
VITREOUS SILICA



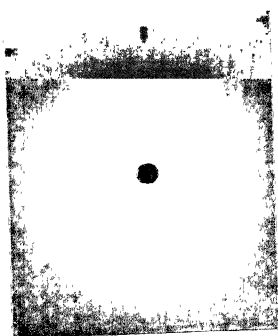
$\alpha$ -CRISTOBALITE



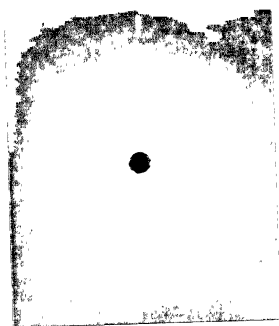
WOLLASTONITE GLASS



PSEUDO-WOLLASTONITE



BORAX GLASS



SODIUM BORATE  $\text{Na}_2\text{B}_4\text{O}_7$

FIG. 118.—A comparison of diffraction patterns of certain compounds in amorphous and crystalline form (Randall)

where  $N$  is the number of atoms in volume  $V$ . Thus if  $E$  is observed experimentally,  $W$  can be deduced as a function of  $(r)$ . Values of  $W$  are plotted against  $r$  in fig. 117.

$W$  is effectively zero for the first two Ångström units, the small oscillations in the dotted curve being an artificial result of the analysis. It then rises to a high peak, falls again, and has further minor peaks. This is to be interpreted as indicating that a mercury atom can have no neighbours nearer than 2 Å. There is a relatively high probability of neighbours at 3 Å., these being clearly atoms in temporary contact with it. The probability of slightly larger distances is small, because such neighbours would

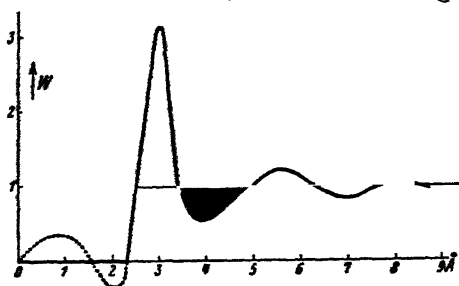


FIG. 117.—Distribution of neighbouring atoms round an atom in liquid mercury (Debye and Menke)

(*Ergebnisse der technischen Röntgenkunde*, II, Akad. Verlag, 1931)

neither be in contact nor allow room for other atoms to come between; but the probability rises again for the next neighbour but one. At larger distances  $W$  becomes unity, since there is no mutual influence.

These results indicate the extent to which the atoms of a liquid assume temporary arrangements due to their packing together. The same must be true in an amorphous solid such as fused silica or glass, where the irregular structure is frozen into place. The figures in Pl. XV are taken from a paper by Randall, and compare the haloes given by crystalline and amorphous forms of the same material. Speaking broadly, the haloes of the amorphous material are due to the most probable relative arrangement of nearest neighbours. It is therefore to be expected that they should correspond to the most intense lines of the powder photographs, much broadened out because the regions of arrangement can only extend over a few atoms. The photographs show that this is the case.

Diffraction by amorphous bodies has been the subject of an



immense amount of research, and there is no room in this account for a description which is in any way representative of the numerous important contributions. A few examples have been chosen to illustrate the main principles.

### CRYSTAL ORIENTATION

If the crystals of a microcrystalline solid are oriented completely at random, a photograph obtained by passing a narrow pencil of monochromatic radiation through the specimen in any direction will show the uniform circular haloes of the usual 'powder' photograph. In many cases, however, the crystalline particles have what is termed a 'preferred orientation,' a definite crystal axis or crystal plane of each particle being approximately parallel to a certain direction or plane. Examples are found in metals which have been drawn, rolled, or hammered, or have been deposited electrolytically, in minerals such as asbestos, and in inorganic and organic bodies which have been produced by living organisms. In such cases a photograph does not give uniform circular haloes. The restriction upon the orientations of the particles causes certain parts of each halo to be enhanced and other parts to be weakened, until in an extreme case each halo reduces to a number of spots. Fig. 119, Pl. XVI, p. 197, shows, for example, one of Hull's early powder photographs of aluminium, and a very perfect photograph of drawn aluminium wire, obtained by Clark. The five innermost haloes, which are on almost the same scale in the two photographs, are due to planes with indices 111, 200, 220, 311, 222. The two inner rings are badly resolved in Hull's picture. In the photograph of the wire the rings are still to be seen, but are faint over the 'greater part of the circle. Their intensities are gathered into short arcs, proving that the orientation of the crystalline particles with a common axis is almost complete. The picture resembles a 'rotation photograph,' in which a single crystal is completely rotated about a definite zone axis. In the present case, analysis shows that this axis of the aluminium crystal is  $[111]$ , the cube diagonal. All the crystalline particles of the metal are so oriented that their  $[111]$  axes are parallel to the axis of the wire. Apart from this, their orientation is a random one. It is not necessary to rotate the specimen, because the individual crystals have all positions around this axis. It can be seen that the common axis is  $[111]$



PLATE XVI



Powder photograph of aluminium (Hull)

Drawn aluminium wire (Clark)

FIG. 119

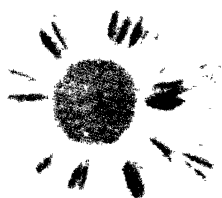


FIG. 123.—Asterism produced by distorted crystal grains  
(By courtesy of George L. Clark)

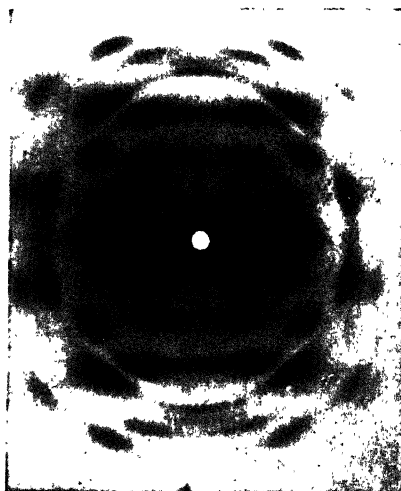


FIG. 125.—Fibre photograph of Ramie fibres (cellulose). The fibre direction is vertical (Astbury)

(*Journal of the Textile Institute*,  
xxiii, pl. iii, 1932)

(P. 197)

by drawing the 'layer lines' appropriate to this rotation axis. When the specimen is rotated about  $[111]$ , the spots on the central layer line have indices  $h\ k\ l$  such that

$$h+k+l=0.$$

The successive layer lines above and below pass through spots for which  $h+k+l=\pm 1, \pm 2, \pm 3$ . In fig. 120 the systems of rings corresponding to random orientation and of layer lines corresponding to rotation about the  $[111]$  axis have both been drawn.

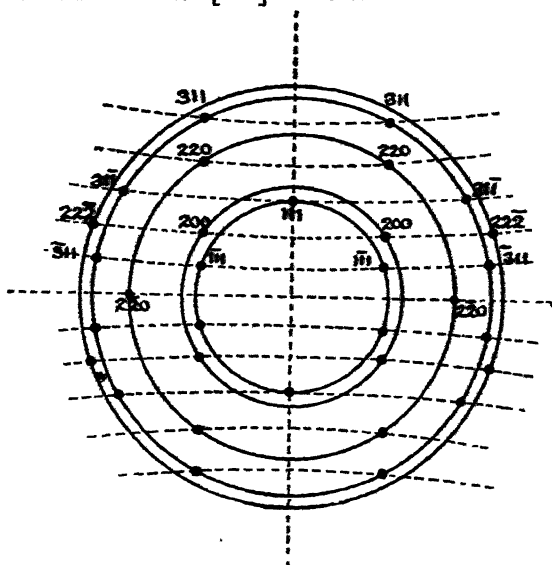


FIG. 120.—Characteristic array of spots due to the rotation of the face-centred cubic structure about the cube diagonal

If we now consider the innermost ring, any corresponding diffracted beam must have indices  $\pm 1, \pm 1, \pm 1$ . The sum  $h+k+l$  of these indices is  $\pm 1$ , or  $\pm 3$ . There should therefore be spots where the first and third layer lines intersect the ring above and below, and by comparing the photograph with fig. 120 it can be seen that this is the case. The second ring, for which the indices are  $\pm 2, 0, 0$ , can only have spots where it intersects the second layer lines, for which  $h+k+l=\pm 2$ . The third ring,  $\pm 2, \pm 2, 0$ , has spots where  $h+k+l=4, 0$ , or  $-4$ , and the fourth ring,  $\pm 3, \pm 1, \pm 1$ , where  $h+k+l=\pm 1, \pm 3, \pm 5$ . The outermost ring,  $\pm 2, \pm 2, \pm 2$ , has only four spots, which are on

the layer lines  $h+k+l=\pm 2$ , because the layer lines  $h+k+l=\pm 6$  do not intersect the ring. In this way every spot in the picture is accounted for.

The streaks in the photograph, which extend from the centre towards each spot, are due to the 'white' or continuous radiation. The effect of varying wave-length is a corresponding variation in all dimensions of the figure, which otherwise retains the same appearance. Hence the continuous radiation, which in this case has its maximum intensity in a region 0.4 Å., produces a streak pointing towards each spot formed by the  $\text{MoK}\alpha$  line with a wave-length 0.71 Å.

The explanation of the selective orientation of the crystals must be sought for in the behaviour of the individual crystals under the influence of the forces to which they are subjected in the process of drawing. The realisation of this has led to very extensive researches into the mechanical properties of single metal crystals, and the technique of preparing single crystals has been brought to a high pitch of perfection. The curious behaviour of large metal crystals was first studied by Andrade in 1914 and Czochralski in 1918. Polanyi, Schmid, Taylor and Elam, Bridgeman and Carpenter, have developed this new study. One type of technique depends upon the slow crystallisation of the metal from a nucleus, either by starting the solidification at a point in the melt, or slowly drawing the solidified mass in the form of a wire out of the melt. Another method (Carpenter) depends upon the recrystallisation of the metal after previous strain and heat treatment. Beautiful specimens have been made by Hausser, as spheres several centimetres in diameter, which when etched have a very striking appearance.

Single crystals of metals have the most remarkable properties. When stretched the crystal elongates under the influence of extremely small forces, and can be extended to double its length before breaking. The elongation takes place by a gliding motion along certain planes in a series of discontinuous jerks. The crystal begins to yield under the influence of so small a force that it is still an open question whether, in the case of a perfect crystal of pure metal, there is any range of strictly elastic extension. It has been shown that this movement takes place by a shearing of the crystal like a pack of cards along certain 'glide planes.' Further, the relative movement occurs along a definite crystallographic axis lying in the plane, the 'glide direction.' In

aluminium, for instance, the glide plane is (111) and the glide direction [110]. The cubic aluminium crystal contains a number of such planes and directions; when a stress is applied, the crystal yields in the direction in which the resolved component of the stretching force has its largest shearing value.

Fig. 121 (a) illustrates the simpler case of extending a cylindrical rod, consisting of a single crystal of zinc, which has only one glide plane. The figure is due to Polanyi. The hexagonal crystal yields by a gliding of the basal planes (0001) over each other, the glide direction being the twofold axis indicated by the arrow. Actually, when a test-piece is being extended the crystal

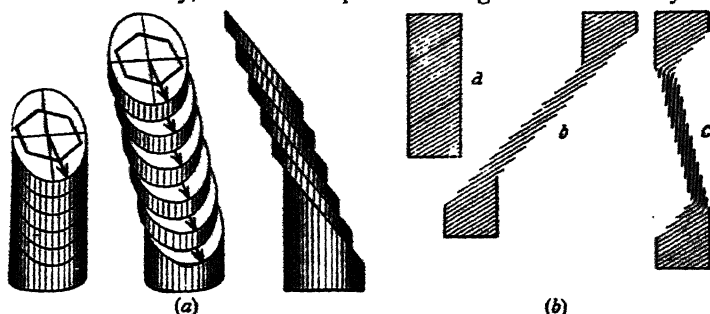


FIG. 121.—(a) Gliding in zinc, after Polanyi. (b) Flexural gliding  
(From *Physics of Solids and Fluids*, P. P. Ewald; Blackie, 1930)

is distorted by flexural gliding at each end, as shown in fig. 121 (b), because the axis of the deformed specimen must remain parallel to the direction of stress.

We may now consider which of the many possible glide planes and glide directions in a symmetrical crystal like aluminium will be most favourably placed so as to yield first when a distorting force is applied. If a given glide direction makes an angle  $\lambda$  with the direction of the applied force  $T$  along the axis of the specimen, the component of the force in the direction of the glide is  $T \cos \lambda$ . If the area of cross-section of the specimen is  $q$  and the glide plane is inclined to the axis at an angle  $\chi$ , the area over which gliding takes place is  $q/\sin \chi$  (fig. 122 (a)). Hence the component of shearing force in the gliding direction per unit area is equal to

$$\frac{T \cos \lambda \sin \chi}{q}$$

It follows from this expression that both glide planes which are

nearly perpendicular to the axis and glide planes nearly parallel to it are unfavourably placed as compared with a plane of moderate slope. In the former case the component of  $T$  parallel to the plane is very small, and in the latter case the glide plane has so large an area owing to its steeply inclined section that the shearing force per unit area is very small. For example, when one of the glide directions is symmetrically placed so that the plane containing it and the direction of tension is perpendicular

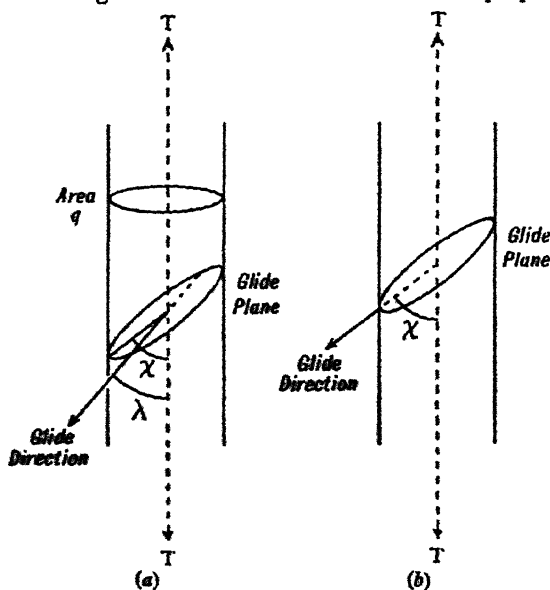


FIG. 122.—Glide planes and glide directions

to the glide plane,  $\lambda$  and  $\chi$  are equal (fig. 122 (b)). The shearing force per unit area is then

$$\frac{T \cos \chi \sin \chi}{q},$$

which has a maximum value when  $\chi$  is  $45^\circ$ .

Consider now a single crystal in an aluminium wire which is undergoing extension in the drawing process. Gliding will first take place along the glide plane and glide direction for which the force is greatest, but continued extension will rotate this plane into a less favourably placed position, as is seen in fig. 121. Finally, as extension proceeds another (111) plane and  $[1\bar{1}0]$  direction

will become equally favourably placed. Extension then takes place, as has been shown by Taylor and Elam, by alternate slips along both planes. This continues until a third direction of gliding becomes equally favourable, and slipping takes place along all three. The result is an orientation of the crystal such that these glide directions are symmetrically disposed along the direction of extension, or, in other words, such that the threefold axis [111] of the crystal is parallel to the direction of extension. This explains why the crystals in drawn aluminium wire are finally all oriented, so that their [111] axes are parallel to the axis of the wire.

Though crystal orientation is often less perfect than in the case considered above, it is a general phenomenon in metals which have been subjected to drawing, rolling, or other processes of cold working. Copper, silver, and gold behave like aluminium when drawn. Zinc and cadmium yield by gliding along the hexagonal basal plane (0001). Tungsten and iron, which are body-centred cubic, have the cube diagonal [111] as gliding direction. In general, gliding takes place along the most closely packed planes or axes. The orientation due to rolling and hammering is more complicated, and the final result depends considerably on the manner in which the cold working has been carried out.

The importance of studying crystal orientation in relation to the properties of the metal as a whole will be clear. The elasticity and tenacity of the polycrystalline material, as contrasted with a single crystal, are due to the different orientations of the glide planes in neighbouring crystalline particles. The properties of the single crystal give an insight into the cause of 'work-hardening.' The crystal at first yields on the application of a very minute force, but the force required rapidly increases as deformation sets in. The perfect crystal structure has become distorted, and a continuous glide plane can no longer be developed.

The distortion by cold-working of what were initially single crystals in a polycrystalline mass is shown by the phenomena known as 'asterism' in Laue photographs. The photograph of the annealed metal has a number of sharp spots, as in the examples shown in fig. 114, PL XIV. The undistorted crystals act as little plane mirrors, each deflecting a narrow beam of the incident radiation. It is to be remembered that in the Laue photograph the only condition for the existence of the diffracted beam is that of



reflection in the crystal plane, since the appropriate wave-length is selected from the range of available 'white' radiation. If the individual crystals are distorted by working, however, each spot becomes drawn out into a diffuse band, with a radial length much greater than its width. This 'asterism' is well shown in fig. 123, Pl. XVI, p. 197, which is due to Clark.

The elongated streaks are at first sight rather striking, and suggest that the crystal planes are more curved in one direction than in another. The diagram (fig. 124) will show, however, that such an effect is to be expected if there is a random deviation

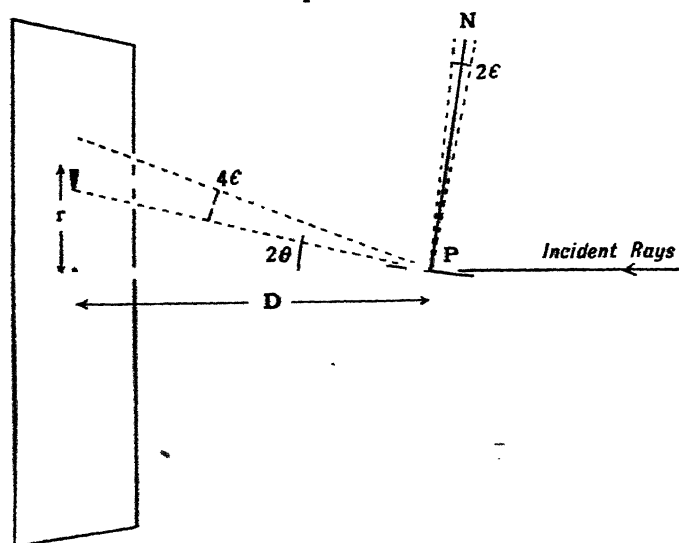


FIG. 124.—Explanation of 'asterism'

of the normal to the crystal plane all round its mean direction owing to a distortion of the crystal grain. Suppose that a mirror is reflecting a narrow beam at a small glancing angle whose mean value is  $\theta$ , and that it is rocked so that its normal moves around a cone of semivertical angle  $\epsilon$  (see fig. 124). The reflected beam will then trace out a very elongated ellipse on the screen. The rocking of the normal in the plane of incidence makes a difference of  $2(\theta + \epsilon) - 2(\theta - \epsilon)$  or  $4\epsilon$  in the direction of the reflected beam, so that the major axis of the ellipse is approximately  $4D\epsilon$ . The rocking at right angles to the plane of incidence gives a lateral movement of approximately  $2\theta D$ ,  $2\epsilon$  or  $r \cdot 2\epsilon$  to the spot. The ratio of major to minor axis is thus  $1/\theta$ . If  $\theta$  is  $3^\circ$ , for

instance, the major axis is twenty times as long as the minor axis. Thus we can see that if the originally perfect plane of a crystal grain is so warped by distortion that its normals have a random distribution around a mean value, the reflected Laue beams will give radial streaks such as the photograph shows.

### THE STRUCTURE OF NATURAL FIBRES

Many substances of organic origin show, by the manner in which they diffract X-rays, that an ordered arrangement is present which is akin to that of a crystal. The structure which is thus revealed is due to their being highly polymerised compounds. The very complicated molecule is composed of a number of similar units, each of which consists of a group of atoms, and these units are linked together by chemical bonds to form a long molecular fibre. The units are therefore repeated at regular intervals along the fibres, so that when the fibres are oriented in a more or less parallel direction there is a repetition of pattern like that in a series of unit cells of a crystal. The lateral forces between neighbouring fibres also create a regularity in arrangement in directions at right angles to the fibre. The result is a structure like that of a very imperfectly crystallised body, though in this case the unit of pattern is only a small part of a single molecule. When the fibres are mounted with their axis perpendicular to the monochromatic beam of X-rays a rotation photograph is obtained, but owing to the limited extent of the ordered arrangement the spots of the photograph are diffuse.

*Cellulose.*—The photograph in fig. 125, Pl. XVI, p. 197, is characteristic of the cellulose chain. Such photographs were first obtained in 1921 by Polanyi, who examined natural cellulose fibres of various kinds. There is a well-marked series of layer lines whose spacing corresponds to a repetition of pattern along the fibre at intervals of  $10\cdot3$  Å. The definition of the layer lines shows that this repetition is regular over a large number of units. The diffuse way in which the spots are spread is evidence that the crystal structure is not so perfect in directions at right angles to the fibre axis as along it.

The chemical investigations of Haworth and others have shown that cellulose is a polymer of anhydro- $\beta$ -glucose. The molecule of the sugar  $\beta$ -glucose has the formula  $C_6H_{12}O_6$ . When

the molecules are linked by covalent bonds to form the cellulose chain a molecule of water is lost, and the chain has the structure shown in fig. 126 (a).

At first sight it would seem an almost hopeless task to find the positions of the atoms of so complicated a molecule when the only basis for computation is a rotation photograph with a limited number of diffuse spots. However, much patient and careful work has been devoted to the problem owing to the great technical importance of the cellulose fibre as well as its scientific interest, and there is strong evidence that the structure of fig. 126 (b) is essentially correct.

In the first place, the dimensions of the unit pseudo-cell appear to be unambiguous. Polanyi, in his first investigation in 1921, found an approximately rhombic cell of dimensions  $a = 8.6$  A.,  $b = 10.3$  A.,  $c = 7.8$  A. Meyer and Mark (*Der Aufbau der Hochpolymeren Organischen Naturstoffe*) summarise the most reliable measurements as giving a monoclinic cell :

$$a = 8.3, \quad b = 10.3, \quad c = 7.9, \quad \beta = 84^\circ.$$

A cell of these dimensions contains four glucose units.

In the next place, the linked double rings of fig. 126 account immediately for the spacing of 10.3 A. along the fibre axis, whatever the arrangement of the groups around this axis.

The detailed arrangement of the atoms in the unit cell is arrived at by using the knowledge of the chemical constitution. The distances between carbon and oxygen, and carbon and carbon, when linked by homopolar bonds are now well known, and the bonds may be reasonably assumed to have an approximately tetrahedral disposition. The minimum interspace between atoms of neighbouring chains is also roughly known from a study of simpler compounds. Hence the possible arrangements are limited in number, and each can be tested by comparing observed and calculated diffracted beams. The positions of the atoms in fig. 126 (b) have been shown by Andress to explain in a satisfactory way the intensities of all the spots of the cellulose photograph, accounting for those absent as well as the relative strength of the remainder.

*Rubber.*—The results of the examination of rubber are unexpected and extremely interesting. Unstretched rubber gives a very diffuse ring system, like that of a liquid or amorphous solid. Katz first showed that quite sharp diffraction spots are formed

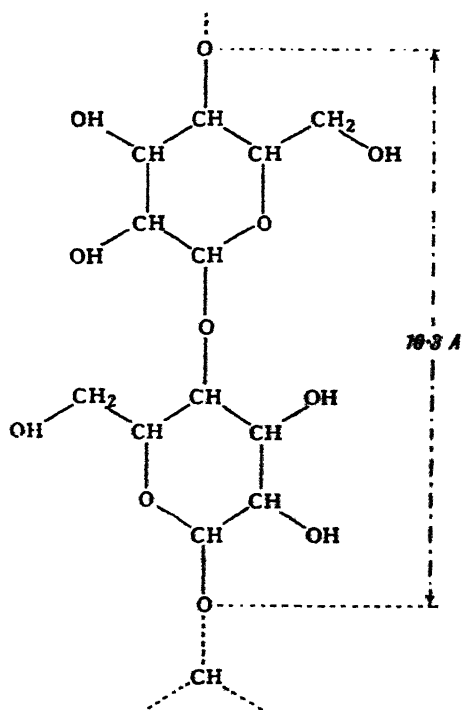
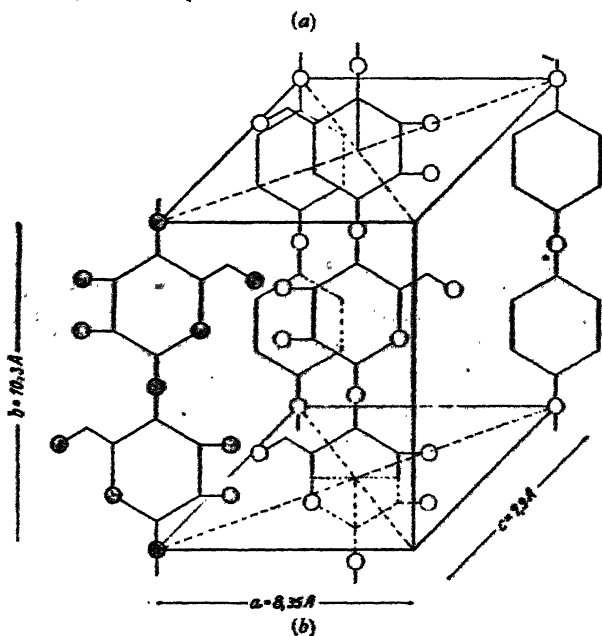


FIG. 126.—(a) The constitution of the chain of cellulose. (b) Atomic positions in the cellulose structure, according to Andress. Oxygen atoms are shown as shaded circles and the carbon atoms occur where bonds meet. The hydrogen atoms are not indicated

(Der Aufbau der Hoch. Org. Nat., Meyer and Mark, Akad. Verlag, 1930)



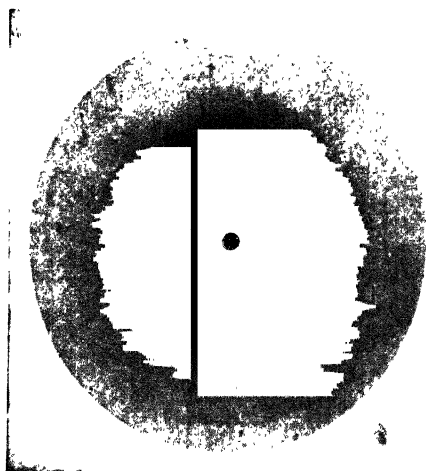
when the rubber is stretched. The pattern begins to appear when the extension is about 100 per cent. The spots remain unaltered in position, but grow in intensity as the rubber is stretched further up to its breaking-point. The process is reversible, the spots disappearing again when the tension is relaxed and the rubber returns to its original form. Photographs of unstretched and stretched rubber are shown in Pl. XVII.

Rubber is composed of polymerised isoprene,  $C_5H_8$ . Apparently the extension of the rubber pulls out the tangled long chains composed of these units until they assume a parallel position, fitting into each other laterally as well as having a regular repetition longitudinally. The sharpness of the spots shows that there is a nearer approach to the crystalline state than in the case of cellulose. Hengstenberg deduces that the 'crystallites' of stretched rubber have dimensions of about  $600 \times 500 \times 150$  Å.

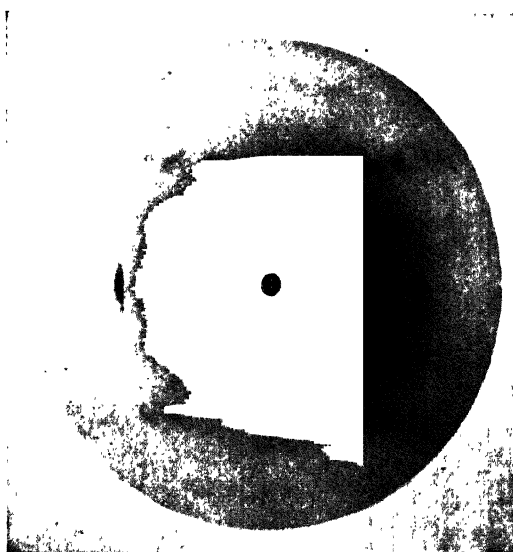
In another series of researches the structure of the compound keratin, which is the common basis of hair, wool, animal spines, and horn, has been examined. All these substances yield similar rotation photographs. They are so diffuse, however, that it is difficult to be certain of the dimensions of the unit cell, and deductions as to the atomic arrangement are still speculative. An important feature, however, has been revealed by the work of Astbury and others on hair and wool. Two types of photograph are obtained, one characteristic of the fibre in the unstretched state and the other of the same fibre when stretched, and it appears certain that each link of the chain has nearly doubled in length in the second case. Apparently the mechanical tension is sufficient to alter the form of the molecule. The association of reversible changes in molecular form with external forces of this small order of magnitude is extremely interesting, because it opens up vistas of inquiry into the mechanism of processes occurring in living matter. The substance of wool and hair, keratin, is a protein. It is formed by linking amino-acids into a long chain, but this case differs from those already considered in that the complex amino-acid groups are not strung together end to end, but rather are attached as pendants to a chain formed by a comparatively simple linking of similar groups at one end of each. We are here coming very near to the structure of living matter.

A detailed study of such complex bodies, difficult though it may now seem, is not beyond the bounds of possibility. Not

PLATE XVII



Amorphous photograph of unstretched rubber



Fibre photograph of rubber stretched seven times its original length

FIG. 127

(*Journal of the Textile Institute*, **xxiii**, pls. v and vi, 1932)



many years ago it seemed hopeless to apply X-ray methods to any but the simplest crystals containing one or two parameters, but they were rapidly extended to complex bodies like the silicates. Improved methods are partly responsible for the advance, but a greater part has been played by increasing knowledge of the nature of the structures and the laws they obey. The rules of interatomic distance, orientation of bonds, and probable associations of atoms are discovered by studying simple structures, and are then applied to those that are more complex. Stage by stage the latter are built up on a theoretical basis, X-rays always serving as a control to check whether the structure has been correctly guessed.



## CHAPTER IX

### X-RAY OPTICS

IN the previous chapters we have considered the directions in which diffracted beams are built up when X-rays fall upon a crystal, the absence of certain spectra owing to space-group symmetry, and the effect of the atomic arrangement in causing certain spectra to be strong and others to be weak. This last feature has been treated in a purely qualitative way; it has been sufficient to associate powerful reflections with large values of the structure amplitude  $F(hkl)$  due to the scattered waves combining together, and weak reflections with small values of  $F(hkl)$ . A great deal more is to be learnt about crystalline and atomic structure when accurate measurements of the diffracted beams are made, and formulæ are devised which make such measurements significant. The problem is complicated, and only an outline can be given here. The diffraction of X-rays by the three-dimensional crystal pattern is a new branch of physical optics, and when it is treated by precise methods many elegant and novel relationships appear.

#### THE SCATTERING OF X-RAYS BY THE ATOM

When a wave-train of X-rays sweeps over an atom, a certain amount of the radiation is scattered. Part of this scattered radiation has a wave-length somewhat greater than that of the incident radiation; this alteration was first measured by Compton, and is known as the Compton Effect. Such radiation plays no part in the diffraction by a crystal, because the waves from different atoms have no phase relationship. Another part of the scattered radiation is termed 'coherent'; it has a wave-length identical with that of the incident rays, and its phase is definite. A quantitative treatment of diffraction must be based on a formula for the efficiency with which each individual atom scatters coherent waves, for it is these waves which interfere.

The scattering can only be calculated accurately by the quantum mechanics, but an expression which depends upon a classical treatment provides a very convenient scale by which the scattering efficiency may be measured. According to classical electromagnetic theory, when a wave of amplitude  $A$  passes over a free electron which is then set vibrating, the electron scatters a wave whose amplitude at a distance  $r$  from the source is equal to

$$\frac{A}{r} \cdot \frac{e^2}{mc^2}.$$

The direction of electric force is supposed to be at right angles to the plane containing incident and scattered rays. When it lies in this plane, the amplitude is

$$\frac{A}{r} \cdot \frac{e^2}{mc^2} \cdot \cos 2\theta,$$

where  $2\theta$  is the angle between the incident and scattered ray. It is to be noted that this simple expression does not involve the wave-length.

The atom contains a number of electrons, distributed throughout a space whose dimensions are comparable with the X-ray wave-length. If each electron be considered as scattering according to the classical formula, the wave scattered by the atom as a whole will be the resultant of contributions from all its electrons. The nucleus has no effect, since its mass is so large. At a small angle  $2\theta$  the diffracted waves are very nearly in phase, because the total paths traversed by the incident and scattered radiation are closely the same. The resultant is therefore  $Z$  times the effect of one electron,  $Z$  being the number of electrons in the atom. As the angle of scattering  $2\theta$  increases, the waves become increasingly out of phase, and interference reduces the resultant to a value  $f \cdot \frac{A}{r} \cdot \frac{e^2}{mc^2}$ . The factor  $f$  is a function of the

angle of scattering, which approaches  $Z$  when  $\theta$  is small and falls off as  $\theta$  increases. It is termed the 'atomic scattering factor,' and measures the scattering efficiency of the atom as compared with that of a single electron according to classical theory.

The solution of the problem by the wave-mechanics is different in principle, but has certain analogies with the classical solution, as is so often the case when classical and wave-mechanical

treatments are compared. An electron which is bound to an atom is represented as a continuous wave-function, the analytical expression of which is like that of a set of standing waves. The probability of the electron being at a given place is proportional to the square of the amplitude of the waves at that point, or what may be thought of as their intensity. The electron bound to a proton in the hydrogen atom, for instance, is represented by a probability function which is very dense near the nucleus and falls away rapidly at greater distances. When the wave-mechanics is set the problem of finding the coherent scattering by such an electron, its answer may be interpreted by a classical analogy. Every part of this electron cloud scatters radiation in proportion to its density, and the contributions from the various parts interfere according to optical principles.

The consequences of this solution are interesting. If the angle at which the scattered radiation is observed is small, the contributions from the various parts of the electron cloud are nearly in phase, and so their resultant is the sum of the contributions. In this case, the amplitude of the radiation is given by precisely the same expression as that found by the classical treatment. It is

$$\frac{A}{r} \cdot \frac{e^2}{mc^2}.$$

On account of this identity, the classical expression may be retained as providing a suitable unit in terms of which the scattering by an atom may be measured. Whereas the classical formula for scattering by a single electron is the same at all angles of scattering  $2\theta$ , however, the new treatment will make the amplitude fall off as  $2\theta$  increases, because of interference from the different parts of the electron cloud. The single electron, in other words, has a scattering factor  $f$  which is unity at small angles and falls away as the angle increases. The intensity of the scattered radiation is proportional to  $f^2$ .

The wave-mechanical treatment also gives the amount of non-coherent radiation scattered with change of wave-length, and, measured on the same scale, this turns out to have an intensity proportional to  $1 - f^2$ . The sum of coherent and non-coherent intensities is equal to that given by the classical formula. These relations were first formulated by Waller and Wentzel. Other consequences may be summarised as follows.

(a) If the electron is loosely bound, the electron cloud is widely spread. In this case interference rapidly destroys the amount of coherent radiation in passing to higher angles, because the path differences are large. In other words, most of the radiation is scattered with change of wave-length.

(b) As the angle of scattering increases, the proportion of coherent to non-coherent radiation diminishes.

(c) If scattering of different wave-lengths be compared, other conditions being the same, phase differences will be greater when the wave-length is short, and so a smaller proportion of coherent radiation will be scattered.

When there are many electrons in the atom the rigorous solution is complex, but an approximate solution which suffices for the problem of crystal diffraction can be simply stated. Each electron is supposed to move in the field of the nucleus and the other electrons, and a corresponding wave-function is formed. The atom is treated as the sum of a number of electron clouds each corresponding to one electron, and each cloud adds its contribution to the resultant wave scattered by the atom as a whole. The atom is thus regarded as an atmosphere of electrons surrounding the nucleus, which is dense towards the centre, and fades away rapidly at the confines of the atomic structure, and the whole may be treated as a single scattering unit.

We can now see what goal we may hope to reach if X-ray analysis of a crystal structure is made with every possible refinement. The analysis is actually an indirect method of viewing the crystal structure illuminated by X-rays, or of looking at it by means of an 'X-ray microscope.' The crystal structure will appear as a continuous distribution of scattering matter, which rises at certain points to a high density. These dense nodes in the structure represent the situation of atomic centres. We cannot hope to see more than the variations in density which correspond to the probability of finding electrons in each region.

The electron densities around the nuclei of a number of atoms have been calculated theoretically by Hartree. The results of his calculations may be represented by plotting a quantity  $U(r)$  against the radius  $r$  measured from the nucleus.  $U(r)$  is defined by making  $U(r)dr$  equal to the number of electrons between the radii  $r$  and  $r+dr$ ; this definition is convenient, because the free atom or ion is spherically symmetrical as regards its electron atmosphere. The expression for the scattering factor  $f$  follows a

well-known optical formula, for it can be shown that each shell acts like a transmitting slit of width  $2r$ :

$$f = \int_0^{\infty} U(r) \frac{\sin \phi}{\phi} dr,$$

where

$$\phi = \frac{4\pi r \sin \theta}{\lambda}.$$

When  $\frac{\sin \theta}{\lambda}$  is small,  $\frac{\sin \phi}{\phi}$  is nearly unity, and the integral  $f$  tends to the value  $\int_0^{\infty} U(r) dr$ , which is equal to the total number of electrons in the atom. At larger angles it falls away, as has

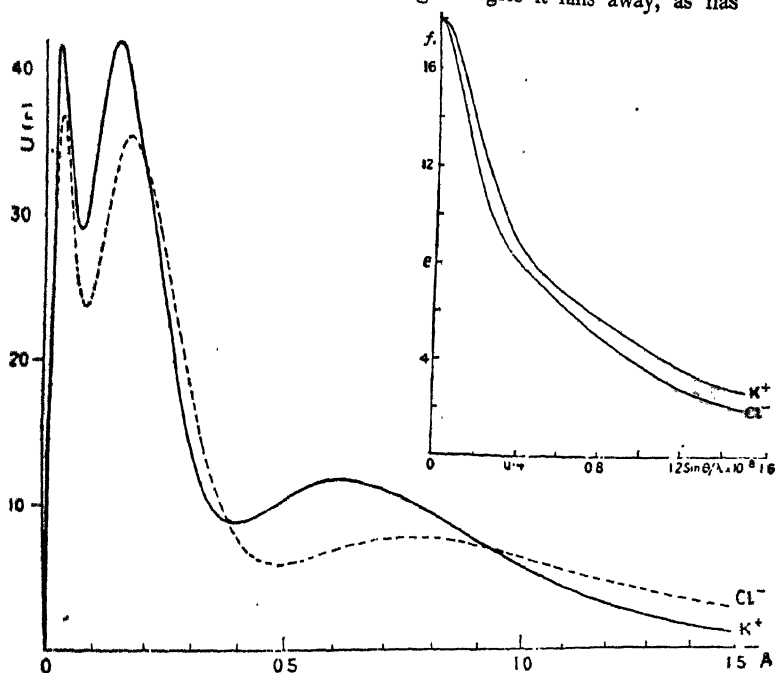


FIG. 128.—Radial distribution of electron density in the potassium and chlorine ions according to Hartree, and the  $f$  curves calculated from these distributions (James and Brindley)

(*Proc. Roy. Soc., A*, 121, 166, 1928)

already been seen qualitatively. Further,  $f$  is seen to be a function of  $(\sin \theta)/\lambda$  alone, so that a curve in which  $f$  is plotted against  $(\sin \theta)/\lambda$  for a given atom can be used to represent its scattering for all wave-lengths and angles.

As an example, the  $U(r)$  curves for potassium and chlorine calculated by Hartree, and the corresponding  $f$  curves plotted against  $(\sin \theta)/\lambda$ , are given in fig. 128. The peaks in the  $U(r)$  curves correspond to the K, L, M electron groups in the atomic structure. The area under both curves represents 18 electrons, the electron distribution in chlorine being displaced further from the centre than that in potassium. Its  $f$  curve therefore has a steeper fall. The  $U(r)$  curves give an impression of the electron density which may be misleading, because they do not indicate its great increase towards the centre of the atom.  $U(r)$  is small near the centre, because the shell has a volume  $4\pi r^2 dr$ , and this

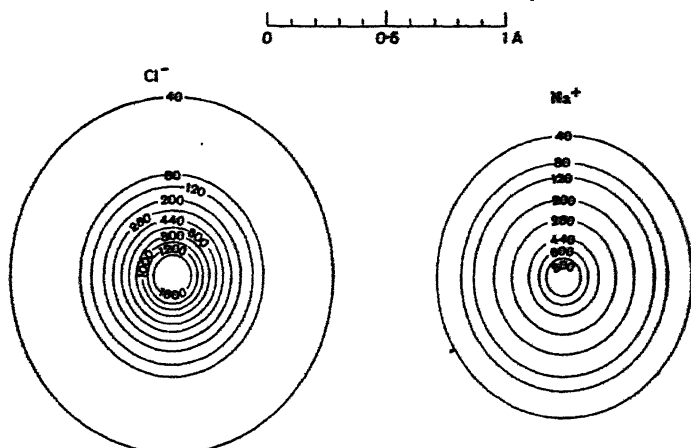


FIG. 129.—The projection upon a plane of the electron density in ions of chlorine and sodium. The numbers signify the number of electrons per  $\text{\AA}^2$  (Bragg and West)

(*Phil. Mag.*, 2, 829, 1930)

rapidly diminishes with decreasing  $r$ . A projection of the electron cloud upon a plane gives a more graphic picture. Such projections for  $\text{Na}^+$  and  $\text{Cl}^-$  are shown in fig. 129; the contour lines mark out areas of equal density, expressed in electrons per  $\text{\AA}^2$  of the projection.

#### THE INTENSITY OF DIFFRACTION BY A CRYSTAL

The quantitative treatment of diffraction by the whole crystal would at first sight appear to be an extremely complex problem. An ideal case for mathematical treatment would be that of a parallel monochromatic beam falling upon an absolutely

perfect crystal. In actual fact, crystals rarely approach this condition. They almost invariably consist of a mosaic of small crystalline blocks, which are inclined at small angles to each other so that there is necessarily an interruption of the regular pattern at the intervening boundaries. The efficiency of X-ray reflection by a crystal face cannot be measured by comparing the incident and reflected beams, as if the face were a mirror, because a glancing angle which is correct for some elements of the mosaic will be wrong for the remainder. Each specimen of a given crystal would give a different result if measurements were made in this way.

This difficulty is surmounted, and significant measurements are made, by a device first employed by W. H. Bragg. The crystal is turned through a small angular range, including the position for reflection, and the total amount of radiation at all angles is integrated. Each small block has an equal opportunity to reflect radiation and contribute to the total. If the crystal reflects an amount  $R(\theta)$  per second when set at the angle  $\theta$ , and the incident radiation measured in the same way is  $I$  per sec., the 'integrated reflection' is defined as

$$\rho = \int_{\theta_0 - \epsilon}^{\theta_0 + \epsilon} R(\theta) d\theta / I.$$

The limits  $\theta_0 + \epsilon$ ,  $\theta_0 - \epsilon$  are chosen at a sufficient interval on either side of the mean angle of reflection  $\theta_0$  to ensure that all the crystalline blocks contribute their reflections.

The measurement of  $\rho$  is conveniently made by rotating the crystal with angular velocity  $\omega$ , and measuring the total amount of radiation  $E$  received by an ionisation chamber as the crystal passes through the reflecting range. The energy reflected in a short time  $dt$ , during which the crystal rotates through an angle  $d\theta$  in the region of the glancing angle  $\theta$ , is  $R(\theta)dt$ . But  $dt = d\theta/\omega$ , since  $\omega$  is the angular velocity. Hence the total energy  $E$  received by the ionisation chamber is given by

$$E = \int_{\theta_0 - \epsilon}^{\theta_0 + \epsilon} R(\theta) \frac{d\theta}{\omega} = \rho \cdot \frac{I}{\omega}.$$

Thus

$$\rho = E\omega/I.$$

It is found experimentally that the integrated reflection of a crystal face measured in this way is the same for different

specimens. As a crystal turns, the diffracted beams flash out irregularly one after another from each speck of the crystalline mosaic, and a curve of  $R(\theta)$  plotted against  $\theta$  is different for every specimen. Nevertheless, the area under the curve is constant, being a characteristic of the substance and of the face examined.

The reason for this constancy appears in a mathematical treatment of the reflection. As each block of crystal turns through the reflecting position, it contributes to the integrated reflection an amount proportional to its volume. This result appears at first sight paradoxical. The reflected wave is built up of wave-trains reflected from each of the crystal planes. If two small crystal blocks be compared in which the areas of reflecting surface are the same, but the number of planes twice as great in the one case as the other, the amplitude of the reflected waves from the thicker block will be twice as great. The thicker block, which is double the volume of the second, will therefore reflect a beam of intensity four times that given by the second, since intensity is proportional to the square of the amplitude. However, it will only reflect radiation over half as great a range. Each crystal block reflects for a small range on either side of the angle  $\theta_0$ , because it is composed of a limited number of planes. This effect is analogous to the finite width of a line in a spectrum given by an optical grating. The width of the line in the case of a grating, or the range of reflection in the case of a crystal block, are inversely proportional to the number of diffracting elements. Although the larger crystal block at its best setting reflects four times as much as the smaller block, this is partly compensated for by its range of reflection being half as great, and the net result is a total contribution twice as great, *i.e.* proportional to its volume.

Since every block of the mosaic contributes an amount proportional to its volume, the resultant effect is independent of the size and angular distribution of the blocks, and the integrated reflection from different specimens is the same. A full treatment shows that a proviso must be made; the blocks of perfect crystal must not be too large, or an effect termed 'extinction' sets in which diminishes the total effect. A discussion of this effect will not be made here, as its satisfactory treatment would be too long. (See Appendix V.)

To sum up, it is possible to deduce a precise formula for the



integrated reflection if the mosaic blocks of a crystal are sufficiently small. A crystal which satisfies this condition is termed an 'ideally imperfect crystal,' and quantitative measurements have a definite meaning when made with a crystal in this state. We might say that as it is impossible to get an absolutely perfect crystal, the alternative is to use a crystal which is thoroughly imperfect; if it is not so naturally, it can often be reduced to a satisfactory state by grinding its surface.

#### FORMULÆ FOR DIFFRACTION BY A MOSAIC CRYSTAL

The diffracted beam may be measured in many ways, and an appropriate formula calculated for each. A speck of crystal may be bathed in the incident radiation; the speck must in this case be so small that absorption is inappreciable. A beam of rays may be reflected from a crystal face, or pass through a thin crystal section and be reflected at internal planes. A formula can be calculated for the intensity in the case of a powder photograph. The only requisite for calculating a formula is that the conditions of the experiment should permit of precise definition.

The formula for reflection by a crystal face may be quoted as an example. It runs as follows:—

$$\rho(hkl) = \frac{1}{2\mu} \left\{ \left( \frac{Ne^2 F(hkl)}{mc^2} \right)^2 \cdot \lambda^3 \cdot \frac{1}{\sin 2\theta} \cdot \frac{1 + \cos^2 2\theta}{2} \right\}.$$

The integrated reflection  $\rho(hkl)$  has been defined above. The linear absorption coefficient  $\mu$  of X-rays in the crystal enters into the formula, because the X-rays penetrate into the interior of the crystal, and the value of  $\mu$  determines the extent to which the deeper layers contribute to the reflection.  $N$  is the number of unit cells in one cubic centimetre.  $F(hkl)$  is the structure amplitude appropriate to the diffracted beam which is being observed. The factor  $\frac{1 + \cos^2 2\theta}{2}$  is termed the polarisation factor,

and arises because rays polarised in, and at right angles to, the plane of incidence are reflected differently.

The formula is often written as  $\rho = Q/2\mu$ , where  $Q$  stands for the expression within brackets above.  $Q$  is common to all formulæ for the intensity of diffraction by mosaic crystals. It arises from the simplest case of all, which is the basis of calculation; a minute crystal of volume  $V$ , which is bathed in

radiation of intensity  $I_0$  per square centimetre, gives the following integrated reflection :—

$$\frac{E\omega}{I_0} = Q \cdot V.$$

The formula makes it possible to determine  $F(hkl)$  for each diffracted beam. An ionisation chamber is first placed so as to receive the incident beam  $I$ , and then placed so as to catch the total diffracted radiation  $R$  as the crystal is turned.  $I$  must be monochromatic, so it is necessary that the incident beam be already reflected from a crystal so as to select one wave-length. Alternatively, a crystal with a known value of  $\rho$  can be used as a comparison standard. Many experimental devices are possible ; the point to be made is that measurements of diffraction lead to an estimate of the scattering power  $F(hkl)$  of the crystal unit.

Formulae applicable to other methods of measurement are as follows :—

*Powder Method.*—Radiation of intensity  $I_0$  per square centimetre falls upon a total volume  $V$  of powdered material. The total amount of radiation  $P$  in the whole cone of radiation with semivertical angle  $2\theta$  is given by

$$P/I_0 = Q \cdot p \cdot \frac{\cos \theta}{2} \cdot V,$$

where  $p$  is the number of planes in the form  $\{hkl\}$  of the crystal (see p. 49).

*Reflection by internal planes of a crystal section, which is cut normal to the planes*

$$\rho = Qte^{-\mu t},$$

where  $t$  is the total length of an incident and reflected ray path in the interior of the crystal.

#### THERMAL MOVEMENTS. THE TEMPERATURE FACTOR

A very interesting application of the measurements determines the extent to which the atoms are vibrating at different temperatures. The movements reduce the value of  $F(hkl)$ , as was predicted by Debye and found by W. H. Bragg in 1914. The first measurements are reproduced in fig. 130, which shows the effect very graphically. The curves represent the reflections 400

and 600 of a rock-salt crystal at  $15^{\circ}\text{C.}$  and  $370^{\circ}\text{C.}$  The displacement of the peaks to the left is due to thermal expansion, which increases the lattice spacing and so reduces the glancing angle. The reduction in height is due to thermal agitation. This agitation makes the reflecting planes more diffuse, and their reflecting power is reduced; a poor grating with diffuse lines similarly gives weaker spectra than one in which the lines are clearly defined. It might appear that temperature movement would make the spectra broader, because the lattice spacing varies from point to point. This is not the case, because

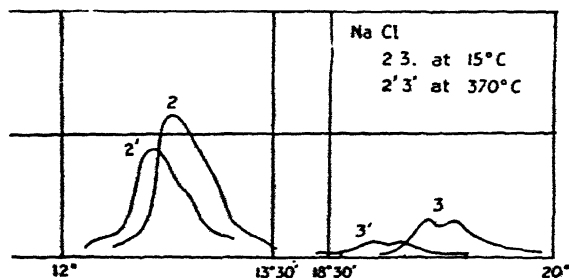


FIG. 130

the sharpness of the spectra depends only upon the number of planes in the single crystal, which is not altered by increase of temperature.

If the mean square displacement of an atom at right angles to the reflecting planes is  $\overline{u^2}$ , supposed to be the same for all atoms in the cell, the structure amplitude  $F$  is

$$F = F_0 e^{-8\pi^2 \overline{u^2} (\sin^2 \theta) / \lambda^2},$$

where  $F_0$  is the corresponding structure amplitude for atoms at rest. The mean square of the displacement increases linearly with the absolute temperature when the latter is high.

The effect is interesting, because it is so direct a way of measuring the atomic oscillations at different temperatures. The crystal is warmed by a surrounding electric furnace, or cooled in liquid air. The vibrations have a marked effect, and when a crystal is cooled in liquid air the higher orders of spectra often increase to several times their value at room temperature. James finds that the root mean square displacements in NaCl are 0.23 Å. at room temperature and 0.58 Å. at  $900^{\circ}\text{K.}$

By a justifiable extrapolation from liquid-air temperature,

James and Waller were also able to measure the amplitude of vibration of the atoms at absolute zero. It was necessary to use the Hartree models as a standard of comparison. In this way they showed that at the absolute zero the atoms still appear to be in a state of vibration to an extent which corresponds precisely to the 'zero-point energy.'

#### TESTS OF THE THEORY OF DIFFRACTION WITH SIMPLE CRYSTALS

On the one hand, atomic models such as those of Hartree make it possible to calculate the atomic scattering factor  $f$  as a function of  $(\sin \theta)/\lambda$ . On the other hand,  $f$  can be determined experimentally by taking simple crystals such as Al, NaCl, or  $\text{CaF}_2$  and measuring the diffracted beams. Many comparisons of theory and experiment have been made by Compton, Bragg, James, Bosanquet, Bearden, and others. The agreement is so good that it gives confidence both in the correctness of the atomic models and the theory of diffraction.

A test of this kind on Al is shown in fig. 131. The curves are calculated on the basis of Hartree's model of aluminium. The upper curve A is the scattering factor for an aluminium atom at rest. The intermediate curve C applies to an atom with the heat motion of room temperature alone, and the lowest curve B to an atom which has also got the zero-point energy of the aluminium crystal. The experimental points, represented by triangles, fit closely on the lowest curve, in conformity with theory and justifying the assumption of zero-point energy. It may be said incidentally that this zero-point energy should be regarded, not as an irregular heat motion of the atoms at the absolute zero, but as the wave-mechanical probability of their being near their mean point. According to the wave-mechanics, atoms like electrons have no definite location.

#### THE USE OF 'ABSOLUTE MEASUREMENTS' IN CRYSTAL ANALYSIS

By 'absolute measurement' is meant the determination of the structure amplitude  $F(hkl)$  for a number of crystal planes by comparing incident and diffracted intensities, as contrasted with merely qualitative estimates of the diffracted beams as 'strong' or 'weak.' Such determination can be made by measuring the

integrated reflection  $\rho$  with the ionisation spectrometer. It is inconvenient to use as incident radiation a monochromatic beam selected by previous crystal reflection, because it is so weak. The difficulty is overcome by using some crystal face as a standard

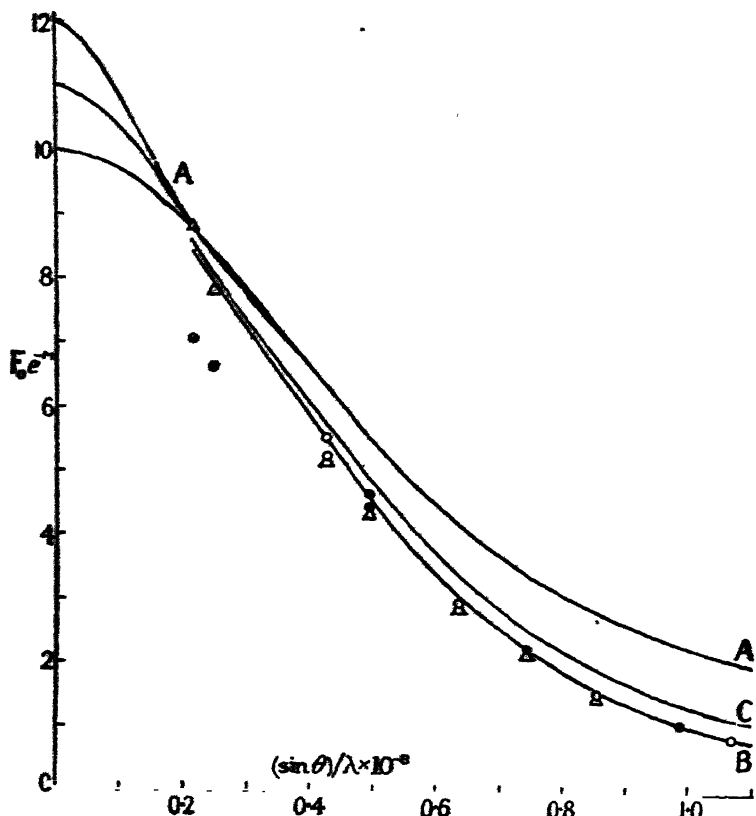


FIG. 131.—A comparison of the  $f$  curve for aluminium deduced from Hartree's model, and corrected both for thermal vibration and zero-point energy (curve B) with the  $f$  values deduced experimentally, indicated by triangles (James and Brindley)

(*Proc. Roy. Soc., A*, 125, 415, 1929)

whose integrated reflection has been measured in absolute units, and comparing other crystals with it.

Absolute measurements provide a very powerful method of analysis when a difficult structure is being examined. We may find, for instance, that some particular reflection is so strong that its value of  $F(hkl)$  is very nearly the maximum which could

be given if all the atoms of the crystal were contributing waves in the same phase. This shows at once that the atoms are so arranged that they lie in sheets on the crystal planes ( $hkl$ ), and analysis is simplified. The numerical data provide a definite basis on which to work. Since the measurements are tedious, they are only used when other methods fail, but they are particularly valuable when the crystal is of a new type and previous experience fails to suggest the solution.

### THE REPRESENTATION OF THE CRYSTAL AS A FOURIER SERIES

The relation between the distribution of scattering matter in the crystal, and its diffraction of X-rays, can be expressed in a very elegant way if the crystal structure is regarded as a three-dimensional Fourier series.

A periodic function of a variable  $x$ , which repeats its value whenever  $x$  is increased by an amount  $a$ , can be expressed as the sum of a number of cosine terms. The lowest term is a constant, the next a cosine curve with one complete wave in the range  $a$ , the next a curve with two waves in the range, and so forth.

$$\begin{aligned} F(x) &= A_0 + A_1 \cos(2\pi x/a + a_1) + A_2 \cos(2\pi \cdot 2x/a + a_2) + \dots \\ &= \sum_0^\infty A_h \cos(2\pi hx/a + a_h). \end{aligned}$$

This sum is a simple Fourier series;  $A_0, A_1, A_2, \dots$  are the amplitudes of the cosine terms, and  $a_1, a_2, \dots$  are their phases. The analysis of certain musical notes into fundamental and higher harmonics is a well-known example.

The scattering matter in a crystal is a similar periodic function, but one which depends on three co-ordinates  $x, y, z$ , measured parallel to the crystal axes  $a, b, c$ . The densities at  $x, y, z$  and  $x+n_1a, y+n_2b, z+n_3c$  are the same, where  $n_1, n_2, n_3$  are any integers. It is therefore possible to express the density (number of electrons per unit volume) at any point  $xyz$  in the crystal by a triple Fourier series:

$$\rho(xyz) = \sum_{-\infty}^{\infty} \sum_{-\infty}^{\infty} \sum_{-\infty}^{\infty} A(hkl) \cos(2\pi hx/a + 2\pi ky/b + 2\pi lz/c + a_{hkl}).$$

Each term of this expression may be thought of as a series of sheets of positive and negative density, parallel to the plane  $hx/a + ky/b + lz/c = 0$ , with a ripple-like distribution of amplitude  $A(hkl)$ . The  $a, b, c$  edges of the unit cell intersect  $h, k, l$  crests

respectively. The density of the crystal is the sum of these components crossing each other in all directions, including a constant term  $A_0$  for which  $h = k = l = 0$ .

When a diffracted beam with indices  $hkl$  is formed by the crystal structure, we can show that it is produced by the Fourier term with corresponding indices alone. All the other terms have no effect on its intensity. If, for instance, we had a mother-of-pearl-like structure with a fluctuation in density normal to its sheets which could be represented by a single cosine term, this structure would give the first-order reflection from the sheets but no other spectra whatever. The significance of this relation in X-ray analysis was first pointed out by W. H. Bragg. Every measurement of an X-ray reflection is in reality a measurement of the corresponding Fourier component in the crystal structure.

The precise form of the relationship may be quoted here, though all its implications cannot be included. It is necessary to use complex quantities in order to put the relationship in a symmetrical form. We must express the density as follows:—

$$\rho(x, y, z) = \sum_{-\infty}^{\infty} \sum_{-\infty}^{\infty} \sum_{-\infty}^{\infty} A'(hkl) e^{2\pi i(hx/a + ky/b + lz/c)},$$

where  $A'$  is complex. It looks strange at first sight that complex quantities should be introduced into an expression for  $\rho$ , but this is necessary in order to cover cases where phase change on scattering must be taken into account. In the normal case, where all the matter scatters with the same phase change,  $\rho$  is everywhere real. This involves the condition that  $A'(hkl)$  and  $A'(\bar{h}\bar{k}\bar{l})$  are conjugate (*i.e.* have the relation  $p + iq, p - iq$ ); the imaginary terms then cancel out in the expression for  $\rho$ .

It may be shown that \*

---

\* This result follows from the expression for the structure amplitude. Since there is a continuous distribution in the unit cell, the waves scattered from various points must be integrated instead of being summed as on p. 97. The structure amplitude for a reflection  $h'k'l'$  becomes

$$F(h'k'l') = \int_{-\frac{a}{2}}^{+\frac{a}{2}} \int_{-\frac{b}{2}}^{+\frac{b}{2}} \int_{-\frac{c}{2}}^{+\frac{c}{2}} \rho(xyz) e^{2\pi i\left(\frac{h'x}{a} + \frac{k'y}{b} + \frac{l'z}{c}\right)} \cdot \frac{V dx dy dz}{abc}$$

Substituting the Fourier series for  $\rho(xyz)$ , every term vanishes on integration except the term for which

$$h = -h', \quad k = -k', \quad l = -l',$$

which integrates to  $V \cdot A'(\bar{h}'\bar{k}'\bar{l}')$ .

$$F(hkl) = A'(\bar{h}\bar{k}\bar{l}) \cdot V,$$

$$F(\bar{h}\bar{k}\bar{l}) = A'(hkl) \cdot V,$$

where  $V$  is the volume of the unit cell.  $F(hkl)$  and  $F(\bar{h}\bar{k}\bar{l})$  are thus also complex and conjugate. As complex quantities they represent both the amplitude and phase of the diffracted beam, the latter being referred to the chosen origin in the crystal. Since they are conjugate the amplitudes are the same, as has already been seen when describing Friedel's Law, but their phases referred to the origin are opposite in sign, as must be true for reflections  $hkl$  and  $\bar{h}\bar{k}\bar{l}$  from opposite faces.

If variations in phase change enter in, as happens when the X-ray wave-length is near an atomic absorption edge,  $\rho$  becomes complex, and it is no longer true that  $|F(hkl)| = |F(\bar{h}\bar{k}\bar{l})|$ ; in this case Friedel's Law breaks down.

The density  $\rho$  throughout the crystal cell is therefore given by

$$\rho(xyz) = \frac{1}{V} \sum_{-\infty}^{\infty} \sum_{-\infty}^{\infty} \sum_{-\infty}^{\infty} F(hkl) e^{-2\pi i(hx/a + ky/b + lz/c)}.$$

The relationship has been given in its complex form because other methods of statement are either incomplete or cumbrous. The constant term, for which  $h=k=l=0$ , is equal to  $Z_n$ , the total number of electrons in the unit cell of volume  $V$ . We may think of the corresponding  $F(000)$  as characteristic of the spectrum of zero order, or radiation scattered in the direction of the transmitted beam.

This relation suggests the possibility of a direct method of crystal analysis. Instead of trying to adjust the positions of atoms in an attempt to explain the X-ray results, values of  $F(hkl)$  for a number of reflections are measured, and the density throughout the crystal is calculated by means of the Fourier series. The centres of the atoms should then be shown as positions of large density, and the atoms can be identified by summing up the concentration of scattering matter and so the number of electrons associated with each.

This can in fact be done, as was first shown by Duane, but only when certain conditions are fulfilled. The X-ray measurements are measurements of intensities, and so they give the amplitudes of the diffracted beams, but not their phases. The lack of knowledge of the phases makes the Fourier method very difficult except in the case of crystals with a centre of inversion. All the Fourier terms must have a maximum or minimum at such



a centre. Hence all values of  $A$  and of  $F$  must be real, when a centre of inversion is used as origin. An ambiguity still remains as to the sign, positive or negative, of each coefficient. This point can be settled, however, by an approximate preliminary analysis of the positions of important atoms in the structure, which suffices to give a verdict for one sign or the other. The Fourier series can then be found.

### EXAMPLES OF FOURIER SERIES

In order to build up the three-dimensional Fourier series,  $F(hkl)$  must be measured for a continuous range of  $hkl$  values. The greater the range of the integers, the more accurate will the representation of the crystal be. The range must be of the order  $+10$  to  $-10$  for a reasonable interpretation to be possible. This implies an enormous number of terms, 4000 in all, which it is impracticable to measure. A more limited representation of the structure may be achieved as follows.

If all the orders of reflection from a given crystal plane are measured, and the values of  $F$  used in a simple Fourier series, the summation of the series gives the distribution of scattering matter in sheets parallel to the plane. This method was first given accurate quantitative expression by Compton. The formula for this case is as follows:—

$$\rho(x) = \frac{1}{d} \sum_{-\infty}^{\infty} F_n e^{-2\pi i n x / d},$$

where  $\rho(x)$  is the density between  $x$  and  $x+dx$  measured normal to the planes whose spacing is  $d$ , and  $F_n$  is the structure amplitude of the  $n$ th order. As before, the constant term  $F_0$  is equal to the number  $Z_0$  of electrons in the unit cell.

In the simple case of a crystal with a centre of inversion, where all  $F$  values are real and  $F_n = F_{-n}$ , this becomes

$$\rho(x) = \frac{1}{d} \left\{ Z_0 + 2F_1 \cos(2\pi x/d) + 2F_2 \cos(4\pi x/d) + \dots \right\}$$

due regard being paid to the signs of the coefficients.

The (111) planes of rock-salt, consisting of alternate layers of sodium and chlorine atoms, may be taken as an instance. Fig. 132 shows the Fourier representation of the fluctuation in density, measured by James and Miss Firth. The higher peaks represent

the chlorine atoms, the lower peaks the sodium atoms. The three curves are taken at temperatures of  $86^\circ$ ,  $290^\circ$ , and  $900^\circ$  Abs. As the temperature rises, the peaks are lowered and flattened out owing to the thermal vibration of the atoms, although the area enclosed beneath them, which is proportional to the total number of electrons, remains constant. The curves show the effect of temperature motion in a very graphic way.

The analysis of the alums by Cork is an example of a direct

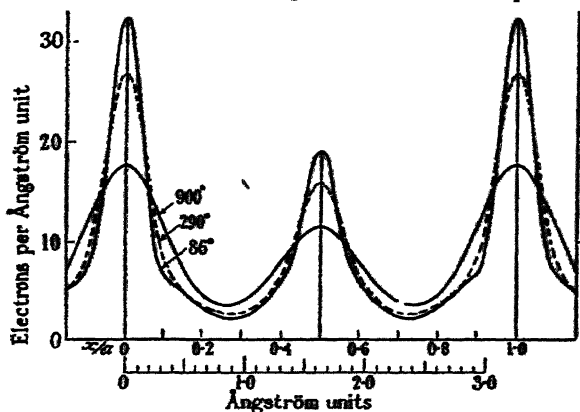


FIG. 132.—The vibration of the atoms when NaCl is heated. The octahedral crystal planes consist of alternate sheets of chlorine and sodium atoms, represented in the figure by the large and small peaks respectively. As the temperature is raised the sheets become broader and more diffuse, owing to thermal movement (James and Firth)

(*I.E.E. Journal*, 60, 1243, 1931)

application of the Fourier method to an unknown crystal structure. An alum has the formula  $R'R''(SO_4)_2 \cdot 12H_2O$ , where  $R'$  may be ammonium, potassium, rubidium, caesium, or thallium, and  $R''$  aluminium, chromium, or iron. The cubic space-group symmetry shows that  $R'$  and  $R''$  are arranged like Na and Cl in rock-salt. The crystal has a centre of symmetry, and values of  $F(hkl)$ , of which a large number were measured by Cork, are therefore positive or negative with no phase factor. The problem is to find the appropriate sign for each in order to build up a Fourier series.

This was done by measuring  $F(hkl)$  in different alums. The origin was chosen at the atom  $R'$ . If  $F(hkl)$  for a rubidium alum is compared with the corresponding  $F(hkl)$  for a potassium alum, then the heavier rubidium atom will make a larger positive contribution to  $F$ . If  $F$  is already positive, its numerical value

will be increased, and if negative, diminished. The comparison of the measured values of  $F$  thus immediately decides the sign. Cork measured the amplitudes and found the signs for a number of alums, and plotted the results for the (111) planes shown in fig. 133. Since  $R'$  and  $R'''$  have a rock-salt arrangement, there are alternate (111) planes of  $R'$  and  $R'''$ , with a complex mass of  $SO_4$  and  $H_2O$  lying between them.

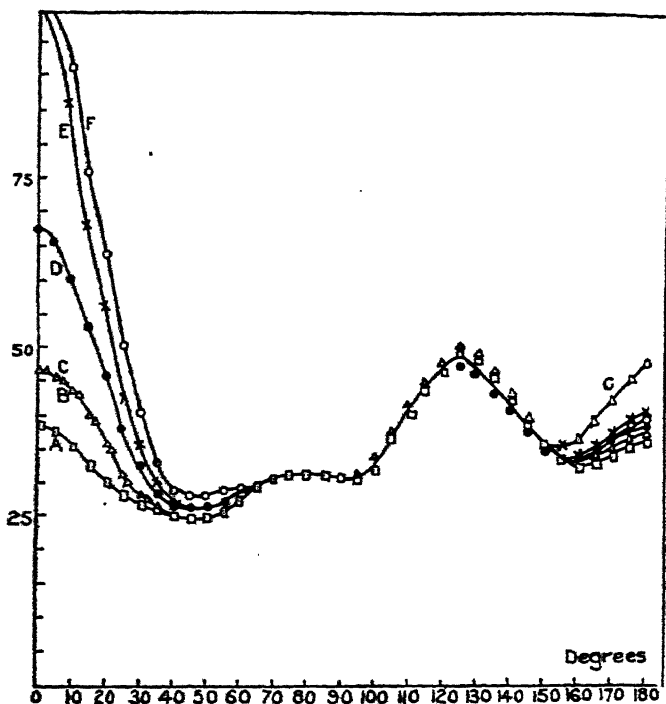


FIG. 133.—Fourier representation of (111) planes in alum (Cork)  
(*Phil. Mag.*, iv, 694, 1927)

The peaks on the left represent the atom  $R'$ , those on the extreme right the atom  $R'''$ . The curves A, B, C, D, E, F are for  $NH_4Al$ ,  $KAl$ ,  $KCr$ ,  $RbAl$ ,  $CsAl$ , and  $TlAl$  alums respectively. The curves nearly coincide in the centre portion, because this represents a similar mass of  $SO_4$  and  $H_2O$  groups. All the Al peaks coincide on the right, but the single Cr peak lies above them. The regular increase in the peaks on the left when heavier atoms occupy the  $R'$  position is very evident.

More complete representation of a structure can be got by



PLATE XVIII

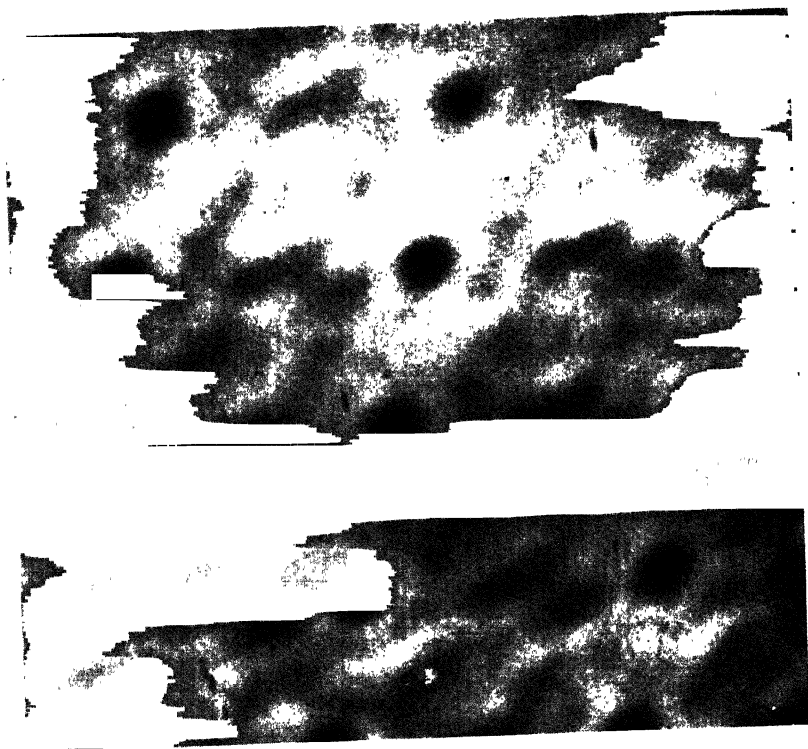


FIG. 137.—Image of crystal structure, projected on face (010)

(*Zeit. f. Krist.*, 70, 489, 1929)

forming a double Fourier series. If all reflections around a crystal zone are measured, and a double series is formed, it gives the electron density per unit area in a projection of the crystal structure upon any convenient plane, the projection being made in a direction parallel to the zone axis. We can see what the

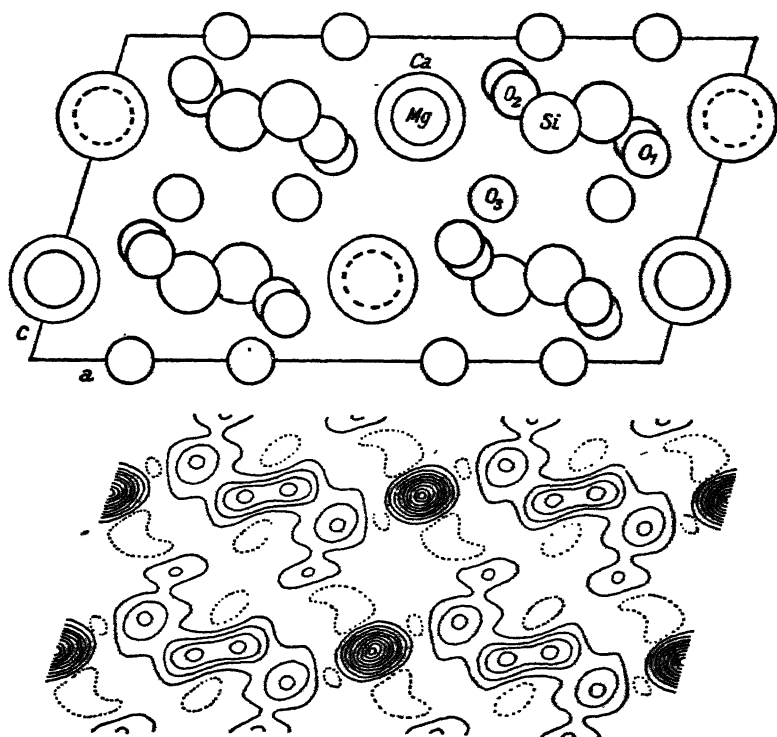


FIG. 134.—Projections of the diopside structure upon (010)  
(*Zeit. f. Krist.*, 70, 488, 1909)

crystal would look like when viewed along the zone axis. In this case, one or two hundred terms in the Fourier series suffice to give a close representation of the structure, and such a number can be measured without excessive labour. The appropriate formula for a two-dimensional projection is

$$\rho(y, z) = \frac{1}{A} \sum_{k=-\infty}^{\infty} \sum_{l=-\infty}^{\infty} F(okl) e^{-2\pi i(ky/b + lz/c)}.$$

The unit cell must be chosen appropriately. Its  $a$  axis is here supposed to be parallel to the zone or direction of projection,

and its  $b$  and  $c$  axes outline the face of area  $A$  on which the projection of the pattern is made.

The results may be represented graphically by calculating the

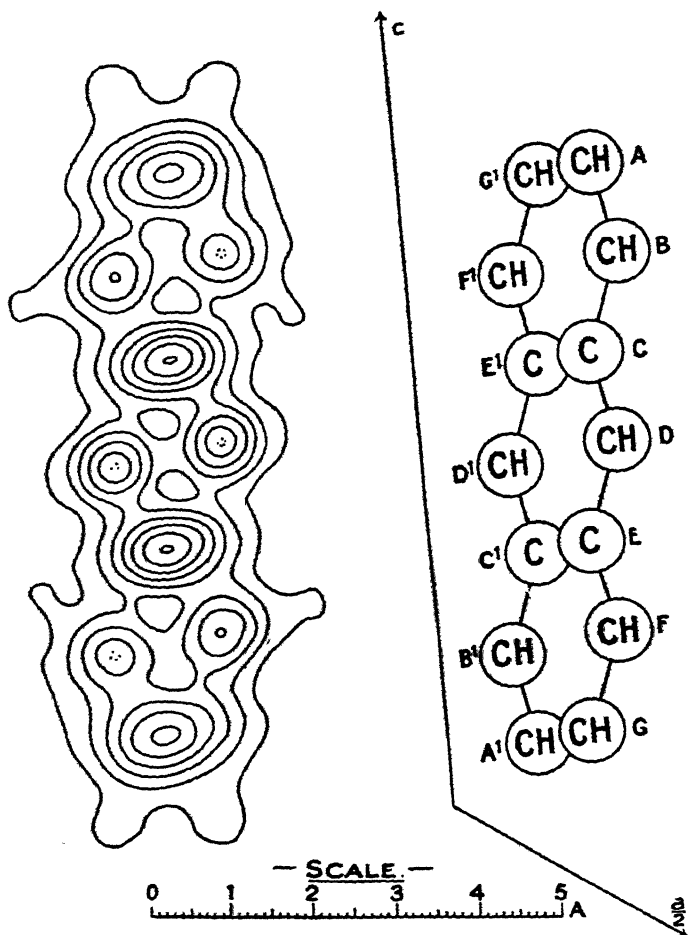


FIG. 135.—Projection upon (010) of the structure of anthracene  $C_{14}H_{10}$  (Robertson)

electron density at a number of points over the projection, and joining points of equal density by lines like the contour lines of equal height on a map. Atoms are then shown by 'peaks' surrounded by concentric contours. Fig. 134 shows a projection

of the structure of diopside,  $\text{CaMg}(\text{SiO}_3)_2$ . The crystal is monoclinic, and has been projected on the  $ac$  face. Calcium and magnesium atoms came on top of each other when viewed in the direction of the  $b$  axis, and account for the very high peaks. The silicon and oxygen atoms are less dense concentrations, but their positions are clearly marked. The position of the atomic centres as analysed by X-rays in the usual way, are shown in the accompanying diagram, with which the Fourier representation may be compared.

Fig. 135 shows a similar diagram for anthracene,  $\text{C}_{14}\text{H}_{10}$ . The carbon atoms alone appear in the diagram, because the hydrogen atoms are too light. The higher peaks occur where two carbon atoms are superimposed. The hexagonal rings are seen almost edgewise from this point of view.

Such Fourier representations sum up in the one diagram all the information about the structure which has been obtained by means of X-rays. They do not constitute an exact image, because a limited number of terms in the series has been taken. The distortion due to the cutting off of the series while its coefficients are still appreciable is analogous to the effect of limited resolving power on an optical image. In interpreting the diagram, these 'diffraction effects' must be borne in mind because they produce false details.

### THE FOURIER REPRESENTATION AS AN OPTICAL IMAGE

The analogy between the projection upon a plane given by the double Fourier series, and the image found by an optical instrument, is a very close one. The projection represents what we should see if we looked at the crystal through an 'X-ray microscope.'

Fig. 136 illustrates Abbe's method of regarding the formation of an image by a microscope. A train of monochromatic waves falls upon an object consisting of a plane grating with transparent lines  $O_1, O_2, O_3$ , etc. Waves spread from these lines, and the lens (represented as a vertical line in the diagram) brings these waves to a focus at the image points  $I_1, I_2, I_3$ . The formation of the image of the whole grating may be thought of as taking place in two stages. In the first stage, the waves scattered by all the lines combine to form parallel trains, the 'spectra' due to the grating. The lens focuses these spectra at  $S_0, S_1, S_1'$ , etc. All the light which has passed through the grating is concentrated at these points, and



we could put a stop in the microscope tube at this point without in any way modifying the appearance of the image, if this stop were pierced with holes at the points  $S$ . These points may be regarded as sources of waves, which proceed to the region of the image and there interfere. The construction shows that the waves from the  $S$  points come into phase at  $I_1 I_2 I_3$ , so that the images of the lines are built up by reinforcement at these points. Each pair of spectra, such as  $S_1$  and  $S_1'$ , or  $S_2$  and  $S_2'$ , produces a band of interference fringes, and the whole image is built up by the superposition of these bands.

It is not hard to see that the amplitudes at the  $S$  points are

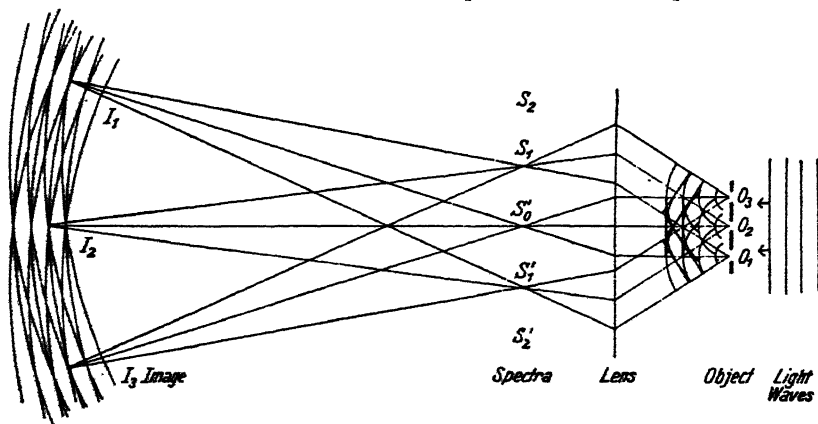


FIG. 136.—Abbe's treatment of image formation in the microscope  
(*Zeit. f. Krist.*, 70, 478, 1929)

proportional to the coefficients of a Fourier series which represents the periodic fluctuations in the amplitude of the light coming through the grating. The formation of the spectra automatically makes a Fourier analysis of the grating. In turn, the elements of the Fourier series recombine in the image space, so that the image resembles the object. The resemblance is not complete, because only the first terms of the Fourier series are included, and Abbe based his theory of resolving power upon the extent of the resemblance.

In the case of X-ray analysis, we cannot form an optical image of the crystal structure. Even if a physical method of image formation were available, the waves scattered by a single atom are too feeble to be recorded. We can, however, measure the spectra  $S$ . To construct a Fourier series to represent the results



# PLATE XIX

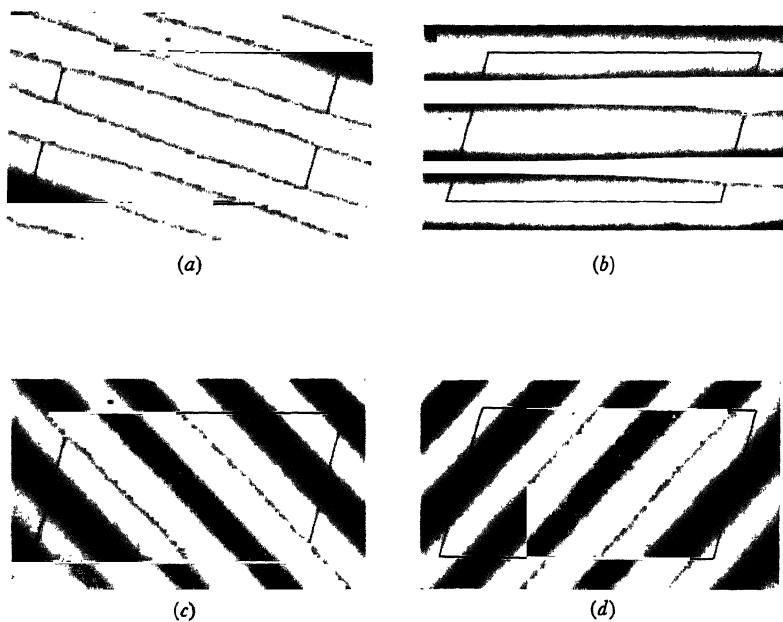


FIG. 138.—Sinusoidal alternations of light and shade. The bands in the figure represent the contributions to the image due to the following spectra:

- |                               |                                     |
|-------------------------------|-------------------------------------|
| (a) $F(102)$ , phase negative | (b) $F(002)$ , phase positive       |
| (c) $F(302)$ , phase negative | (d) $F(30\bar{1})$ , phase positive |

(*Zeit. f. Krist.*, 70, 483, 1929)

of X-ray analysis is in effect to achieve by calculation what is done automatically by the optical system. It is as if we placed a thermopile at the S points in the microscope, and then calculated the image from their observed energies instead of viewing it through the eyepiece.

An optical device can be used to make realistic pictures of what would be seen through the X-ray microscope. The image is the superposition of a number of interference fringes. When a line grating is being viewed, the fringes all lie parallel to each other and form a simple Fourier series. If a cross grating is being viewed, we get in the S region a two-dimensional pattern of spectra, and the corresponding fringes cross each other in all directions. They form a two-dimensional Fourier series which reproduces the pattern of the cross grating in the image space.

A similar X-ray image can be formed artificially. A series of light and dark fringes, like interference fringes, are made on a lantern slide which is placed in a projector. The outline of one face of the unit cell is drawn on a sheet of photographic paper pinned to a board. The projector throws an image of the fringes on the paper, and it is so adjusted that the fringes correspond to some component of the Fourier series. For instance, if the projection is upon the face (010), the fringes of fig. 138, Pl. XIX, represent the components with indices 102, 002, 302, 307 respectively. The paper is exposed to the light for a time proportional to the amplitude of each component  $F(hol)$  as measured by X-rays. In this way the effects of the fringes are summed up, and when the paper is developed it shows an image of the crystal structure as projected upon the crystal face. The image of diopside upon (010) is given in fig. 137, Pl. XVIII, p. 227, and may be compared with fig. 134. Such a picture may be called an 'X-ray microphotograph,' in which the magnification is of the order of 100,000,000 diameters. Projections of the same structure, the Fourier representation, and the image upon the (001) and (100) faces, are given in figs. 139 and 140, A and B, and Pls. XX and XXI, pp. 232 and 234.

### THE RECIPROCAL LATTICE

The reciprocal lattice, first applied to crystal structure by Ewald, sums up the relationship between structure and spectra described above.

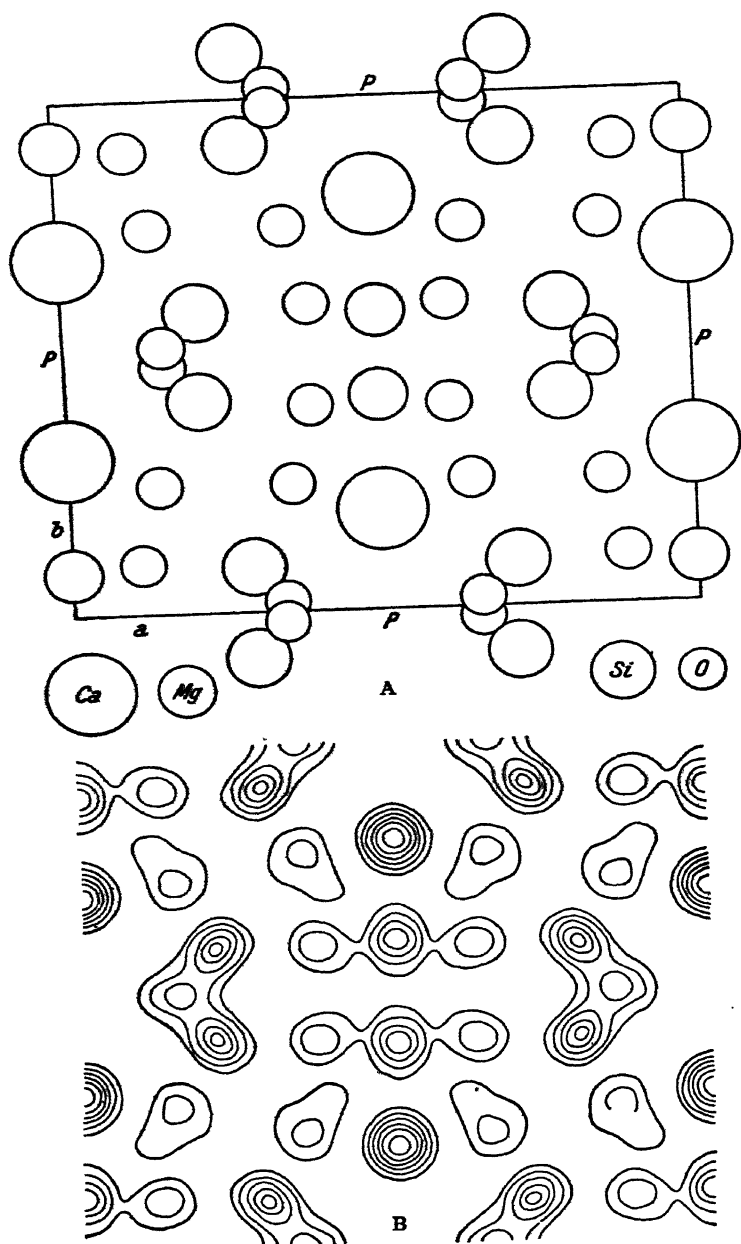


FIG. 139.—A. Atomic positions, projection on face (001). B, Summation of Fourier series, projection on face (001)  
(*Zeit. f. Krist.*, 70, 490, 1929)

PLATE XX

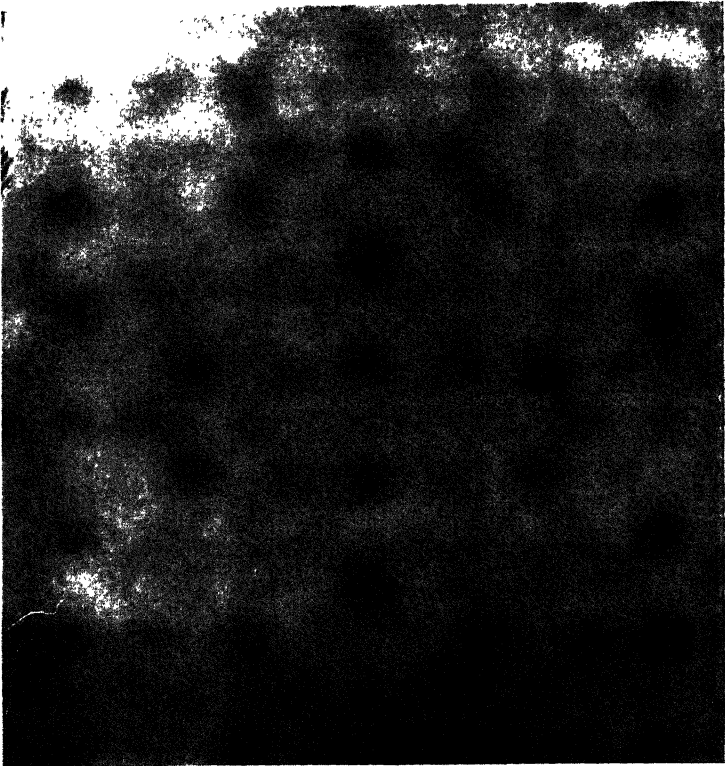


FIG. 139.—C. Image of crystal structure, projected on face (001)

(*Zeit. f. Krist.*, 70, 491, 1929)



The reciprocal lattice is in effect an alternative way of describing the structure. The planes ( $hkl$ ) of the crystal lattice are planes which make intercepts of  $a/h$ ,  $b/k$ ,  $c/l$  on the crystal axes. The reciprocal lattice is constructed by representing each set of planes ( $hkl$ ) of the original lattice by a point  $hkl$ , such that the line joining this point to the origin is normal to the planes, and its distance from the origin is inversely proportional to the spacing  $d(hkl)$  of the planes. Since all multiples of  $hkl$  are to be considered, this point is one of an equally spaced row. When such points are found for all values of  $hkl$ , it follows from the construction that they lie upon a new lattice, the reciprocal lattice. We may now attach a weight of  $F(hkl)$  to each point, and by using complex quantities denote the phase of  $F(hkl)$ . The origin is labelled with a weight corresponding to the total number of electrons in the unit cell. We thus get a constellation of weighted points around the origin, which lie on a lattice, and which show a general falling off in weight at greater distances because the higher orders of  $F(hkl)$  are smaller.

This constellation may be regarded in two ways. It is a way of tabulating the components of the Fourier series which represents the crystal pattern. Alternatively, it is a simultaneous representation of all the spectra given by the crystal when monochromatic X-rays fall upon it. When monochromatic light falls upon a line grating, a linear series of orders results. If it falls upon a cross grating, a pattern of spectra is formed. It is physically impossible to form simultaneously all the spectra of a three-dimensional pattern, but the reciprocal lattice represents analytically the result of such an ideal experiment. It is a pattern of spectra in space (fig. 141).

The relationship which has been traced is an example of a reciprocal action between light and scattering object. If the transparency of a grating follows a cosine form, and composite light falls upon it, the grating analyses the light into its Fourier components, a process termed giving the 'spectrum' of the light. On the other hand, if the grating has a complex form and monochromatic light falls upon it, the spectra give the Fourier components of the grating. In this same way a single crystal periodicity can be used to analyse composite X-rays and determine the components of their spectrum, or a monochromatic beam of X-rays can be used to analyse the crystal structure into its separate periodicities.



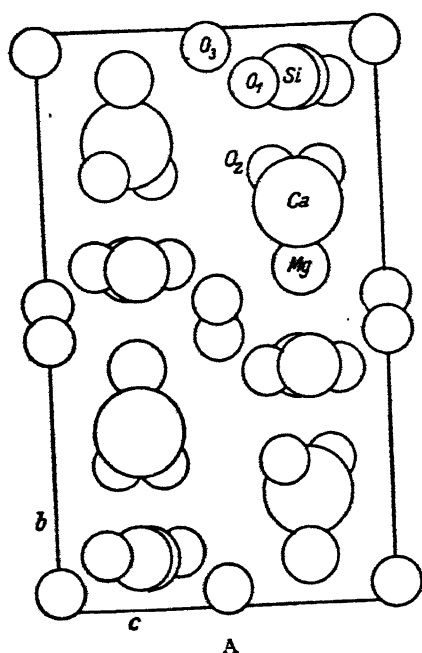


FIG. 140.—A. Atomic positions projected on face (100). B. Summation of Fourier series for projection on face (100). The distribution of scattering matter is indicated by contour lines drawn through points of equal density in the projection

(*Zeit. f. Krist.*, 70, 486, 1929)

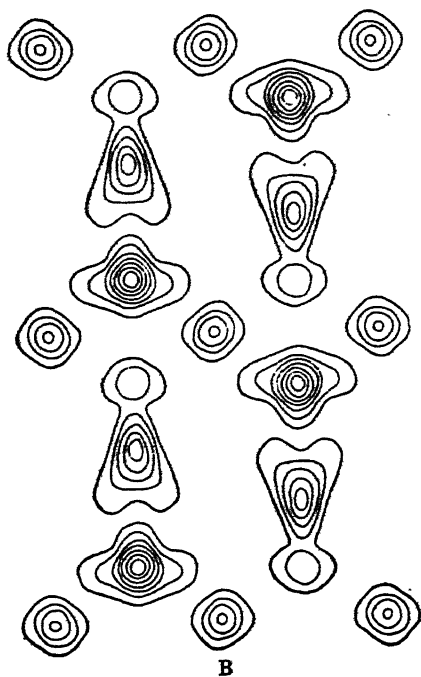


PLATE XXI

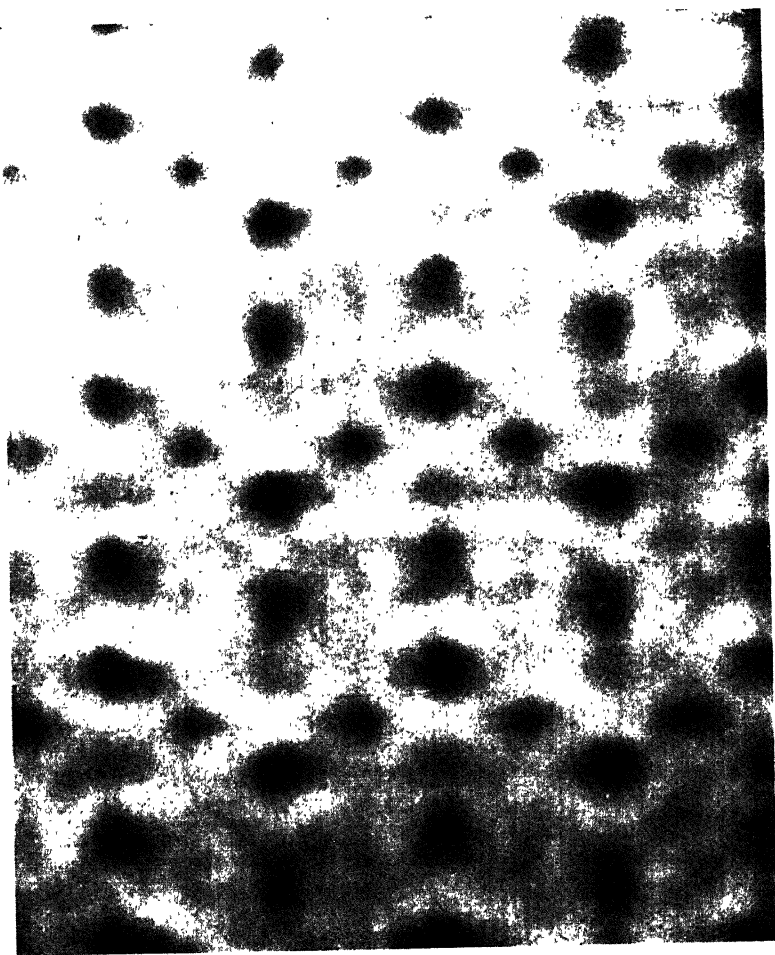


FIG. 140.—C. Image of crystal structure, projected on face (100)

(*Zeit. f. Krist.*, 70, 487, 1929)



Geometrical problems of crystal analysis are often more conveniently treated by using the reciprocal lattice rather than the crystal lattice. This is true in particular of rotation photographs. A geometrical condition concerning a set of planes of the crystal lattice becomes a condition affecting a point of the reciprocal lattice, and such a condition is more simple in form. We may take a case which has already been referred to, where a photograph

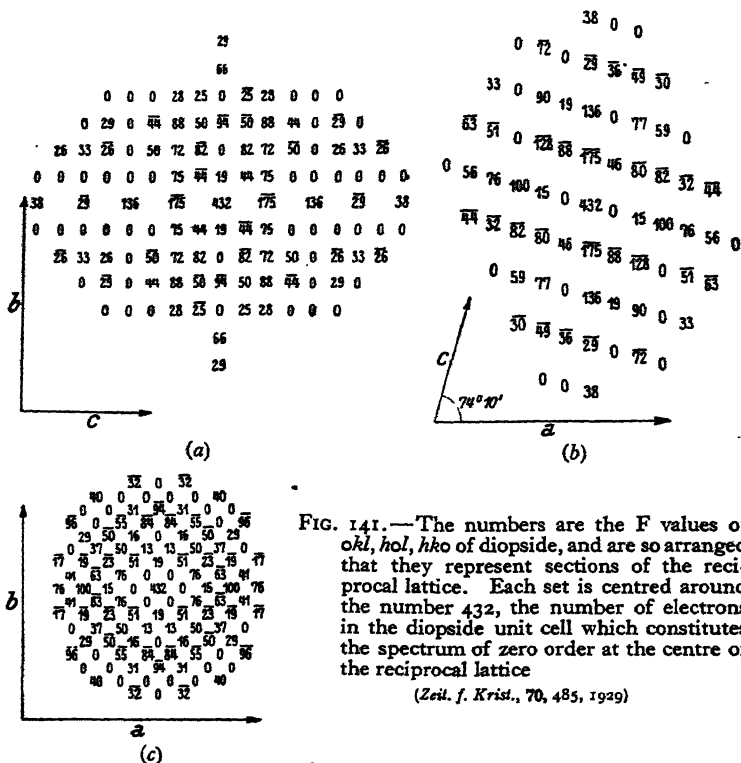


FIG. 141.—The numbers are the  $F$  values of  $okl$ ,  $hol$ ,  $hko$  of diopside, and are so arranged that they represent sections of the reciprocal lattice. Each set is centred around the number 432, the number of electrons in the diopside unit cell which constitutes the spectrum of zero order at the centre of the reciprocal lattice

(*Zeit. f. Krist.*, 70, 485, 1929)

is formed by rotating the crystal through a small arc which includes an axis, the  $a$  axis, for example. A number of  $okl$  planes then come into position to reflect, and a pattern like that given by a cross grating is formed upon the plate. This photograph is in effect a distorted image of part of the reciprocal lattice, for each spot in the picture corresponds to a point  $okl$  of the lattice. They are arranged in a pattern like that of a sheet of points in the lattice (see fig. 141), and they are correspondingly strong and weak.

## SUMMARY

The theory of interaction between diffracting matter arranged in a three-dimensional pattern, and waves whose wave-length is less than the distance between neighbouring lattice-points, is an extension of physical optics. It has only been possible in this chapter to give a brief survey of its main features, and to deduce the effects to a first approximation. The diffracted waves have in effect been considered as being so small in amplitude as compared with the incident wave sweeping through the crystal, that the latter is unaffected by them. Actually this approximation is not sufficient in many cases. The interaction of diffracted and incident waves must be taken into account, a subject which has been treated very fully by Darwin and Ewald. Extinction is due to this interaction, and in the case of a highly perfect crystal a more complete treatment shows that the reflected beam is as strong as the incident beam over a range of a few seconds of arc. The interaction gives rise to the refraction and specular reflection of X-rays described in Appendix I, which might also be included under the heading of X-ray Optics. The object of the present account is to outline the basis of a quantitative treatment of X-ray diffraction, and to indicate the extent of the agreement between theory and experiment.

## CHAPTER X

### APPLICATIONS OF X-RAY METHODS TO PROBLEMS OF PURE AND APPLIED SCIENCE

#### A SUMMARY

X-RAY analysis is complementary to other methods of analysis. It attacks from a new angle, and supplies information which cannot be obtained in other ways. All compounds which exist as gases or liquids will assume the crystalline form if cooled sufficiently, but the converse does not hold. Many compounds can only exist in the crystalline state, and break down into simpler constituents if an attempt is made to convert them into the dissolved, liquid, or gaseous form necessary for chemical investigation. Their nature can only be understood if they are studied as solids. In chemical analysis the structure of the compound is inferred by studying its reactions, or by breaking it down into simpler constituents which can be recognised; it is essential to change the substance in the process. In crystal analysis, on the other hand, the material remains unchanged. Very minute quantities suffice for an examination, and it is not necessary to separate it from other constituents with which it may be mixed if these latter do not bulk too largely. Hence there are many cases where X-ray analysis is indispensable. This holds not only in purely scientific investigations, but also in problems of applied science where X-ray analysis can be used in conjunction with other methods as a means of studying bodies whose properties are of technical importance.

An account has been given in the preceding chapters of the methods and results of the analysis of structure. Although an accurate fixation of atomic positions is of fundamental importance, there are many cases where much can be learnt without complete analysis, or where variations from a known type of structure are being studied. Such cases often arise in technical investigations,

and may be included in the present review of the application of X-ray methods.

### CHEMICAL COMPOSITION

A measurement of the unit cell, together with a knowledge of the density of a crystal, makes it possible to calculate the mass of the compound which is included in the unit cell. The accuracy with which this can be carried out is high, if the substance be homogeneous and well crystallised. Crystal spacings can be measured to one part in twenty thousand by the usual powder method, and the main factor influencing the accuracy of the final result is the determination of density. Since the unit cell contains an integral number of units of pattern, or of molecules in the case of organic compounds, the X-ray measurements provide a reliable means of deciding the formula of constitution of a body in the solid state.

Mauguin's preliminary work on the micas may be quoted as an example. Owing to isomorphous replacement of one constituent by another, there is a wide variation in the composition of the mica minerals. Chemical analysis tells us the relative proportion of the constituents such as H, K, Mg, Fe, Al, Si, F, and O, but in order to assign a formula to the mica structure it is necessary to discover what amount of each of these elements is contained in the structural unit. The relative proportions vary widely, and there is no *a priori* reason to anchor the formula to one constituent more than to another; this uncertainty is reflected in the conflicting views of the constitution of mica which have appeared from time to time. Mauguin made simultaneous determinations of chemical composition, density, and cell dimensions, for a number of varieties, and was able to show that the constant factor in terms of which all compositions must be expressed is the sum total of oxygen and fluorine atoms in the unit cell. This total is always forty-eight. Once this constant character is established, the chemical analyses give the amounts of the other constituents in the unit cell, and so make it clear how isomorphous replacement is taking place. An ideal muscovite mica, for instance, has the formula  $H_2KSi_3Al_3O_{12}$ , or  $(OH)_2KAl_2(Si_3AlO_{10})$  as the subsequent complete analysis of mica has indicated, and there are four such units in the cell. F may be substituted for OH. The relative amounts of Si and





# PLATE XXII

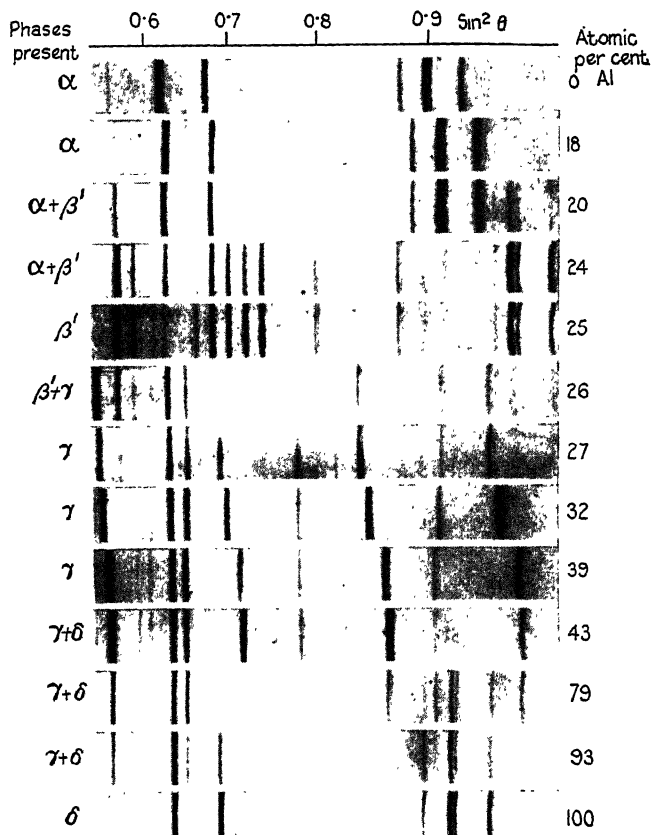


FIG. 142.—Powder photographs of silver-aluminium alloys.  
FeK radiation (Westgren and Bradley)

(*Phil. Mag.*, 6, 280, 1928)

Al in the  $(\text{Si}_3\text{AlO}_{10})$  structure may vary, and the variations are balanced by alterations in the amount of the large cation K, or by the substitution of Ca for K. In the small cation group  $\text{Mg}_3$  may be substituted for  $\text{Al}_2$ , and  $\text{Fe}^{++}$  may replace  $\text{Mg}^{++}$ , or  $\text{Fe}^{+++}$  replace  $\text{Al}^{+++}$ . These substitutions lead to varieties of composition which are very puzzling until the structural formula is established, when they all fall into their places in an extremely simple scheme.

The typical formula of an amphibole has generally been quoted in text-books as  $\text{CaMg}_5(\text{SiO}_3)_4$ . Analyses have shown, however, that amphiboles contain a small proportion of hydrogen (generally expressed as 2.2 per cent.  $\text{H}_2\text{O}$ ), and Warren's analysis of the structure showed this to be an essential constituent. The true formula is  $(\text{OH})_2\text{Ca}_2\text{Mg}_5(\text{Si}_4\text{O}_{11})_2$ . Al may partly take the place of Si in the  $\text{Si}_4\text{O}_{11}$  group, and this is balanced by the inclusion of additional ions such as K in certain spaces in the unit cell. The presence of OH' as an essential part of the structure was proved by applying Pauling's rule of the balancing of valencies. Another example is that of hemimorphite, usually written  $\text{H}_2\text{Zn}_2\text{SiO}_5$ . Analysis shows the true constitution to be  $\text{H}_2\text{O} \cdot (\text{OH})_2 \cdot \text{Zn}_4 \cdot \text{Si}_2\text{O}_7$ . Many other cases might be quoted. The very large group of compounds which includes the phosphotungstic and phosphomolybdic acids, for instance, presents problems analogous to those of the silicates, and similar methods may be used to arrange these compounds in an ordered scheme.

In the case of organic compounds where the unit is the molecule, the molecular weight can generally be determined by classical methods. As investigation is extended to more complex bodies, however, the determination of molecular weight by X-rays may become increasingly important. In such substances as cellulose it has already proved its value. The atomic arrangement of the cellulose chain may be uncertain owing to the diffuse nature of the diffraction effects, but these are sufficient to identify the repeated unit in the chain with the linked glucose groups shown in fig. 126, and so to justify the conclusion reached by Haworth on chemical evidence. Interesting work has been carried out in the identification of the long-chain constituents in paraffins, such as that of Piper and Malkin on solid solutions of these compounds in each other. Mention may also be made of Shearer's work on long chains to which a ketone oxygen is attached (p. 165). The chains are placed side by side in the

crystal structure, and the oxygen which is attached to one of the carbon atoms in the chain gives rise to an increased scattering of X-rays at that point. The distribution of intensity in the different orders of reflection from the long spacing of the cell is determined by the interaction between the increased scattering at this point, and the decreased scattering where the ends of the chains are in contact. The distribution of intensity immediately shows at what point in the chain the ketone oxygen is attached, and it is therefore possible to identify the compound. An interesting test of this method was reported in *Nature*, 11th July 1925. Professor R. Robinson submitted to Shearer four long-chain keto-acids which he had synthesised, without indicating their formulæ, and Shearer was able to give the number of carbon atoms in the chain and the position of the oxygen merely by inspection of the spectra.

#### THE STRUCTURE OF ALLOYS

The study of alloys by X-ray methods enables the various phases to be identified with a certainty which was previously not possible in all cases. Similar phases can be recognised in different alloy systems, and this has given a great impetus to the search for general laws which will enable the properties of a given alloy system to be predicted. Since the range of possible metal combinations is so immense, any general laws of this kind are of the greatest technical importance. An important feature of the X-ray method is that the boundary between two phases in a phase diagram can be determined very accurately by studying a few samples with compositions on either side of the critical composition. As has been explained in Chapter VII, the alteration in composition in a single-phase region is accompanied by a regular alteration in lattice dimensions. The measurement of alloys of known composition in the single-phase region establishes this relation, and therefore a measurement of the spacings of the limiting phase in the adjacent two-phase region enables its exact composition to be determined. It is also possible to examine the alloy by X-rays at different temperatures, so that the phase diagram can be studied in a very complete way. The study of the distribution of atoms amongst the positions of the structure in a single-phase region has already been described (p. 153).

An example of alloy powder photographs is given in Chapter VII. Another example which illustrates the points summarised



PLATE XXIII



FIG. 143.—Powder photographs of two kinds of opal glass  
Opal 1. Mainly calcium fluoride  
Opal 2. Mixture of sodium and calcium fluorides

here is shown in Pl. XXII, p. 239. The photographs, due to Westgren, are of silver-aluminium alloys, and the transition from one phase to the next is very clearly shown. It will be noted that the first and last phases have an almost identical structure, which is actually face-centred cubic.

The preparation and heat treatment of the alloys remains as essential a part of metallurgical technique in X-ray investigation as formerly; the method can only report the nature of the sample studied and cannot control the conditions of its formation. So much information can be obtained, however, that an X-ray equipment should be considered as necessary in any extended scheme of metallurgical investigation.

### IDENTIFICATION

The powder method may be used to identify the constituents of very small quantities of crystalline matter. Each structure gives a characteristic pattern of lines, and the constituents can be recognised by matching these powder photographs against those of known substances whose presence is suspected. It is impossible to unravel the crowded lines if too many substances are present, and trial has shown that it is difficult to recognise a constituent if it is present to an extent of less than about 10 per cent.; but there are many cases where the method is extremely useful, especially as the substance can be examined *in situ*. Powder photographs have been used, for instance, to identify the coating of a valve-filament, to study the course of the reactions in the action of bleaching-powder, and to analyse the lead compounds on the plates of a storage battery during charge and discharge. Fig. 143, Pl. XXIII, shows photographs of opal glass. The glass, being amorphous, gives rise to diffuse diffracted bands, but the photograph shows in addition sharp lines due to the crystals which give the opal glass its character. They are seen to be crystals of calcium and sodium fluoride, by comparison with the standard photographs in the lower part of the figure. The powder method distinguishes allotropic modifications of the same substance, such as quartz and cristobalite (fig. 144, Pl. XXIV, p. 242). By heating or cooling the powder, the transition from one allotropic form to another can be followed. A classical instance of such an investigation was Westgren's proof that  $\alpha$ -,  $\beta$ -, and  $\delta$ -iron have a body-centred structure, while  $\gamma$ -iron

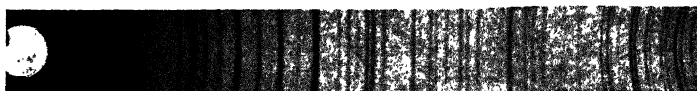
is face-centred. Cases occur where similar structures possess a number of closely related forms, and it may be important to know which modification is present. As an instance, there is a range of compounds (mullites) which are closely related in their structures to sillimanite,  $\text{Al}_2\text{SiO}_5$ , but which have a different ratio of  $\text{Al}_2\text{O}_3$  to  $\text{SiO}_2$ , and often contain other constituents. Fig. 145, Pl. XXIV, shows photographs of these compounds. The obvious similarity in the three patterns shows that their structures are analogous, but closer inspection reveals characteristic differences, especially between the lines of higher order on the right of each film. These compounds are of technical interest, because the varieties of porcelain are included amongst them.

The approximate quantitative analysis of a mixture of crystals may be made by comparing the intensities of their respective lines in the photographs. Though the method is simple in principle, difficulties arise when it is carried into practice. An ingenious modification has been developed by Nahmias, which consists in exposing the powder mounted upon a standard thin aluminium wire. A weighed quantity of the powder is placed upon the wire, and the lines of one of its constituents are compared with the aluminium lines. A weighed quantity of the pure constituent is then placed upon a similar wire and an exposure made in the same camera. The relative strength of the aluminium lines in the photographs indicates the relative 'doses' of X-rays in the two cases, and the comparison of the powder lines then makes it possible to estimate the amount of the constituent in the powder.

#### COEFFICIENTS OF THERMAL EXPANSION

The lines of a powder photograph which correspond to reflections through nearly  $180^\circ$  are very sensitive to small changes in crystal spacing. An alteration in the position of the reflected line from  $175^\circ$  to  $176^\circ$ , for instance, corresponds to an alteration in spacing of 0.034 per cent., and much smaller angular variations can be accurately measured. A crystalline powder may be cooled by liquid air or heated in a resistance furnace, and the alterations in the position of its powder lines at high angles make it possible to measure its coefficients of expansion to an extremely high degree of accuracy, dependent mainly on the accuracy to which the temperature can be estimated. When the

PLATE XXIV



(a)



(b)

FIG. 144.—Powder photographs of quartz (a) and cristobalite (b)  
(Bradley and Roussin)



FIG. 145.—Powder photographs of aluminosilicates  
(Bradley and Roussin)

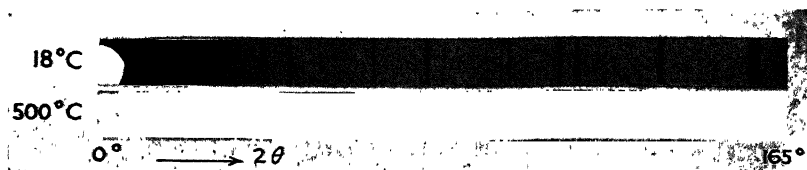


FIG. 146.—Powder photographs illustrating the thermal expansion of silver (Jay)





crystal is not isotropic, different lines give the coefficients of expansion in different directions. Suitable lines are brought into the sensitive position by using an anticathode which gives a beam of the requisite wave-length. This is a rapid and accurate way of measuring coefficients for which only small quantities of crystalline powder are required.

In fig. 146, Pl. XXIV, p. 242, two powder photographs of silver are compared. The upper photograph is produced by powdered silver at 18° C., the lower by the same powder heated to 500° C. in a furnace enclosed in the Debye camera. The expansion of silver is shown by the displacement of the lines, which is very considerable in the region of high dispersion on the right. The photograph illustrates at the same time the Debye temperature effect. The times of exposure were identical, and it will be seen that whereas the lines of low order are little affected by the thermal movement, those of high order are much reduced in intensity.

### TECHNICAL APPLICATIONS

In assessing the value of X-ray investigations to industry, it is to be remembered that they can only constitute one factor in any technical advance. As in the case of other methods of analysis, it will only exceptionally be possible to record a direct connection between an investigation and a consequent improvement in technique. Its main function must be to provide accurate information about the materials which are being utilised, and so indirectly to aid the technical expert who can put this knowledge to practical use. A works laboratory has its chemical analysts and metallurgists who examine the materials in order to arrive at a better understanding of their nature and properties, the causes of their breakdown, and the reasons for their usefulness. The general value of such knowledge is unquestioned, and X-ray methods take their place along with the older methods as a means of obtaining it.

To be of service, any method of analysis must be understood and trusted by the technical expert, whose imagination is stimulated by the knowledge it affords.

## CHAPTER XI

### THE DIFFRACTION OF ELECTRONS

THE discovery that an electron beam is diffracted by matter, as if it were a train of waves, has provided a new means of investigating crystalline and molecular structure. The new diffraction effects were observed independently by Davisson and Germer and by G. P. Thomson. They are analogous to the effects obtained with X-rays, and can be used in the same way to analyse atomic arrangement. The amount of matter required to produce electron diffraction, however, is extremely small compared with that required for X-ray diffraction, and the times of exposure required for a photographic record are measured in fractions of a second. These new features make it possible to apply electron diffraction to problems where it is difficult or impossible to use X-rays, such as to the structure of surface films or to the analysis of the molecules of a gas, and the applications which have already been made indicate how useful the method will be.

### THE WAVE-MECHANICS OF ELECTRONS

The behaviour of an electron in large-scale electric or magnetic fields is satisfactorily explained by assuming it to be a particle with mass and electrical charge, subject to the ordinary laws of mechanics. On the other hand, the mechanisms of spectral emission, the photo-electric effect, and other phenomena are of such a nature that they cannot be explained by these laws. The quantum theory formulated rules which arranged and co-ordinated these phenomena, but its combination of new rules with the classical laws was a temporary expedient in the search for something more fundamental. The new mechanics, developed by L. de Broglie, Schrödinger, Heisenberg, Born, and Dirac, has brought the classical and quantum mechanics within a single scheme. It leads to the same result as classical mechanics in such problems

as the latter explained satisfactorily. It solves the problems of atomic mechanics where the older quantum theory had a very restricted success, and reconciles the quantum and wave aspects of light.

The analytical handling of these problems by the new mechanics may be conveniently carried out by a process which resembles the classical treatment of waves, and hence this method of treatment is known as the wave-mechanics. The electrons are in no way to be identified with the waves which appear in the mathematical analysis. Our knowledge about the initial conditions of an experiment, such as the positions and velocities of the interacting particles, is expressed in a wave-form. By tracing what happens to these waves in a given interval of time, and then reinterpreting the final wave-form as a distribution of particles, we are able to make successful predictions as to the result of the experiment.

A beam of electrons which have a kinetic energy  $\frac{1}{2}mv^2$  is represented by a wave-train with a wave-length  $h/mv$ , where  $h$  is Planck's constant. If electrons with initial energy  $E$  enter a field of force so that at a given point an electron has potential energy  $V$ , then the kinetic energy of an electron at this point will be given by

$$\frac{1}{2}mv^2 = E - V.$$

The wave-length associated with the electrons thus becomes

$$\lambda = h/mv = h/\sqrt{2m(E - V)}.$$

The wave-length therefore varies from point to point in the field, as if the waves travelled in a medium with a variable refractive index.

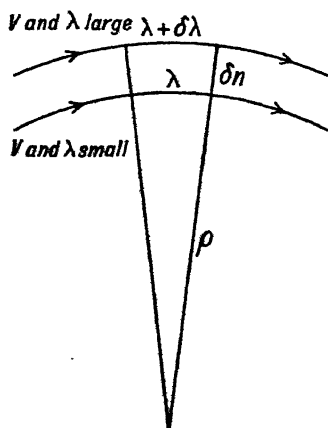
A beam of monochromatic waves entering a medium where the refractive index varies from point to point follows a curved path in the medium. When an electron beam enters an electric field it describes a curved path. Owing to the above relation between the kinetic energy of the electron and the associated wave-length, it follows from the construction in fig. 147 that the curved path of the beam of waves exactly reproduces the trajectory of the electrons.

According to classical mechanics there is a component of force  $\frac{\delta V}{\delta n}$  acting on the particle normal to its trajectory,  $\delta n$  being

measured along the direction normal to the curve in which the force is greatest. The curvature  $\rho$  of the path at this point is given by

$$\frac{mv^2}{\rho} = \frac{\delta V}{\delta n},$$

and the electrons will be deflected away from the region where the potential energy is greatest. The rays normal to the waves will curve in the same direction, because the wavelength is less when  $V$  is less. It can be seen from the diagram that the curvature of the ray is given by



$$\frac{\delta \lambda}{\delta n} = \frac{\lambda}{\rho}.$$

Since  $\lambda = \frac{h}{mv}$  and  $\frac{1}{2}mv^2 = E - V$ , it follows that

$$-\frac{h}{mv^2} \frac{dv}{dn} = \frac{h}{mv\rho},$$

$$-mv \frac{dv}{dn} = \frac{mv^2}{\rho},$$

$$-\frac{d}{dn} \left( \frac{1}{2}mv^2 \right) = \frac{mv^2}{\rho},$$

$$-\frac{d}{dn} (E - V) = \frac{mv^2}{\rho}.$$

FIG. 147.—The identical curvature of path for particles and waves in potential field.

Thus  $\frac{mv^2}{\rho} = \frac{\delta V}{\delta n}$ , since  $E$  is constant and the equation is the same for the curvature of the rays as for the curvature of the trajectory of a particle.

The representation of the electron beam as a homogeneous wave-train leaves quite uncertain the position of any electrons in the train. Suppose, however, an initial experiment locates an electron within a certain limited space. This knowledge about the position of the electron is represented in the wave-picture by a 'wave-packet' or limited wave-group. Apart from its spreading by diffraction, we have already seen that such a wave-group will travel along the electron's path in the field. It can also be shown that it travels as a whole with the velocity of the electron. The limited wave-packet must be regarded as the sum of a series of

wave-trains of varying wave-length, which conspire to form a large amplitude of vibration in the packet and are destroyed by interference outside it. The group velocity of such a packet is equal to  $\frac{dv}{dN}$ , where  $\nu$  is the frequency of waves whose wave-number  $1/\lambda$  is  $N$ . Without specifying the absolute frequency of the vibrations, and so the absolute velocity of the individual waves composing the group, the quantum relationship  $E = h\nu$  leads to the equation

$$\frac{dv}{dN} = \frac{d\left(\frac{mv^2}{2h}\right)}{dN} = \frac{d\left(\frac{mv^2}{2h}\right)}{d\left(\frac{mv}{h}\right)} = v,$$

so that the group velocity of the packet is equal to the velocity of the electron which it represents.

Knowledge about the initial momentum and position of the electron can always be adequately represented by the appropriate wave-packet, in spite of its diffuseness, because of Heisenberg's 'Principle of Uncertainty.' Any observation on the electron necessarily leaves the observer uncertain as to its precise momentum and position, because the light-signal which the electron has sent out in betraying its presence alters the constants of its motion to an extent which, within certain limits, is indeterminate. The possible errors in position  $x$  and momentum  $mv$  are related by the equation

$$\Delta(x)\Delta(mv) \approx h.$$

The representation of the electron by a wave-packet has just the same uncertainty. A short wave-packet defines  $x$  closely, but must be built up of waves of widely varying  $\lambda$ , so that  $mv$  is uncertain. A long wave-packet, necessary to define  $mv$  closely, makes the precise position of the electron uncertain. In such a packet  $\Delta x \cdot \Delta N \approx 1$ , leading to the above relation when  $mv/h$  is substituted for  $N$ .

These are examples of problems where the classical mechanics and the new mechanics lead to corresponding results. The path of a particle can only be compared with the path of a wave-group, however, when the relative change of kinetic energy is small for distances comparable with the wave-length. This is no longer true when the field is that of the atom and the

conception of an electron following an orbit breaks down. However, the same differential equations which represent the propagation of the waves can be used in this case, and lead to an explanation of the stationary states of the atom.

Another case in which the new mechanics leads to results which have no counterpart in classical mechanics is that of elastic scattering of the electron beam by a number of centres, such as the regularly arranged atoms in a crystal. When the electron beam is treated as a wave-train, the waves scattered by the centres interfere with each other. Strong beams are diffracted in certain directions and weak beams in others. Correspondingly, electrons will be observed to proceed in large numbers when the waves have a large amplitude, and *vice versa*. Just as in the case of light the number of light-quanta observed is proportional to the intensity of the light or square of its amplitude, so the number of electrons is proportional to the square of the quantity  $\psi$  which represents the amplitude of the vibration in the wave treatment.

It was first suggested by Elsasser in 1925 that this prediction of wave-mechanics might be tested by diffraction of electrons by a crystal, and in 1928 this was verified experimentally by Davisson and Germer, and by G. P. Thomson, whose results were published almost simultaneously. Thomson's results are more closely analogous to the diffraction of X-rays by crystals, and will be described first.

#### POWDER PHOTOGRAPHS OF ELECTRON DIFFRACTION

G. P. Thomson, by passing a narrow beam of electrons through thin crystalline films, obtained diffraction effects which were similar to the haloes of the Debye-Scherrer and Hull X-ray powder photographs. The apparatus which he used is shown in fig. 148. The electron beam is produced in the discharge tube A, the applied potential being between 10,000 and 60,000 volts. The electrons pass through the narrow tube B, which has a diameter of  $\frac{1}{2}$  mm. and a length of 6 cm. The crystalline film is mounted at C. The diffraction pattern can be viewed on a fluorescent screen E, and when desired it can be recorded upon a photographic plate D, which is lowered by a winch into a position in front of the beam. The space between E and C is highly evacuated so as to avoid scattering of the electrons by gas atoms.

An exposure of a few seconds' duration is sufficient to record the pattern.

Two patterns obtained by Thomson in his first investigation are shown in fig. 149, Pl. XXV, p. 250. A thin celluloid film gives diffuse rings, and a gold film gives a series of rings corresponding to its cubic face-centred lattice. The indices of the innermost rings in the picture are 111, 200, 220, and a close pair 311 and 222 which are not resolved and appear in consequence as a broad ring.

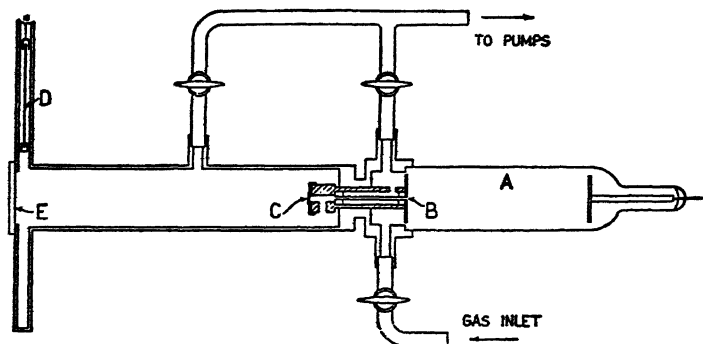


FIG. 148.—Apparatus for electron diffraction

(From *The Wave Mechanics of Free Electrons*, G. P. Thomson; McGraw-Hill, 1930; by courtesy of the University of Cornell)

If a magnetic field is applied which deflects the central spot the ring pattern moves with it. This proves that it is formed by electron beams, and the equal displacement of the central spot and of the rings shows that the pattern is formed by electrons which have not lost velocity in traversing the film. A certain proportion of the electrons do lose velocity owing to inelastic collisions, and a drawn-out 'tail' extends from the deflected central spot owing to the greater deflection in the magnetic field of the slower electrons.

Thomson further showed that the wave-length of the electron waves, calculated from the diameters of the rings and the known grating spacings of gold, platinum, and aluminium, was in agreement with the equation  $\lambda = h/mv$ . The potential was measured by means of a spark gap between 4 cm. aluminium spheres. The velocity of the electrons is calculated by the relation  $eV = \frac{1}{2}mv^2$ . The agreement is best shown by comparing the edge  $a_w$  of the unit cube as calculated from the dimensions of the rings with the value of  $a_w$  determined by X-rays.



*Size of Unit Cube  $a_0$  (G. P. THOMSON)*

Metal	X-rays	Cathode rays
Aluminium . . .	$4.046 \times 10^{-8}$	$4.03 \times 10^{-8}$
Gold . . . . .	$4.06 \times 10^{-8}$	$4.09 \times 10^{-8}$
Platinum . . . .	$3.91 \times 10^{-8}$	$3.89 \times 10^{-8}$
Lead . . . . .	$4.92 \times 10^{-8}$	$4.99 \times 10^{-8}$

The film traversed by the electron beam must be very thin. Theory shows that interference only takes place between the diffracted beams which correspond to perfectly elastic collisions in which the electrons lose no velocity. As the thickness of the film is increased, the probability of electrons undergoing an inelastic collision becomes high; the rings then show up faintly against a dense continuous background of inelastically scattered electrons or disappear altogether. The thickness which gives the best results lies between  $10^{-5}$  and  $10^{-6}$  cm. The preparation of such thin films demands a special technique, and various ways of obtaining the crystalline matter in the most suitable form have been devised. Examples are shown in fig. 150, Pl. XXVI, p. 258.

#### THE EXPERIMENTS OF DAVISSON AND GERMER

The apparatus used by Davisson and Germer is shown in fig. 151. G is the 'electron gun,' by means of which electrons with velocities between 65 and 600 volts were projected upon the target T. T was a single nickel crystal, cut so that a face (111) was normal to the electron beam. The diffracted electrons are received in a Faraday cylinder C connected to a galvanometer. The crystal face could be rotated through  $360^\circ$  in its own plane by the plunger P, which engaged a toothed wheel, and C could be swung round an arc by tilting the apparatus. The whole was enclosed in a highly evacuated vessel.

The effects which were obtained were more complex than those of G. P. Thomson's experiments, but were equally indicative of electron diffraction. Instead of a general scattering in all directions, it was found that the electrons were scattered most strongly in definite directions which were related to the symmetry of the crystal. There are three variables in the experiment, these being the potential applied to the electron gun, the

PLATE XXV



A. Celluloid

B. Gold

FIG. 149.—Early diffraction patterns obtained by G. P. Thomson

(From *Wave Mechanics of Free Electrons*, G. P. Thomson; McGraw-Hill, 1930;  
by courtesy of the University of Cornell)

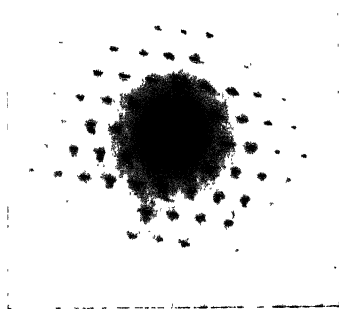


FIG. 156.—A Kikuchi N pattern, given by mica (Trillat)



'azimuth' or setting of the crystal face, and the 'colatitude' or position of the collector.

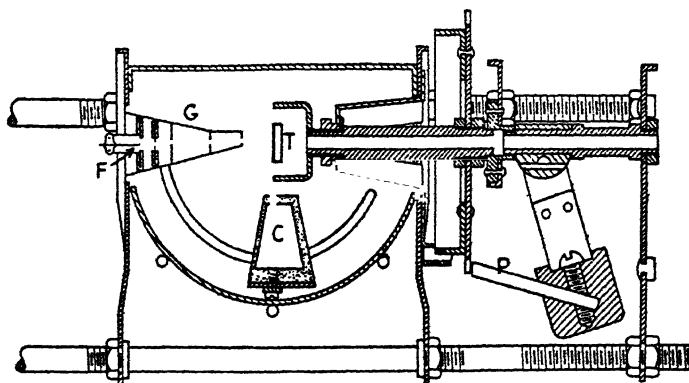


FIG. 151.—Apparatus for electron diffraction (Davisson and Germer)

(*Bell Tel. Lab.*, 4th January 1928)

The atomic arrangement of the crystal face (111) is shown in fig. 152, nickel having a face-centred cubic structure. In one

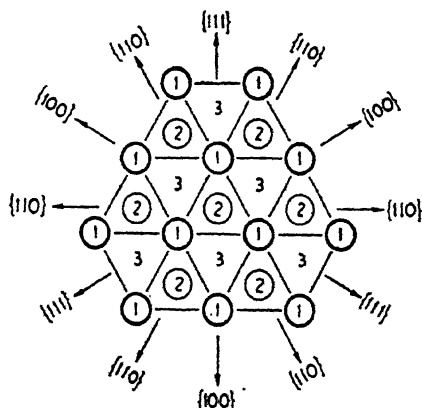


FIG. 152.—Arrangement of atoms and designation of azimuths, (111) face of nickel. Atoms 1, 2, 3 are on successive layers (Davisson and Germer)

(*Bell Tel. Lab.*, 8th January 1928)

series of experiments, the apex of the triangle pointed towards the arc in which the collector swung, this position being termed azimuth A (111). A curve is plotted showing the number of

electrons collected at various settings of the collector, the voltage being kept at some constant value. Similar curves for other voltages are drawn (fig. 153), the effect being plotted radially for each angular setting of the collector. With certain voltages a 'spur' develops on the curve. If now the voltage and position of the collector are kept fixed at values corresponding to the largest spur, and the crystal is rotated in azimuth, the curve at the bottom of fig. 153 is obtained. The spur appears three times

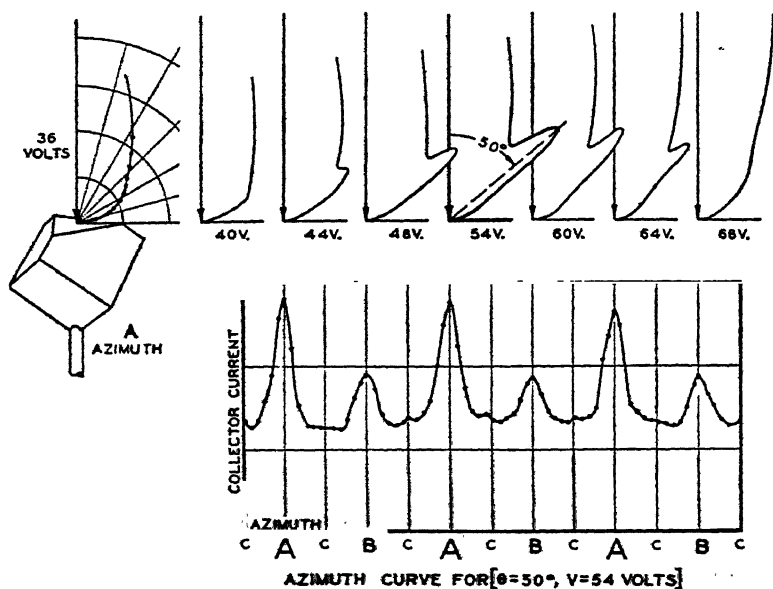


FIG. 153.—Curves showing development of diffracted beam in the A azimuth (above) and variation of intensity as the crystal is rotated (below) (Davisson and Germer)

(Bell Tel. Lab., 6th February 1928)

in a complete rotation, corresponding to the threefold symmetry of the crystal. Subordinate maxima occur at intermediate positions.

The conditions for reinforcement of the scattered waves in one of the special positions, such as the azimuth (100), may be considered as depending upon two factors. In the first place, the rows of atoms in the upper sheet act like a line grating, and the waves from successive lines must be in phase. Since the incident waves fall normally on the face, the condition is

$$n\lambda = b \sin \phi,$$

where  $b$  is the spacing of the lines. This relation enables a check to be made upon the relation  $\lambda = h/mv$ . It was found, for instance, that the 54-volt peak in fig. 153 was a first-order spectrum of the electrons diffracted by the atomic rows, the wave-length in this case being 1.67 Å. Naturally this diffracted beam is strongest in azimuth A, when the rows of atoms are at right angles to the diffracted beam.

If this were the sole condition to be satisfied, a spur should appear at an appropriate angle for any arbitrary voltage. Actually it only appears for a certain small range of voltage owing to the existence of a second condition, the reinforcement of the waves from the uppermost plane by those from lower planes. The electrons only penetrate a few planes in depth, and the condition is not precise. The effect is complicated by the existence of a 'refractive index' due to the inner potential of the metal, which is important in the case of such slow electrons. It will be clear, however, that both voltage and colatitude are fixed by the necessity of satisfying both conditions, and this corresponds to the result of experiment.

#### THE WAVE-LENGTH OF THE ELECTRON BEAM —

The wave-length of a beam of electrons which have all acquired the same velocity owing to a constant potential applied to the discharge tube is given by the equation  $\lambda = h/mv$ . The velocity of the electron is most conveniently expressed in terms of the potential  $P$  applied to the tube,  $P$  being measured in volts.

$$\frac{1}{2}mv^2 = eV = eP/300,$$

whence

$$\lambda = h/mv = h\sqrt{\frac{150}{ePm}}.$$

To within the order of accuracy with which  $h$ ,  $e$ ,  $m$  are known,

$$h/\sqrt{em} = 10^{-8}.$$

Thus

$$\lambda = \sqrt{\frac{150}{P}} \times 10^{-8} \text{ cm.} = \sqrt{\frac{150}{P}} \text{ Å.}$$

A more accurate expression takes account of the relativity correction, which is appreciable when potentials higher than 10,000 volts

are used. Thomson gives the corrected formula in the form

$$\lambda = h \sqrt{150 / e P m_0} / (1 + e P / 1200 m_0 c^2).$$

Wave-lengths corresponding to potentials between 10,000 and 80,000 are given below :

P	$\lambda \times 10^8$	P	$\lambda \times 10^8$
10,000	0.1227	50,000	0.0536
20,000	0.0858	60,000	0.0487
30,000	0.0697	70,000	0.0447
40,000	0.0601	80,000	0.0417

These wave-lengths are ten to twenty times as short as the wave-lengths of X-rays ordinarily used in crystal analysis (cp.  $\text{CuK}\alpha$  1.54 Å.,  $\text{MoK}\alpha$  0.710 Å.). The angles through which the waves are diffracted by crystal planes are therefore much smaller. The powder photographs shown in figs. 149 and 150 are included within an angular range of a few degrees, and it is necessary to have a considerable distance between specimen and plate or fluorescent screen in order that the haloes may be resolved.

### THE ATOMIC SCATTERING FACTOR FOR ELECTRON WAVES

In the case of X-rays we have seen that there is a typical curve for each atom, the  $f$  curve, which describes the amplitude of the wave diffracted by the atom in a direction making an angle  $2\theta$  with the primary beam. The  $f$  curve is given by the relation

$$f = \int_0^\infty U(r) \cdot \frac{\sin\left(\frac{4\pi r \sin \theta}{\lambda}\right)}{\frac{4\pi r \sin \theta}{\lambda}} dr,$$

where  $U(r)$  is the number of electrons between  $r$  and  $r+dr$ , so that

$$\int_0^\infty U(r) dr = Z,$$

the total number of electrons in the atom.

When X-rays of unit amplitude fall on an atom, the scattered wave at a distance  $r$  has an amplitude

$$\frac{1}{r} \cdot \frac{e^2}{mc^2} \cdot f,$$

where  $f$  is a function of  $(\sin \theta)/\lambda$ , as described in Chapter IX.

The corresponding formula for electron diffraction, which was first calculated by Born, may be compared directly with that for X-ray scattering if expressed in the convenient form due to Mott. If the incident electron beam is assigned unit amplitude, the scattered wave at a distance  $r$  from the atom has an amplitude,

$$\frac{1}{r} \cdot \frac{e^2}{2mv^2} (Z-f) \frac{1}{\sin^2 \theta},$$

where  $v$  is the velocity of the electrons.

The appearance of  $Z-f$ , instead of  $f$ , in the formula is due to the effect of the nucleus with its positive charge  $Ze$ , which acts in a contrary sense to the surrounding electron atmosphere. At very small angles of scattering by the neutral atom both  $Z-f$  and  $\sin^2 \theta$  tend to zero, but it can be shown that the complete expression tends to a finite value. It can also be expressed in a form which shows that it is a function of  $(\sin \theta)/\lambda$ , like the expression for  $f$ . Since  $\lambda = h/mv$ ,

$$\frac{1}{r} \frac{e^2}{2mv^2} \cdot (Z-f) \frac{1}{\sin^2 \theta} = \frac{1}{r} \cdot \frac{e^2 m}{2h^2} \cdot (Z-f) \frac{\lambda^2}{\sin^2 \theta}.$$

The curve in which  $(Z-f)\lambda^2/\sin^2 \theta$  is plotted against  $(\sin \theta)/\lambda$  has been termed the 'E' curve,\* by analogy with the  $f$  curve.

\* A convention for the definition of E has not yet been generally adopted. Mott has used

$$E(\theta) = \frac{\lambda^2(Z-f)}{16\pi^2 \sin^2 \theta}.$$

In theoretical papers, the notation  $f(\theta)$  has been used, where  $\theta$  is the angle of scattering, and so equal to twice the angle in the above formula. This is undesirable, because  $f$  has been so widely adopted for the expression which appears in X-ray scattering. Since E cannot be expressed conveniently in a dimensionless form, a possible solution is to employ the complete expression for scattering at unit distances,

$$E(\theta) = \frac{e^2}{2mv^2} (Z-f) \cdot \frac{1}{\sin^2 \theta} = \frac{e^2 m}{2h^2} \cdot (Z-f) \frac{\lambda^2}{\sin^2 \theta},$$

which is plotted in fig. 154. In cases where relative values of E are alone required, the expression

$$E' = (Z-f) \left( \frac{\lambda \times 10^8}{\sin \theta} \right)^2$$

is convenient, since it is readily calculated and leads to numbers of convenient magnitude.

If a beam containing  $N$  electrons per square centimetre falls upon an atom, the number scattered in a solid angle  $d\omega$  is  $N(E(\theta))^2 d\omega$ .



This convenient definition of  $E$  has been used by Mott and Thomson. It should be noted, however, that  $E$  is not dimensionless like  $f$ .

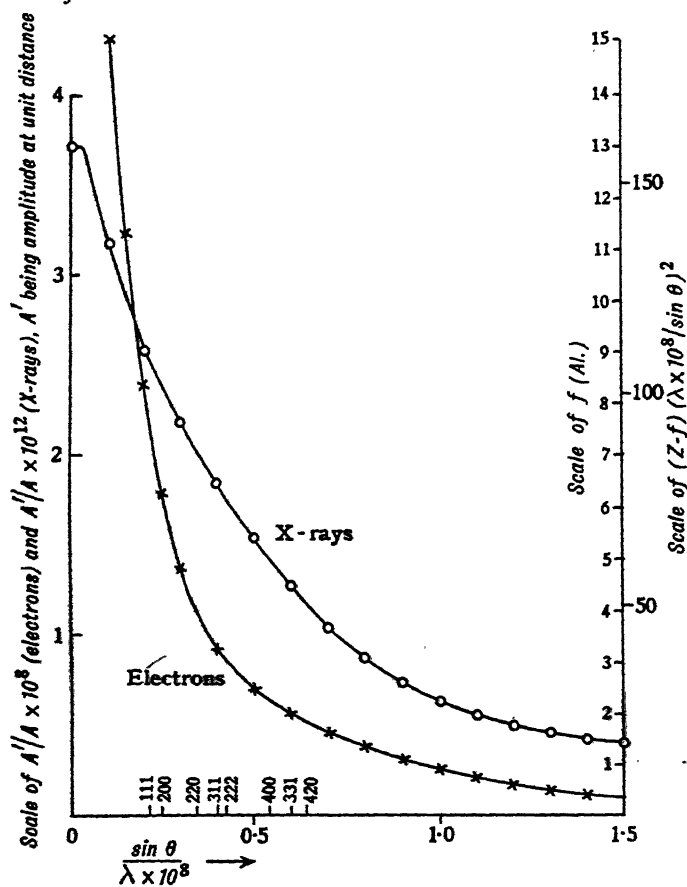


FIG. 154.—A comparison of the scattering of X-rays and of electrons by aluminium

On substitution of the values of the constant, the formulæ for electron scattering and X-ray scattering become:

$$\text{Electrons} \quad A'/A = \frac{1}{r} \cdot 2.38 \times 10^{-10} (Z - f) \cdot \left( \frac{\lambda \times 10^8}{\sin \theta} \right)^2,$$

$$\text{X-rays} \quad A'/A = \frac{1}{r} \cdot 2.82 \times 10^{-13} \cdot f,$$

where  $A$  is the amplitude of the incident wave and  $A'$  that of the

scattered wave at distance  $r$ . It is important to note how much more efficiently the atoms scatter electrons than X-rays, for the characteristics of electron diffraction are largely due to the difference.

The difference is illustrated by the curves for aluminium shown in fig. 154. The abscissæ are values of  $\frac{\sin \theta}{\lambda \times 10^8}$ ; it will be remembered that a given crystal reflection occurs at the same value of  $(\sin \theta)/\lambda$  whatever the wave-length, so that this is a convenient scale for both curves. The points at which reflections

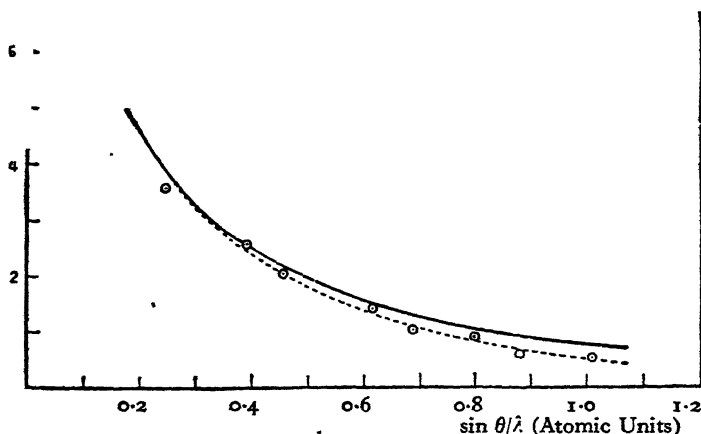


FIG. 155.—Comparison of experimental and theoretical  $E$  curves for gold (G. P. Thomson and Mott)

(From *The Wave Mechanics of Free Electrons*, G. P. Thomson; McGraw-Hill, 1930; by courtesy of the University of Cornell)

from the Al crystal (face-centred cubic) occur are marked. The scale of ordinates is such that values of  $A'/A$  for electron and X-ray scattering, at unit distance from the atom, can be compared. The ordinates for electron scattering have to be reduced by a factor of  $10^{-4}$  in order to bring them on to the same scale as the ordinates for X-ray scattering. Owing to this enormously greater efficiency of the atom in scattering electrons, a minute speck of crystal is sufficient to give diffraction effects.

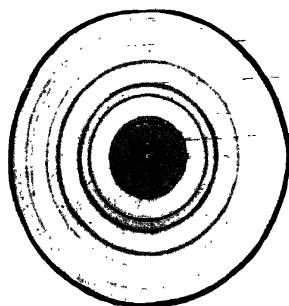
The scales of ordinates on the right of the graph enable the  $f$  values and  $E$  values to be read. The  $E$  curves for other atoms can be calculated from their  $f$  curves, and they have similar characteristics, falling rapidly as  $(\sin \theta)/\lambda$  increases.

The above formula for electron scattering only applies when the kinetic energy of the electron is large compared with its

(FIG. 150)

- A. The thin film of silver was prepared by a method due to Rupp. The metal is deposited from the vapour in a high vacuum upon a highly polished plate of rock-salt, the rock-salt is dissolved in water, and the film is caught upon a brass sheet pierced with a hole, over which it is mounted.
- B. The film of zinc oxide is made by melting zinc, and slowly withdrawing from the melt a wire loop on which a sheet of zinc and zinc oxide forms. This sheet contains transparent patches, which consist of extremely thin films of oxide.
- C, D. The substances are vaporised upon thin celluloid or collodion sheets *in vacuo*. This process may be carried out in a separate apparatus, or in the diffraction apparatus itself. In C the  $\text{CdI}_2$  crystals deposit with the (001) axis normal to the collodion sheet. Hence only the planes around this zone reflect, and the powder photograph shows 'correspondingly few lines.
- E. The film of copper oxide is formed by passing a copper sheet through a flame, and it is separated from the metal by making the latter the anode in an electrolytic cell, when it peels off.
- F. The bismuth is deposited from vapour on a collodion sheet, which is then inclined to the electron beam so that the preferred orientation of the crystals around the normal to the sheet introduces asymmetry into the haloes.

PLATE XXVI



B. Zinc oxide

(Bragg and Darbyshire)

(*Trans. Far. Soc.*, 133, vol. xxviii, 1932)

A. Silver. 36 kV electrons  
Exposure  $\frac{1}{8}$  second (Mark and Wierl)

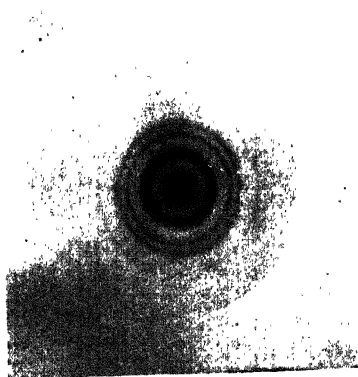
(*Zeit. f. Physik*, 60, 743, 1930)

C. Cadmium iodide,  $\text{CdI}_2$  (Kirchner)

(*Zeit. f. Physik*, 76, 580, 1932)

D. Mercurous chloride,  $\text{Hg}_2\text{Cl}_2$  (Kirchner)

(*Zeit. f. Physik*, 76, 590, 1932)



E. Cuprous oxide,  $\text{Cu}_2\text{O}$  (Darbyshire)



F. Bismuth (Kirchner)

FIG. 150



potential energy when in the atomic field. This condition is sufficiently satisfied for fast electrons, even for the heavier atoms, for it is only in the neighbourhood of the nucleus and K ring that it breaks down. Tests by Mott, G. P. Thomson, and Mark and Wierl have shown that theory and experiment are in good accord. In fig. 155, the experimental points are relative values of  $E$  deduced by G. P. Thomson from measurements of haloes given by gold, and the dotted curve is a theoretical  $E$  curve calculated by Mott's formulæ, allowing for the heat motion of the gold atoms; the agreement is good. Mark and Wierl have obtained similar results with films of aluminium and silver.

### DIFFRACTION BY SINGLE CRYSTALS

Certain phenomena occur in electron diffraction which have no counterpart in the case of X-rays. When a monochromatic X-ray beam falls on a single crystal, the crystal must be set at an appropriate angle in order that any given reflection may appear. The diffracted beams flash out one by one as the crystal is turned through the correct setting for each. On the other hand, an electron beam falling on a small single crystal may give rise to an extended pattern of diffracted beams, which appear on the photographic plate like the spectra of a 'crossed grating' in optics.

The first photographs of this type were obtained by Kikuchi with thin sheets of mica ( $10^{-5}$  to  $10^{-6}$  cm. thick). The photograph (fig. 156, Pl. XXV, p. 250) shows a pattern of spots arranged at the corners of equilateral triangles. The cleavage plane of mica is parallel to the (001) face of the monoclinic crystal, and contains points of the space-lattice which are arranged almost exactly at the corners of equilateral triangles, the basal plane being face-centred. Kikuchi showed that the positions of the spots on the plate correspond to diffraction by a two-dimensional crossed grating of this form, as if interference were only taking place between electron waves scattered by a single sheet of lattice-points in the crystal. Fig. 157, C and D, Pl. XXVII, p. 260, kindly supplied by M. Trillat, shows a very regular example of the 'N' pattern, as it was termed by Kikuchi. Similar effects have been obtained in other ways. Fig. 157, Pl. XXVII, shows: A, a pattern obtained by Kirchner which is due to a crystal of unknown nature, and which appears when a thin sheet of collodion is in the path of the electron beam; B, a

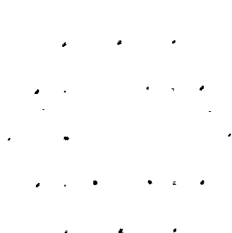
pattern obtained by G. P. Thomson when electrons fall at a small glancing angle upon the (100) surface of a copper crystal; C, a pattern due to Trillat obtained with a small single crystal in a gold leaf; and D, a similar pattern of platinum leaf obtained by the same investigator.

Though the effect appears at first sight to be due to the diffraction of waves by a two-dimensional crossed grating and not the three-dimensional grating of the crystal pattern, there can be no doubt that a three-dimensional crystal is causing it. The spacings deduced from the position of the spots are precisely those of the three-dimensional crystal as found by X-rays, and this could not be the case if we were dealing with monomolecular sheets. The apparent two-dimensional effect must be ascribed to the very small angle at which electron diffraction takes place, and to the very efficient scattering of the electron beam by the atoms so that a few atomic planes suffice to build up a powerful diffracted beam. The effect may be explained in several ways, and it is probable that more than one cause is operative in typical cases.

#### DISTORTION OF THE SMALL CRYSTAL

Let us suppose that a small crystal is set so that a zone axis is nearly parallel to the electron beam. There will be a number of crystal planes parallel to this zone axis, and if the crystal is viewed along the axis these planes will be seen on edge, and will resemble the lines, or two-dimensional pattern, of a crossed grating. Each plane can reflect the electrons if the angle of incidence is appropriate. These angles are very small, varying from a fraction of a degree to a few degrees for fast electrons. If, therefore, the crystal is slightly distorted so that the zone-axis direction varies from point to point in it, reflection at all the planes around the zone will be possible at one point or another of the crystal. Trillat has advanced convincing arguments to show that this distortion is the cause of such patterns as that in fig. 157, C. The gold crystal is in a hammered sheet, and the process of hammering orients the small crystals so that an axis [100] is perpendicular to the plane of the sheet. The spreading of the spots along arcs shows that one is not dealing with a perfect single crystal, but with a mass of nearly parallel crystals which are derived from a single crystal distorted by the hammering. The distortion also tilts the crystal in slightly different directions

# PLATE XXVII



A. Single crystal on collodion sheet (Kirchner)  
(*Natura.*, 22, 463, 1931)



B. Single crystal of copper (G. P. Thomson)  
(*Proc. Roy. Soc., A*, 133, pl. i, fig. 2, 1931)



C. Single crystal in beaten gold sheet,  $[100]$  parallel to beam (Trillat)



D. Single crystal in beaten platinum sheet,  $[110]$  parallel to beam (Trillat)

FIG. 157





from the normal, so that planes around a zone [100] are set so as to reflect. The cross-grating pattern is the result.

An explanation of Kikuchi's mica patterns along these lines was put forward in 1929 by W. L. Bragg, but it is not certain whether the distortion of the mica is responsible in this case or whether the pattern is due to other causes described below.

### DIFFRACTION BY A SMALL CRYSTAL

Let us suppose again that a zone axis of the crystal is parallel to the electron beam and that the crystal is so small that only a limited number of lattice-points lie on the axis. The crystal may be considered as a number of these rows side by side, their centres lying on a cross-grating (fig. 158). The conditions for interference depend upon two factors. The first is responsible for the cross-grating effect, and is the condition that the waves coming from atoms in a single horizontal sheet reinforce each other. This condition determines the possible positions of spots on the plate. The second factor depends upon the reinforcement of waves coming from the points in a vertical row, and the spots will be strong when it is large and weak when it is small. Now it is easy to see that the phase difference between successive points in a row is extremely small, and in fact the whole phase difference between the first and last points of the row may be so small as to be negligible; in that case the whole row will act as a single scattering unit, and we shall get the whole of the cross-grating pattern. To take an example, let us suppose the spacing  $d$  of the points in a vertical row to be 4 Å. and the angle  $\phi$  (fig. 158, *b*) to be  $2^\circ$ . The path difference for waves from successive atoms is  $d\phi^2/2$ , which in this case is 0.0024 Å., or  $\lambda/20$  for 60,000-volt electrons. The crystal may be twenty planes thick and yet act as a two-dimensional grating. An equal breadth of the crystal, so that there are a corresponding number of elements each way in the cross-grating, will give sharp spots, and therefore a little three-dimensional crystal acts as a two-dimensional grating. As the crystal is turned the two-dimensional pattern flashes out when any important zone comes parallel to the electron beam, the pattern always corresponding to the projection of the crystal on the plane normal to the incident beam.

In coarse powder photographs showing spots due to individual crystals the spots often appear as pairs on opposite sides of the centre.

They are then due to a setting of some small crystal such that one of its planes is parallel to the electron beam. Its projection is then a line grating, and a row of orders appears on each side.

Very beautiful effects, first obtained by Kikuchi, appear when

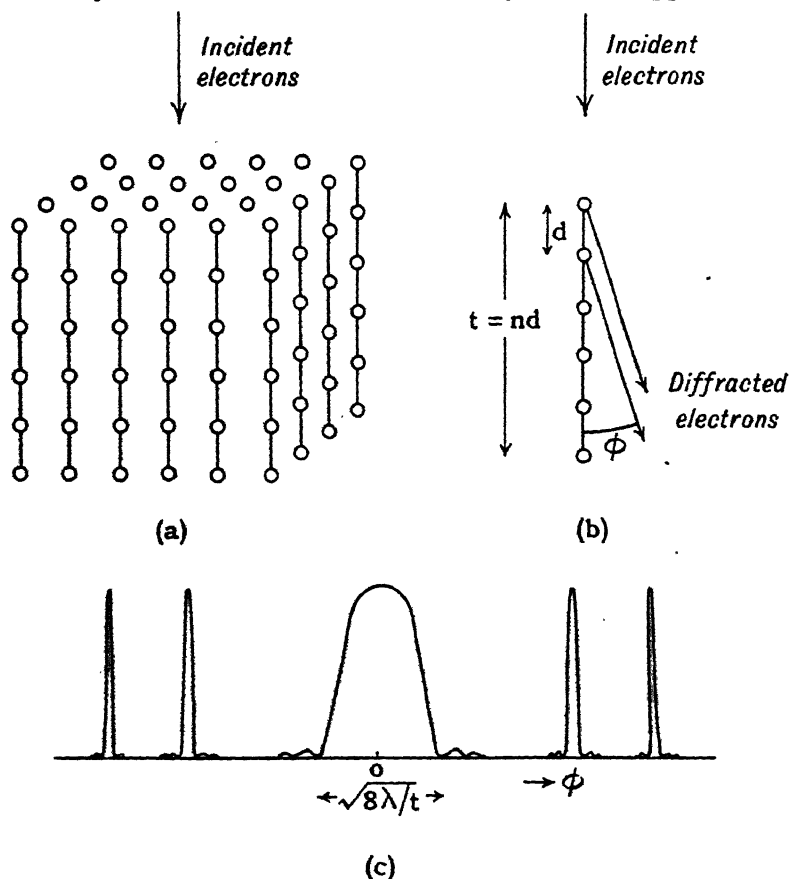


FIG. 158.—Electron diffraction by a small crystal

the crystal is somewhat thicker, so that the factor for reinforcement by atoms of a row becomes important. This factor is plotted in fig. 158 (c). There is a broad central maximum of zero order inside which the whole row scatters waves which are nearly in phase. This is surrounded by a series of narrowing rings for which the path difference from successive points in a row is  $\lambda$ ,  $2\lambda$ ,  $3\lambda$ , etc. Only such cross-grating spots as are inside one of the peaks can be strong, for their intensities depend upon both



PLATE XXVIII



A. Mica, zone axis inclined to electron beam (Kikuchi)  
(*Japanese Journal of Physics*, v, 2, 1928)



B. Mica, zone axis parallel to electron beam (Kirchner)

FIG. 159

(P. 263)

factors. The effect is well shown in the mica photograph of fig. 159, B, Pl. XXVIII, due to Kirchner. If the zone axis is inclined to the beam, the factor gives a series of broad circular fringes with the zero order passing through the central spot (fig. 159, A). These fringes are analogous to those obtained with Fabry-Perot plates.

#### INTERACTION BETWEEN THE INCIDENT AND DIFFRACTED BEAMS

So far the diffraction effect has been treated as if it were due to a simple conversion of a primary beam sweeping through the crystal into a series of diffracted beams. A numerical calculation shows, however, that this treatment is too elementary.

If a beam of amplitude  $A$  falls normally upon a single sheet containing  $N$  atoms per sq. cm., the diffracted wave has an amplitude  $A' = NE\lambda A$ . This follows from the construction of Fresnel zones, and a substitution of numerical values shows that  $NE\lambda$  is of the order of several parts in one hundred. The simple treatment would therefore indicate that, after traversing a small number of atomic planes whose effects add together directly, the diffracted beams surpass the incident beam in amplitude. This impossible result is due to neglecting the interaction between primary and diffracted beams. In reality there must be a continuous give-and-take between them, each being converted into the other as the crystal is traversed by the waves. Though this complicated effect has not been analysed in detail, it is clear that there must be a whole series of interdependent beams at any stage of the passage of the electrons through the crystal. Even a thick crystal cannot give merely a primary and single diffracted beam as is the case of X-rays, for the last few sheets of the crystal would suffice to turn each of these beams into a multitude of diffracted beams. Though the appearance of single crystal photographs can be explained in a qualitative way, a more accurate investigation is difficult owing to the last effect.

Many other examples of diffraction by single crystals might be given from the work of Kikuchi, G. P. Thomson, Kirchner, Trillat, Rupp, and others. It is possible to see that a number of factors conspire to produce the cross-grating pattern, and it is not surprising that it so frequently turns up in electron-diffraction investigations though the explanation of its origin is often incomplete.

## THE KIKUCHI 'P' PATTERN

Another effect observed by Kikuchi can be seen in fig. 160, A, Pl. XXIX. Black and white lines stretch across the plate, and these lines are related in position to crystal planes in the mica. They occur in pairs, and analysis shows that a plane of the mica lattice with low indices would, if projected, cut the plate midway between a black and white line. The explanation given by Kikuchi is that the lines are due to electrons which have been scattered in the mica and then reflected by the crystal planes. The dark line is formed by reflected electrons which would otherwise have met the plate on the accompanying white line. A similar effect is seen in fig. 160, B, Pl. XXIX, kindly supplied by Dr Kirchner. The electron beam is reflected from the cleavage face of rock-salt, and Kikuchi lines are well marked in addition to the cross-grating pattern.

## ELECTRON DIFFRACTION BY THE MOLECULES OF A GAS

Mark and Wierl have applied electron diffraction to the study of the structure of gaseous molecules. Their apparatus is shown in fig. 161. The success of the method is due to the high efficiency of molecules in scattering the electron waves. A jet of rarefied gas issues from D, traverses the electron beam issuing

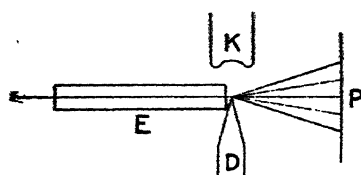


FIG. 161.—Electron diffraction by gaseous molecules (Mark and Wierl)  
(*Leipziger Vorträge*, 1930; Verlag Hirzel)

through E, and is condensed on K, which is cooled by liquid air, so that the space between the jet and the photographic plate P remains highly evacuated. The electrons are diffracted by the molecules in the jet, and a pattern of haloes is formed on P. In this case the interfering beams come from

the atoms of a single molecule, and owing to their limited number the haloes are very broad. Typical photographs are shown in fig. 162, Pl. XXX, p. 266.

The appropriate formula for such interference effects has been calculated by Debye and has already been discussed in Chapter VIII. The simplest case is that of molecules each consisting of two atoms  $a$  and  $b$  a distance  $l$  apart. The intensity of the waves scattered through an angle  $2\theta$  by a number of molecules, with all

PLATE XXIX

21



A. 'P' pattern of mica (Kikuchi)  
(*Japanese Journal of Physics*, 7, 2, 1928)

B. 'P' pattern of rock-salt (Kirchner)  
FIG. 160





possible orientations, will then be proportional to

$$E_a^2 + E_b^2 + 2E_a E_b \frac{\sin x_{ab}}{x_{ab}},$$

where

$$x_{ab} = \frac{4\pi l \sin \theta}{\lambda}.$$

The corresponding expression for a complicated molecule consisting of  $n$  atoms is

$$\sum_1^n \sum_1^n E_a E_b \frac{\sin x_{ab}}{x_{ab}}.$$

The photographs show the diffraction rings due to carbon tetrachloride,  $\text{CCl}_4$ . In this case the central carbon atom can almost be neglected in comparison with the heavier chlorine atoms, and since the latter are arranged at the corners of a tetrahedron all distances  $l_{ab}$  are alike. The haloes have therefore a simple gradation of intensity, and their maxima and minima correspond to those of the expression  $\frac{\sin x_{ab}}{x_{ab}}$ . Several successive haloes are

evident, and their scale makes it possible to deduce the distance between the Cl atoms in the  $\text{CCl}_4$  group. Wierl has measured the distance for a series of tetrahedral groups, and compared them with distances deduced from X-ray data.

	$\text{CCl}_4$	$\text{SiCl}_4$	$\text{GeCl}_4$	$\text{TiCl}_4$	$\text{SnCl}_4$
Measured ( $\pm 0.03$ A.)	2.97	3.28	3.45	3.76	3.92
According to Goldschmidt	2.96	3.28	3.34	3.60	3.90

Wierl has applied the method to more complex organic molecules. For instance, he has attempted to measure the distance between carbon atoms in the benzene ring,  $\text{C}_6\text{H}_6$ , and to compare it with the distance in cyclopentane,  $\text{C}_5\text{H}_{10}$ , where the carbon atoms are united by single bonds. The appropriate formulæ are:

$$\text{Benzene, } I \propto 6E_c^2 \left( 1 + 2 \frac{\sin x}{x} + 2 \frac{\sin \sqrt{3}x}{\sqrt{3}x} + \frac{\sin 2x}{2x} \right).$$

$$\text{Cyclopentane, } I \propto 5E_c^2 \left( 1 + 2 \frac{\sin x}{x} + 2 \frac{\sin (\sqrt{5}+1)x/2}{(\sqrt{5}+1)x/2} \right).$$

The composition of the curve in the case of cyclopentane is shown in fig. 163. The heavy line represents the factor within the brackets, and the dotted line is obtained when this is multiplied by  $E_0^2$ . A comparison of the size of the observed rings with the theoretical maxima and minima gives the distance  $l$  between the

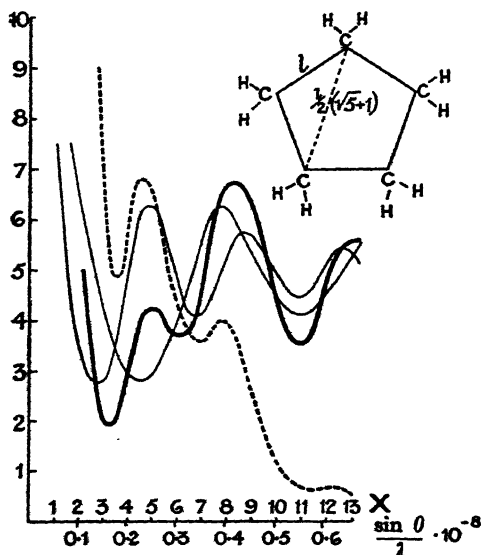


FIG. 163.—Theoretical distribution of intensity in diffraction haloes of cyclopentane (Wierl)

(*Leipziger Vorträge*, 1930; Verlag Hirzel)

carbon atoms. Wierl finds 1.4 Å. in benzene and 1.5 Å. in cyclopentane.

An interesting application of electron diffraction is exemplified by the attempt to find whether the single bond between carbon atoms allows of rotation. In 1,5-dichloropentane the chlorine atoms are attached to each end of the carbon chain. If the chain has a rigid form, the two chlorine atoms would give a series of haloes corresponding to a fixed distance apart shown in fig. 164. Since they are heavy in comparison with the carbon atoms, these haloes would stand out. If, on the other hand, free rotation about the single bond is possible, the chain may twist into a number of forms. The distance between chlorine atoms would then be variable, and on the average much less than in the figure. The haloes to be expected are widely different in the

PLATE XXX

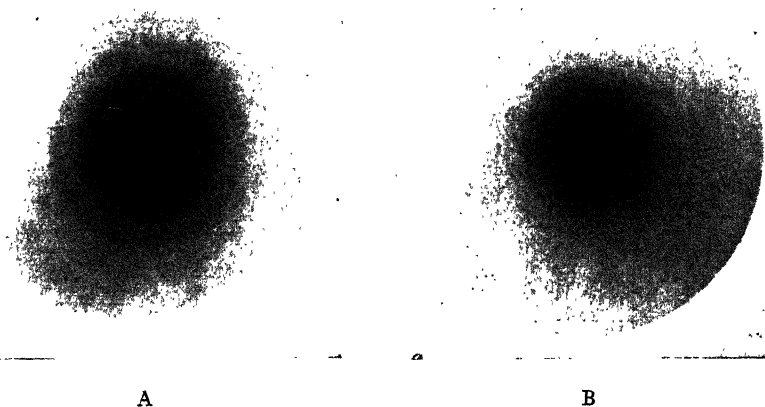


FIG. 162.—Electron diffraction by gaseous  $\text{CCl}_4$  (Mark and Wierl)

A. 36 kV electrons.

B. 60 kV electrons

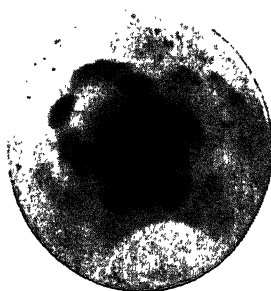


FIG. 166.—The first photograph of X-ray diffraction  
by a crystal

(*Naturw.*, 18, 365, 1922)



two cases, and the experimental evidence supports the idea of free rotation.

Electron diffraction by a gas is thus a powerful method of testing molecular models. A direct deduction of the structure from the haloes is hardly possible since they are so diffuse. It is necessary to proceed by assuming a molecular model, and comparing the calculated effect with that observed experimentally. In many cases an approximate model can be reasonably assumed,

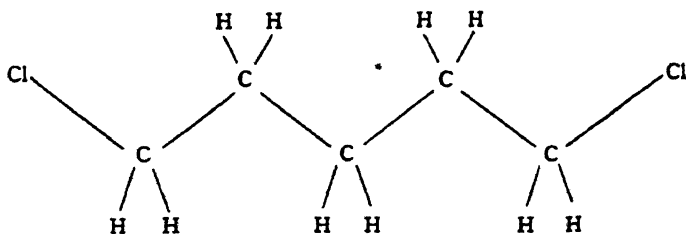


FIG. 164.—The 1,5 dichloropentane molecule

and the results then make it possible to choose between alternatives and to measure the scale of the structure. The results are so interesting because the molecule is studied when it is part of a gas and free from the influence of its neighbours, whereas in a crystal it may be distorted and artificially rigid.

Electron diffraction is a new method of analysis, and the exploration of its possibilities is in its initial stages. It is not yet possible to give as complete and logical an account as in the case of X-ray analysis, and in this chapter we have merely attempted to give typical illustrations of the interesting new effects.

## CHAPTER XII

### HISTORICAL

#### THE THEORY OF CRYSTAL STRUCTURE BEFORE THE DISCOVERY OF X-RAY DIFFRACTION

HAÛY'S *Essai d'une théorie sur la structure des cristaux* was published in 1784, and may be regarded as the foundation of the science of crystallography. He recognised that the different forms which a given crystalline substance assumes are based on a common underlying structure. He was led to this by the observation that a typical rhomb of calcite would be obtained by successive cleavages from any of the various forms of calcite crystal. He showed that all the faces of the calcite crystal could be reproduced by stacking together elementary cleavage rhombs in a regular way, as units of structure, the rhombs being supposed so small that the resulting face appeared smooth. He was thus led to formulate the 'law of rational indices,' as a consequence of the regular stepping of the units in the building of a crystal face. The conception of a regular arrangement of units in the calcite crystal had, indeed, been put forward by Huygens nearly 100 years before Haüy's *Essai*. In his *Treatise on Optics*, published in 1690, he pictured the crystal as composed of flattened spheroids, and so explained the rhombohedral cleavage. It is interesting to read in the *Treatise* that he determined the form of the calcite rhomb by measuring, not the more obvious angles between its edges, but the angles between neighbouring faces, which he observed to be a more accurate method. Huygens' chief interest lay, however, in the optical properties of the crystal, rather than in its form and structure.

In the work of Frankenheim and Bravais the problem assumed a more purely geometrical aspect. The idea of juxtaposed units of structure was replaced by that of an assembly of points. Frankenheim in 1842 concluded that there were fifteen different

symmetrical ways of arranging networks of points in space. Bravais in 1848 showed that two of them were identical, and divided the fourteen space-lattices into the seven systems in which all types of crystalline symmetry may be grouped. These fourteen space-lattices, however, only represented the seven holohedral types of symmetry, and did not account for the other known types. Actually, Hessel had shown in 1830 that as many as thirty-two classes of symmetry were possible for crystals based on space-lattices, but his work remained unnoticed till Sohnke recognised its significance sixty years later. Bravais accounted for the hemihedral types by assigning a lower symmetry to the units of structure situated at the points of the space-lattice, which he regarded as similarly oriented molecular groups.

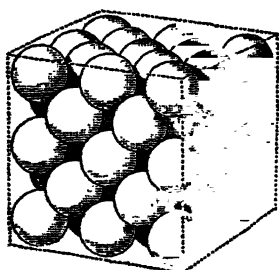
The next milestone is the work of Sohnke (*Entwicklung einer Theorie der Krystallstruktur*, 1879). Sohnke considered the number of symmetrical ways of arranging points in space, such that the environment around each point was precisely the same as that around any other point, but not necessarily similarly oriented as in the case of a space-lattice. This necessitated the introduction of screw axes as well as rotation axes. He showed that there are sixty-five such point-systems, whose symmetry is in correspondence with the majority of crystal classes. It is not possible to explain all the classes, however, by means of Sohnke's point-systems. In order to do this, units of structure must be introduced which are similar in every respect except that they are enantiomorphous, or bear to each other the relation of object and image in a mirror.

The further step of considering such units, and the new elements of symmetry which they imply, was made independently and almost simultaneously by Fedorov, Schoenflies, and Barlow. Reflection and glide planes of symmetry, axes of rotatory inversion, and centres of inversion are elements of symmetry of the second kind which relate the right-handed to the left-handed units. Their inclusion in the symmetry scheme raises the number of types to two hundred and thirty. Fedorov first established the existence of the two hundred and thirty space-groups during the years 1885-90, but his memoirs were in Russian and did not become generally known until after the publication of Schoenflies' work in 1891. Barlow published his results in 1894. The three authors attacked the problem from different view-points. Fedorov divided space into polyhedra,

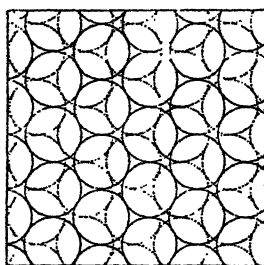


Schoenflies filled it with a system of groups of movements, and Barlow pictured the symmetry of the generalised three-dimensional 'pattern' or homogeneous structure composed of a repetition of similar units.

Speculations on the nature of the atomic arrangement which gives rise to the crystalline structures were made by many of

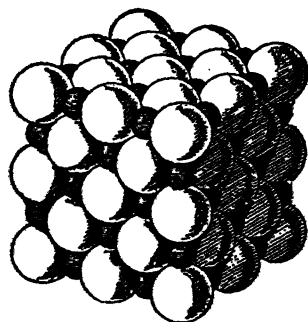


(a)

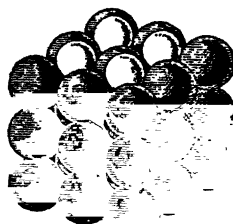


(b)

The packing of identical atoms



(c)



(d)

The packing of equal numbers of atoms of two kinds

FIG. 165.—Barlow's predictions of the structures of elements and simple binary compounds

(From *A Mechanical Cause of Homogeneity of Structure and Symmetry*, William Barlow; by permission of the Royal Dublin Society)

those who studied the geometrical laws. It is extremely interesting to read, now that the structures of crystals have been analysed, Barlow's paper in the *Proceedings of the Royal Dublin Society*, 1897, entitled "A Mechanical Cause of Homogeneity of Structure and Symmetry." Barlow pictured the atoms in the crystal as spheres which, under the influence of attractions and repulsions varying as a power of the interatomic distance, packed themselves together into as small a volume as

possible. He considered the arrangements which might arise when the spheres were of one, two, or more kinds, with various relationships in their sizes. In this way he arrived at a number of hypothetical structures which have since been discovered actually to exist. For instance, four of Barlow's figures are shown in fig. 165. He describes (a) and (b) as ways of packing when the atoms are all alike, and we recognise them as the cubic and hexagonal close-packed structures in which the majority of metals crystallise. The figures (c) and (d) are given as methods of packing two sets of atoms, equal in number but unequal in size. They are the NaCl and CsCl structures so common amongst the AX compounds. A later development by Pope and Barlow of this idea of packing spheres, the 'Valency Volume' theory, proved to be founded upon a fallacious principle. The author would like to take the opportunity, however, to acknowledge the inspiration he personally derived from Barlow's work. In the early days of crystal analysis it provided a rich store of symmetrical arrangements of all kinds, which one could explore when trying to explain the result of X-ray diffraction. In particular, one sees in many of Barlow's structures the absence of any molecular association, the very feature which the new X-ray results established.

A work of outstanding importance is Groth's *Chemische Krystallographie*. This record of the form, preparation, and physical properties of crystals has been the familiar book of reference to all workers on crystal structure, and its influence in the development of the new methods has been immense.

#### THE EARLY X-RAY INVESTIGATIONS

A fascinating account by Friedrich of the events which gave rise to Laue's discovery in 1912 will be found in *Naturwissenschaften* for April 1922. The conditions in Munich at that time were peculiarly favourable to the event which gave rise to a new branch of science. Laue himself was profoundly interested in interference phenomena, Sommerfeld in the nature of X-rays and their excitation by the stopping of cathode rays, and Groth was the world's most famous authority on crystallography. The actual incident which precipitated the discovery was a doctor's dissertation by Ewald. We may note here the great part which Ewald has played in all subsequent developments of X-ray

analysis. As an editor of the *Zeitschrift für Kristallographie* and of the *Strukturbericht*, he has come to occupy much the same high position of authority which Groth himself held in the older crystallography. At that time he had undertaken under Sommerfeld's guidance the study of the passage of light waves through a crystal space-lattice of scattering atoms. When discussing Ewald's problem, Laue was led to ask what would happen if the waves became so short that their wave-length was less than the inter-atomic distances in the crystal. He realised that spectra should be formed, and that waves so short as to be diffracted in this way would be X-rays. An informal discussion on the possibility of observing this phenomenon took place after one of the colloquium meetings, and Friedrich, who was then Sommerfeld's assistant, volunteered to carry out some experiments. After several failures, the photograph shown in fig. 166, Pl. XXX, p. 266, was obtained.\* Friedrich gives a vivid picture of his feelings when he saw it in the developing-dish.

At that time W. H. Bragg was one of the chief protagonists of the theory that X-rays were corpuscular and not undulatory in nature. He was led to this conception by a study of the ionisation effects of X-rays, which he concluded to be due entirely to electrons produced by the X-rays and not directly to the X-rays themselves. We now know through such experiments as Wilson's cloud-chamber photographs that this conclusion was correct; the appearance of the X-ray energy at isolated points is reconciled with the wave-nature of the rays by the quantum theory. At the time, however, it was logical to suppose that rays which could produce such effects must be corpuscular. The author, who had just then taken his degree at Cambridge, was naturally a staunch upholder of the parental theory. When Laue's results were published, and seemed to prove the wave-nature of X-rays, he tried various experiments to find an alternative explanation such as the production of the spots by electrons liberated in the crystal and travelling through channels in the structure. The conclusion that Laue was essentially correct was soon found to be inevitable, but at the same time it appeared that Laue's explanation of the details of his zincblende photographs was unnecessarily complicated. The author approached the problem with the idea that electromagnetic pulses, equivalent to 'white light' in the X-ray region, were *reflected* from the crystal planes.

\* *Sitzb. Math. phys. Klasse Bayer. Akad. Wiss. München*, p. 303, 1912.

This was suggested by the behaviour of the spots when the crystal was tilted, and by their shape. Analysis of the ZnS photographs \* then showed that its main features could be explained by supposing the atoms to be arranged in a face-centred cubic lattice, and not in a simple cubic lattice. An account of the results was given to the Cambridge Philosophical Society in November 1912. At the suggestion of C. T. R. Wilson, the author † tried the direct experiment of allowing a beam of X-rays to fall upon a mica sheet, mica being chosen because well-defined sheets of atoms parallel to the cleavage flakes were to be expected. A strong reflected beam, which followed alterations in its angle of incidence, was at once found. A great interest was taken in these experiments by Pope, Professor of Chemistry at Cambridge, who suggested experiments with KCl and NaCl. These were found to give even simpler Laue photographs ‡ than ZnS, and the structures of the crystals were deduced. These two structures were the first to be analysed.

In the meantime both W. H. Bragg,§ and Moseley and Darwin,|| made a test of the reflected beam with ionisation chamber and absorbing screens, in order to see if it had all the properties of the incident X-ray beam. This was found to be the case, and the Ionisation Spectrometer was the result of W. H. Bragg's experiments.¶ This instrument showed a new feature. In addition to the white radiation reflected over a wide range of angle, the peaks of the characteristic line spectrum appeared.

The discovery of the line spectrum had two results. In the first place, it made crystal analysis enormously more powerful. Its first success was the structure of diamond,\*\* which the author was engaged in trying to solve by means of its Laue photograph, and which was immediately solved by W. H. Bragg's measurements with the spectrometer. The author was able to work with the new apparatus during the summer of 1913, and so to use the results which the spectrometer gave. The structures of ZnS, FeS<sub>2</sub>, CaF<sub>2</sub>, CaCO<sub>3</sub> were the immediate result.††

In the second place, the wide scope of the earliest results in 1913 in the field of X-ray spectroscopy, partial and imperfect though they were, may perhaps be recalled.‡‡ The wave-lengths

\* *Proc. Camb. Phil. Soc.*, 17, 43, 1913. † *Nature*, 90, 410, 1912.

‡ *Proc. Roy. Soc.*, A, 89, 248, 1913. § *Nature*, 90, 572, 1913.

|| *Ibid.*, 90, 594, 1913. ¶ *Proc. Roy. Soc.*, A, 88, 428, 1913.

\*\* *Ibid.*, A, 89, 277, 1913. †† *Ibid.*, A, 89, 468, 1914.

‡‡ *Ibid.*, A, 89, 246, 1913; and A, 89, 430, 1914.

of the rays given by anticathodes of platinum, osmium, iridium, palladium, rhodium, copper, and nickel were all measured. Their absorption coefficients identified them with the K or L characteristic radiations of Barkla. Their energy quanta according to Planck's relationship could now be calculated, since the wave-lengths were known, and these were found to be in agreement with the cathode-ray energies necessary to excite the corresponding X-rays, which Whiddington had measured. The  $K\alpha$  and  $K\beta$  lines were discovered to be similar in the last four elements, and it was shown that their frequency was not quite proportional to the square of the atomic weight. This was indeed a first hint of the subsequent brilliant generalisations of Moseley,\* who by using an extended range of anticathodes was able to formulate the laws relating frequency to atomic number. The positions of the absorption edges were measured by using crystals containing various absorbing elements and noticing the effect on the spectra. The study of the absorption edges was further developed by de Broglie† at about this time. Siegbahn, who has since become the recognised leader in the field of X-ray spectroscopy, commenced his investigations into X-ray spectra in 1915.

Two theoretical contributions were made in 1913 and 1914, which were remarkable for the influence they had upon subsequent developments, and for their insight into essentials although the experimental work was in its initial stages. Debye in 1913‡ calculated the effect of thermal movements in weakening the spectra, and his predictions were afterwards verified by W. H. Bragg. Darwin,§ in two remarkable papers in the *Philosophical Magazine* in 1914, covered almost the whole ground of the theory of X-ray reflection. He gave the formula for what is now called the mosaic crystal, on which all intensity measurements are based. He also gave the formula for reflection from the perfect crystal, and discussed the conditions under which either formula is applicable. The latter formula was arrived at independently by Ewald some years later, Darwin's results being so much ahead of practical realisation at the time they were published that most X-ray investigators had forgotten their existence. The

\* *Phil. Mag.*, 26, 1024, 1913; and 27, 703, 1914.

† A series of papers in the *Comptes rendus* from 1914 onwards.

‡ *Verh. deut. phys. Gesell.*, 15, 678, 1913.

§ *Phil. Mag.*, 27, 315 and 675, 1914.

same was true for Darwin's proof of the existence of a refractive index and of the departure from the simple law of reflection, for which he gave formulæ in these original papers. The actual effect was observed by Stenström, and explained by Ewald, many years later.

In 1914 W. H. Bragg\* evolved a method of defining and measuring the intensity of reflection satisfactorily; he measured the Debye thermal effect, and observed the 'extinction' or extra absorption of X-rays when passing through a crystal at the reflecting angle. In 1915 he gave the elementary theory of the Fourier analysis of X-ray measurements in the Bakerian Lecture to the Royal Society.† The early history of the developments may be conveniently ended at this stage, since the War interrupted work in most laboratories.

#### THE DEVELOPMENT OF X-RAY TECHNIQUE

The two outstanding advances in experimental technique, apart from the methods of the Laue photograph and spectrometer which were used in the earliest researches, have been the methods of the powder photograph and the rotating crystal. The powder photographic method was devised by Debye and Scherrer in Zurich in 1916,‡ and independently a year later by Hull in America.§ It immensely increased the range of crystals which could be examined, since so many substances can only be obtained in a finely divided crystalline form. Its main applications have been to metals and alloys, and to the compounds of simple formula. The earliest powder photographs were crude as compared with modern examples, and perhaps Westgren has been responsible more than any other single worker for their improvement. Bradley has shown what high accuracy can be obtained in measurement of spacing, and what complex structures can be successfully analysed, by powder photographs treated in the right way. Recent powder photographs are remarkable both for the beauty of their appearance and the elegance of the methods used in analysing them.

The development of the rotating-crystal method was more gradual. Photographs in which a rotating crystal was used were

\* *Phil. Mag.*, 27, 881, 1914.

† *Phil. Trans. Roy. Soc.*, 215, 253, 1915.

‡ *Physikal. Zeit.*, 17, 277, 1916.

§ *Phys. Rev.*, 10, 661, 1917.

obtained by de Broglie in 1913.\* They showed both the main layer line and the subsidiary layer lines above and below. Seeman in 1919 † obtained a large number of simultaneous spectra by directing a convergent bundle of monochromatic X-rays upon a crystal. The first proposal to use the spectra given by a rotating crystal for purposes of crystal analysis appears, however, to have been made by Schiebold in 1919. Various papers by his pupils appeared in this and in subsequent years in which the space-groups of crystals were deduced, using the Niggli criteria for the presence or absence of reflections. In 1921 Polanyi ‡ obtained the first photographs of fibre structures, and showed that they were in principle identical with photographs of a single rotating crystal. With Weissenberg, he is responsible for the simple interpretation of the approximately horizontal rows of points which they called *Schichtlinien* or 'layer lines.'

The interpretation of rotation photographs is beset with pitfalls for the unwary. The method is responsible for more tragedies in the form of crystals wrongly analysed through mistakes in assigning the space-group than any other of the standard methods. A paper by Bernal in 1926,§ "On the Interpretation of X-ray Single Crystal Rotation Photographs," has had a great influence in introducing general and accurate methods of solution. In the type of camera introduced by Weissenberg || the difficulties of assigning indices to the lines are overcome by mechanical means.

Though the Laue method was used to analyse the first crystals it has not been widely adopted owing to its complexity. Its greatest exponent has been Wyckoff, who raised to a fine art the indexing of the photographs, the deduction of the space-group, and the determination of crystal parameters. From 1920 onwards he and his co-workers have analysed a series of crystals, generally characterised by a relatively small number of parameters, but of interesting and important types.

### SPACE-GROUP CRITERIA

We owe to Niggli the idea of a systematic deduction of the space-group by means of X-ray data. Niggli published in 1919

\* *Compt. rend.*, 157, 924 and 1413; 158, 177, 1913.

† *Physikal. Zeit.*, 20, 55 and 169, 1919.

‡ *Naturw.*, 9, 337, 1921; *Zeit. f. Physik*, 7, 149, 1921,

§ *Proc. Roy. Soc., A*, 113, 117, 1926.

|| *Zeit. f. Physik*, 23, 229, 1924.

the *Geometrische Kristallographie des Diskontinuums*.<sup>\*</sup> He described the positions of the symmetry elements in the 230 space-groups, and gave the co-ordinates of equivalent points in general and special positions. He proceeded to consider the spacings of the planes which give rise to X-ray reflection. His statement (p. 487) runs: "Since they (the relative spacings of the planes as deduced by X-rays) are different for almost every space-group of a given symmetry class, it must thus be possible when a relatively heavy atom is present in the most general position to determine the space group for a given type of crystal and crystal class." He showed that restrictions as to indices affecting all reflections determined whether the lattice were simple, face-centred, or body-centred, and that restrictions affecting certain classes of reflection were evidence of screw axes and glide planes. He also showed that Laue photographs, although they did not give spacings directly, could be used for space-group determination by a statistical survey of the indices of the spots and their dependence upon the short-wave limit of the white radiation. He gave a set of tables for use in assigning the correct space-group.

At the time when Niggli's book appeared, the crystals which had as yet been analysed were of extremely simple type. A general survey of space-groups was hardly necessary for their analysis, because the results could be justified on first principles. A complete outline may be found in the book, however, of all the methods which have since been used to determine space-groups.

Other space-group tables have been published by Wyckoff † in 1922, and Astbury and Yardley ‡ in 1924. Wyckoff from the first has been a staunch adherent of the view that in all crystal analysis a deduction of the space-group must precede any attempt to fix the atomic positions. In his book he confined himself to a description of the space-groups and lists of general and special positions, and did not tabulate the criteria for distinguishing between them by means of X-rays. These criteria were published by him in a series of separate papers, for cubic crystals in 1922, monoclinic and orthorhombic in 1925, hexagonal in

<sup>\*</sup> *Geometrische Kristallographie des Diskontinuums*, P. Niggli, Leipzig, 1919.

† *The Analytical Expression of the Results of the Theory of Space Groups*, R. W. G. Wyckoff, Carnegie Inst., Washington, Publ. No. 318, 1922.

‡ *Phil. Trans. Roy. Soc., A*, 224, 221, 1924.



1926, and tetragonal in 1927. Wyckoff's indexing of the special positions has been widely used in the description of the results of analysis.

The tables of Astbury and Yardley are based on precisely the same principles as those of Niggli. They were constructed, however, at a time when many organic crystals of low symmetry were being examined, and when routine methods of indexing reflections had become standardised. Their merit lies in their conciseness. The space-group criteria, expressed in a convenient form, occupy about twenty pages, and figures of all space-groups are given in twenty plates. In practice, condensed tables of this kind will probably be found sufficient by most X-ray workers. The difficulty of space-group determination is essentially experimental, and lies in lack of knowledge of crystal class and uncertainty in the indexing of the reflections. Given these data, the space-group is immediately deduced. The barest description of its nature or most simplified diagram is sufficient to indicate the position of all the symmetry elements and the special positions, and many workers who have had experience of analysis will find it possible to dispense with lengthy tables of these properties.

#### THE USE OF INTENSITY MEASUREMENTS IN ANALYSIS

Up till about 1924 the successes of X-ray analysis had all been confined to very simple crystals. In an attempt to extend its scope and to develop methods for crystals with any number of parameters, the author, with R. W. James and J. West, introduced measurements of absolute intensity as part of the routine of crystal analysis. For their interpretation it was necessary to know the scattering curves or  $f$  curves for all atoms. Hartree in Cambridge was at this time engaged in calculating the Bohr orbits for a number of atoms, and he applied his results to the calculation of the scattering curves.\* The much greater power of intensity measurements was immediately shown. The analysis of the orthorhombic crystal aragonite by the author,† and of the barytes group by James and Wood,‡ may perhaps be classed amongst the first successes of the new methods, and it was then applied to a series of silicate structures which were successfully analysed although they contained twenty or thirty parameters.

\* *Phil. Mag.*, 50, 289, 1925.

† *Proc. Roy. Soc., A*, 105, 16, 1924.

‡ *Ibid.*, A, 109, 598, 1925.

Once the laws governing these structures became known, other crystals could be worked out without such methods of prolonged siege, but they were necessary in the first place in order to extend analysis to quite a new field. A summary by Bragg and West\* in 1928, "A Technique for the X-ray Examination of Crystal Structures with many Parameters," summarises the methods employed.

### X-RAY OPTICS

Apart from Laue's original demonstration of the conditions for interference, the theory of X-ray reflection was founded by two papers of Darwin in 1914, which have already been quoted. He gave expressions for the ratio of the intensities of incident and reflected beams in the case of imperfect and perfect crystals, and for the refractive index. W. H. Bragg soon afterwards measured the relative intensities of different orders of reflection, but no comparison of incident and reflected beams was made till 1917, when the experiment was carried out by Compton.† Compton showed that Darwin's formula for the mosaic crystal gave results of the right order in the case of rock-salt, and he was able to get an approximate idea of the distribution of electrons in the sodium and chlorine atoms. An exhaustive investigation was undertaken by Bragg, James, and Bosanquet in 1921.‡ Absolute measurements of a large number of rock-salt reflections were made, which justified the mosaic formula and enabled the electron distribution to be deduced with considerable accuracy.

The comparison of theory and experiment could not be complete, however, until a satisfactory atomic model was available. Hartree commenced the calculation of atomic models by means of wave-mechanics in 1928.§ Scattering curves calculated for the Hartree models have now been experimentally tested in a number of cases, and agreement has always been found within the error of experiment. The influence of temperature is one uncertain factor, and it has recently been shown how important is the relation of the X-ray frequency to the characteristic frequencies of the atom. Wyckoff in particular has examined this point.|| The most complete check of the reflection formulæ

\* *Zeit. f. Krist.*, 69, 118, 1928.

† *Phys. Rev.*, 9, 29, 1917.

‡ *Phil. Mag.*, 41, 309, and 42, 1, 1921; also 44, 433, 1922.

§ *Camb. Phil. Soc. Proc.*, 24, 89, 111, 1928; also 25, 310, 1929.

|| *Phys. Rev.*, 35, 215 and 583; 36, 1116, 1930.

is perhaps that of James, Waller, and Hartree in 1928,\* where the Hartree scattering curves, the Debye-Waller temperature formula, elastic constants, zero-point energy, and the Darwin reflection equation, were all taken into account and found to be in accurate correspondence with the experimental results.

The most complete treatment of the theory of X-ray interference is due to Ewald. He published in 1917† his *Crystal Optics of X-rays*, in which he considered the diffraction effect by a rigid analysis. The simple treatment merely takes into account the interference of weak scattered waves set up by a strong primary beam traversing the crystal. The rigid treatment considers also the further scattering of the diffracted beam. In this way he obtained formulæ for the diffraction by a perfect crystal, and for the refractive index. Darwin had previously arrived at the same formulæ, but Ewald's treatment is more profound. Ewald is also responsible for applying the elegant method of the 'Reciprocal Lattice' to X-ray diffraction, and for showing how exactly it is suited to the problem.

The principles of the Fourier analysis were outlined in 1915 by W. H. Bragg.‡ They were rediscovered by Duane§ in 1925, and applied by Havighurst|| to give representations of scattering density in crystals. Compton in his book, *X-rays and Electrons* (1926), introduced absolute intensity measurements into the Fourier expression. Their most complete application has been found in the two-dimensional pictures of the crystal density projected upon a plane, of which diopside¶ is an example amongst inorganic crystals, and anthracene\*\* amongst organic crystals. Such pictures enable us to see just how much information we have gained about a crystal structure by means of the X-ray analysis.

### CRYSTAL CHEMISTRY

The first crystal analysis had an effect on conceptions of chemical combination which was of the very highest importance, for it proved that in the typical inorganic salt NaCl there is no

\* *Proc. Roy. Soc., A*, 118, 334, 1928.

† *Ann. Physik*, 54, 519, 1917.

‡ *Phil. Trans. Roy. Soc., A*, 215, 253, 1915.

§ *Proc. Nat. Acad. Sci.*, 11, 489, 1925.

¶ *Proc. Roy. Soc., A*, 123, 537, 1929.

\*\* *Ibid.*, A, 140, 79, 1933.

|| *Ibid.*, 11, 502, 1925.

molecular grouping, and the same was found to be the case in the subsequent analysis of other simple inorganic salts. The inference that the structure consists of alternate ions of sodium and chlorine was an obvious one to make, though the evidence in its support was largely indirect. Madelung in 1910 had shown that the *Reststrahlen* of NaCl indicate an ionic structure. The idea of the chemical molecule is fundamental in organic chemistry, but its general extension to inorganic compounds in the solid state had in the past been the chief obstacle to an understanding of their nature, notwithstanding Abegg's division of chemical compounds in 1904 into *heteropolar* and *homopolar*. Crystal analysis removed this false conception, and opened the way to much new research into ionic compounds. Born's lattice theory, and the work of Fajans, Grimm, and Wasastjerna on the properties of ions, may be cited as examples. The conception of the simple ions as bodies with a charge, an effective 'size' which could be measured in Ångström units, and a characteristic polarisability, was launched on its way and had as an immediate effect a much better understanding of the mechanics of inorganic structures. This was a natural consequence of the analysis of crystal structure, since for the first time definite data were available on which theories could be based. Kossel and Lewis in 1916, and Langmuir in 1919, used the new knowledge of crystal structure, and the new understanding of atomic structure, to explain the nature of chemical combination in heteropolar and homopolar compounds. All this work was inevitably incomplete and largely empirical, but it had the great advantage of presenting the molecular or atomic arrangement as something objective, of which scale models could be made. We have by now become so accustomed to the new ideas that it is difficult to recapture the first thrill of Langmuir's work on surface films, in which, for instance, he confidently assigned to molecules soluble ends immersed in a water surface, and inactive or insoluble ends protruding outwards. The distinction between physical forces on the one hand, and on the other the mysterious chemical forces into whose nature it had been thought almost presumptuous to inquire, was swept away for ever.

In the inorganic field Wasastjerna's work on ionic structures occupies a very important place. The author in 1920\* had shown that interatomic distances obeyed in many cases an

\* *Phil. Mag.*, 40, 169, 1920.

additive law. Wasastjerna\* reinterpreted the author's figures in terms of *ionic* sizes, which he checked by means of ionic refractivities. He must be regarded as the founder of the list of ionic radii so widely used in analysis. The author's figures as altered by Wasastjerna correspond very closely to those now established by the investigations of Goldschmidt.

Goldschmidt's monumental work on the crystal chemistry of simple compounds was commenced about the year 1925. With a band of assistants, amongst whom were Machatschki, Oftedal, and Zachariasen, he examined many complete series of substances and sought for general laws of structure. A summary of the earlier work is given in his contribution to a discussion held by the Faraday Society in 1929, on "Crystal Structure and Chemical Constitution," and a full account of Goldschmidt's work is to be found in the series *Geochemische Verteilungsgesetze der Elemente*.† The division of the structures into types, and the rôles of ionic size and polarisation, were surveyed in a broad way; the crystal chemistry of inorganic compounds has been built upon the foundations which he laid.

The author's work on the silicates ‡ dealt with a highly complex series of bodies, for which similar general laws were found to exist. Silicates figure so largely in mineralogy that it is possible to rewrite much of the subject from the new view-point.

Pauling's paper on "The Principles Determining the Structures of Complex Ionic Crystals" § has had an outstanding influence on the study of inorganic compounds. In it he collected the existing knowledge of the features of these compounds, and by adding new generalisations he was able to lay down the laws governing their structure and stability. These laws have greatly increased the assurance with which inorganic analysis of all types can be carried out.

The chief contributors to our knowledge of co-ordination compounds have been Wyckoff and Hassel. Papers by the former author have appeared from 1926 onwards in the *American Journal of Science* and other periodicals, and by the latter in the *Zeitschrift für physikalische Chemie* and the *Zeitschrift für anorganische Chemie*.

\* *Soc. Scient. Fenn. Comm. Phys. Math.*, 38, 1, 1923.

† *Norske Videnskaps-Akademi*, Oslo, 1924 onwards.

‡ *Zeit. f. Krist.*, 74, 237, 1930.

§ *J. Amer. Chem. Soc.*, 51, 1010, 1929.

The development of the study of alloy structures will always be associated with Westgren's name. He commenced in 1921 his investigations upon the structure of iron and steel. Since that date many papers on particular alloy structures, and reviews of the nature of alloys, have appeared from his laboratory. His work has been characterised by the precision of its metallurgical technique, and the clearness of its powder photographs. He has been responsible, more than any other investigator, for unravelling the intricacies of phase diagrams by the X-ray method.

Westgren has concentrated his energies rather upon a broad review of alloy structures than upon the close analysis of individual alloys. Though most structures are simple, some complicated cases occur. The analysis of  $\gamma$ -brass \* and  $\alpha$ -manganese † by Bradley, and of certain other alloys, marked a turning-point in the analysis of highly complex structures by the unaided powder method.

The researches of Gunnar Hägg into the metallic hydrides, nitrides, borides, and carbides have appeared from 1930 onwards, and represent a very wide survey of these structures.

Another outstanding contribution was Hume - Rothery's ‡ divination that the electron-atom ratio is a major factor in determining the type of an alloy structure. This rule, and others which he has developed, have played a prominent part in enabling analogies to be drawn between the various alloy systems.

The analysis of organic crystals commenced with the comparison of the naphthalene and anthracene cells by W. H. Bragg § in 1921. Although the atomic positions could not be determined the results promised further developments, for they showed that the structural arrangement was in conformity with the chemist's scheme of linked benzene rings, and that these rings had approximately the dimensions of the rings in diamond and graphite. This foreshadowed the development of rules for the interpretation of the complicated molecular structures which are usual to organic compounds.

In the long-chain carbohydrates the dispositions of the diamond are also followed. The first measurements of these substances were made by Müller and Shearer, || by Piper and

\* *Proc. Roy. Soc., A*, 112, 678, 1926.

† *Ibid.*, A, 115, 456, 1927.

‡ *J. Inst. Metals*, 35, 295, 1926.     § *Proc. Phys. Soc.*, 34, 33, 1921.

|| *J. Chem. Soc.*, 123, 2043 and 3156, 1923.

Grindley,\* and by de Broglie and Friedel.† The regular increase in spacing with increased number of carbon atoms in the chain, and the constancy of the 'side spacings,' provided a basis for further development.

The complete solution of a long-chain carbohydrate by Müller,‡ of hexamethyl benzene by Mrs Lonsdale,§ and of anthracene by Robertson|| have confirmed these first results. The analysis of Urea,  $(\text{NH}_2)_2\text{CO}$ , by Wyckoff ¶ also determines atomic positions with exactitude. The analysis of more complicated molecules will be based in future on such determinations of the configuration of characteristic groups, and they are therefore of fundamental importance.

The first work on the structure of cellulose was carried out in 1920 by Herzog, Jancke, and Polanyi.\*\* They obtained the earliest 'fibre-diagrams,' and realised their significance as indicating an orientation of crystalline particles with an axis parallel to the fibre axis, though otherwise irregular. Polanyi deduced dimensions for the unit of structure, now identified with two linked glucose units, which correspond almost exactly to those determined by the later work of Mark and Andress.††

Other highly polymerised organic substances which have been studied are rubber, and hair and wool. The discovery of interference effects produced by stretched rubber was made by Katz in 1925,‡‡ and the structure of rubber has been studied extensively by Hauser. The work on hair and wool has been carried out by Astbury.§§ Though the interference effects are of a very diffuse type, an entirely new field has been opened up by the discovery that stretched and unstretched fibres yield patterns which indicate different molecular arrangements. Since these substances are proteins this observation has an immense importance.

Meyer and Mark's book, *Der Aufbau der Hochpolymeren Organischen Naturstoffe*,||| was the first to be devoted to this subject and gives an excellent summary of it.

\* *Proc. Phys. Soc.*, 35, 269, 1923.

† *Compt. rend.*, 176, 738, 1923.

‡ *Proc. Roy. Soc., A*, 120, 437, 1928. § *Ibid.*, A, 123, 494, 1929.

|| *Ibid.*, A, 140, 79, 1933.

¶ *Zeit. f. Krist.*, 75, 529, 1930.

\*\* *Zeit. f. Physik*, 3, 196 and 343, 1920; *Naturw.*, 9, 288, 1921.

†† *Zeit. physikal. Chem.*, 4, 431, 1929. ‡‡ *Naturw.*, 13, 411, 1925.

§§ *Phil. Trans. Roy. Soc., A*, 230, 75, 1931.

||| Akademische Verlagsgesellschaft, Leipzig, 1930.

## CRYSTAL PHYSICS

Crystal physics covers so wide a field that it is difficult to know where to delimit a survey. There are two aspects, however, which are very closely connected with the intimate structure of the crystal.

The first of these is represented by Born's *Atomtheorie des Festen Zustandes*,\* which is a more elaborate account of an earlier *Dynamik der Kristallgitter* published in 1915. The crystal is treated as a system in stable equilibrium, the interatomic forces being regarded as existing between atoms which are spherically symmetrical. The energy of the crystal lattice, elastic constants, optical constants, and other properties are calculated on this basis. The method is eminently suitable for ionic crystals and has been used to link up their energies of formation, the heats of solution, the electron affinities of the ions, and so forth. Grimm, Fajans, Lennard-Jones, and many others have related the physical properties of crystals to the properties of the ions of which they are composed. Hund † broke new ground in a very suggestive work, "An Attempt to Derive the Lattice Type from the Assumption of Isotropic Polarizable Ions." The data were too uncertain to yield accurate results, but the new ideas he brought forward were of the greatest interest. The author ‡ in 1924 gave a successful quantitative explanation of the birefringence of calcite and aragonite, which was based on a very simple treatment essentially the same as in Born's exhaustive *Atomtheorie des Festen Zustandes*. A recent paper by Born and Mayer § on the dynamics of crystals of NaCl and CsCl types has carried analysis further, and has given for the first time an insight into the factors which decide whether an ionic crystal assumes one or other of these types. It has also justified theoretically the empirical law of constant ionic radii.

The other aspect of crystal physics on which a vast amount of research has been carried out is the deformation of metal crystals, and the alteration in crystal texture due to cold-working. Here Polanyi has been the pioneer. His researches have appeared from 1922 onwards and are the foundation of the theory of single-crystal deformation. Other workers in this field have been

\* Teubner, Leipzig, 1923. † *Zeit. f. Physik*, 34, 833, 1925.

‡ *Proc. Roy. Soc., A*, 109, 370, 1924.

§ *Zeit. f. Physik*, 75, 1, 1931.



Carpenter, and Taylor and Elam in this country, and Mark and Schmid in Germany.

In the study of the 'real crystal,' or of the dependence of physical properties upon the irregularities of crystal growth, Smekal and Zwicky have been the foremost exponents. Joffé's book on *The Physics of Crystals* is a standard work on the macroscopic properties of crystalline material.\* Kapitza and Goetz have developed methods of the highest ingenuity in the preparation and study of perfect crystals, and have insisted upon the necessity of explaining the physical properties of such crystals before attempting to explain the properties of a crystalline aggregate.

Many important investigations have necessarily been omitted in this survey, since the field is so vast. It has been impossible to do more than indicate the nature of the pioneer investigations which have given rise to the various branches of the subject. An historical account of the more recent developments, such as the investigation of electron diffraction and of diffraction by liquids and gases, has not been repeated here because it will be found in previous chapters devoted to these fields.

\* McGraw-Hill Book Company, 1928.

## BIBLIOGRAPHY

Many books dealing with X-ray analysis have appeared in recent years. A brief selection only from this extensive literature is given here, these being books which may be of use to the reader for the information they contain about the results of analysis, and for their descriptions of X-ray technique.

### DESCRIPTIVE CRYSTALLOGRAPHY

*Mineralogy.* H. A. Miers. 2nd edition, Macmillan & Co., 1929.

This classic gives an account of the methods of studying external crystal form and optical properties which is a very good introduction for the student of X-ray analysis.

*An Introduction to Crystallography.* F. C. Phillips. Longmans, Green & Co., 1946.

A concise but thorough account of the geometry of crystals.

### CRYSTAL SYMMETRY

*Mathematical Crystallography.* H. Hilton. Clarendon Press, 1903.

Included because of its historical interest, but formal in treatment. Later books on space-group derivation are better adapted to X-ray analysis.

*Geometrische Kristallographie des Diskontinuums.* P. Niggli. Gebrüder Borntraeger, Leipzig, 1919.

A thorough treatment of space-groups.

*The Analytical Expression of the Results of the Theory of Space-Groups.* R. W. G. Wyckoff. Carnegie Inst. Washington Publications, No. 318, 2nd edition, 1930.

### X-RAY OPTICS

*Röntgenstrahl-Interferenzen.* M. von Laue. Akademische Verlagsgesellschaft, Leipzig, 1941.

*Materiewellen und ihre Interferenzen.* M. von Laue. Akademische Verlagsgesellschaft, Leipzig, 1944.

*X-ray Diffraction in Crystals.* W. H. Zachariasen. John Wiley & Sons, New York, 1945.

*The Diffraction of X-rays and Electrons by Free Molecules.* M. H. Pirene. Cambridge University Press, 1946.

*Wave Propagation in Periodic Structures.* L. Brillouin. McGraw Hill Book Co., New York, 1946.

*Volume II of The Crystalline State (The Optical Principles of the Diffraction of X-rays)* by R. W. James. G. Bell & Sons, and Oxford University Press, 1937.

### PHYSICAL AND CHEMICAL CRYSTALLOGRAPHY. TECHNIQUES

*An Introduction to Crystal Chemistry.* R. C. Evans. Cambridge Univ. Press, 1939.

This book deals with the relationship of internal structure to physical and chemical properties.

*Atomic Structure of Minerals.* W. L. Bragg. McGraw Hill Book Co. and Oxford University Press, 1937.

A general review of mineral structures, in particular the silicates.

*Structural Inorganic Chemistry.* A. F. Wells. O.U.P., 1945.

A systematic description of structures, with especial relation to their chemical properties.

- Structure of Metals.* C. S. Barrett. McGraw Hill Book Co., 1943.  
*An Introduction to X-ray Metallography.* A. Taylor. Chapman & Hall, 1945.  
*The Structure of Metals and Alloys.* W. Hume-Rothery. The Institute of Metals, London, 1936.  
*The Diffraction of X-rays and Electrons by Amorphous Solids, Liquids and Gases.* J. T. Randall. Chapman & Hall, 1934.  
*The Structure of Crystals,* 1912-30. R. W. G. Wyckoff. Chemical Catalog Co., New York, 1931.  
*Supplement to above for 1930-34.* Reinhold Publishing Corporation, New York, 1935.  
*High Polymers.* Interscience Publishers. For reference, parts of Vol. II, H. Mark, 1940, and Vol. IV, K. H. Meyer, 1942, are very useful.  
*Chemical Crystallography.* C. W. Bunn. Clarendon Press, 1945. An introduction to optical and X-ray methods.  
*X-ray Crystallography.* M. J. Buerger. John Wiley & Sons, 1942.  
*Radiocristallographie.* A. Guinier. Dunod, Paris, 1945.  
*Applied X-rays.* G. L. Clark. McGraw Hill Book Co., 1940.  
*The Interpretation of X-ray Diffraction Photographs.* N. F. M. Henry, H. S. Lipson and W. A. Wooster. Macmillan & Co. (shortly).  
*X-ray Analysis and Application of Fourier Series Methods to Molecular Structures.* J. M. Robertson. Reports on Progress in Physics Vol. IV, Physical Society, London, 1938.

#### WORKS OF REFERENCE

- International Tables for the Determination of Crystal Structure.* Vols. I and II. Borntraeger, Berlin, 1935.  
*Structure Factor Tables.* K. Lonsdale. G. Bell & Sons, 1936. A series of formulae for structure factor and electron density for the 230 space groups.  
 The "International Tables" listed above is useful for reference.  
*Strukturbericht.* Akademische Verlagsgesellschaft, Leipzig.  
 Vol. I, 1913-28. P. P. Ewald and C. Hermann; Vol. II, 1928-32. C. Hermann, O. Lohrmann and H. Philipp; Vol. III, 1933-35. C. Gottfried and F. Schossberger; Vol. IV, 1936. C. Gottfried; Vol. V, 1937. C. Gottfried; Vol. VI, 1938. K. Herrmann; Vol. VII, 1939. K. Herrmann.

All volumes of the *Strukturbericht*, and also the *International Tables*, have been re-published by Edwards Bros., Ann Arbor, Michigan.

The following books, now mainly of historical interest, played a part in the early development of the subject :—

- X-rays and Crystal Structure.* W. H. Bragg and W. L. Bragg. G. Bell & Sons, London, 1924.  
*Kristalle und Röntgenstrahlen.* P. P. Ewald. Julius Springer, Berlin, 1923.  
*La Structure des Cristaux.* C. Mauguin. Presses Universitaires, Paris, 1924.

## APPENDIX I

### THE PRODUCTION AND PROPERTIES OF X-RADIATION

#### THE PRODUCTION OF X-RAYS

THE X-ray bulb or tube is an apparatus in which a high vacuum is maintained so that an electron stream can be projected with sufficient velocity and without hindrance against a target which arrests the motion. The electrons are driven across the tube by a high potential from a transformer, induction coil, or large storage battery. Potentials normally applied vary from 30,000 to 70,000 volts, though higher and lower potentials are sometimes used.

Most of the energy in the electron stream is dissipated as heat in the anticathode, but a small fraction of it is converted into the very short electromagnetic waves which we term X-rays. These radiations vary greatly in quality; the original classification into 'hard' or penetrating, and 'soft' or easily absorbed, corresponds to the short-wave and long-wave regions. The average quality of the radiations tends towards the harder type as the potential on the tube is increased.

The radiation from a given anticathode consists of a continuous spectrum with a superimposed line spectrum. A curve which shows the distribution of energy amongst the wave-lengths for the continuous or 'white' radiation commences sharply at a short-wave limit which depends on the applied voltage, rises to a maximum, and falls away again in the long-wave region. The 'line' spectrum is characteristic of the element of which the anticathode is made, and consists of groups of 'monochromatic' components of definite wave-lengths. For each group there is a limiting voltage which must be surpassed if it is to be excited.

Fig. 167, due to Webster, shows the effect of bombarding a rhodium target with electrons of different velocities. The source

of high tension is a large storage battery. The radiation is analysed into different wave-lengths by a crystal spectrometer, and the energy in different parts of the spectrum is plotted against the wave-length. Owing to absorption in the walls of the tube, and different reflecting power of the crystal for different wave-lengths, the curve gives merely a qualitative representation of the true energy distribution.

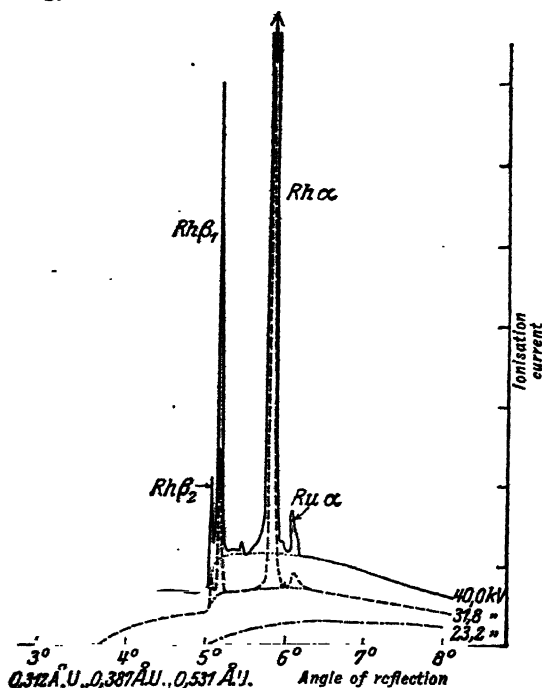


FIG. 167.—Analysis of X-radiation from a rhodium target, for various voltages

(From *The Spectroscopy of X-rays*, Siegbahn; O.U.P., 1925)

When the applied potential is 23,200 volts or less, the electrons have not sufficient energy to excite the line spectrum. At higher voltages (31,800 volts in the case of the second curve) the line spectrum of rhodium appears, and at the same time the curve representing white radiation is raised and moved to the left or short-wave side. With 40,000 volts the characteristic line spectrum is much enhanced. It will be noticed in each case how abruptly the continuous spectrum begins at a definite wave-length on the left or short-wave side. The small peaks are the

$K\alpha$  and  $K\beta$  lines of ruthenium, which was present as an impurity in the rhodium.

### LINE SPECTRA

The two peaks in the above figure represent two characteristic K wave-lengths in the X-ray spectrum of rhodium. Soon after the discovery of X-rays, Barkla commenced a series of researches on absorption coefficients, during the course of which he proved the existence of characteristic X-radiations. A metal emits secondary rays when a primary beam of X-rays falls upon it, and Barkla found that these rays were much more homogeneous than the direct beam from an X-ray tube. Each element was found to give a characteristic hard 'K' radiation and a soft 'L' radiation. Both types get harder as the atomic weight of the element increases.

The characteristic radiations are excited both when the element forms the anticathode of a tube and when it scatters X-rays. The discovery that a crystal diffracted X-rays made it possible to measure the wave-length of the radiation, and one of the first achievements of the X-ray spectrometer was to show that the K radiation consisted of two spectral lines  $K\alpha$  and  $K\beta$ , and the L radiation of three lines  $L\alpha$ ,  $L\beta$ ,  $L\gamma$  (it is now known that these lines are complex, and that other weaker lines are present in each group).

Moseley examined the X-ray spectra of a number of elements, and showed that they varied in a regular manner from one element to the next in the periodic table. He was thus able to found his famous law governing the number and order of the elements. When the wave-length of corresponding lines is plotted against the *atomic number*  $N$ , defining the position of the element in the periodic table, a regular curve is the result. A vacant place in the table, corresponding to an unknown element, is shown by the absence of the corresponding wave-length in the series of X-ray spectra. Fig. 168 is drawn from Moseley's original observations of the K spectra. Curves which are nearly straight lines are obtained when the square root of the frequency is plotted against the atomic number, the wave-length scale being denoted above. Moseley found, for instance, that the frequency of the  $K\alpha$  lines is given very closely by the formula

$$\nu = \frac{3}{4}\nu_0(N-1)^2,$$

where  $\nu_0$  is the constant which appears in optical spectral series. If  $\nu$  and  $\nu_0$  are expressed as wave numbers  $1/\lambda$ ,  $\nu_0$  is the Rydberg constant  $R$ , 109,737.

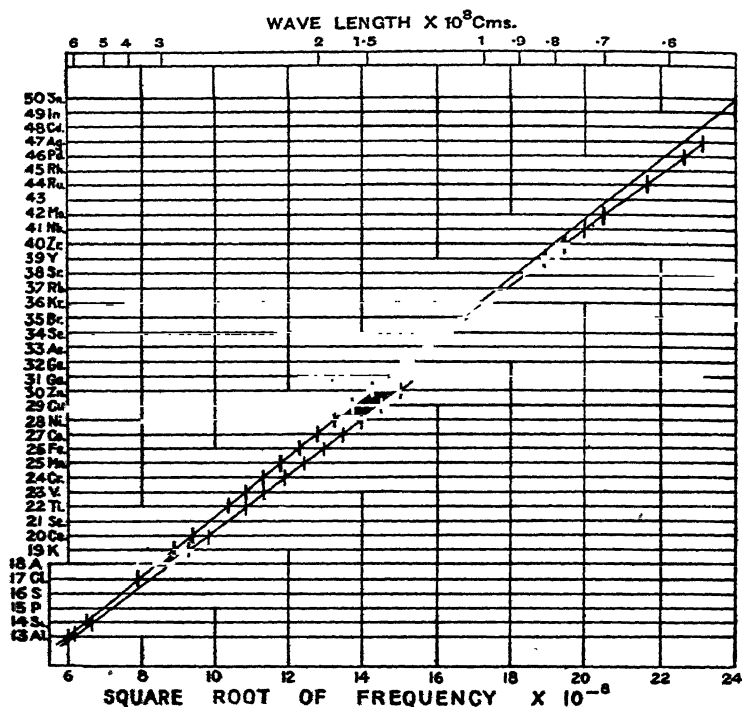


FIG. 168.—K spectra of the elements from aluminium to tin  
After Moseley

The X-ray spectra of the elements have been exhaustively studied by Siegbahn and his school. Fig. 169, due to Siegbahn, represents his measurements on the L series of elements from calcium to uranium. The original survey of the elements showed that 43, 61, 72, and 75 were missing from the periodic table, in addition to the gaps at 85 and 87 amongst the radioactive elements. These elements have since been discovered and identified by means of their X-ray spectra:

- 43 Masurium.
- 61 Illinium.
- 72 Hafnium.
- 75 Rhenium.

The heaviest elements yield also an M spectrum which is much softer than the L spectrum, and in one or two cases lines of the

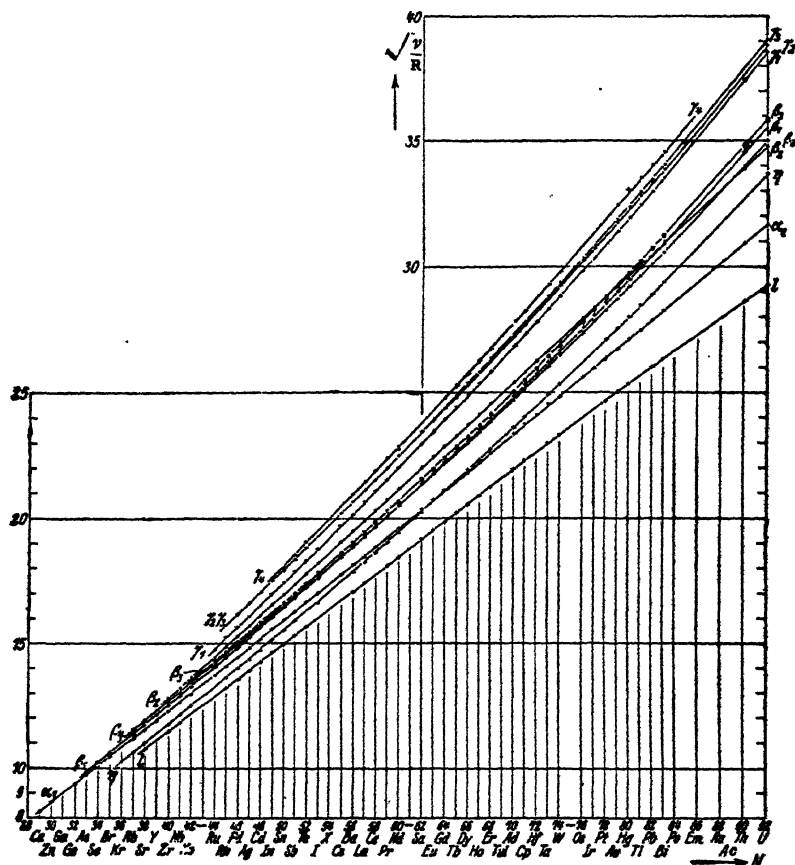


FIG. 169.—Moseley diagram of the L spectra of elements from calcium to uranium.  $\sqrt{\frac{\nu}{R}}$  is plotted vertically against  $N$  plotted horizontally,  $R$  being the Rydberg constant and  $\nu$  expressed as  $a/\text{wave number}$ .

(From *The Spectroscopy of X-rays*, Siegbahn; O.U.P., 1925)

N spectrum have been observed. In fig. 170, due to Siegbahn, the wave-lengths of every third element (to avoid overcrowding in the figure) have been plotted against the atomic number. This gives a convenient survey of the whole range of X-ray spectra, and illustrates their general simplicity as contrasted with optical spectra. This simplicity is due to their origin in the



interior of the atomic structure, so that they are little affected by the periodic changes in external electronic arrangement which govern the physical and chemical properties of successive elements.

Certain wave-lengths are especially useful for the purposes of crystal analysis. The very short wave-lengths must be excited by a very high voltage, and are so penetrating that it is difficult to limit them by screens. Such are the K lines given by tungsten

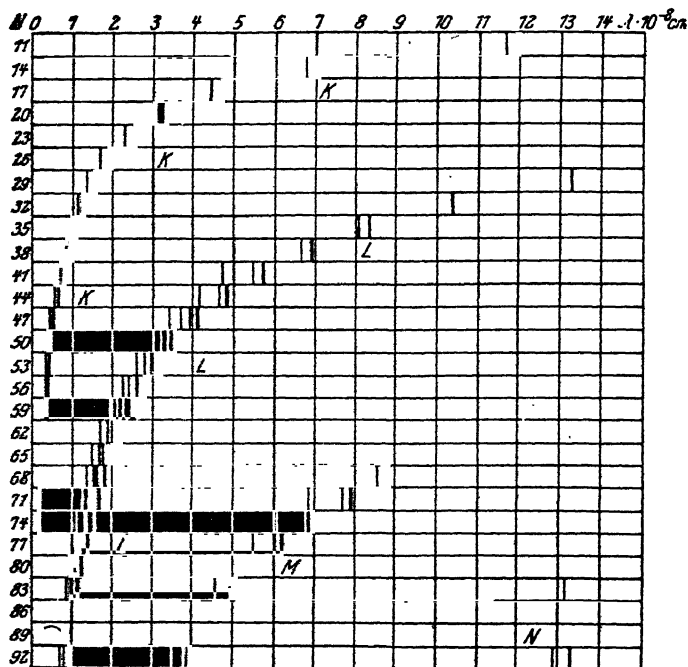


FIG. 170.—The strongest lines of the X-ray series, for every third element from aluminium to uranium

(From *The Spectroscopy of X-rays*, Siegbahn; O.U.P., 1925)

with wave-lengths 0.213, 0.209, 0.189 Å. On the other hand, waves longer than the K lines of chromium (2.29 Å. and 2.08 Å.) are very easily absorbed, both by any window in the walls of the X-ray tube and by the diffracting substance. Suitable sources are further limited by the requirements that the anticathode must be a tough metal with high melting-point and good thermal conductivity in order that it may stand the electron bombardment.

The anticathodes most used are molybdenum, copper, and iron, the former for shorter and more penetrating waves, and the latter

two for the longer wave-length region. Rhodium and palladium also make excellent anticathodes and were much used in early experiments, but they are expensive and apt to be impure. A survey of the list of elements in fig. 168 will show that there are no suitable elements between copper and molybdenum in the periodic table. Lines of the L series are not convenient as sources of monochromatic waves since they are relatively weak and belong to so complex a group (the L series of tungsten, for example, contains twenty-two lines).

The wave-lengths of radiations ordinarily employed for analysis are given below, the unit being the Ångström  $10^{-8}$  cm.\* The  $K\alpha$  doublet is used for crystal analysis, being the most intense.

	$K\alpha_2$	$K\alpha_1$	$K\beta_1$	Absorption edge
24 Chromium . . .	2.2889	2.2850	2.0806	2.0661
26 Iron . . .	1.9360	1.9321	1.7530	1.7393
27 Cobalt . . .	1.7892	1.7853	1.6174	1.6043
28 Nickel . . .	1.6583	1.6545	1.4970	1.4846
29 Copper . . .	1.5412	1.5374	1.3893	1.3778
42 Molybdenum . .	0.71280	0.70783	0.63098	0.61848
45 Rhodium . . .	0.61637	0.61202	0.54449	0.53303
46 Palladium . . .	0.58863	0.58427	0.51947	0.50795
47 Silver . . .	0.56267	0.55828	0.49601	0.48480

### ENERGY LEVELS AND X-RAY SPECTRA

X-ray spectra are reduced to an ordered scheme, like optical spectra, by considering each line of the spectrum as due to a transition between two energy states of the atom. It has been seen that the K lines are not produced unless the voltage applied to a tube exceeds a value characteristic of the element. This critical voltage endows the electrons from the cathode with an energy which is just sufficient to eject electrons from the innermost K shell of atoms in the target. The K spectrum is emitted on the return of the atoms to their normal state. Energy is

\* The *relative* values of X-ray wave-lengths are known with much greater accuracy than their *absolute* wave-lengths, since the estimate of crystal spacing depends upon atomic constants and crystal density. The (200) spacing of a standard crystal, calcite at 18° C., is taken to be 3.02945 Å., and wave-lengths calculated on this basis may be measured to six significant figures.

released when an electron from an outer shell takes the place of the electron lost by the K shell, and this energy appears as X-rays of frequency  $\nu$  given by the Bohr relationship,

$$h\nu = W_1 - W_2,$$

when  $W_1 - W_2$  represents the change in potential energy of the system, and  $h$  is Planck's constant. The L spectrum is similarly excited when electrons have been removed from the L shells of atoms and their place is taken by electrons from outer shells.

A definite amount of energy is required to remove a K electron from a given atom. By the quantum relationship  $E = h\nu$  this energy corresponds to a definite frequency, and so to a wavelength which marks the K *absorption edge* of the element. As will be seen in the following paragraph, there is a sharp rise in the absorption of X-rays by the element as the absorbed wavelength passes from the long-wave to the short-wave side of the absorption edge. X-rays of lower frequency have too small an energy quantum to remove K electrons, whereas X-rays of higher frequency can dissipate their energy by doing so. A determination of the K absorption edge therefore makes it possible to measure the energy of binding of a K electron. There is only one K absorption edge, but there are three L absorption edges ( $L_1$ ,  $L_{11}$ ,  $L_{111}$ ), five M absorption edges, and so forth, in atoms of sufficient complexity to have complete electron shells of these categories.

Each frequency in an X-ray spectrum is equal to the difference between the frequencies associated with two absorption edges. For instance,

$$\begin{aligned}\nu(Ka_1) &= \nu(K_1) - \nu(L_{11}), \\ \nu(Ka_2) &= \nu(K_1) - \nu(L_{111}).\end{aligned}$$

This relationship, first pointed out by Kossel, is a result of the quantum equation. The change in potential energy of the atom, when a gap in the K shell is filled by an electron from an L shell, must be equal to the difference between the energy required to remove a K electron and that required to remove an L electron:

$$h\nu(Ka_1) = h\nu(K_1) - h\nu(L_{11}).$$

Similarly, a  $K\beta_1$  line is produced when the gap in the K shell is filled by an electron drawn from an M shell, and a  $K\beta_2$  line when the electron comes from the N shell.

A complete scheme of the energy-levels in uranium is shown in fig. 171, due to Siegbahn. The heights of the horizontal lines are not proportional to the actual energies involved, for the diagram merely indicates the transitions which give rise to X-ray spectra. Only such transitions occur as are in accord with the selection rules developed by the theory of spectra.

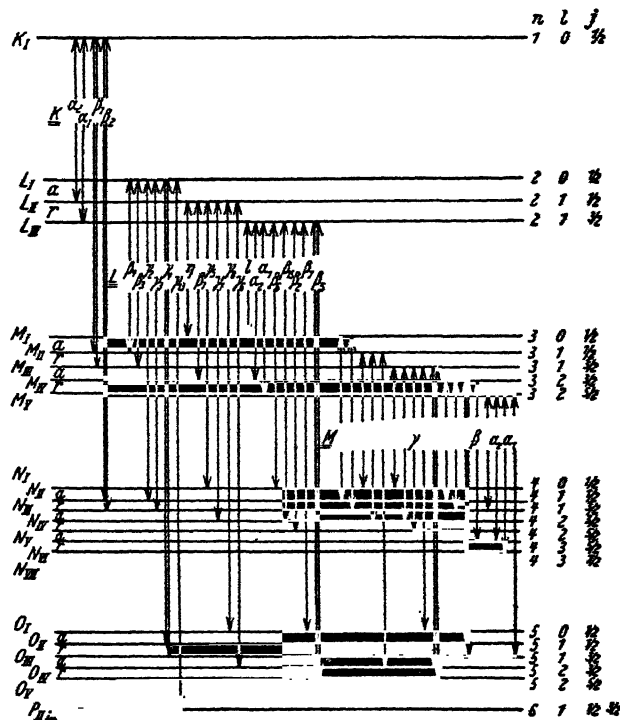


FIG. 171.—Scheme of energy-levels in uranium  
(From *Spektroskopie der Röntgenstrahlen*, Siegbahn; Julius Springer)

As the potential in a tube is raised to a value sufficiently high to remove K electrons in the target, all lines of the K spectra appear simultaneously. The same holds for each of the three sets of L lines, and so forth. The production of a spectrum commences abruptly at a critical potential  $V_0$ , given by

$$eV_0 = h\nu_a,$$

where  $\nu_a$  is the frequency of the absorption edge. Beyond that point the intensity for constant current is proportional to  $(V - V_0)^{3/2}$

according to Webster and Clark, or to  $(V - V_0)^2$  according to Wooten. Thus as the voltage is increased beyond the critical point the output of characteristic rays rises very rapidly, relatively to that of the continuous radiation. For this reason, when monochromatic X-rays are required it is best to employ a potential considerably in excess of the critical potential. The K rays of molybdenum appear as soon as the voltage exceeds 20 kV, but it is desirable to apply about 60 kV in order to obtain a strong monochromatic beam. Similarly, voltages of the order of 35 kV are desirable for the anticathodes in the copper-chromium series.

### THE CONTINUOUS SPECTRUM

Three features of the continuous spectrum may be briefly referred to here. As already stated, the spectrum ends abruptly at a definite short-wave limit, shown by fig. 167. When the potential  $V$  applied to the tube is increased, this limit moves towards the region of shorter wave-lengths. The highest frequency  $\nu_m$  is fixed by the equation

$$Ve = h\nu_m.$$

Putting this in terms of the minimum wave-length,

$$\begin{aligned}\lambda &= hc/Ve \\ &= 1.234 \times 10^{-4}/V',\end{aligned}$$

where  $V'$  is expressed in volts.

All electrons hit the anticathode with an energy equal to  $Ve$ , but only in a few cases is the energy converted into radiation immediately on impact; most electrons dissipate the greater part of their energy by repeated collisions, when it appears as heat. Hence the frequency given by the quantum relationship appears as an upper limit to the spectrum of continuous radiation.

Fig. 172, due to Urey, shows that as the voltage increases, the white radiation from a given anticathode both increases in total amount and shifts towards the high frequency region. It is found that the total amount of white radiation is approximately proportional to  $V^2$ . Fig. 173, which is also due to Urey, shows the effect of using different metals for the anticathode, the voltage being kept constant. The short-wave limit is of course always the same, since this depends on the maximum voltage, which is 35,000 in this case. Chromium has no lines in its spectrum of so short a

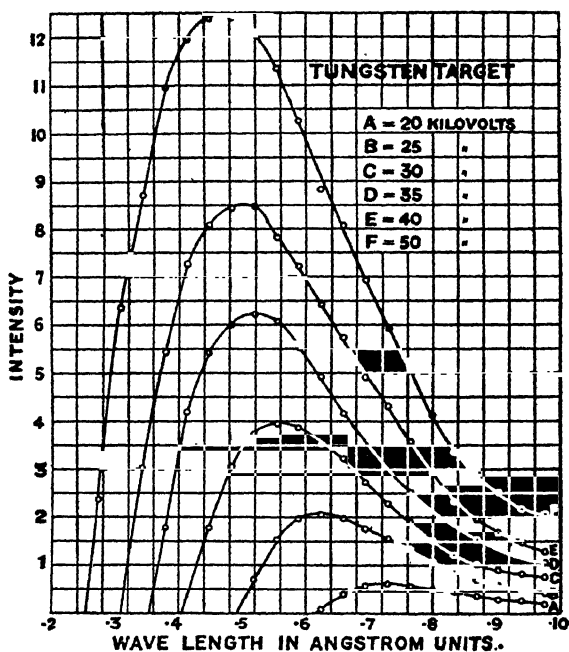


FIG. 172.—Excitation of the continuous spectrum at various potentials

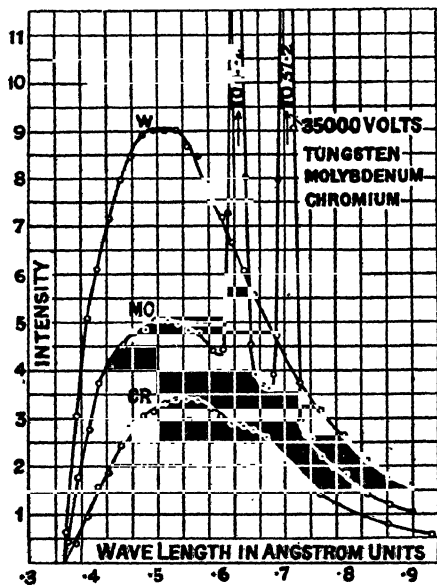


FIG. 173.—X-ray spectrum with different anticathodes

wave-length as to come within the range of the figure. The potential is not sufficient to excite the tungsten K lines, and its L lines are again in the long-wave region outside the figure. Hence it is only in the case of molybdenum that a spectrum appears, the K peaks being so high that they exceed the limits of the graph. It is found that the total amount of white radiation is approximately proportional to the atomic number  $Z$ . Since it is also proportional to  $V^2$ , whereas the energy input for a given current is proportional to  $V$ , the efficiency of production is greater when the voltage is high. Summing up the effect of both of the above laws, it is best to use a high voltage and an anticathode of a metal with high atomic number when a range of continuous radiation is required, such as for Laue photographs.

### X-RAY ABSORPTION

A beam of X-rays loses energy as it traverses matter, partly by scattering and partly by transformation of the energy into that of moving electrons and of secondary X-radiation. Unless the atomic weight of the absorbing substance is small and the wave-length of the X-rays short, the loss by scattering is negligibly small in comparison to that by transformation.

If the original beam of X-rays is homogeneous, the energy  $I$  of a beam of initial energy  $I_0$ , after traversing a layer of thickness  $t$ , is given by

$$I = I_0 e^{-\mu t},$$

where  $\mu$  is termed the *linear absorption coefficient*. It is simpler to express absorption coefficients in terms of mass traversed rather than of thickness, since it is the amount of matter which determines the absorption and not its distribution in space. The equation can be written,

$$I = I_0 e^{-\frac{\mu}{\rho} \cdot \rho t},$$

where  $\mu/\rho$  is the mass absorption coefficient, and  $\rho t$  is the mass per square centimetre of the absorbing screen. The coefficient  $\mu/\rho$  is then independent of the physical or chemical state of any given constituent in the absorbing screen, whose contribution to the absorption is determined by the coefficient multiplied by its mass per square centimetre. We can further divide  $\mu/\rho$  into a scattering coefficient and transformation coefficient

$$\mu/\rho = \sigma/\rho + \tau/\rho.$$

The scattering coefficient  $\sigma/\rho$  is approximately constant and is equal to 0.2. The transformation coefficient  $\tau/\rho$ , on the other hand, varies very greatly for different materials and different wave-lengths.

We can only give a brief summary here of the laws of absorption. Absorption increases very rapidly with increasing wave-length of the radiation and with increasing atomic number of the absorbing element. If the mass absorption coefficient is multiplied by the atomic weight, a quantity is obtained proportional to the absorption per atom of the element. It is found that the relation between the atomic transformation coefficient and variables defining the radiation and the atom respectively may be expressed to a first approximation at least by the formula,

$$\text{Atomic transformation coefficient} = CN^4\lambda^3$$

or

$$\text{Mass transformation coefficient} = C'N^4\lambda^3/A,$$

where  $N$  is the atomic number of the element forming the absorbing screen,  $A$  is the atomic weight, and  $\lambda$  the wave-length of the radiation.

According to this law, a straight line should be obtained when  $(\tau/\rho)^{\frac{1}{2}}$  for a given element is plotted against the wave-length  $\lambda$ . Actual absorption coefficients show a close approximation to the relation, but there are discontinuities at the absorption edges. The constant  $C$  has several values; one value applies to the region in which the absorbed radiation has a shorter wave-length than the K absorption edge, the next to the region between the K and L edges, and so forth. In the first region, where the radiation can excite the K, L, M spectra of the absorbing screen,  $C$  has the value 0.0225 when  $\lambda$  is expressed in A. This constant applies, for instance, to the absorption of a wide range of wave-lengths in aluminium whose K edge is far out in the long wave region. When  $\lambda$  exceeds the value for the K edge of the absorber, the coefficient drops to 0.0031. There is a further decrease in  $C$  of about the same ratio when the L edges are surpassed.

Fig. 174 is an ideal diagram calculated with these values of the constants,  $(\tau/\rho)^{\frac{1}{2}}$  being plotted as ordinate against  $\lambda$  as abscissa for a series of absorbing elements. The absorption in aluminium is represented by a straight line across the graph. Copper shows a similar straight line up to its K absorption edge, at 1.378 A., where there is a sudden drop and a new straight line



is followed. In the case of platinum, the discontinuities both at the K edge (0.1581) and at the three L edges come within the range of the graph.

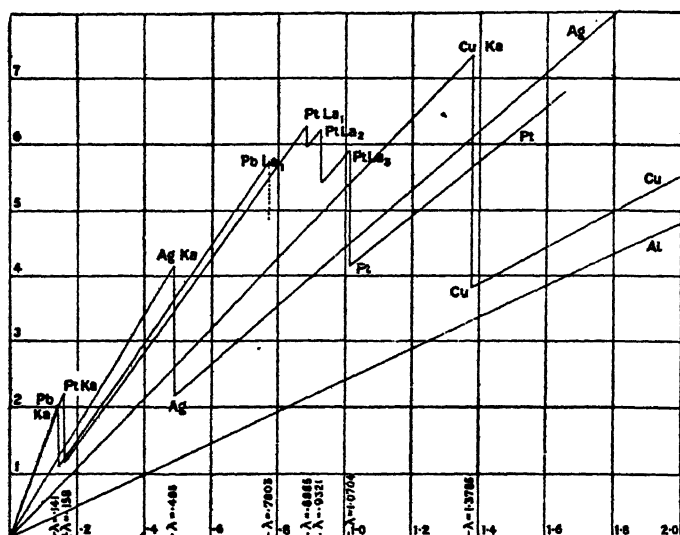
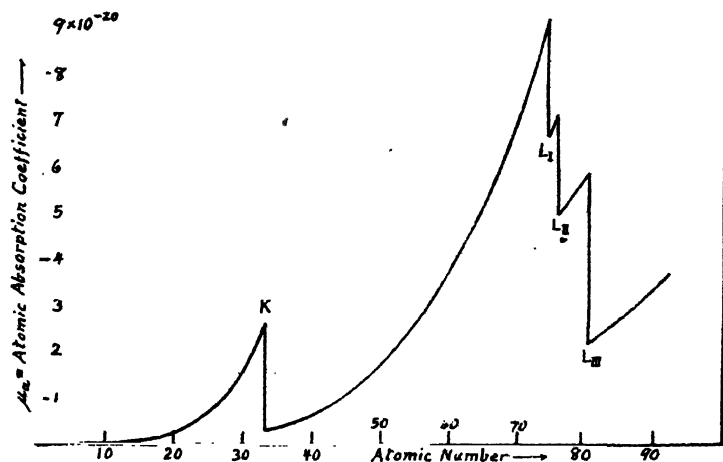
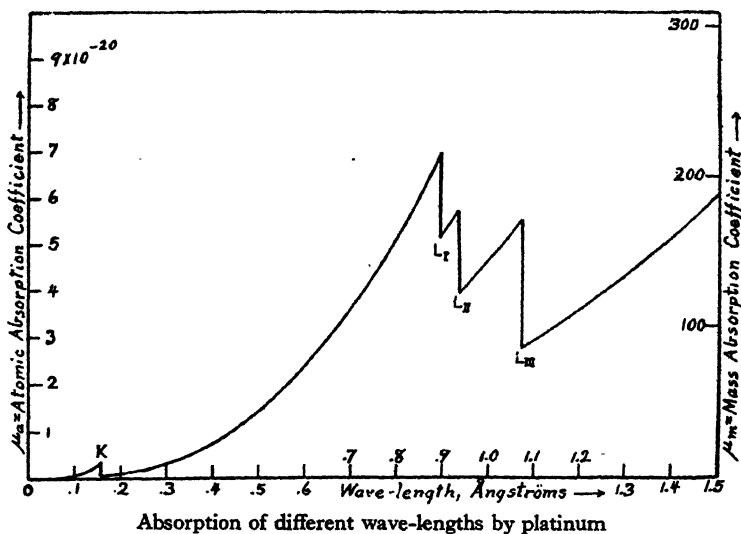


FIG. 174.—Variation of  $(\tau/\rho)^{1/2}$  with wave-length

A better conception of the wide range of absorption coefficients can be got from the graphs in fig. 175, which are due to Compton. The upper curve shows the absorption of various wave-lengths by platinum, the atomic absorption coefficient being plotted against the wave-length of the rays. Alternatively, we may take a definite wave-length, such as 1.00 Å., and plot the atomic absorption coefficient against the atomic number of various absorbing screens, as in the lower graph. In both cases it will be seen that the coefficient decreases by five or six times as an edge or group of edges is passed.

Though these graphs give a general idea of the dependence of absorption coefficients upon wave-length and atomic number, a table of absorption coefficients, such as is given in a subsequent appendix, must be consulted for accurate values. In order to find the absorption by a composite screen, the mass absorption coefficients for the different elements in the screen are multiplied by the mass per unit area of the respective elements, and the products are added:

$$I = I_0 e^{-\sum m_k \cdot \mu_k / \rho_k}$$



Absorption of wave-length 1.00 Å. by different elements

FIG. 175.—Variation of  $\tau/\rho$  with wave-length and with atomic number

(By courtesy of D. Van Nostrand Company, Inc.)

The absorption coefficient plays an important part in X-ray analysis. It is necessary to know its value when absolute measurements are being made. Further, in the rotation and powder methods it is desirable to avoid the use of a radiation which is

just on the short-wave side of the absorption edge of an element in the crystal. Such radiation is strongly absorbed, and there is an intense production of secondary X-rays which fog the record.

Advantage is taken of the difference in absorption coefficient on either side of an absorption edge to 'filter' the radiation from a tube. In powder and rotation photographs, measurements made with the diffracted  $K\alpha$  radiation are required, and the lines or spots due to  $K\beta$  radiation merely confuse the record. By

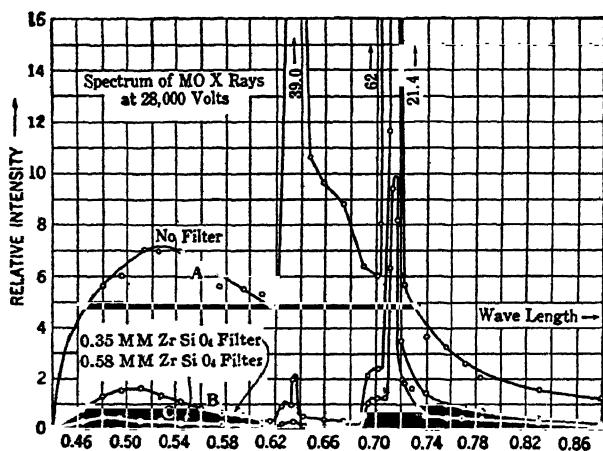


FIG. 176.—Use of filter to reduce  $K\beta$  radiation of molybdenum

(From *X-Ray Studies*, General Electric Company)

choosing a screen containing an element whose K edge lies between the  $K\alpha$  and  $K\beta$  lines of the anticathode, the shorter  $K\beta$  rays can be heavily absorbed, while the  $K\alpha$  rays are transmitted with relatively small loss of intensity. Fig. 176, for instance, shows the effect of a filter containing zirconium upon the rays from a molybdenum anticathode. A screen of  $ZrSiO_4$ , 0.35 mm. in thickness, reduces the height of the  $K\beta$  peak from 39 to 2 in the graph, whereas the  $K\alpha$  peak is only reduced from 62 to 21. Much of the white radiation is absorbed at the same time, and such filters have a most pronounced effect in improving photographs. Appropriate filters for anticathodes of silver, molybdenum, and copper contain palladium, zirconium, and nickel respectively.

## THE COMPTON EFFECT

It has already been mentioned in the chapter on X-ray Optics that X-rays scattered by an atom are of two types, coherent and incoherent. The coherent rays are scattered without change of wave-length, and are responsible for the diffraction phenomena. The incoherent radiation is of longer wave-length than the incident rays, and its scattering is accompanied by the ejection of an electron from the atom. These ejected electrons were first observed by C. T. R. Wilson as short cathode-ray tracks in his cloud-chamber photographs, which he termed 'fish-tracks' because they were all heading in a direction nearly parallel to the incident rays, like fish in a stream. The change in wave-length of the scattered radiation was first measured by Compton, who gave an explanation of the effect as being due to the scattering of a quantum by an electron, with a consequent recoil of the electron.

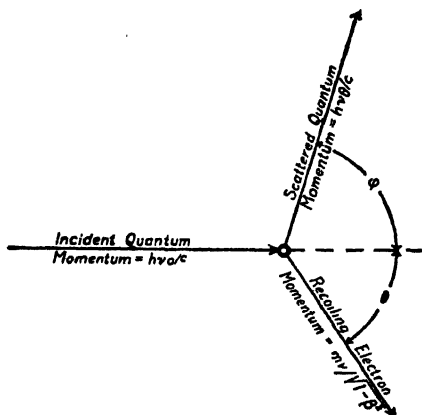


FIG. 177.—The Compton effect  
(By courtesy of D. Van Nostrand Company, Inc.)

Compton considered the incident quantum to have an energy  $h\nu_0$  and a momentum  $h\nu_0/c$ . On collision with an electron of mass  $m$ , the electron recoils with velocity  $v$  in a direction making an angle  $\theta$  with the incident ray, while the quantum is deflected through an angle  $\phi$  and its frequency is changed to  $\nu_\theta$ . Compton treated the problem as a dynamical process, subject to the conservation of energy and momentum. The conservation of energy leads to the equation

$$h\nu_0 = h\nu_\theta + mc^2 \left( \frac{1}{\sqrt{1-\beta^2}} - 1 \right),$$

where  $\beta = v/c$ . The conservation of momentum parallel and perpendicular to the ray direction leads to (see fig. 177)

$$\frac{h\nu_0}{c} = \frac{h\nu_\theta}{c} \cos \phi + \frac{mv}{\sqrt{1-\beta^2}} \cos \theta,$$

$$0 = \frac{h\nu_0}{c} \sin \phi + \frac{mv}{\sqrt{1-\beta^2}} \sin \theta.$$

The solution of these equations gives the change  $\delta\lambda$  in wavelength of rays scattered through an angle  $\phi$ ,

$$\delta\lambda = \frac{h}{mc}(1 - \cos \phi),$$

which Compton verified by spectrometer measurements.

The contribution to the absorption coefficient of both scattering processes is included in the  $\sigma/\rho$  term in

$$\mu/\rho = \sigma/\rho + \tau/\rho.$$

The relative parts played by coherent and incoherent scattering have been discussed in the chapter on X-ray Optics.

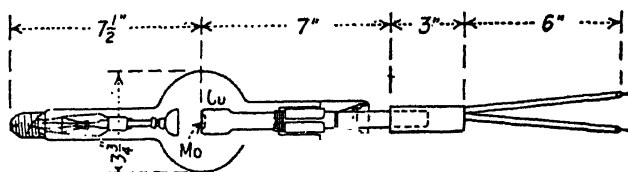
#### APPARATUS

The current in an X-ray tube may be carried either by a discharge through gas at low pressure in the tube, or by an electron stream which in general is produced by a heated filament. In tubes of the 'sealed off' type, *i.e.* those which are not connected to a pump while running, it is now universal to employ an electron source, such as a hot filament, and to have the highest possible vacuum in the tube. The current is governed by the temperature of the filament, which avoids the instability of the earlier type of gas tube.

Two types of tube are shown in fig. 178. The Coolidge tube represents the first practical realisation of the hot-wire principle. A special filament is contained in the cathode on the left, and it is heated by a current from an auxiliary transformer or a battery. The anticathode on the right is a molybdenum button set in a copper tube, which is water-cooled. The anticathode surface is at right angles to the axis of the tube, since greater intrinsic brightness of the focal spot is obtained when rays come off the surface at a small glancing angle. The Philips tube is constructed of glass and chromium-iron alloy fused together. The reservoir on the left contains water which cools the anticathode. The window through which the rays emerge is made of a soda-glass which is highly transparent to X-rays. An advantage of the

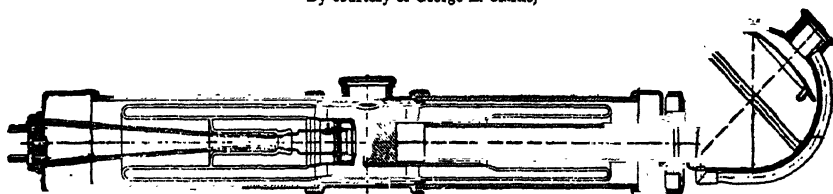
Philips metalix tube is the absorption by the metal of the tube of all radiation except that passing through the window. Tubes are made with anticathodes of molybdenum, rhodium, copper, chromium, or iron.

Tubes which are attached to pumps are of two types, depending on gas discharge or on a hot filament for the maintenance of



(a) Coolidge tube

By courtesy of George L. Clarke)



(b) Philips metalix tube

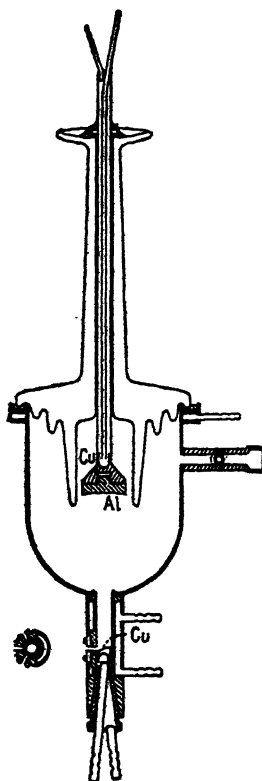
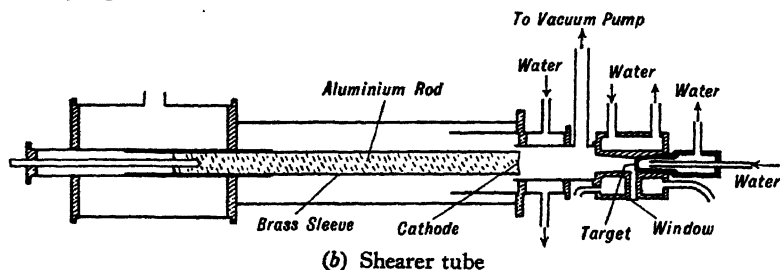
(From *Philips Metalix, X-Ray Tubes for Research Work*)

FIG. 178

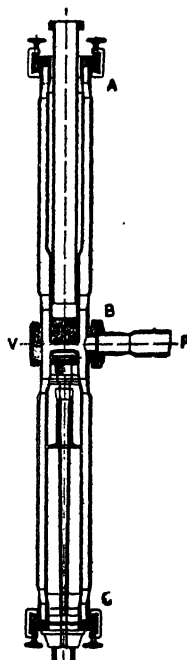
the current. Famous tubes of the former type are due to Hadding and to Shearer (fig. 179). These tubes are continuously evacuated while running, the gas pressure in the tube being maintained at a suitable level by balancing the action of the pump against a small adjustable leak. The figure also shows a demountable tube of the Philips type, which works on the hot-wire cathode principle. In this case, of course, the tube is evacuated as completely as possible by the pump while running. The advantage of all these tubes consists in the ease with which cathode and anticathode can be replaced or changed. In the Philips tube, for example, the vacuum seal is effected by means of a rubber washer gripped between two flanges by the screws seen at the upper and lower ends of the tube. If a filament burns out, or an anticathode of a different metal is desired, it is a very simple matter to take the tube to pieces and effect the change.

The source of high tension most widely employed is a transformer. The high-tension leads can be connected directly to any

tube which has a hot-wire cathode, since these tubes are self-rectifying. A current in the reverse direction, which would soon



(By courtesy of George L. Clarke)



(From *Philips Metalix, X-Ray Tubes for Research Work*)

FIG. 179

break down the tube, cannot pass, since the electron stream only originates at the cathode. Some gas tubes, such as the

Shearer tube, also possess the self-rectifying property when the degree of vacuum is correctly adjusted. The best results are obtained, however, by the more elaborate installation of a rectifying valve and condenser system which provides a nearly steady source of unidirectional current at high tension to a tube with a hot-wire cathode.

### REFRACTION, REFLECTION, AND INTERFERENCE OF X-RAYS.

*The Refractive Index.*—The velocity of X-rays traversing matter is slightly different from their velocity *in vacuo*. Considered classically, the electrons vibrate under the influence of the radiation. If the X-ray frequency is higher than the frequency associated with the electrons, as will generally be the case for the majority of electrons in the atom, the displacement of an electron at a given moment will always be opposite to the force exerted on it by the electromagnetic wave. The case is the reverse of that ordinarily met with in optics, where the electrons are displaced in the direction of the force acting on them because they are firmly bound and the light frequency is small. In optical dispersion, the electronic displacement gives rise to a refractive index greater than unity; in the case of X-rays, the reversed electronic displacement implies a refractive index smaller than unity. This may be expressed more precisely by quoting Sellmeier's formula for the refractive index

$$\mu^2 = 1 + (e^2/\pi m) \sum_1^N n_s/(\nu_s^2 - \nu^2),$$

where  $n_s$  is the number of electrons per unit volume with characteristic frequency  $\nu_s$ , and there are  $N$  different kinds of electrons. When  $\nu$  is very large compared with all values of  $\nu_s$ , this becomes

$$\mu^2 = 1 - e^2 n / \pi m \nu^2,$$

where  $n$  is the total number of electrons per unit volume. The frequency  $\nu$  is very much larger in the case of X-rays than in that of light, hence the value of  $\mu$  differs only slightly from unity. This expression may therefore be written

$$\mu = 1 - ne^2/2\pi m \nu^2,$$

where  $n$  is the total number of electrons in unit volume.

The Sellmeier formula is based on classical dynamics and



the assumption of electrons with characteristic free periods. A similar result is yielded by quantum mechanics, however, on account of the correspondence between the classical and wave-mechanical expressions for scattering by the electrons described in the chapter on X-ray Optics. If waves of amplitude  $A$  fall on an atom containing  $N$  electrons, the scattered amplitude at a distance  $r$  in the forward direction will be  $N \cdot A/r \cdot e^2/mc^2$ , because  $f$  is equal to  $N$ ; all the scattered radiation is also coherent. Each electron, in other words, contributes an amount  $A/r \cdot e^2/mc^2$ . Consider a depth  $t$  of the material, containing  $n$  electrons per unit volume. By drawing Fresnel zones in the usual way, it follows that the scattered waves build up a wave-train whose amplitude is given by

$$A' = nt\lambda A \cdot e^2/mc^2.$$

This wave-train is one-quarter of a wave-length *ahead*\* of the primary wave, and its amplitude is small in comparison with  $A$ . The resultant of the two trains is therefore a wave-train of amplitude  $A$  whose phase is slightly ahead of the incident train in phase, by an amount  $\phi$  (fig. 180), where

$$\phi = A'/A = nt\lambda \cdot e^2/mc^2.$$

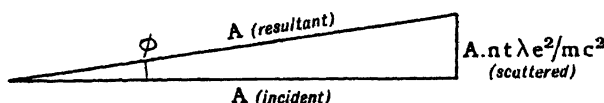


FIG. 180.—Refraction of X-rays

The corresponding path difference is  $\lambda\phi/2\pi$ :

$$\lambda\phi/2\pi = nt\lambda^2 e^2/2\pi mc^2 = t \cdot ne^2/2\pi mv^2.$$

The medium has therefore acted upon the waves as if it had a refractive index

$$1 - ne^2/2\pi mv^2.$$

According to this formula, the refractive index depends only upon the frequency and the number of electrons in unit volume. It is not affected by the state of the body whether crystalline or amorphous. A few values chosen from a table given by

\* The individual scattered wavelets are in opposite phase to the transmitted primary wave, and their combination to form a plane wave introduces a lag of one quarter of a wave-length. The result of the two effects is equivalent to a wave-train which is one quarter of a wave-length in advance of the primary beam.

Compton \* will serve to show the magnitude of the effect. The figures are values of  $(1 - \mu) \times 10^6$ , which is positive, since  $\mu$  is less than unity. Calculated values are in good accord with values measured experimentally by the various methods described below.

$\lambda$	Substance	$(1 - \mu) \times 10^6$ (calc.)	$(1 - \mu) \times 10^6$ (exp.)
0.52 A.	Glass	0.9	0.9
0.708	Calcite	1.84	2.03
0.708	Speculum	4.90	4.77
1.538	Glass	8.14	8.12
1.933	Glass	12.8	12.4

The above formula requires modification when the X-ray wave-length is greater than that of any absorption edges in the material. In this case there is an effect analogous to anomalous dispersion in optics. The study of this effect is in fact a branch of X-ray optics with important theoretical implications; the  $f$  curves, and consequently the refractive indices, need special consideration when the K edge of the atom, for instance, has a higher frequency than the X-rays. It is only possible here to draw attention to this effect.

The existence of this refractive index, and the interesting implication that the law of reflection  $n\lambda = 2d \sin \theta$  cannot be strictly true, was first deduced by Darwin in 1914. He showed that when X-rays are reflected from a crystal face which is parallel to the atomic planes, the actual glancing angle  $\theta'$  will differ slightly from the above angle  $\theta$  by an amount

$$\theta' - \theta = (1 - \mu) / \sin \theta \cos \theta.$$

The X-rays are bent away from the normal when they enter the body, and their effective wave-length is increased, so that both factors make the glancing angle greater than that given by the simple reflection law. This deviation from the reflection law is less for high orders than for low orders, hence a calculation of the apparent wave-length of X-rays, using the formula  $n\lambda = 2d \sin \theta$ , will give different results for different orders. Such an effect was first noticed by Stenström with soft X-rays, and was interpreted by Ewald as due to refraction.

The correction due to the refractive index is extremely small,

\* *X-Rays and Electrons*, p. 211.

being only a few seconds of arc. An ingenious method due to Davis and von Nardroff greatly increases the deviation, and enables accurate measurements to be made. This consists in cutting the crystal so that the face makes an angle with the crystal planes very nearly equal to the glancing angle of reflection. When either the incident beam enters or the reflected beam leaves the crystal at a small glancing angle, the effects of refraction are greatly increased. By cutting a face of iron pyrites so as to make an angle of  $6^{\circ} 32'$  with the crystal plane (100), Davis and von Nardroff obtained a deviation of  $39''$  for the Mo  $K\alpha$  line, and  $160''$  for the Mo  $K\beta$  line, which are reflected at  $7^{\circ} 31'$  and  $6^{\circ} 43'$  at the normal cube face.

A direct observation of the refractive index by passing a narrow beam of X-rays through a prism had often been attempted, but the first successful measurement of this kind was made in 1924 by Larsson, Siegbahn, and Waller. The prism was so placed that the incident rays (Cu or Fe K lines) fell at a very small glancing angle upon the first face, and left the second face nearly normal. Advantage was thus taken of the comparatively large deviation due to refraction when the glancing angle is small, and they were able to photograph a refracted ray making an angle of several minutes with the direct beam.

*Total Reflection.*—A very interesting consequence of the refractive index, first realised and shown experimentally by Compton, is that it is possible to obtain total reflection of an X-ray beam at a plane surface. In the corresponding optical phenomenon, a ray travelling in a medium of refractive index  $\mu_1$ , and falling upon an interface where the refractive index changes to a smaller value  $\mu_2$ , is totally reflected when the critical angle of incidence exceeds the value given by

$$\sin \phi = \mu_2 / \mu_1.$$

The ray, travelling in the denser medium, undergoes total internal reflection. In the case of X-rays, the refractive index is smaller in the solid than in air or *in vacuo*, hence X-rays may be said to be totally externally reflected. Moreover, although  $\mu$  differs so little from unity, the critical glancing angle  $\theta$  is quite appreciable. It is given by

$$\begin{aligned} \cos \theta &= 1 - \theta^2/2 = \mu, \\ \theta &= \sqrt{2(1 - \mu)}. \end{aligned}$$

Critical angles for values of  $(1 - \mu)$  are given below.

$(1 - \mu) \times 10^6$	Critical angle in minutes of arc
1	4.8
5	11.1
10	15.7

The existence of this critical angle was demonstrated by Compton with the apparatus shown in fig. 181. The slit S can be set so as

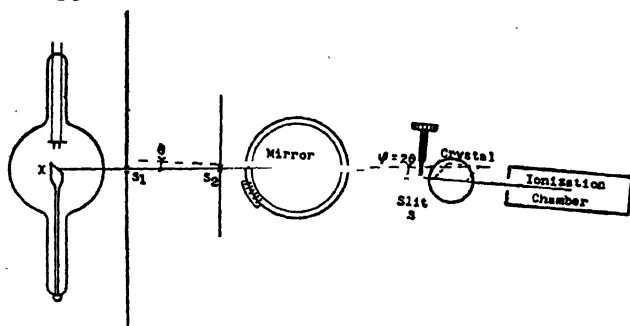


FIG. 181.—Specular reflection of X-rays (Compton)

(*Phil. Mag.*, **xlv**, 1123, 1923)

to select a beam which has been deviated through a known angle  $2\theta$ , and the reflected radiation can then be analysed spectrally by the crystal. As an instance, Compton reflected the rays from a tube with a tungsten anticathode at a series of angles, measuring for each angle the intensity of the L line  $1.279 \text{ \AA}$ . in the reflected beam. Using a glass mirror of density  $2.52$ , Compton calculated a value of  $5.2 \times 10^{-6}$  for  $(1 - \mu)$ , corresponding to a critical angle of  $11'$ . The curve in fig. 182, A, shows that the reflected beam is constant at small angles, and then falls rapidly to zero as the critical angle is reached. Fig. 182, B, shows a similar curve for a silvered plate covered with lacquer, in which the critical angles for both silver and lacquer surfaces are evident. Compton also showed that over 90 per cent. of the incident beam is reflected at angles inside the critical angle.

*Diffraction by a Ruled Grating.*—The deviation of X-rays by total reflection through an angle without appreciable loss of

intensity makes it possible to obtain a series of interference effects which have their analogies in optics, the characteristic feature of the X-ray effects being that they must be looked for within a small angular range measured in minutes of arc. The most important of these is the production of X-ray spectra from a ruled reflection grating, which was also first demonstrated by Compton. The incident beam falls upon the grating at a small

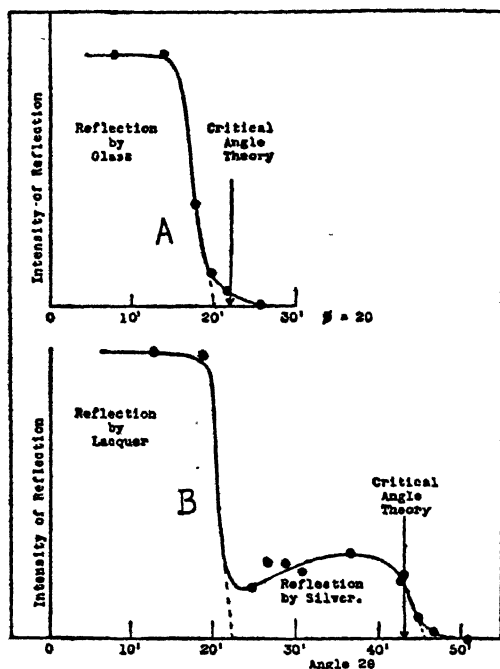


FIG. 182.—Critical angle of reflection (Compton)

(*Phil. Mag.*, xlv, 1127, 1923)

glancing angle. Spectra appear on either side of the reflected beam, which may be considered as the spectrum of zero order. The rulings on the grating are quite coarse (500 to the centimetre in Compton's first experiment), and it is at first sight surprising that measurable deviations should be obtained with such very short waves. To state it broadly, by presenting the grating to the incident light at an extremely fine angle, its effective spacing has been greatly diminished.

Compton's formula for the positions of the spectra is derived as follows:—



# PLATE XXXI

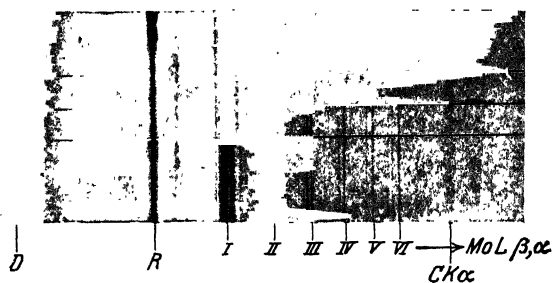
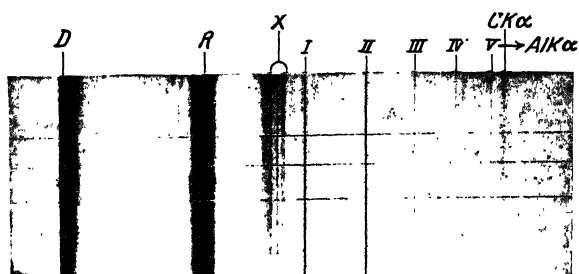


FIG. 183.—X-ray spectra with a ruled grating (Bäcklin). The direct beam is marked D, the reflected beam R, and the spectra are numbered

(*Spektroskopie der Röntgenstrahlen*, Siegbahn; Julius Springer, 1931)



FIG. 184.—Diffraction of X-rays by a narrow slit (Larsson)

(*Spektroskopie der Röntgenstrahlen*, Siegbahn; Julius Springer, 1931)

Let  $\theta$  be the glancing angle at which the incident beam falls upon the grating whose spacing is  $D$ , and let  $\alpha$  be the angle which the spectrum of  $n$ th order makes with the reflected ray. Then

$$\begin{aligned} n\lambda &= D (\cos \theta - \cos (\theta + \alpha)), \\ \lambda &= (D/n)(\alpha\theta + \alpha^2/2), \end{aligned}$$

whence

$$\alpha = \sqrt{(2n\lambda/D) + \theta^2} - \theta.$$

To take a numerical instance, if  $D = 2 \times 10^{-3}$  cm.,  $\lambda = 0.708 \times 10^{-8}$  cm.,  $\theta = 10' = 2.92 \times 10^{-3}$  radians, it follows that

$$\begin{array}{ll} \alpha = -5.9' & \text{for } n = -1 \\ = 0 & n = 0 \\ = 3.5' & n = 1 \\ = 6.3' & n = 2 \end{array}$$

Fig. 183, Pl. XXXI, shows very fine spectra of the Al  $K\alpha$  line, and the Mo  $L\beta$  and  $L\alpha$  lines, obtained by Bäcklin. Six orders can be seen in each case.

The production of X-ray spectra by a ruled grating has been developed by Siegbahn, Thibaud, and others, and has attained a high degree of accuracy. It has been used to explore the range between X-ray and optical frequencies. By comparing the diffraction of a given X-ray wave-length by grating and by crystal, one is in effect measuring the crystal spacing in terms of the spacing ruled on the grating. This constitutes a new method of measuring the values of atomic constants, for the measurement of crystal spacing gives the mass of the scattering unit in the crystal, and so the masses of atoms. Hence increases in the accuracy of the grating measurements are of the greatest importance.

*Interference Fringes.*—The list of interference effects obtained with X-rays which are analogous to optical interference is being rapidly extended. Larsson, in 1929, produced typical diffraction patterns by passing a beam of X-rays through a narrow slit, about  $6 \mu$ . in width. The fringes were so well defined (fig. 184, Pl. XXXI) that it was possible to estimate to 1 per cent. the width of the slit, which was used in his experiments on dispersion by a prism. The wave-length in these experiments was  $8.3 \text{ \AA}$ ., the  $K\alpha$  line of aluminium. Equally striking interference effects have been observed with X-rays of shorter wave-length. Linnik, for



instance, has obtained fringes by the Lloyd's mirror method, using the  $K\alpha$  lines of copper ( $1.54 \text{ \AA}$ .) and iron ( $1.93 \text{ \AA}$ .). His apparatus is shown in fig. 185, and is most ingeniously designed so as to make possible the very precise adjustments which are necessary. The slit through which the X-rays pass is formed between the polished plates A and B, and is  $0.1 \mu$  in width. X-rays emerge as coherent waves with a divergence of  $2'$  from so narrow a slit. The slit is made parallel to the Lloyd's mirror S by observing optical interference fringes in the air film between A and S, and these fringes are also used to measure the distance of the slit from the plane of the mirror. Part of the beam issuing from the slit is intercepted and reflected by the mirror, and interference fringes are produced at P where this beam crosses the path of that

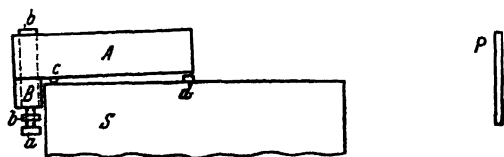
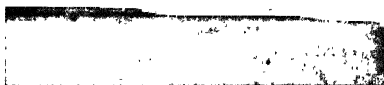
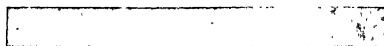


FIG. 185.—Lloyd's mirror arranged for X-ray interference (Linnik)  
(*Zeit. f. Physik*, 85, 108, 1930)

part of the original beam which has escaped reflection. The fringes are shown in fig. 186, A, Pl. XXXII. Estimates of  $1.56 \pm 0.02 \text{ \AA}$ . for Cu  $K\alpha$ , and  $1.96 \text{ \AA}$ . for Fe  $K\alpha$ , were obtained.

Kuhlenkamp has obtained interference fringes corresponding to those formed by light reflected by thin films. A narrow beam of monochromatic X-rays (Ni  $K\alpha$ ,  $1.66 \text{ \AA}$ .) is reflected from a surface consisting of a deposit of nickel,  $1400 \text{ \AA}$  in thickness, upon a flat glass plate. The plate is slowly turned during the experiment, and the reflected beam is recorded on a photographic plate. For all angles within the critical angle for nickel, the beam is totally reflected and makes a continuous band on the plate (fig. 186, B). As the critical angle is passed, a fraction of the radiation enters the nickel and is reflected by the nickel-glass surface below. The two beams reflected at the upper and lower surfaces interfere, reinforcing each other for some angles of incidence and destroying each other at intermediate points. A fine series of fringes outside the continuous band is formed, shown in fig. 186, B. It is surprising to note how far apart the fringes are, the reproduction being only enlarged three times; this wide spacing is due to the fact that the rays in the nickel film are travelling very nearly parallel to

PLATE XXXII



A. Lloyds mirror fringes (Linnik)

(*Zeit. f. Physik*, 65, 109, 1930)



↑  
Direct beam

Range of reflection

B. Reflection by thin film (Kuhlenkamp)

FIG. 186



the surface, so that the optical path difference for rays reflected by the upper and lower surfaces is extremely small.

We may sum up by saying that the gap between optical and X-ray interference phenomena has been completely bridged. In many cases the X-ray and optical effects are similar, and in others there is a continuous transition from one characteristic type to the other as the wave-length increases. The peculiar effects which form the subject of this book only arise because X-ray wave-lengths are less than interatomic distances.

## APPENDIX II

### EMISSION SPECTRA AND ABSORPTION EDGES

THE following tables give the strongest lines in the K, L, and M spectra, and also a list of absorption edges. In the case of the L and M series the most pronounced edge is alone given. The wave-lengths are in X-units. One X-unit is approximately  $10^{-11}$  cm., but actually owing to the uncertainty in estimating a standard crystal spacing it is necessary to base the measurements upon an assumed value for calcite (200) of 3029.45 X-units.\*

The values are from Siegbahn's *Spektroskopie der Röntgenstrahlen*, 2nd edition.

TABLE X  
*K Emission Spectra and Absorption Edges*

Element	Atomic No.	$\alpha_2$	$\alpha_1$	$\beta_2$	$\beta_1$	$\beta_2$	Absorption edge
Sodium .	11	11885		Here $\beta_2$ is not resolved from $\beta_1$	11594	$\beta_2$ decreases rapidly in intensity with decreasing atomic numbers below 42, and is not observed below nickel	
Magnesium .	12	9869			9539		9496.2
Aluminium .	13	8320.5			7965		7935.6
Silicon .	14	7111.06			6754.5		6731.0
Phosphorus .	15	6142.5			5792.1		5774.9
Sulphur .	16	5363.7	5361.3	Here $\beta_2$ is not resolved from $\beta_1$	5021.1	$\beta_2$ decreases rapidly in intensity with decreasing atomic numbers below 42, and is not observed below nickel	5008.8
Chlorine .	17	4721.2	4718.2		4394.2		4383.8
Potassium .	19	3737.07	3733.68		3446.8		3431.0
Calcium .	20	3354.95	3351.69		3083.4		3064.3
Scandium .	21	3028.40	3025.03		2773.9		2751.7
Titanium .	22	2746.81	2743.17		2509.0		2491.2
Vanadium .	23	2502.13	2498.35		2279.7		2263.0
Chromium .	24	2288.91	2285.03		2080.6		2065.9
Manganese .	25	2101.49	2097.51		1906.20		1891.6
Iron .	26	1936.012	1932.076		1753.013		1739.4

\* This value is taken to be the actual spacing of the crystal planes. Owing to the correction for refraction, the value to be inserted in the reflection formula for the order 200 is 3029.04 X-units.

TABLE X—continued  
K Emission Spectra and Absorption Edges

Element	Atomic No.	$\alpha_2$	$\alpha_1$	$\beta_3$	$\beta_1$	$\beta_2$	Absorption edge
Cobalt .	27	1789.19	1785.29	Here $\beta_3$ is not resolved from $\beta_1$	1617.44		1604.0
Nickel .	28	1658.35	1654.50		1497.05	1485.61	1483.9
Copper .	29	1541.232	1537.395		1389.35	1378.24	1377.4
Zinc .	30	1436.03	1432.17		1292.55	1281.07	1280.5
Gallium .	31	1340.87	1337.15		1205.20	1193.8	1190.2
Germanium	32	1255.21	1251.30	Here $\beta_3$ is not resolved from $\beta_1$	1126.71	1114.59	1114.6
Arsenic .	33	1177.43	1173.44		1055.10	1042.81	1042.63
Selenium .	34	1106.52	1102.48		990.13	977.91	977.73
Bromine .	35	1041.66	1037.59		930.87	918.53	918.09
Krypton .	36	978			875		
Rubidium .	37	927.76	923.64	827.49	826.96	814.76	814.10
Strontium .	38	877.61	873.45	781.83	781.30	769.21	768.37
Yttrium .	39	831.32	827.12	739.72	739.19	727.13	725.5
Zirconium .	40	788.51	784.30	700.83	700.28	688.50	687.38
Niobium .	41	748.89	744.65	664.96	664.38	652.80	651.58
Molybdenum	42	712.105	707.831	631.543	630.978	619.698	618.48
Ruthenium .	44	646.06	641.74	571.93	571.31	560.51	558.4
Rhodium .	45	616.37	612.02	545.09	544.49	533.96	533.03
Palladium .	46	588.63	584.27	520.09	519.47	509.18	507.95
Silver .	47	562.67	558.28	496.65	496.01	486.03	484.48
Cadmium .	48	538.32	533.90	474.71	474.08	464.20	463.13
Indium .	49	515.48	511.06	454.23	453.58	444.08	442.98
Tin .	50	494.02	489.57	434.95	434.30	424.99	423.94
Antimony .	51	473.87	469.31	416.23	407.10	406.09	406.09
Tellurium .	52	454.91	450.37	399.26	390.37	389.26	389.26
Iodine .	53	437.03	432.49	383.92	383.15	374.71	373.44
Xenon .	54	417			360		
Cæsium .	55	404.11	399.59	354.36	353.62	345.16	344.04
Barium .	56	388.99	384.43	340.89	340.22	332.22	330.70
Lanthanum .	57	374.66	370.04	328.09	327.26	319.66	318.14
Cerium .	58	361.10	356.47	315.72	315.01	307.70	306.26
Praseodymium	59	348.05	343.40	304.39	303.60	296.25	295.1
Neodymium	60	335.95	331.25	293.51	292.75	285.73	284.58
Samarium .	62	313.02	308.33	273.25	272.50	265.75	264.4
Europium .	63	302.65	297.90	263.86	263.07	256.45	254.8
Gadolinium	64	292.61	287.82	254.71	253.94	247.62	246.2
Terbium .	65	282.86	278.20	246.29	245.51	239.12	237.6
Dysprosium	66	273.75	269.03	237.87	237.10	231.28	230.1
Holmium .	67	264.99	260.30	...	...	...	222.64
Erbium .	68	256.64	251.97	223.00	222.15	216.71	

TABLE X—*continued*  
*K Emission Spectra and Absorption Edges*

Element	Atomic No.	$\alpha_2$	$\alpha_1$	$\beta_3$	$\beta_1$	$\beta_2$	Absorption edge
Thulium .	69	248.61	243.87	215.58	214.87	...	208.5
Ytterbium .	70	240.98	236.28	209.16	208.34	203.22	201.6
Lutecium .	71	233.58	228.82	202.52	201.71	196.49	195.1
Hafnium .	72	226.53	221.73	195.83	195.15	190.42	190.1
Tantalum .	73	219.73	214.88	189.91		184.52	183.6
Tungsten .	74	213.45	208.62	184.22		178.98	178.22
Osmium .	76	201.31	196.45	173.61		168.75	167.55
Iridium .	77	195.50	190.65	168.50		163.76	162.09
Platinum .	78	190.04	182.23	163.70		158.87	157.70
Gold .	79	184.83	179.96	159.02		154.26	153.20
Thallium .	81	174.66	169.80	150.11		145.39	144.41
Lead .	82	170.04	165.16	146.06		141.25	140.49
Bismuth .	83	165.25	160.41	142.05		136.21	136.78
Thorium .	90	136.8	132.3	116.9		113.4	112.70
Uranium .	92	130.95	126.40	111.87		108.42	106.58?
Approximate relative intensities		50	100	7	14	< 5	

TABLE XI  
L Emission Spectra and  $L_{III}$  Absorption Edges

Element	Atomic Number	$\lambda$	$\eta$	$a_2$	$a_1$	$\beta_1$	$\beta_2$	$\beta_3$	$\beta_4$	$\beta_5$	$\gamma_1$	Absorption edge $L_{III}$
Copper .	29	15190	14830	13306	13030	...	...	12100	...	...	...	6841.3
Zinc .	30	13950	13610	12230	11960	...	...	11160	...	...	...	6362.0
Gallium .	31	12890	12560	11270	11010	...	...	...	...	...	...	5944.4
Germanium .	32	11922	11587	10415	10153	...	...	...	...	...	...	...
Arsenic .	33	11048	10711	9652	9395	...	...	8912	...	...	...	...
Selenium .	34	10272	9939	8972	8718	...	...	...	...	...	...	...
Bromine .	35	9564	9235	8358	8109	...	...	...	...	...	...	...
Rubidium .	37	...	...	...	...	...	...	...	...	...	...	...
Strontium .	38	7822	7506	6848.6	6610.0	...	...	6769.4	6800.9	6358.2	6968.1	6841.3
Yttrium .	39	...	7031.0	6435.7	6203.9	...	...	5974.1	6391.8	6007.7	6508.1	6362.0
Zirconium .	40	6899	6593.9	6056.7	5823.6	...	...	5618.6	5651.7	5574.2	5373.8	5561.0
Niobium .	41	6510	6196	5718	5480.3	...	...	5297.1	5330.6	5226.0	5024.8	5212.1
Molybdenum .	42	...	5836	5401	5166.5	...	...	5004.7	5041.0	4910.0	...	4904.2
Ruthenium .	44	5486.4	...	4843.7	4611.0	...	...	4476.4	4512.6	4361.9	4172.8	4360.4
Rhodium .	45	5207.0	4911.2	4595.6	4364.0	...	...	4244.7	4280.2	4122.1	3935.7	4121.2



TABLE XI—continued  
L Emission Spectra and  $L_{III}$  Absorption Edges

Element	Atomic Number	$\lambda$	$\eta$	$a_1$	$a_2$	$\alpha_1$	$\beta_1$	$\beta_2$	$\beta_3$	$\beta_4$	$\beta_5$	$\gamma_1$	Absorption edge $L_{III}$
Palladium .	46	4939.6	4650.2	4366.6		4358.5	4137.3	3900.7	4025.7	4062.3		3716.4	3903.9
Silver .	47	4697.6	4410.1	4153.8		4145.6	3926.6	3693.8	3824.5	3861.1		3514.9	3690.8
Cadmium .	48	4471.3	4187.5	3956.4		3947.8	3730.1	3506.4	3636.4	3674.3		3328.0	3496.3
Indium .	49	4259.3	3976.1	3772.4		3703.7	3547.8	3331.2	3461.9	3499.0		3155.3	3315.5
Tin .	50	4063.3	3781.8	3601.1		3592.2	3377.9	3167.9	3298.9	3336.3		2994.9	3149.3
Antimony .	51	3880.3	3599.6	3440.8		3431.8	3218.4	3016.6	3145.1	3184.3		2845.1	2990.7
Tellurium .	52	3710.1	...	3291.0		3282.0	3070.0	2876.1	3001.3	3040.0		2706.5	2845.7
Iodine .	53	3549.7	...	3150.9		3141.7	2930.9	2746.1	2868.2	2905.9		2577.5	2713.9
Cæsium .	55	3259.6	2983.3	2895.6		2886.1	2677.8	2566.4	2622.9	2660.5		2342.5	2467.4
Barium .	56	3128.7	2857.1	2779.0		2769.6	2562.2	2399.3	2511.0	2549.8		2236.6	2356.8
Lanthanum .	57	3000	2734	2668.9		2659.7	2453.3	2298.0	2405.3	2443.8		2137.2	2253.7
Cerium .	58	2885.7	2614.7	2565.1		2556.0	2351.0	2204.1	2305.9	2344.2		2044.3	2159.5
Praseodymium	59	2778.1	2507	2467.6		2457.7	2253.9	2114.8	2212.4	2250.1		1956.8	2072.8
Neodymium .	60	2670.3	2404.2	2375.6		2365.3	2162.2	2031.4	2122.2	2162.2		1873.8	1990.7
Samarium .	62	2477	2214	2205.7		2195.0	1993.6	1878.1	1958.0	1996.4		1723.1	1840.8
Europium .	63	2390.3	...	2127.3		2116.3	1916.3	1808.2	1882.7	1922.1		1654.3	1771.7
Gadolinium .	64	2307.1	...	2052.6		2041.9	1842.5	1741.9	1810.9	1849.3		1588.6	1706.0
Terbium .	65	2229.0	...	1982.3		1971.5	1772.7	1679.0	1742.5	1781.4		1526.6	1645.3
Dysprosium .	66	2154.0	1892.2	1915.6		1904.6	1706.6	1619.8	1677.7	1716.7		1469.7	1576
Holmium .	67	2082.1	1822.0	1852.1		1841.0	1643.5	1563.7	1616.0	1655.3		1414.2	1532.2

TABLE XI—continued  
L Emission Spectra and  $L_{III}$  Absorption Edges

Element	Atomic Number	$l$	$\eta$	$a_2$	$a_1$	$\beta_1$	$\beta_2$	$\beta_3$	$\beta_4$	$\beta_5$	$\gamma_1$	Absorption edge $L_{III}$
Erbium	68	2015.1	1754.8	1791.4	1780.4	1583.4	1510.6	1557.9	1596.4	1563.6	1362.3	1479.19
Thulium	69	1951.1	1692.3	1733.9	1722.8	1526.8	1460.2	1502.3	1541.2	1511.5	1312.7	1429.9
Ytterbium	70	1890	1631	1678.9	1667.8	1472.5	1412.8	1449.4	1482.5	1462.7	1264.8	1382.64
Lutecium	71	1831.8	1573.8	1626.36	1615.51	1420.7	1367.2	1398.2	1437.2	1414.3	1220.3	1337.5
Hafnium	72	1777.4	1519.7	1577.04	1566.07	1371.1	1323.5	1349.7	1389.3	1371.1	1176.5	1293.0
Tantalum	73	1724.9	1467.9	1529.78	1518.85	1324.23	1281.90	1304.09	1343.07	1328.4	1135.58	1251.7
Tungsten	74	1675.0	1418.1	1484.38	1473.36	1279.17	1242.03	1259.92	1298.79	1287.0	1096.30	1212.9
Rhenium	75	1627.3	1370.6	1441.0	1429.97	1236.03	1204.1	1217.6	1256.3	1248.1	1058.7	1175.5
Osmium	76	...	...	1398.66	1388.59	1194.90	1168.84	...	...	...	1022.96	1139.0
Iridium	77	...	1281.7	1359.8	1348.47	1155.40	1132.97	1138.47	1177.15	1175.45	988.76	1103.8
Platinum	78	1496.4	1240.3	1321.55	1310.33	1117.58	1099.74	1101.65	1139.86	1141.00	955.99	1071.0
Gold	79	1456.9	1200.3	1285.02	1273.77	1081.28	1068.01	1065.50	1104.22	1108.63	924.61	1038.2
Mercury	80	1418.41	1161.6	1249.51	1238.63	1046.52	1037.70	1030.46	1069.2	1076.8	894.6	1007.5
Thallium	81	1381.9	1125.4	1216.26	1204.93	1012.99	1008.22	998.50	1036.99	1047.48	865.71	977.8
Lead	82	1347.4	1090.0	1184.08	1172.58	980.83	980.83	967.21	1005.63	1019.06	838.01	949.2
Bismuth	83	1313.7	1056.5	1153.01	1141.50	950.02	953.24	936.66	975.01	991.31	811.43	922.1
Thorium	90	1112.8	852.8	965.85	954.05	763.56	791.92	753.24	791.92	826.46	651.76	760.0
Protoactinium	91	1088.5	827.8	942.7	930.9	740.7	772.1	730.7	768.3	806.2	632.5	
Uranium	92	1064.9	803.5	920.62	908.74	718.51	753.07	708.79	746.4	786.79	613.59	720.8
Approximate relative intensities for elements of high atomic number		3	2	12	100	50	25	10	5	1	10	

TABLE XII

*M Emission Spectra and  $M_v$  Absorption Edges*

Element	Atomic Number	$\alpha_2$	$\alpha_1$	$\beta$	$\gamma$	Absorption edge [ $M_v$ ]
Tantalum .	73	...	7237	7008	6299	...
Tungsten .	74	...	6969	6743	6076	6702
Rhenium .	75	...	6715	6491	5875	...
Osmium .	76	...	6477	6254	5670	6194
Iridium .	77	6262	6249	6025	5490	5961
Platinum .	78	6045	6034	5816	5309	5746
Gold .	79	5842	5828	5612	5135	5529
Thallium .	81	5461	5450	5239	4815	5136
Lead .	82	5288	5274	5065	4665	4945
Bismuth .	83	5119	5108	4899	4522	4762
Thorium .	90	4143	4130	3934	3672	3722
Uranium .	92	3916	3902	3708	3473	3491

## APPENDIX III

### ABSORPTION COEFFICIENTS

THE following table gives for all elements the mass absorption coefficients  $\mu/\rho$  of the radiations most frequently used in X-ray analysis.

The linear absorption coefficient for a substance of mixed composition, which is the constant required for X-ray analysis, is given by the formula

$$\mu = d \sum p \cdot \mu/\rho,$$

where  $d$  is the density of the substance, and  $p$  is the proportion by weight of a constituent element with mass absorption coefficient  $\mu/\rho$ , the sum being taken for all constituents.

TABLE XIII

*Mass Absorption Coefficient of Elements  $\frac{\mu}{\rho}$ , including Scattering*

Radiation		Ag Ka $\lambda$ 0.5604	Rh Ka 0.6149	Mo Ka 0.7097	Cu Ka 1.5392	Ni Ka 1.6565	Fe Ka 1.9344	Cr Ka 2.2869
Absorber Z								
He	2	0.16	0.16	0.18	0.37	0.43	0.64	0.86
Li	3	0.18	0.20	0.22	0.68	0.87	1.48	2.11
Be	4	0.22	0.25	0.30	1.35	1.80	3.24	4.74
B	5	0.30	0.35	0.45	3.06	3.79	5.80	9.37
C	6	0.42	0.51	0.70	5.50	6.76	10.73	17.9
N	7	0.60	0.70	1.10	8.51	10.7	17.3	27.7
O	8	0.80	1.00	1.50	12.7	16.2	25.2	40.1
F	9	1.00	1.32	1.93	17.5	21.5	33.0	51.6
Ne	10	1.41	1.80	2.67	24.6	30.2	46.0	72.7
Na	11	1.75	2.25	3.36	30.9	37.9	56.9	92.5
Mg	12	2.27	2.93	4.38	40.6	47.9	75.7	120.1
Al	13	2.74	3.60	5.30	48.7	58.4	92.8	149
Si	14	3.44	4.52	6.70	60.3	75.8	116.3	192
P	15	4.20	5.36	7.98	73.0	90.5	141.1	223
S	16	5.15	6.65	10.03	91.3	111.5	175	273

TABLE XIII—continued

Mass Absorption Coefficient of Elements  $\frac{\mu}{\rho}$ , including Scattering

Radiation	Ag Ka $\lambda$ 0.5604	Rh Ka 0.6149	Mo Ka 0.7097	Cu Ka 1.5392	Ni Ka 1.6565	Fe Ka 1.9344	Cr Ka 2.2869
Absorber Z							
Cl 17	5.86	7.50	11.62	103.4	125.6	199	308
A 18	6.40	8.00	12.55	112.9	141	217	341
K 19	8.05	10.7	16.7	143	179	269	425
Ca 20	9.66	12.8	19.8	172	210	317	508
Sc 21	10.5	13.8	21.1	185	222	338	545
Ti 22	11.8	15.8	23.7	204	247	377	603
Va 23	13.3	17.7	26.5	227	275	422	77.3
Cr 24	15.7	20.4	30.4	259	316	490	89.9
Mn 25	17.4	22.6	33.5	284	348	63.6	99.4
Fe 26	19.9	25.8	38.3	324	397	72.8	114.6
Co 27	21.8	28.1	41.6	354	54.4	80.6	125.8
Ni 28	25.0	32.3	47.4	49.2	61.0	93.1	145
Cu 29	26.4	34.0	49.7	52.7	65.0	98.8	154
Zn 30	28.2	37.7	54.8	59.0	72.1	109.4	169
Ga 31	30.8	39.7	57.3	63.3	76.9	116.5	179
Ge 32	33.5	42.8	63.4	69.4	84.2	128.4	196
As 33	36.5	46.0	69.5	76.5	93.8	142	218
Se 34	38.5	49.0	74.0	82.8	100.6	152	235
Br 35	42.3	53.5	82.2	92.6	112.4	169	264
Kr 36	45.0	57.5	88.1	100.4	122	182	285
Rb 37	48.2	62.8	94.4	109.1	133	197	309
Sr 38	52.1	68.3	101.2	119	145	214	334
Y 39	55.5	74.0	108.9	129	158	235	360
Zr 40	61.1	80.9	117.2	143	173	260	391
Nb 41	65.8	86.0	118.7	153	183	279	415
Mo 42	70.7	91.6	120.2	164	197	299	439
Ru 44	$a_1$ 79.9 $a_2$ 12.2	15.4	23.4	185	221	337	488
Rh 45	13.1	16.6	25.3	198	240	361	522
Pd 46	13.8	17.6	26.7	207	254	376	545
Ag 47	14.8	19.1	28.6	223	276	402	585
Cd 48	15.5	20.1	29.9	234	289	417	608
In 49	16.5	21.7	31.8	252	307	440	648
Sn 50	17.4	22.9	33.3	265	322	457	681
Sb 51	18.6	24.6	35.3	284	342	482	727
Te 52	19.1	25.0	36.1	289	347	488	742
I 53	20.9	27.3	39.2	314	375	527	808
Xe 54	22.1	28.5	41.3	330	392	552	852
Cs 55	23.6	30.0	43.3	347	410	579	844
Ba 56	24.5	31.1	45.2	359	423	599	819
La 57	26.0	33.0	47.9	378	444	632	218

TABLE XIII—continued

Mass Absorption Coefficient of Elements  $\frac{\mu}{\rho}$ , including Scattering

Radiation	Ag Ka $\lambda$ 0.5604	Rh Ka 0.6149	Mo Ka 0.7097	Cu Ka 1.5392	Ni Ka 1.6565	Fe Ka 1.9344	Cr Ka 2.2869
Absorber Z							
Ce 58	28.4	35.8	52.0	407	476	636	235
Pr 59	29.4	37.2	54.5	422	493	624	251
Nd 60	30.5	38.8	57.0	437	510	651	263
Sm 62	33.1	41.2	62.3	467	519	183	289
Eu 63	35.0	44.5	65.9	461	498	193	306
Gd 64	35.8	45.7	68.0	470	509	199	316
Tb 65	37.5	47.9	71.7	435	140	211	333
Dy 66	39.1	49.9	75.0	462	146	220	345
Ho 67	41.3	52.7	79.3	128	153	232	361
Er 68	42.6	54.6	82.0	133	159	242	370
Tm 69	44.8	57.6	86.3	139	168	257	387
Yb 70	46.1	59.4	88.7	144	174	265	396
Lu 71	48.4	62.6	93.2	151	184	281	414
Hf 72	50.6	65.0	96.9	157	191	291	426
Ta 73	52.2	67.7	100.7	164	200	305	440
W 74	54.6	70.7	105.4	171	209	320	456
Os 76	58.6	76.3	112.9	186	226	346	480
Ir 77	61.2	80.0	117.9	194	237	362	498
Pt 78	64.2	83.8	123	205	248	376	518
Au 79	66.7	87.1	128	214	260	390	537
Hg 80	69.3	90.1	132	223	272	404	552
Tl 81	71.7	92.4	136	231	282	416	568
Pb 82	74.4	95.8	141	241	294	429	585
Bi 83	78.1	100.4	145	253	310	448	612
Nt 86	84.7	109	159	278	341	476	657
Ra 88	91.1	117	172	304	371	509	708
Th 90	97.0	119	143	327	399	536	755
U 92	104.2	129	153	352	423	566	805

## APPENDIX IV

### ATOMIC SCATTERING FACTORS

THE atomic scattering factors in the following tables are given for a series of values of  $(\sin \theta)/\lambda$ , and are therefore adapted for use with radiation of any wave-length. It is to be remembered, however, that the factor has an abnormal value when the wave-length is in the neighbourhood of an absorption edge of the scattering atom. The factor  $f_0$  decreases by several units near this point.

Tables XIV and XV give a series of  $f_0$  values for atoms at rest, which will be modified in an actual crystal by the heat motion. They are taken from a paper by James and Brindley (*Zeitschrift für Kristallographie*, **78**, 470, 1931). Most common atoms will be found in these tables. If  $f$  values for other atoms are required, they may be calculated from Table XVI. The Thomas-Fermi electron distribution represents the density of the electron atmosphere around an atom of high atomic number. This ideal distribution is sufficiently close to the actual distribution for it to be possible to calculate a general  $f_0$  curve, applicable to all atoms of higher atomic number than Rb. The  $f_0$  values for Rb calculated from the Hartree model and from the Thomas-Fermi distribution will be seen to agree closely in Table XIV.

To use Table XVI for an atom of atomic number  $Z$ , each value of  $f_0$  in the table must be multiplied by  $Z/55$ , and each value of  $(\sin \theta)/\lambda$  must be multiplied by  $(55/Z)^{1/3}$ . A curve of  $f_0$  against  $(\sin \theta)/\lambda$  is then plotted with the modified values. The table is calculated for caesium, the atomic number of which is 55.

TABLE XIV  
Atomic Scattering Factors  $f_0$ 

$\frac{\sin \theta}{\lambda} \cdot 10^{-3}$	0	0.1	0.2	0.3	0.4	0.5	0.6	0.7	0.8	0.9	1.0	1.1	Remarks
H	1.0	0.81	0.48	0.25	0.13	0.07	0.04	0.03	0.02	0.01	0.00	0.00	<i>W</i>
He	2.0	1.88	1.46	1.05	0.75	0.52	0.35	0.24	0.18	0.14	0.11	0.09	<i>H</i>
Li <sup>+</sup>	2.0	1.96	1.8	1.5	1.3	1.0	0.8	0.6	0.5	0.4	0.3	0.3	<i>H</i>
Li (neut.)	3.0	2.2	1.8	1.5	1.3	1.0	0.8	0.6	0.5	0.4	0.3	0.3	<i>H</i>
Be <sup>++</sup>	2.0	2.0	1.9	1.7	1.6	1.4	1.2	1.0	0.9	0.7	0.6	0.5	<i>I</i>
Be (neut.)	4.0	2.9	1.9	1.7	1.6	1.4	1.2	1.0	0.9	0.7	0.6	0.5	<i>I</i>
B <sup>+++</sup>	2.0	2.0	1.9	1.8	1.7	1.6	1.4	1.3	1.2	1.0	0.9	0.7	<i>I</i>
B (neut.)	5.0	3.5	2.4	1.9	1.7	1.5	1.4	1.2	1.2	1.0	0.9	0.7	<i>I</i>
C	6.0	4.6	3.0	2.2	1.9	1.7	1.6	1.4	1.3	1.2	1.0	0.9	<i>I</i>
N <sup>+</sup>	2.0	2.0	2.0	1.9	1.9	1.8	1.7	1.6	1.5	1.4	1.3	1.16	<i>I</i>
N <sup>+</sup>	4.0	3.7	3.0	2.4	2.0	1.8	1.65	1.55	1.5	1.4	1.3	1.15	<i>I</i>
N (neut.)	7.0	5.8	4.2	3.0	2.3	1.9	1.65	1.55	1.5	1.4	1.3	1.15	<i>I</i>
O (neut.)	8.0	7.1	5.3	3.9	2.9	2.2	1.8	1.6	1.5	1.4	1.35	1.25	<i>H</i>
O <sub>2</sub>	10.0	8.0	5.5	3.8	2.7	2.1	1.8	1.6	1.5	1.4	1.35	1.25	<i>I+H</i>
F <sup>-</sup>	10.0	8.7	6.7	4.8	3.5	2.8	2.2	1.9	1.7	1.55	1.5	1.35	<i>H</i>
F (neut.)	9.0	7.8	6.2	4.45	3.35	2.65	2.15	1.9	1.7	1.6	1.5	1.35	<i>H</i>
Ne	10.0	9.3	7.5	5.8	4.4	3.4	2.65	2.2	1.9	1.65	1.55	1.5	<i>I</i>
Na <sup>+</sup>	10.0	9.5	8.2	6.7	5.25	4.05	3.2	2.65	2.25	1.95	1.75	1.6	<i>H</i>
Na	11.0	9.65	8.2	6.7	5.25	4.05	3.2	2.65	2.25	1.95	1.75	1.6	<i>H</i>
Mg <sup>++</sup>	10.0	9.75	8.6	7.25	5.05	4.8	3.85	3.15	2.55	2.2	2.0	1.8	<i>I</i>



TABLE XIV—continued  
Atomic Scattering Factors  $f_0$ 

$\frac{\sin \theta}{\lambda} \cdot 10^{-3}$	0	0.1	0.2	0.3	0.4	0.5	0.6	0.7	0.8	0.9	1.0	1.1	Remarks
Mg	12.0	10.5	8.6	7.22	5.05	4.8	3.85	3.15	2.55	2.2	2.0	1.8	I
Al <sup>+++</sup>	10.0	9.7	8.9	7.8	6.65	5.5	4.45	3.65	3.1	2.65	2.3	2.0	H
Al <sup>++</sup>	11.0	10.3	9.0	7.75	6.6	5.5	4.5	3.7	3.1	2.65	2.3	2.0	H
Al <sup>+</sup>	12.0	10.9	9.0	7.75	6.6	5.5	4.5	3.7	3.1	2.65	2.3	2.0	H
Al	13.0	11.0	8.95	7.75	6.6	5.5	4.5	3.7	3.1	2.65	2.3	2.0	H+I
Si <sup>++</sup>	10.0	9.75	9.15	8.25	7.15	6.05	5.05	4.2	3.4	2.95	2.6	2.3	H
Si <sup>+</sup>	12.0	11.1	9.55	8.2	7.15	6.05	5.05	4.2	3.4	2.95	2.6	2.3	H+I
Si	14.0	11.35	9.4	8.2	7.15	6.1	5.1	4.2	3.4	2.95	2.6	2.3	H+I
P <sup>++</sup>	10.0	9.8	9.25	8.45	7.5	6.55	5.65	4.8	4.05	3.4	3.0	2.6	I
P (neut.)	15.0	12.4	10.0	8.45	7.45	6.5	5.65	4.8	4.05	3.4	3.0	2.6	I
P <sup>-3</sup>	18.0	12.7	9.8	8.4	7.45	6.5	5.65	4.85	4.05	3.4	3.0	2.6	I
S (neut.)	16.0	13.6	10.7	8.95	7.85	6.85	6.0	5.25	4.5	3.9	3.35	2.9	I
S <sup>++</sup>	10.0	9.85	9.4	8.7	7.85	6.85	6.05	5.25	4.5	3.9	3.35	2.9	I
S <sup>-2</sup>	18.0	14.3	10.7	8.9	7.85	6.85	6.0	5.25	4.5	3.9	3.35	2.9	I
Cl	17.0	14.6	11.3	9.25	8.05	7.25	6.5	5.75	5.05	4.4	3.85	3.35	H+I
Cl <sup>-</sup>	18.0	15.2	11.5	9.3	8.05	7.25	6.5	5.75	5.05	4.4	3.85	3.35	H
A	18.0	15.9	12.6	10.4	8.7	7.8	7.0	6.2	5.4	4.7	4.1	3.6	I
K <sup>+</sup>	18.0	16.5	13.3	10.8	8.85	7.75	7.05	6.44	5.9	5.3	4.8	4.2	H
Ca <sup>++</sup>	18.0	16.8	14.0	11.5	9.3	8.1	7.35	6.7	6.2	5.7	5.1	4.6	H
Sc <sup>+3</sup>	18.0	16.7	14.0	11.4	9.4	8.3	7.6	6.9	6.4	5.8	5.35	4.75	I

TABLE XIV—continued  
Atomic Scattering Factors  $f_0$

$\frac{\sin \theta}{\lambda} \cdot 10^{-3}$	0	0.1	0.2	0.3	0.4	0.5	0.6	0.7	0.8	0.9	1.0	1.1	Remarks
Ti <sup>++</sup>	18.0	17.0	14.4	11.9	9.9	8.5	7.85	7.3	6.7	6.15	5.65	5.05	I
Ti <sup>+</sup>	20.0	18.7	15.5	12.5	10.1	8.5	7.8	7.25	6.7	6.15	5.65	5.05	I
Cu <sup>+</sup>	28.0	27.0	24.0	20.7	17.3	14.0	11.3	9.4	8.0	7.3	7.0	6.7	I
Cu <sup>+</sup>	28.0	26.3	23.0	19.2	15.8	13.0	11.2	9.7	8.4	7.4	6.7	6.5	II approx.
Cu	29.0	25.8	21.4	17.8	15.2	13.3	11.7	10.2	9.1	8.1	7.3	6.7	T
Rb <sup>+</sup>	36.0	33.6	28.7	24.6	21.4	18.9	16.7	14.6	12.8	11.2	9.9	8.9	H
Rb	37.0	33.4	28.2	23.6	20.4	17.9	15.9	14.0	12.4	11.2	10.2	9.3	T

I calculated by method of interpolation.

H calculated from Hartree distribution.

T calculated from Thomas model.

W calculated from hydrogen wave-function (ground state).

TABLE XV  
Values of  $\epsilon_0$  calculated from the Thomas Field

$\frac{\sin \theta}{\lambda} \cdot 10^{-4}$	0	0.1	0.2	0.3	0.4	0.5	0.6	0.7	0.8	0.9	1.0	1.1
Va	23.0	20.3	16.6	13.5	11.6	10.1	8.7	7.6	6.7	6.0	5.4	4.8
Cr	24.0	21.4	17.4	14.3	12.2	10.6	9.2	8.1	7.2	6.4	5.7	5.2
Mn	25.0	22.1	18.2	14.9	12.8	11.2	9.6	8.5	7.5	6.7	6.0	5.5
Fe	26.0	23.1	19.1	15.6	13.4	11.7	10.2	8.9	7.9	7.1	6.4	5.8
Co	27.0	24.0	19.9	16.3	13.9	12.2	10.7	9.3	8.2	7.4	6.7	6.0
Ni	28.0	24.9	20.7	17.0	14.6	12.8	11.2	9.8	8.7	7.8	7.0	6.4
Cu	29.0	25.8	21.4	17.8	15.2	13.3	11.7	10.2	9.1	8.1	7.3	6.7
Zn	30.0	26.9	22.4	18.6	15.8	14.0	12.2	10.6	9.5	8.5	7.7	7.0
Ga	31.0	27.8	23.3	19.3	16.5	14.5	12.7	11.2	9.9	8.9	8.1	7.3
Ge	32.0	28.7	24.1	20.0	17.1	15.1	13.3	11.7	10.3	9.3	8.4	7.6
As	33.0	29.6	24.9	20.7	17.7	15.6	13.8	12.1	10.7	9.7	8.8	7.9
Se	34.0	30.6	25.8	21.5	18.4	16.2	14.3	12.6	11.2	10.1	9.1	8.2
Br	35.0	31.5	26.6	22.2	19.0	16.7	14.8	13.0	11.6	10.4	9.5	8.6
Rb	37.0	33.4	28.2	23.6	20.4	17.9	15.9	14.0	12.4	11.2	10.2	9.3
Sr	38.0	34.4	29.2	24.5	20.9	18.5	16.4	14.5	12.9	11.5	10.5	9.6
Y	39.0	35.4	30.0	25.3	21.6	19.1	17.0	15.0	13.3	12.0	10.9	9.9
Zr	40.0	36.4	30.9	26.1	22.3	19.7	17.5	15.5	13.9	12.4	11.2	10.3
Mo	42.0	38.2	32.6	27.5	23.5	20.8	18.6	16.5	14.8	13.2	12.0	11.0
Rh	45.0	41.1	35.1	29.8	25.4	22.6	20.2	18.0	16.1	14.5	13.1	12.0
Pd	46.0	42.0	36.0	30.6	26.2	23.1	20.7	18.6	16.6	14.9	13.5	12.4

TABLE XV—continued  
*Values of  $f_0$  calculated from the Thomas Field*

$\frac{\sin \theta}{\lambda} \cdot 10^{-3}$	0	0.1	0.2	0.3	0.4	0.5	0.6	0.7	0.8	0.9	1.0	1.1
Ag	47.0	43.0	36.9	31.3	26.8	23.7	21.3	19.0	17.0	15.3	13.9	12.8
Cd	48.0	43.9	37.8	32.1	27.5	24.3	21.8	19.5	17.4	15.7	14.3	13.2
Sn	50.0	45.9	39.4	33.6	28.9	25.5	23.0	20.5	18.5	16.6	15.0	13.8
Sb	51.0	46.8	40.3	34.5	29.6	26.1	23.5	21.1	18.9	17.0	15.4	14.1
Te	52.0	47.7	41.1	35.2	30.2	26.7	24.0	21.6	19.3	17.4	15.8	14.4
I	53.0	48.7	42.0	36.0	30.9	27.4	24.6	22.1	19.8	17.9	16.2	14.8
Cs	55.0	50.7	43.8	37.6	32.4	28.7	25.8	23.2	20.8	18.8	17.0	15.6
Ba	56.0	51.7	44.8	38.4	33.1	29.3	26.4	23.7	21.3	19.2	17.4	16.0
Ta	73.0	68.1	59.7	52.1	45.2	40.1	36.2	32.9	29.9	27.1	24.7	22.6
W	74.0	69.0	60.5	53.0	46.0	40.6	36.8	33.5	30.4	27.6	25.1	23.0
Pt	78.0	72.9	64.2	56.3	48.9	43.3	39.1	35.7	32.5	29.5	26.9	24.7
Au	79.0	74.0	65.0	57.0	49.7	43.9	39.8	36.3	33.0	30.0	27.4	25.1
Hg	80.0	74.9	65.9	57.8	50.3	44.6	40.3	36.9	33.5	30.5	27.8	25.4
Tl	81.0	75.8	66.8	58.6	51.2	45.2	41.0	37.5	34.0	30.9	28.3	25.8
Pb	82.0	76.9	67.8	59.5	51.9	45.9	41.6	38.0	34.6	31.4	28.7	26.2
Bi	83.0	77.9	68.7	60.3	52.7	46.6	42.2	38.6	35.2	31.9	29.2	26.8

TABLE XVI

*f<sub>0</sub> Values for Cs calculated on the Thomas-Fermi Distribution*

$\frac{\sin \theta}{\lambda} \cdot 10^{-8}$	<i>f</i>	$\frac{\sin \theta}{\lambda} \cdot 10^{-8}$	<i>f</i>
0	55	1.0	17.0
0.1	50.7	1.1	15.6
0.2	43.8	1.2	14.5
0.3	37.6	1.3	13.2
0.4	32.4	1.4	12.3
0.5	28.7	1.5	11.3
0.6	25.8	1.6	10.4
0.7	23.2	1.7	9.6
0.8	20.8	1.8	9.2
0.9	18.8	1.9	8.6
		2.0	8.1

## APPENDIX V

### DEDUCTION OF THE FORMULÆ FOR INTENSITY OF REFLECTION

IT has been seen in the chapter on X-ray Optics that reflection formulæ contain a quantity  $Q$  defined as follows. A crystal of volume  $V$ , so small that absorption in it may be neglected, is bathed in monochromatic radiation of intensity  $I_0$  per square centimetre. It is turned with constant angular velocity  $\omega$  about an axis lying in the reflection plane, through a small angular range  $2\epsilon_0$  which includes all settings at which reflection is appreciable. The amount  $R$  of radiation reflected per second at each setting is a function of the glancing angle. The total amount of radiation reflected is  $E$ , and the 'Integrated Reflection,' which is a constant characteristic of the crystal for a reflection  $hkl$ , is defined as

$$\int_{\theta_0 - \epsilon_0}^{\theta_0 + \epsilon_0} R d\theta / I_0,$$

and is given by  $\int_{\theta_0 - \epsilon_0}^{\theta_0 + \epsilon_0} R d\theta / I_0 = \frac{E\omega}{I_0} = QV$ ,

where  $Q = \left( \frac{Ne^2 \cdot F(hkl)}{mc^2} \right)^2 \cdot \lambda^3 \cdot \frac{1}{\sin 2\theta} \cdot \frac{1 + \cos^2 2\theta}{2}$ .

This expression for  $Q$  is the basis of reflection formulæ for a mosaic crystal, and the method of its derivation will be indicated here.

In the first place, a single unit of pattern of the crystal scatters radiation to an extent given by

$$\frac{A'}{A_0} = \frac{1}{r} \cdot \frac{e^2}{mc^2} \cdot F(hkl),$$

where  $A_0$  is the incident amplitude,  $A'$  the scattered amplitude at a distance  $r$ , and for the present the electrical vibration is supposed to be perpendicular to the plane of incidence. The 'polarisation

factor' can be introduced later. A train of plane monochromatic waves of amplitude  $A_0$  is now supposed to fall at glancing angle  $\theta$  upon a single sheet of these pattern-units, and we wish to find the amplitude of the reflected beam. By a well-known optical principle, the required amplitude at a given point P is equal to one-half the contribution from the first Fresnel zone, drawn for that point. If the distance of P from the point of reflection is  $r$ , the area of the zone is

$$\pi \lambda r / \sin \theta.$$

Let there be  $n$  pattern-units per square centimetre. The amplitude  $A$  at P is given by  $\frac{1}{2} \cdot \frac{2}{\pi} \cdot (\text{area of zone}) \cdot n \cdot A'$ .

$$A = \frac{1}{2} \cdot \frac{2}{\pi} \cdot \frac{\pi \lambda r}{\sin \theta} \cdot n \cdot \frac{1}{r} \cdot \frac{e^2}{mc^2} \cdot F(hkl) \cdot A_0.$$

$$\frac{A}{A_0} = \frac{n \lambda}{\sin \theta} \cdot \frac{e^2}{mc^2} \cdot F(hkl) = q(hkl).$$

The factor  $2/\pi$  in the expression is the same as that which appears in the treatment of Fresnel's circular zones, representing the effect of summing up the contributions from the elements of the first zone. It will be noted that  $r$  cancels out, as must be the case since both incident and reflected wave-trains have plane wave-fronts.

The next step consists in calculating the effect of a group of  $p$  planes, spaced a distance  $d$  apart, as in fig. 187 (a). The reflection is strongest at an angle  $\theta_0$  given by  $\lambda = 2d \sin \theta_0$ , but reflection occurs over a small range of angles on either side.

In the neighbourhood of the point P, reflected waves are being contributed by the planes enclosed in the dotted lines. We will find how much energy is passing per unit time through a small area  $S$  around P, for a setting of the crystal  $\theta = \theta_0 + \epsilon$ . When  $\epsilon$  is zero, the contributions from all the planes are exactly in phase, and since each contributes an amplitude  $A_0 q$  (see above), the total amplitude will be  $p A_0 q$ . The intensity through  $S$  will thus be proportional to  $S(p A_0 q)^2$ , and so equal to  $S \cdot p^2 q^2 \cdot I_0$  by definition of  $I_0$ . At each setting  $\epsilon$ , by a well-known formula of diffraction, this intensity is modified by the factor \*

---

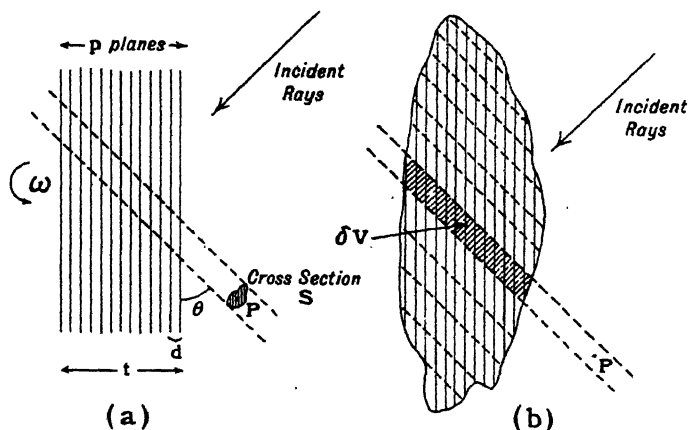
\* It will be realised that this expression, as in the case of a diffraction grating, is not strictly accurate, but it is a very close approximation when  $p$  is large.

$$\frac{\sin^2 \phi}{\phi^2},$$

where  $2\phi$  is the total phase difference between waves coming from the first and last planes, the number of planes being large.

$$2\phi = p \cdot \epsilon \cdot \frac{d}{d\theta} \left( \frac{2\pi}{\lambda} \cdot 2d \sin \theta \right)$$

$$\phi = p \cdot \pi \cdot \epsilon \cdot \frac{2d \cos \theta}{\lambda}.$$



(c)  
FIG. 187

The total amount of energy passing through  $S$  when the crystal is rotated with velocity  $\omega$  is therefore

$$E = \int_{-\epsilon_0}^{+\epsilon_0} S p^2 q^2 I_0 \cdot \frac{\sin^2 \phi}{\phi^2} \cdot \frac{d\epsilon}{\omega},$$

since the time  $dt$  during which the crystal reflects with this intensity is equal to  $\frac{d\epsilon}{\omega}$ . The angle  $\theta$  may be treated as a constant



in the integration, and equal to  $\theta_0$ . The expression becomes,

$$\text{since } d\epsilon = \frac{\lambda}{2\pi p d \cos \theta} \cdot d\phi,$$

$$E = Sp^2 q^2 I_0 \cdot \frac{1}{\omega} \cdot \frac{\lambda}{2\pi p d \cos \theta} \cdot \int \frac{\sin^2 \phi}{\phi^2} \cdot d\phi,$$

where the integral is taken over all appreciable values of  $\sin^2 \phi / \phi^2$ . The following substitutions are made:—

$$\int_{-\infty}^{+\infty} \frac{\sin^2 \phi}{\phi^2} d\phi = \pi,$$

$$q = \frac{n\lambda}{\sin \theta} \cdot \frac{e^2}{mc^2} \cdot F(hkl) \text{ as above,}$$

$n = Nd$ ,  $N$  being the number of pattern-units *per unit volume*,  
 $t = pd$ ,  $t$  being the total thickness of the crystal block.

We then obtain

$$E = \frac{I_0}{\omega} \left\{ \frac{Ne^2 \cdot F(hkl)}{mc^2} \right\}^2 \cdot \lambda^3 \cdot \frac{1}{\sin 2\theta} \cdot \frac{St}{\sin \theta}.$$

Now  $St/\sin \theta$  is equal to the volume  $\delta V$  of crystal enclosed between the dotted lines, which outline a cylinder of cross-section  $S$  and length  $t/\sin \theta$ . Thus

$$\frac{E\omega}{I_0} = \left\{ \frac{Ne^2 \cdot F(hkl)}{mc^2} \right\}^2 \cdot \lambda^3 \cdot \frac{1}{\sin 2\theta} \cdot \delta V.$$

When we have an irregular small crystal as in fig. 187 (b) it can be split up into a number of parallel cylindrical elements as in the figure. Some of these elements contain many planes and some few; the former give a strong reflection over a small range and the latter a weak reflection over a large range. However, the contribution from each element is proportional to its volume, and hence the whole crystal of volume  $V$  gives an integrated reflection

$$\frac{E\omega}{I_0} = \left\{ \frac{Ne^2 \cdot F(hkl)}{mc^2} \right\}^2 \cdot \lambda^3 \cdot \frac{1}{\sin 2\theta} \cdot V.$$

The justification of this treatment lies in the fact that it is possible to choose a point  $P$  at which to measure the reflected energy, such that it is sufficiently far from the crystal for the reflected waves to be completely built up, and yet sufficiently close for each crystal plane to contain many zones so that the reflected waves have not spread by diffraction. The volume within the dotted

lines remains effectively constant although the crystal rotates through an angle, because this angular range is so very small. We are thus justified in assuming that the integrated reflection is proportional to the volume of each small block of mosaic, however irregular its form. The treatment of waves whose vibration is in the plane of incidence is precisely the same, except that the intensity of the reflected wave is multiplied by  $\cos^2 2\theta$ . Hence, for unpolarised incident waves, the 'polarisation factor' is

$$(1 + \cos^2 2\theta)/2.$$

The important case of incidence upon a crystal face to which the reflection planes are parallel may be given as an example of the application of this formula. Let us suppose a beam, of intensity  $I_0$  per unit area, and cross-section  $S$ , falls upon the face at glancing angle  $\theta$  (fig. 187 (c)). At a depth  $x$  in the crystal, a layer of thickness  $dx$  is contributing to the total integrated reflection as the crystal turns. Its volume is  $\frac{Sdx}{\sin \theta}$ . The rays entering and leaving the crystal after reflection at this layer pass through a total thickness  $\frac{2x}{\sin \theta}$ , so that they are reduced in intensity by  $e^{-2\mu x/\sin \theta}$ , where  $\mu$  is the linear absorption coefficient of X-rays in the crystal. The total integrated reflection is therefore

$$\begin{aligned} \frac{E\omega}{I_0} &= \int_0^\infty Q \cdot \frac{Sdx}{\sin \theta} \cdot e^{\frac{-2\mu x}{\sin \theta}} \\ &= \frac{Q \cdot S}{2\mu}. \end{aligned}$$

If this be written

$$\frac{E\omega}{SI_0} = \frac{Q}{2\mu}$$

and for  $SI_0$  we put  $I$ , the total X-ray energy falling upon the crystal face, we obtain the expression quoted in Chapter IX:

$$\frac{E\omega}{I} = \frac{Q}{2\mu}.$$

Reflection formulæ for other methods, such as the powder method, can easily be deduced by similar treatments.

Brief mention may be made of a relation between incident

and reflected beam which holds for a *perfect* crystal, though it is not possible to give here the derivation of the formula which was first deduced by Darwin in 1914. If the crystal is a single homogeneous block of perfectly arranged structure, it can then be shown that reflection is total over a small angular range  $\theta_0 - s$  to  $\theta_0 + s$ , where

$$s = q\lambda / 2\pi d \cos \theta$$

$$\frac{Ne^2 F(hkl)}{mc^2} \cdot \frac{\lambda^2}{\pi \sin 2\theta}$$

Within this range the reflected beam is equal in intensity to the incident beam. Thus the integrated reflection over the same range, defined as  $\int R d\theta / I$ , is equal to  $\int d\theta$  or  $2s$ , since  $R = I$ . On either side of the range of perfect reflection there is a region in which the reflection rapidly falls away to zero. The total effect raises the integrated reflection from  $2s$  to  $8s/3$ :

$$\frac{E\omega}{I} = \frac{8s}{3} = \frac{8}{3\pi} \cdot \frac{Ne^2 F(hkl)}{mc^2} \cdot \frac{\lambda^2}{\sin 2\theta} \cdot \frac{1 + |\cos 2\theta|}{2},$$

where the last factor represents the polarisation factor. In general  $2s$  is of the order of several seconds of arc.

The state of the perfect crystal is not attained except in very rare cases, such as that of certain diamonds or of a freshly cleaved calcite surface; it does not present itself in ordinary crystal analysis. The criterion for 'perfection' is that  $pq \gg 1$ , where  $p$  is the number of planes in perfect array. In crystals which approach this condition for strong reflections ( $q$  large), the integrated reflection is less than that calculated by the mosaic formula, an effect called 'primary extinction.' It seems at first sight paradoxical that a perfect crystal which gives total reflection should yet give a smaller integrated reflection than a thoroughly imperfect crystal of the same substance, but this is the case owing to the minute angular range over which the former reflects. It will be noted that the absorption coefficient does not appear in the expression. All reflections ( $hkl$ ) are equally strong at the exact settings since they are total, but the integrated reflections vary because the range  $s$  is large when  $q$  is large, and *vice versa*.

## APPENDIX VI

### NOMENCLATURE OF THE SPACE-GROUPS

THE following table is taken from the "Report of the Abstracts Committee," a report prepared for the *Zeitschrift für Kristallographie* (79, 495, 1931) with the object of introducing uniformity in the description of space-groups and in the reference to them of crystal structures. The first two columns give the classical notation of Schoenflies and the number of the space-group in his arrangement, an order followed in the Astbury and Yardley tables. The third column gives Wyckoff's notation, which has been widely used in the description of structure. The fourth column contains the standard notation whose adoption has been agreed upon by a number of crystallographers in all countries. Its significance and the advantages to be derived from it are described in the chapter on Crystal Symmetry. As has been explained, it not only gives the full symmetry, but also makes it possible in describing a structure to show how the crystal has been 'set up,' *i.e.* to indicate the relation of the  $a$ ,  $b$ ,  $c$  axes to the symmetry elements. The alternative ways of setting up the crystal are given in the fifth column.

[TABLE

	Schoenflies	Wyckoff	Mauguin Normalised	Mauguin Other Orientations
1 2	$C_1^1$ $C_1^1, S_2^1$	$1C-1$ $1Ci-1$	$P1$ $P\bar{1}$	$A1, B1, C1, F1, I1 \dots$ $A\bar{1}, B\bar{1}, C\bar{1}, F\bar{1}, I\bar{1} \dots$
3 4 5 6	$C_2^1, C_2^2$ $C_2^1, C_2^2, C_2^3, C_2^4$ $C_2^1, C_2^2, C_2^3, C_2^4$ $C_2^1, C_2^2, C_2^3, C_2^4$	$2C-1$ $2C-2$ $2C-3$ $2C-4$	$Pm$ $Pc$ $Cm$ $Cc$	$Bm$ $Pa, Pn, Ba, Bc, Bd$ $Am, Im, Fm$ $Aa, Ia, Fd$
7 8 9	$C_3^1$ $C_3^1, C_3^2, C_3^3$ $C_3^1, C_3^2, C_3^3$	$2C-1$ $2C-2$ $2C-3$	$P_2$ $P_{21}$ $C_2$	$B_2$ $B_{21}$ $A_2, I_2, F_2$
10 11 12 13 14 15	$C_2^1, C_2^2, C_2^3, C_2^4$ $C_2^1, C_2^2, C_2^3, C_2^4$ $C_2^1, C_2^2, C_2^3, C_2^4$ $C_2^1, C_2^2, C_2^3, C_2^4$ $C_2^1, C_2^2, C_2^3, C_2^4$ $C_2^1, C_2^2, C_2^3, C_2^4$	$2Ci-1$ $2Ci-2$ $2Ci-3$ $2Ci-4$ $2Ci-5$ $2Ci-6$	$P_2/m$ $P_{21}/m$ $C_2/m$ $P_2/c$ $P_{21}/c$ $C_2/c$	$B_2/m$ $B_{21}/m$ $A_2/m, I_2/m, F_2/m$ $P_2/a, P_2/n, B_2/a, B_2/c, B_2/d$ $P_{21}/a, P_{21}/n, B_{21}/a, B_{21}/c, B_{21}/d$ $A_2/a, I_2/a, I_2/c, F_2/d$
16 17 18 19 20 21 22 23 24 25 26 27 28 29 30 31 32 33 34 35 36 37	$C_1^1, C_1^2, C_1^3, C_1^4, C_1^5, C_1^6, C_1^7, C_1^8, C_1^9, C_1^{10}, C_1^{11}, C_1^{12}, C_1^{13}, C_1^{14}, C_1^{15}, C_1^{16}, C_1^{17}, C_1^{18}, C_1^{19}, C_1^{20}, C_1^{21}, C_1^{22}, C_1^{23}, C_1^{24}, C_1^{25}, C_1^{26}, C_1^{27}, C_1^{28}, C_1^{29}, C_1^{30}, C_1^{31}, C_1^{32}, C_1^{33}, C_1^{34}, C_1^{35}, C_1^{36}, C_1^{37}$	$2C-1$ $2C-2$ $2C-3$ $2C-4$ $2C-5$ $2C-6$ $2C-7$ $2C-8$ $2C-9$ $2C-10$ $2C-11$ $2C-12$ $2C-13$ $2C-14$ $2C-15$ $2C-16$ $2C-17$ $2C-18$ $2C-19$ $2C-20$ $2C-21$ $2C-22$	$Pmm$ $Pmc$ $Pcc$ $Pma$ $Pca$ $Pnc$ $Pmn$ $Pba$ $Pna$ $Pnn$ $Cmm$ $Cmc$ $Ccc$ $Amm$ $Abm$ $Ama$ $Aba$ $Fmm$ $Fdd$ $Imm$ $Iba$ $Ima$	$\dots$ $Pcm$ $\dots$ $Pbm$ $Pbc$ $Pcn$ $Pnm$ $\dots$ $Pbn$ $\dots$ $\dots$ $Ccm$ $\dots$ $Bmm$ $Bma$ $Bbm$ $Bba$ $\dots$ $\dots$ $\dots$ $\dots$ $Ibm$
38 39 40 41 42 43 44 45 46	$V^1, D_2^1, D_2^2, D_2^3, D_2^4, D_2^5, D_2^6, D_2^7, D_2^8, D_2^9, D_2^{10}, D_2^{11}, D_2^{12}, D_2^{13}, D_2^{14}, D_2^{15}, D_2^{16}, D_2^{17}, D_2^{18}, D_2^{19}, D_2^{20}, D_2^{21}, D_2^{22}, D_2^{23}, D_2^{24}, D_2^{25}, D_2^{26}, D_2^{27}, D_2^{28}, D_2^{29}, D_2^{30}, D_2^{31}, D_2^{32}, D_2^{33}, D_2^{34}, D_2^{35}, D_2^{36}, D_2^{37}$	$2D-1$ $2D-2$ $2D-3$ $2D-4$ $2D-5$ $2D-6$ $2D-7$ $2D-8$ $2D-9$	$P_{222}$ $P_{2221}$ $P_{21212}$ $P_{212121}$ $C_{2221}$ $C_{222}$ $F_{222}$ $I_{222}$ $I_{212121}$	$\dots$ $P_{2122}; P_{2212}$ $P_{2121}; P_{21221}$ $\dots$ $A_{2122}; B_{2212}$ $A_{222}; B_{222}$ $\dots$ $\dots$ $\dots$

Synoptical Table—continued

	Schoenflies	Wyckoff	Mauguin Normalised	Mauguin Other Orientations
47	$V_1^1, D_{2h}^1$	2Di-1	<i>Pmmm</i>	...
48	$V_2^1, D_{2h}^2$	2Di-2	<i>Pnnn</i>	...
49	$V_3^1, D_{2h}^3$	2Di-3	<i>Pccm</i>	<i>Pbmb</i> ; <i>Pmaa</i>
50	$V_4^1, D_{2h}^4$	2Di-4	<i>Pban</i>	<i>Pcna</i> ; <i>Pncb</i>
51	$V_5^1, D_{2h}^5$	2Di-5	<i>Pmma</i>	<i>Pmnb</i> ; <i>Pnam</i> ; <i>Pnmc</i> ; <i>Pbmm</i> ; <i>Pcmm</i>
52	$V_6^1, D_{2h}^6$	2Di-6	<i>Pnna</i>	<i>Pnnb</i> ; <i>Pnan</i> ; <i>Pncn</i> ; <i>Pbnn</i> ; <i>Pcnn</i>
53	$V_7^1, D_{2h}^7$	2Di-7	<i>Pmna</i>	<i>Pnnb</i> ; <i>Pman</i> ; <i>Pncm</i> ; <i>Pbmn</i> ; <i>Pcmm</i>
54	$V_8^1, D_{2h}^8$	2Di-8	<i>Pcca</i>	<i>Pccb</i> ; <i>Pbab</i> ; <i>Pbcb</i> ; <i>Pbaa</i> ; <i>Pcaa</i>
55	$V_9^1, D_{2h}^9$	2Di-9	<i>Pbam</i>	<i>Pcma</i> ; <i>Pmcb</i>
56	$V_{10}^1, D_{2h}^{10}$	2Di-10	<i>Pccn</i>	<i>Pbnb</i> ; <i>Pnaa</i>
57	$V_{11}^1, D_{2h}^{11}$	2Di-11	<i>Pbcm</i>	<i>Pbma</i> ; <i>Pcam</i> ; <i>Pcmb</i> ; <i>Pmab</i> ; <i>Pmca</i>
58	$V_{12}^1, D_{2h}^{12}$	2Di-12	<i>Pnmn</i>	<i>Pnmn</i> ; <i>Pmnn</i>
59	$V_{13}^1, D_{2h}^{13}$	2Di-13	<i>Pmnn</i>	<i>Pmnn</i> ; <i>Pnmn</i>
60	$V_{14}^1, D_{2h}^{14}$	2Di-14	<i>Pbcn</i>	<i>Pbna</i> ; <i>Pcan</i> ; <i>Pcnb</i> ; <i>Pnab</i> ; <i>Pnca</i>
61	$V_{15}^1, D_{2h}^{15}$	2Di-15	<i>Pbca</i>	<i>Pcab</i>
62	$V_{16}^1, D_{2h}^{16}$	2Di-16	<i>Pnma</i>	<i>Pnam</i> ; <i>Pbnm</i> ; <i>Pcmn</i> ; <i>Pmnb</i> ; <i>Pmcn</i>
63	$V_{17}^1, D_{2h}^{17}$	2Di-17	<i>Cmcm</i>	<i>Ccmn</i> ; <i>Amma</i> ; <i>Amam</i> ; <i>Bmbb</i> ; <i>Bbmm</i>
64	$V_{18}^1, D_{2h}^{18}$	2Di-18	<i>Cmca</i>	<i>Ccma</i> ; <i>Abma</i> ; <i>Abam</i> ; <i>Bmab</i> ; <i>Bbam</i>
65	$V_{19}^1, D_{2h}^{19}$	2Di-19	<i>Cmmm</i>	<i>Ammm</i> ; <i>Bmmm</i>
66	$V_{20}^1, D_{2h}^{20}$	2Di-20	<i>Cccm</i>	<i>Amaa</i> ; <i>Bbmb</i>
67	$V_{21}^1, D_{2h}^{21}$	2Di-21	<i>Cmma</i>	<i>Abmm</i> ; <i>Bmam</i>
68	$V_{22}^1, D_{2h}^{22}$	2Di-22	<i>Ccca</i>	<i>Abaa</i> ; <i>Bbab</i>
69	$V_{23}^1, D_{2h}^{23}$	2Di-23	<i>Fmmm</i>	...
70	$V_{24}^1, D_{2h}^{24}$	2Di-24	<i>Fddd</i>	...
71	$V_{25}^1, D_{2h}^{25}$	2Di-25	<i>Immm</i>	...
72	$V_{26}^1, D_{2h}^{26}$	2Di-26	<i>Ibam</i>	<i>Ibma</i> ; <i>Imaa</i>
73	$V_{27}^1, D_{2h}^{27}$	2Di-27	<i>Ibaa</i>	...
74	$V_{28}^1, D_{2h}^{28}$	2Di-28	<i>Imma</i>	<i>Imam</i> ; <i>Ibmm</i>
75	$S_4^1$	4C-1	$P_4^1$	$C_4^1$
76	$S_4^2$	4C-2	$I_4^1$	$F_4^1$
89	$C_4^1$	4C-1	$P_4$	$C_4$
90	$C_4^2$	4C-2	$P_{41}$	$C_{41}$
91	$C_4^3$	4C-3	$P_{42}$	$C_{42}$
92	$C_4^4$	4C-4	$P_{43}$	$C_{43}$
93	$C_4^5$	4C-5	$I_4$	$F_4$
94	$C_4^6$	4C-6	$I_{41}$	$F_{41}$
95	$C_{4h}^1$	4Ci-1	$P_{4/m}$	$C_{4/m}$
96	$C_{4h}^2$	4Ci-2	$P_{42/m}$	$C_{42/m}$
97	$C_{4h}^3$	4Ci-3	$P_4/n$	$C_4/a$
98	$C_{4h}^4$	4Ci-4	$P_{42/n}$	$C_{42/a}$
99	$C_{4h}^5$	4Ci-5	$I_{4/m}$	$F_{4/m}$
100	$C_{4h}^6$	4Ci-6	$I_{41/a}$	$F_{41/d}$
77	$V_1^2, D_{3d}^1$	4d-1	$P_4^2$	$C_{4m2}$
78	$V_2^2, D_{3d}^2$	4d-2	$P_{42}^2$	$C_{4c2}$

## Synoptical Table—continued

	Schoenflies	Wyckoff	Mauguin Normalised	Mauguin Other Orientations
191	$D_{2h}^1$	$6D_i-1$	$C6/mmm$	$H6/mmm$
192	$D_{2h}^2$	$6D_i-2$	$C6/mcc$	$H6/mcc$
193	$D_{2h}^3$	$6D_i-3$	$C6/mcm$	$H6/mmc$
194	$D_{2h}^4$	$6D_i-4$	$C6/mmc$	$H6/mcm$
195	$T^1$	$T-1$	$P2_3$	...
196	$T^2$	$T-2$	$F2_3$	...
197	$T^3$	$T-3$	$I2_3$	...
198	$T^4$	$T-4$	$P_{213}$	...
199	$T^5$	$T-5$	$I_{213}$	...
200	$T_h^1$	$T_i-1$	$Pm3$	...
201	$T_h^2$	$T_i-2$	$Pn3$	...
202	$T_h^3$	$T_i-3$	$Fm3$	...
203	$T_h^4$	$T_i-4$	$Fd3$	...
204	$T_h^5$	$T_i-5$	$Im3$	...
205	$T_h^6$	$T_i-6$	$Pa3$	...
206	$T_h^7$	$T_i-7$	$Ia3$	...
207	$T_d^1$	$Te-1$	$P4_3m$	...
208	$T_d^2$	$Te-2$	$F4_3m$	...
209	$T_d^3$	$Te-3$	$I4_3m$	...
210	$T_d^4$	$Te-4$	$P4_3n$	...
211	$T_d^5$	$Te-5$	$F4_3c$	...
212	$T_d^6$	$Te-6$	$I4_3d$	...
213	$O^1$	$O-1$	$P4_3$	...
214	$O^2$	$O-2$	$P4_3$	...
215	$O^3$	$O-3$	$F4_3$	...
216	$O^4$	$O-4$	$F4_3$	...
217	$O^5$	$O-5$	$I4_3$	...
218	$O^6$	$O-6$	$P4_3$	...
219	$O^7$	$O-7$	$P4_3$	...
220	$O^8$	$O-8$	$I4_3$	...
221	$O_h^1$	$O_i-1$	$Pm3m$	...
222	$O_h^2$	$O_i-2$	$Pn3n$	...
223	$O_h^3$	$O_i-3$	$Pm3n$	...
224	$O_h^4$	$O_i-4$	$Pn3m$	...
225	$O_h^5$	$O_i-5$	$Fm3m$	...
226	$O_h^6$	$O_i-6$	$Fm3c$	...
227	$O_h^7$	$O_i-7$	$Fd3m$	...
228	$O_h^8$	$O_i-8$	$Fd3c$	...
229	$O_h^9$	$O_i-9$	$Im3m$	...
230	$O_h^{10}$	$O_i-10$	$Ia3d$	...

## INDEX OF SUBJECTS

- ABSENT Spectra, 91, 100.  
 Absolute Determination of Wave-length, 45.  
 Absolute Measurements, 29.  
     Application to Analysis, 101, 219-221.  
 Absorption Coefficients, 325-327.  
     Edges, 296, 301-304.  
     of X-rays, 300-304.  
 Adamantine Structures, 128.  
 Additive Law of Ionic Radii, 113.  
 Alkaline Halides, Heat of Formation, 173, 176.  
     Refractivity, 182.  
 Alloys, 148-157, 240-241.  
 Alum, Fourier Analysis of, 225.  
 Aluminium Wire, Orientation in, 196.  
 Amorphous Solids, Diffraction by, 191-196.  
 Amphibole, 133, 239.  
 Anthracene, 161.  
     Fourier Analysis of, 229.  
 Aragonite, Twinning of, 177.  
 Aromatic Compounds, 160-165.  
 Asterism, 201.  
 Atomic Number, 291.  
     Refractivity, 182.  
     Scattering Factor, 100-101, 209-213, 328-334.  
     Scattering of Electrons, 254-259.  
     of X-rays, 208-213.  
 Axis of Rotation-Inversion, 68.  
     of Symmetry, 68.  
  
 B SUB-PERIODS, 143.  
 Benzene, 165, 265.  
 Beryl, 104-108, 141.  
 Birefringence, 183.  
 Body-centred Cubic Structure, 145.  
 Borates, 136.  
 Borides, 157.  
 Bragg's Law, 15.  
  
 Brass, 154.  
 Breadth of Powder Lines, 189.  
  
 CALCITE, Birefringence of, 183.  
 Carbides, 157.  
 Carbon Tetrachloride, 192.  
     Electron Diffraction by, 265.  
 Cellulose, 203-204.  
 Centre of Inversion, 68.  
 Classes of Crystal Symmetry, 72-73.  
 Closest Packing, 144-145.  
 Complex Acid Radicals, 129-130.  
 Compton Effect, 305-306.  
 Continuous Spectrum, 298-300.  
 Coolidge Tube, 306-307.  
 Co-ordination, 124, 140.  
     Compounds, 130-131.  
 Critical Angle, 313-314.  
 Cross Spectra, 235.  
     in Electron Diffraction, 259.  
 Crystal Faces, Naming of, 7, 19-20.  
     Lattice, Energy of, 171-176.  
     Zones, 9.  
 CsCl Type, Crystal Dimensions, 126.  
 Cubic Crystal, Symmetry of, 69.  
 Cubic Space-lattices, 43-44, 64.  
 Cyclopentane, 265.  
  
 DEBYE Factor, 217-219.  
 Deviation from Reflection Law, 311.  
 Diamond, Analysis of, 53-55.  
     Symmetry of, 78.  
 Diffraction by Small Crystals, 188.  
     by Three-dimensional Grating, 17-20.  
     of X-rays by Ruled Grating, 313-315.  
 Difluorides, 126-127.  
 Diopside, Fourier Analysis of, 227.  
 Dioxides, 126-127.  
 Double Fourier Series, 227.



E-CURVE, 255-257, 259.  
 Electron Affinities, 174.  
 Electron Diffraction, by Powders, 248-250.  
   Examples, 258.  
 Electron Distribution in Atoms, 121, 211.  
 Electron Sharing, 117.  
 Elements, Structure of, 142-148.  
 Energy Levels, 295-298.  
 Equivalent Positions, 95-96.  
 Excitation of Line-spectra, 297.  
 Extinction, 236.

FACTOR  $f$ , 100-101, 209, 328-334.  
 Fatty Acids, 165-169.  
 Felspar, 136.  
 Fibres, Structure of, 203-207.  
 Filters, Absorbing, 304.  
 Fluor, Analysis of, 55-56.  
 Formulæ for Crystal Diffraction, 216-217, 335 *et seq.*  
 Fourier Analysis, Applied to Liquids, 194.  
   Examples of, 224-229.  
   of Crystal Structure, 221-224.  
 Fourier Representation as Optical Image, 229-231.  
 Friedel's Law, 93-95, 223.

GAMMA Structure, 154.  
 Gases, Diffraction by, 191-193.  
   Electron Diffraction by, 264-267.  
 Glide Plane, 76.  
   Notation, 87.  
 Gliding of Metals, 199.  
 Gnomonic Projection, 25-26.  
 Graphite, 162.

HADDING Tube, 307.  
 Hair, 206.  
 Hemihedry, 75.  
 Hemimorphite, 239.  
 Heteropolar Bond, 112-116.  
 Heteropolyacids, 137-140.  
 Hexagonal Crystal Indices, 67.  
 Holohedry, 75.  
 Homopolar Bond, 116-117.  
 Hull's Graphs, 36.  
 Hume-Rothery's Law, 154.  
 Hydrides, 157.  
 Hydrogen, Binding of, 122.

IDEALLY Imperfect Crystal, 216.  
 Identification, 241-242.  
 Image Formation in Microscope, 229.  
 Indices of Crystal Faces, 7, 19-20.  
   of Reflections or Spectra, 19.  
 Inorganic Compounds, Types AX and AX<sub>2</sub>, 124-129.  
   Crystals, Analysis of, 102-104.  
 Integrated Reflection, 214, 335.  
 Interatomic Distances, Homopolar, 117.  
   Ionic, 115.  
   Metallic, 118.  
 Interatomic Repulsion, 120.  
 Interference Fringes with X-rays, 315-317.  
 Intermetallic Compounds, 148.  
 Interstitial Alloys, 158.  
 Ionic Bond, 112-116.  
   Radii, 115.  
 Ionisation Spectrometer, 27-30.  
 Iron-aluminium Alloys, 152.

K ABSORPTION Edges, 318-320.  
   Emission Spectra, 292, 318-320.  
 Keratin, 206.  
 Ketone Oxygen, 165, 239.  
 Kossel's Law, 296.

L ABSORPTION Edges, 321-323.  
   Emission Spectra, 293, 321-323.  
 Lattice-planes, 5-6.  
 Laue Equations, 18.  
   Pattern, Model Illustrating, 25.  
   Photograph, Method of, 23-27.  
 Layer Lattices, 127.  
   Lines, 31.  
 Line Spectra, 291-295.  
 Liquids, Diffraction by, 191-196.  
 Long-chain Organic Molecules, 165-170.

M ABSORPTION Edges, 324.  
   Emission Spectra, 324.  
 Mercury, Diffraction by, 193-195.  
 Metallic Bond, 118.  
   Structures, Dimensions of, 146.  
 Mica, 133, 238.  
 Missing Elements, 292.  
 Molecular Refractivity, 182.  
   Weight, Determined by X-rays, 238.  
 Mosaic Crystal, 214.  
 Mullite, 242.

N-PATTERN, 259.  
NaCl Type, Crystal Dimensions, 126.  
Naphthalene, 161, 185.  
Nickel Arsenide Type, 128-129.  
Nitrides, 157.  
Notation of Space Groups, 84-88.

OPAL GLASS, 241.  
Operations of First and Second Kind, 68.

Organic Compounds, 159-171.  
Crystals, Analysis of, 108-111.  
Orientation, Crystal, 196-203.  
Orthohexagonal Cell, 85.  
Orthorhombic Space-groups, 81-84.

P-PATTERN, 264.  
Packing of Ions, 103.  
Paraffins, 165-170.  
Parameters, 56-57.  
Pattern, 3.  
Pauling's Principles of Ionic Structures, 103, 140-142.  
Periodic Table after Bohr, 143.  
Periodic Table of the Elements, 123.  
Phase Diagram of Alloy, 149.  
Philips Tube, 307-308.  
Phosphotungstic Acid, 138-139.  
Plane of Symmetry, 68.  
Point-group Symbols, 86.  
Point-groups, 67-75.  
Polar Axis, 79.  
Potassium Chloride, 39-51.  
Analysis by Laue Photograph, 46.  
by Powder Photograph, 47.  
by Spectrometer, 40.  
by Rotation Photograph, 49-50.  
Powder Photograph, 33-37.  
Pyrites, 57-61.  
Symmetry of, 70, 79-80, 95.  
Pyroxene, 133.

QUANTITATIVE Estimation by X-rays, 242.

Quartz, Symmetry of, 81.  
Twinning of, 178-180.

RATIONAL Indices, Law of, 6-8.  
Reciprocal Lattice, 231-235.  
Reflection by Lattice-planes, 13-16.  
by Perfect Crystal, 340.  
Formulae, 216-217, 335-340.  
Refraction of X-rays, 309-312.  
Refractive Index, 180-186.

Resolution of  $K\alpha$  Doublet, 190.  
Resolving Power of Powder Photographs, 36.  
Rotation Photograph, 30-33.  
Indexing of, 32.  
of KCl, NaCl, 50.  
Row Lines, 32.  
Rubber, 204-206.  
Rydberg Constant, 292.

SCREW Axes, 76.  
Notation of, 86-87.  
Segregation in Alloys, 152.  
Shearer Tube, 307-308.  
Silicates, 131-136.  
Silicon-oxygen Groups, 133-136.  
Silver-cadmium Alloys, 149-151.  
Sodium Chloride, 39 *et seq.*  
Analysis by Laue Photograph, 46, 48.  
by Powder Photograph, 47.  
by Spectrometer, 40.  
by Rotation Photograph, 49.  
Sodium Nitrate, Birefringence of, 183.  
Solid Solution, 148.  
Space-group, 75 *et seq.*  
Determination of, 90-93.  
Examples, 88.  
Notation of, 86.  
 $V_h^{16}$ , 98.  
Space-lattice, 3-5, 63-67.  
Determination of, 92.  
the Fourteen Types of, 64-66.  
Standard Plane, 7.  
Stereographic Projection, 25-26, 47-48.  
Structure Amplitude, 96-100.  
Superlattice, 152-154.  
Symmetry Elements of Cubic Crystal, 69.

TEMPERATURE Factor, 217-219.  
Tetartohedry, 75.  
Thermal Expansion, 242-243.  
Thermal Movement, 217-219.  
Fourier Analysis of, 225.  
Total Reflection of X-rays, 312-313.  
Transition Elements, 142.  
Twinning, 176-180.

UNCERTAINTY Principle, 247.  
Unit Cell, 4.

VAN DER WAALS Attraction, 118-120.

WATER of Crystallisation, 131.

Wave-length of Electron Beam, 253-254.

Scale, 295.

Used in Analysis, 295.

Wave Mechanics, 244-248.

Packet, 246.

Weissenberg Goniometer, 37.

Wool, 206.

Wurtzite Type, 128.

X-RAY Microscope, 231.

X-rays, Absorption of, 300-304.

Refraction of, 309-312.

Total Reflection of, 312-313.

Used in Analysis, 295.

Wave-lengths of, 292-295, 318-324.

ZEOLITE, 136.

Zero-point Energy, 219.

Zincblende, Analysis of, 51-53.

Symmetry of, 79.

Type, 128.

Zone Axis, 9.

## INDEX OF AUTHORS

ABBE, 229.

Abegg, 281.

Adam, 169.

Andrade, 198.

Andress, 204, 284.

Astbury, 92, 206, 277, 278, 284.

BÄCKLÉN, 315.

Barkla, 274, 291.

Barlow, 81, 145, 269, 271.

Bearden, 219.

Bernal, 110, 170, 276.

Berzelius, 113.

Bhagavantam, 185.

Bohr, 142, 143, 278, 296.

Born, 113, 171, 172, 174, 176, 244, 255, 281, 285.

Bosanquet, 219, 279.

Bradley, 146, 152, 154, 275, 283.

Bragg, W. H., 160, 161, 214, 217, 222, 272, 273, 274, 275, 279, 280, 283.

Bragg, W. L., 113, 116, 219, 261, 279.

Bravais, 268, 269.

Bridgeman, 198.

Brindley, 328.

Burgers, 35.

CARPENTER, 198, 286.

Clark, 23, 191, 196, 202, 298.

Compton, 30, 208, 219, 224, 279, 280, 305, 311, 312.

Coolidge, 306.

Cork, 225, 226.

Crane, 2.

Czochralski, 198.

DARWIN, 236, 273, 274, 275, 279, 280, 311, 340.

Davis, 312.

Davisson, 244, 248, 250.

De Broglie, 165, 244, 274, 276, 284.

Debye, 33, 188, 192, 193, 217, 248, 264, 274, 275, 280.

Dirac, 244.

Duane, 223, 280.

EKMAN, 156.

Elam, 198, 201, 286.

Elsasser, 248.

Ewald, 126, 231, 236, 271, 274, 275, 280, 311.

FAJANS, 113, 281, 285.

Fedorov, 81, 269.

Fermi, 328.

Firth, 224.

Foz, 122.

Frankenheim, 268.

Friedel, 93, 165, 223, 284.

Friedrich, 12, 165, 271.

GERMER, 244, 248, 250.

Goetz, 286.

Goldschmidt, 113, 124, 127, 282.

Grimm, 113, 128, 281, 285.

Grindley, 284.

Groth, 271, 272.

Gunnar Hägg, 157, 283.

HADDING, 307.

Hartree, 211, 213, 219, 278, 279, 280,  
328.

Hassel, 282.

Hauser, 284.

Hausser, 198.

Häuy, 2, 268.

Havighurst, 280.

Haworth, 203.

Heisenberg, 244, 247.

Heitler, 116.

Helmholtz, 176.

Hengstenberg, 206.

Hermann, 85.

Herzog, 284.

Hessel, 269.

Hilger, 23.

Huggins, 122.

Hull, 33, 36, 196, 248, 275.

Hume-Rothery, 146, 154, 283.

Hund, 127, 285.

Huygens, 268.

JAMES, 218, 219, 224, 278, 279, 280,  
328.

Jancke, 284.

Jay, 152.

Joffé, 286.

Johanssen, 152.

KAPITZA, 286.

Katz, 204, 284.

Keggin, 138.

Kikuchi, 259, 262, 263, 264.

Kirchner, 259, 263, 264.

Knipping, 12.

Kossel, 281, 296.

Kuhlenkampf, 316.

LANDÉ, 171, 172, 173.

Langmuir, 169, 281.

Larsson, 312, 315.

Laue, 12, 18, 23, 271, 279.

Lennard-Jones, 113, 285.

Lewis, 116, 281.

Linde, 152.

Linnik, 315.

London, 116.

Lonsdale, 163, 164, 284.

MACHATSCHKI, 282.

Madelung, 172, 281.

Malkin, 239.

Mark, 169, 193, 204, 259, 264, 284.

Mauguin, 85, 238.

Mayer, 174, 176, 285.

Menke, 193.

Meyer, 204, 284.

Miers, 72.

Miller, 8.

Moseley, 273, 274, 291.

Mott, 255, 256, 259.

Müller, 23, 165, 166, 169, 283, 284.

NAHMIA, 242.

Niggli, 92, 276, 277, 278.

OFTEDAL, 282.

PALACIOS, 122.

Parker, 57, 61.

Pauling, 103, 113, 117, 138, 140, 239,  
282.

Philips, 306, 307.

Piper, 165, 239, 283.

Polanyi, 30, 198, 203, 204, 276, 284,  
285.

Pope, 145, 271, 273.

Preston, 283.

Prins, 193.

RANDALL, 195.

Robertson, 163, 284.

Robinson, 240.

Rupp, 263.

SCHERRER, 33, 188, 190, 248, 275.

Schiebold, 26, 30, 276.

Schmid, 198, 286.

Schoenflies, 81, 84, 269.

Schrödinger, 244.

Seeman, 276.

Shearer, 165, 239, 240, 282, 307.

Siegbahn, 274, 292, 297, 312, 315.

Slater, 117.

Smekal, 286.

Sohnke, 269.

Sommerfeld, 128, 271.

Stenström, 275, 321.

TAYLOR, 198, 201, 286.

Thewlis, 154.

Thibaud, 315.

Thomas, 328.

Thomson, 244, 248, 250, 259, 263.

Trillat, 165, 259, 263.

UREY, 298.

VAN DER WAALS, 118, 176.

Van 't Hoff, 117.

Von Nardroff, 312.

WALLER, 210, 219, 280, 312.

Warren, 239.

Wasastjerna, 113, 116, 182, 281, 282.

Webster, 289, 298.

Weissenberg, 37, 276.

Wentzel, 210.

Werner, 130.

West, 278, 279.

Westgren, 149, 275, 283.

Whiddington, 274.

Whitehouse, 57, 61.

Wierl, 169, 193, 259, 264, 265.

Wilson, 273, 305.

Wood, 278.

Wooster, 298.

Wyckoff, 27, 92, 276, 277, 278, 279,

282, 284.

YARDLEY, 92, 277, 278.

ZACHARIASEN, 136, 282.

Zernicke, 193.

Zwicky, 286.





